INVESTIGATIONS OF THE PHYSICAL AND CHEMICAL PROPERTIES OF AMBIENT FINE PARTICLES IN URBAN SCHOOLS

Leigh R. Crilley
Bachelor of Applied Science (Chemistry)

Submitted in [partial] fulfilment of the requirements for the degree of
Doctor of Philosophy

International Laboratory for Air Quality and Health
Faculty of Science and Engineering
Queensland University of Technology
[2013]

Keywords

Airborne particles

Aerosol Mass Spectrometry

Chemometrics

Children

Diurnal variation

Elements

Elemental carbon/Organic carbon

Exposure

On-road measurements

Organic Aerosols

Positive Matrix Factorisation

Reactive oxygen species

School

Secondary Organic Aerosols

Toxicity

Urban

Vehicle emissions

Abstract

Airborne particles present in urban environments are from a number of sources including vehicle emissions, which have been frequently shown to be the largest primary urban source. There are numerous detrimental health effects associated with exposure to airborne particles, with both the size and chemical composition thought to play a role in the particles toxicity. Due to their immature immune systems, children are one of the more vulnerable sections of the community to exposure of ambient particles. An urban microenvironment where children spend a large portion of their day is school, and thus this is an important site for monitoring exposure to airborne particles. To properly assess children's exposure in schools, source identification along with quantitative estimations of their contributions is necessary; however there is limited literature on children's exposure to vehicle emissions and other sources in schools. Thus, this thesis aimed to determine the sources of ambient particles that children are exposed to at school, the driving factors to the observed concentrations and potential toxicity of the particles.

To achieve these aims, a pilot study was first conducted on the emissions from the Brisbane fleet followed by a comprehensive study on the physiochemical properties of airborne particles at 25 urban schools in Brisbane using selected established and novel analytical techniques. A particular focus was on organic aerosols, as these typically form the largest component of ambient fine particles in urban areas. Based on the chemical composition and size distribution of the particles, the potential toxicity was assessed.

The pilot study was conducted in a Brisbane tunnel to probe the effect of traffic counts and composition on the levels of traffic emissions and its toxicity, as measured by its oxidative potential. On-road mobile measurements were performed in a tunnel as the emissions undergo 'real world' dilution effects with minimal interference from other sources, enabling the contributing factors to be determined. Based on these results, total traffic volume as opposed to traffic composition was found to be a better indicator of vehicle particle emissions and their potential toxicity and was considered as key parameter in assessing children's exposure at school.

The sources of ambient fine particles were identified at the participating schools using techniques which included the elemental carbon, organic carbon and trace elemental analysis as well as aerosol mass spectrometry. The trace elemental results at the schools indicated that the toxic heavy metals (V, Cr, Ni, Cu, Zn and Pb), attributed mostly to vehicle and industrial emissions, were predominantly in the PM_1 fraction (mass concentration of particles with a diameter less than 1 μm). This result points to PM_1 being a potentially better fraction for investigating the health effects of airborne particles, with future work required to confirm this hypothesis.

An Aerodyne Aerosol Mass Spectrometer (AMS) was deployed at 5 of the schools to measure the chemical composition of the ambient non-refractory PM_1. Utilising the high temporal resolution afforded by the AMS found that the levels of organic aerosols during school hours (9 am to 3 pm) to be at a minimum concentration compared to the rest of the day. Pick-up and drop-off times represented the periods of children's maximum exposure to vehicle emissions while at school. As field

deployment of the AMS was not possible for every school, a novel filter based method for the analysis of the organic aerosols by AMS was tested and validated. This method offers a simplified approach to field measurements at multiple sites and extends the application of the AMS to location where deployment is difficult.

A common finding across all the techniques was that, unless schools were near busy roads (<500m) children were mostly exposed to secondary sources rather than primary particle emissions while at school. At the majority of the schools, the secondary organic aerosols were highly oxidised and was therefore attributed to regional sources. Levels of vehicle emissions at the schools were found to be primarily dependent on total traffic counts on surrounding roads and secondly on the wind direction relative to the surrounding roads. Overall, while local meteorology affected the observed concentrations, the range of concentrations measured can be considered as representative of children's exposure to vehicle emissions and secondary organic aerosols at schools with similar traffic conditions.

This thesis represents a comprehensive study of the physicochemical properties of ambient particles in school environments in Australia and forms part of a larger study aimed to determine the effects of traffic emissions on children's health. The result from this thesis will be integrated with other air quality parameters from the study and will be analysed in conjunction with health data from children at the participating schools with the aim of determining the effects of long-term exposure to traffic emissions.

List of Publications

Peer reviewed journal articles

1. Leigh R. Crilley, Luke D. Knibbs, Branka Miljevic, Xiaochun Cong, Kathryn E. Fairfull-Smith, Steve E. Bottle, Zoran D. Ristovski, Godwin A. Ayoko and Lidia Morawska; Concentration and oxidative potential of on-road particle emissions and their relationship with traffic composition: Relevance to exposure assessment. *Atmospheric Environment.* **2012,** 59, 533-539.
2. Leigh R. Crilley, Godwin A. Ayoko, Mandana Mazaheri and Lidia Morawska; Characterisation of carbonaceous aerosols at urban schools to determine the sources of children's exposure. *Atmospheric Environment.* **2013**, Submitted.
3. Leigh R. Crilley, Godwin A. Ayoko, Eduard Stelcer, David D. Cohen, Mandana Mazaheri and Lidia Morawska; Elemental composition of ambient fine particles in urban schools: sources of children's exposure**.** *Science of the Total Environment.* **2013,** Submitted**.**
4. Leigh R. Crilley, Godwin A. Ayoko, E. Rohan Jayaratne, Farhad Salimi and Lidia Morawska; Aerosol Mass Spectrometric analysis of the chemical composition of non- refractory PM_1 samples from school environments in Brisbane, Australia**.** *Science of the Total Environment.* **2013,** 498-460, 81-89.
5. Leigh R. Crilley, Godwin A. Ayoko and Lidia Morawska; First measurements of source apportionment of organic aerosols in the Southern Hemisphere. *Environmental Pollution.* **2014**, 184, 81-88.

6. Leigh R. Crilley, Godwin A. Ayoko and Lidia Morawska; Analysis of organic aerosols collected on filters by Aerosol Mass Spectrometry for source identification. *Analytica Chimica Acta.* **2013**, 803, 91-96.

Table of Contents

List of Figures

List of Tables

List of Abbreviations

AMS	Aerosol Mass Spectrometer
BBOA	Biomass Burning Organic Aerosols
EC	Elemental Carbon
HDV	Heavy-Duty Vehicles
HOA	Hydrocarbon-like Organic Aerosols
LV-OOA	Low-Volatility Oxygenated Organic Aerosols
OA	Organic Aerosols
OC	Organic Carbon
OOA	Oxygenated Organic Aerosols
PCA	Principal Component Analysis
PM_1	Mass concentration of particles with a diameter less than 1 μm
$PM_{2.5}$	Mass concentration of particles with a diameter less than 2.5 μm
PMF	Positive Matrix Factorisation
PNC	Particle Number Concentration
POA	Primary Organic Aerosols
ROS	Reactive Oxygen Species
SOA	Secondary Organic Aerosols
SV-OOA	Semi Volatile Oxygenated Organic Aerosols
TOF-AMS	Time-Of-Flight Aerosol Mass Spectrometer
UFP	Ultrafine Particles

Statement of Original Authorship

The work contained in this thesis has not been previously submitted to meet requirements for an award at this or any other higher education institution. To the best of my knowledge and belief, the thesis contains no material previously published or written by another person except where due reference is made.

Signature: _____

Date: 3/12/2013

Acknowledgements

There have been many people who have supported me through my PhD, and include

Prof Godwin Ayoko, my principal supervisor, for giving me the opportunity to pursue my doctorate, keeping me focussed throughout, supporting and encouraging me and being my sounding board on all issues, great and small.

Prof Lidia Morawska, my associate supervisor, for direction, insightful comments and provision of the top up scholarship.

Dr Rohan Jayaratne, my other associate supervisor for his very helpful discussions and comments on my research.

Dr Mandana Mazaheri for her organisation of the fieldwork and help with the design of the sampling at the schools.

Dr Branka Miljevic for the ROS measurements and training on the AMS sampling and data analysis procedures

Dr Luke Knibbs for his assistance with the planning, data collection and analysis in the Clem7 project.

Fellow UPTECHer's Farhad Salimi, Rusdin Laiman, Megat Mokhtar and Nitika Mishra for assistance with my sampling and fieldwork, making the fieldwork enjoyable and useful discussions regarding the data

Dr Adrian Friend for his chemometric assistance

All other members of staff and colleagues at ILAQH, for their assistance and making it a great group to work in.

Fellow HDR students in the Enviro-Analytical group and Chemistry

My beautiful wife, Karen Crilley for tirelessly editing and formatting my work but most of all for being there for me through the frustrations and highs.

Queensland University of Technology for the provision of an Australian Postgraduate Award scholarship.

Chapter 1. Introduction

Air pollution is ubiquitous in urban environments as a result of the contribution of a number of anthropogenic sources comprising emissions of gases and particles. There are numerous anthropogenic (man-made) and biogenic (natural) sources of airborne particles. Anthropogenic sources include traffic, industrial, cooking emissions and domestic heating by biomass burning. Biomass burning can also be related to biogenic sources, such as bushfires, while other biogenic sources include sea spray, airborne soil and volcanoes. Sources listed thus far are known as primary sources, as they directly emit particles into the atmosphere [1]. Reactions of primary gaseous compounds in the atmosphere, such as the photo-oxidation of volatile organic compounds can result in the formation of aerosols, referred to as secondary sources [2]. Aerosols are suspensions of solid or liquid particles within a gaseous medium with a lifetime sufficiently long to enable detection [3]. Thus within the atmospheric sciences airborne particles in ambient air are also known as aerosols and the terms are used interchangeably and are the topic of this thesis. Atmospheric aerosols have a broad size range that spans several orders of magnitude from a few nanometres to upwards of 10 μm [4].

The size of airborne particles is frequently expressed in terms of its diameter. The definition of the particle diameter depends primarily on the measurement technique employed [3]. One definition is the aerodynamic equivalent diameter, which refers to the size of a particle having the same terminal velocity as an equivalent perfectly spherical particle with unit density [1]. This definition is applicable to particles larger than 0.5 μm as particles smaller than this undergo Brownian diffusion and are thus

characterised by their diffusive diameter [3]. In this thesis the aerodynamic equivalent diameter is appropriate for the techniques utilised and is thus the definition used throughout unless otherwise stated.

In an urban environment, several size modes of ambient particles are frequently observed; coarse, fine, ultrafine and nanoparticle size fractions. The coarse fraction is from 2.5 to 10μm, the fine fraction is < 2.5 μm, ultrafine are < 0.1 μm and nanoparticles are < 50 nm. However, these conventions, particularly for the ultrafine and nanoparticle size fractions are not strictly adhered to in the literature but for this thesis these are the definitions used unless otherwise stated. These particle size fractions have different chemical and physical properties, sources and formation mechanisms [5]. Thus airborne particles demonstrate a high degree of complexity in terms of both their size and chemical composition which makes identification of the sources challenging.

This is particularly true for urban environments where there are multitudes of contributing sources and includes biomass burning, industrial, vehicle emissions, airborne soil as well as secondary sources. Many studies have shown that vehicle emissions are major anthropogenic sources in an urban environment ([6] and references therein). Vehicles emit a range of particles that have different chemical and physical properties as a result of a number of separate processes. These vehicular process are classified as either exhaust emissions (directly from the tailpipe) or non-exhaust emissions, which are abrasion products from engine, brake and tyre wear and also resuspension of road dust [7]. Exhaust and non-exhaust emissions can be responsible for approximately equal contributions by mass to ambient particles in

urban environments [8]. With the continuing introduction of technologies designed to reduce exhaust emissions around the world, the contribution of non-exhaust emissions will only increase [9]. Exhaust and non-exhaust emissions exhibit different properties in terms of their size and chemical composition.

Particles directly emitted by vehicles are mostly carbonaceous in nature consisting of both elemental carbon and organic compounds and are found typically in the ultrafine mode [10]. Non-exhaust emissions also includes organic compounds but are distinguished by the emissions of metals such as Fe, Zn, Cu and Sb, which can act as tracers for the various vehicular sources [7] and are generally in the coarse particle mode [11]. Efforts to characterize the contributions of vehicle emissions to urban environments are discussed further in chapter 2. Due to the semi-volatile nature of the organic compounds emitted by vehicles, once they enter the atmosphere the emissions are quickly transformed by atmospheric processes into secondary organic aerosols (SOA) [12].

Organic aerosols (OA) are frequently the largest component of ambient fine particles in urban atmospheres (up to 90%) and as a result of better analysis techniques and modelling, secondary sources are increasingly being recognized as the main source over primary emissions ([13] and references therein). OA have a highly complex chemical composition with the number of organic compounds estimated to be between 10^4 and 10^5 [14] and consequently are not well understood. Reactions in the atmosphere transform the OA and the processes governing SOA formation are poorly understood [14]. SOA is actually an intermediate of the oxidation of primary emitted organic compounds and the gaseous product (CO_2) [13]. Thus the composition of

SOA is difficult to characterize as it undergoes continuous oxidation, however as shown in Chapter 2 the broad classes of OA can be distinguished using advanced multivariate techniques. The broad classes include hydrocarbon-like OA (HOA) and oxygenated OA (OOA). HOA is a surrogate for vehicle emissions while OOA can be considered as SOA. The OOA can be further deconvolved based upon differences in the level of oxidation and hence age [15]. As will be shown in Chapter 2, the majority of the research on the contributions and source profile of OOA have been conducted in the Northern Hemisphere [16] with little work done in the Southern Hemisphere. Different source influences on the composition of SOA are expected in Southern Hemisphere compared to the Northern Hemisphere [17] and thus warrants further investigation. Overall, the need to determine the different sources of OA and other ambient particles arises in part because of the adverse health effects associated with airborne particles.

Attention began to turn to the harmful health effects of air pollution after the Great Smog event in London during the winter of 1952. Up to four thousand deaths were directly attributed to the heavy smog that covered London for days due to the combination of extreme cold, which prompted a massive increase in burning coal for heating along with windless conditions failing to disperse the emissions [18]. This event, along with others, brought attention to the scientific community of the serious health effects that are associated with elevated levels of air pollution [19] and these health effects are discussed in more detail in chapter 2.

In addition to enabling the source apportionment of aerosols, the size and chemical composition are both thought to be the main influences on the toxicity of airborne

particles. Ambient particles, especially those with an aerodynamic diameter smaller than 2.5 μm ($PM_{2.5}$) are of serious public health concern with clear relationships established between $PM_{2.5}$ concentrations and increased incidences of cardiovascular disease [20] and lung cancer [21]. Particles of a different size have been found to have different health effects, with coarse and nano-particles more associated with respiratory and cardiovascular disease, respectively ([22] and references therein). The different health effects may be due in part to the different sites of deposition of larger and smaller particles in the lungs though the situation is more complex than this. Ultrafine particles are gaining increasing attention as they are thought to be the more harmful size fraction as they can penetrate deeper into the lungs [23] and to cause a greater inflammatory response in the lungs than larger particles of the same material [24]. One contributing factor to different health effects observed between coarser and finer particles may be due to the variation in the chemical composition.

The chemical composition is also thought to contribute to the harmful health effects owing to the presence of many toxic and carcinogenic compounds in ambient particles such as polycyclic aromatic hydrocarbons and heavy metals (Cd, Cr, Pb, and Ni). Transition metals frequently observed in ambient particles such as Ni, Cu, Cr, V and especially Fe can generate reactive oxygen species (ROS) in presence of cellular material and is thought to be one of mechanisms accounting for the detrimental health effects of aerosols [25]. However, as noted by Harrison et al. [26], airborne particles themselves may be inherently toxic and the chemical composition may not matter, though recent evidence would suggest otherwise [27]. In a recent review Chen and Lippmann [28] found evidence that ambient Ni, V, Pb and Zn had harmful health effects. Therefore to fully elucidate the potential health effects of

airborne particles, the size and chemical composition should both be characterized however the relative effect of both parameters is still under debate [26].

The more vulnerable sections of the community are especially susceptible to the harmful health effects of air pollutants and this includes children [29]. Children, owing to their immature immune systems and faster breathing rates, are susceptible to long term effects to the respiratory and cardiovascular health related to both long and short term exposure [29]. Children with long term exposure to vehicle emissions have increased risk of developing asthma [30] and higher incidences of wheezing [31]. One location where children spend a large amount of their day is school. Consequently schools represent an ideal location to monitor children's exposure to vehicle emissions. To properly assess children's exposure in schools, source identification along with quantitative estimations of their contributions is necessary; however there is limited literature on children's exposure to vehicle emissions and other sources in schools [32]. Thus, as outlined in the next section, several gaps in knowledge were identified in the literature related to chemical and physical properties of ambient particles and the sources of children's exposure at urban schools

1.1 GAPS IN KNOWLEDGE

Based upon an extensive review of the relevant literature the following gaps in knowledge were identified related to the sources of children's exposure at school and the potential toxicity of airborne particles based on their size and chemical composition.

- Composition and sources of OA in Southern Hemisphere cities, including Brisbane is unknown
- The extent of the mass spectral variation in the source profiles of OA across multiple sites in an urban area
- Toxicity and physical properties of vehicle emissions under 'real world' dilution effects in a tunnel and its relationship with traffic composition
- Concentration of vehicle emissions that children are exposed to at urban schools
- Contribution of local and school-related traffic to the levels of vehicle emissions at urban schools
- Variation in concentration of the different sources such as vehicle emissions during school hours
- Exposure assessment of children at school based upon the size and chemical composition of ambient particles at school and their relation to the potential toxicity

This research was designed to address these gaps in knowledge and provide significant and original contribution to the body of literature, as outlined by the research aims and objectives in the next section.

1.2 RESEARCH OBJECTIVES

This thesis sets out to address the gaps in knowledge outlined in the previous section by a systematic and comprehensive study of the physical and chemical characteristics of ambient particles in Brisbane, Australia. Children were identified in the literature as being highly susceptible to the harmful health effects related to airborne particles, particularly from vehicle emissions. In addition, schools are locations where children

experience a significant exposure to vehicle emissions and other urban sources. However, as literature on the sources that children are exposed to at schools and the driving factors are limited [32], schools were chosen as the location of study. Thus, the research problem tackled in this thesis is in regards to the sources that children are exposed to at school, the driving factors to the observed concentrations and potential toxicity of ambient particles.

The main aim of this research was to determine the sources of ambient fine particles that children are exposed to at urban schools based on the relevant analytical techniques identified in the literature (Chapter 3-8). With vehicle emissions being identified in the literature as a key source of ambient particles in an urban environment it was a focus of the thesis. A specific objective was to determine the concentrations of vehicle missions to which children were exposed and the driving factors, such as the contribution of local and school-related traffic (Chapter 4-7). Another objective was to examine the potential toxicity of vehicle emissions based upon the size and chemical composition and the contributing parameters (Chapter 3 and 5)

In Brisbane, the composition and sources of the OA, which comprises one of the largest components of ambient particles in urban atmospheres [13] is not known and thus another objective of this thesis was to address this by sampling at the schools. This enabled the contributions of primary and secondary sources at the schools to be determined (Chapters 4, 6-8). Another objective was to establish the diurnal variation in the OA and its source components at the schools to determine what children are actually exposed to during school hours and the variability in concentration (Chapter

6). Variability in the mass spectra of OA sources across the schools was examined as there is limited information in the literature on mass spectral variations due to the influence of local and regional sources within a city (Chapter 7). Finally, a novel methodology for the analysis of the OA mass spectral composition from samples collected on filters was tested and validated to further the scope and application of the AMS (Chapter 8).

To meet these aims and objectives the research methodology outlined in Figure 1-1 and in Section 1.3 was constructed.

1.3 RESEARCH METHODOLOGY

In Figure 1-1, the research plan sets out the work undertaken for this thesis, as a thesis by publication. Initially a thorough review of the literature revealed several gaps in knowledge as outlined in Section 1.1. With vehicle emissions identified in the literature as a major primary source in urban areas a pilot study on the Brisbane fleet was undertaken (Paper 1). In this study, on-road mobile measurements were conducted in a tunnel of the physical and oxidative potential of emitted particles. Measurements were conducted in a tunnel as it allows for a quantitative assessment of vehicle emissions under 'real world' dilution effects with minimal interference from other sources. Physical properties of the particles measured included particle number and $PM_{2.5}$ mass concentrations using a condensational particle counter and a DustTrak, respectively. The oxidative potential of the particles was measured using a new profluorescent nitroxide probe described in more detail in Paper 1, and is a measure of the potential toxicity of the particles (See Chapter 2). Thus the key parameters identified in this study were applied when assessing children's exposure at the schools.

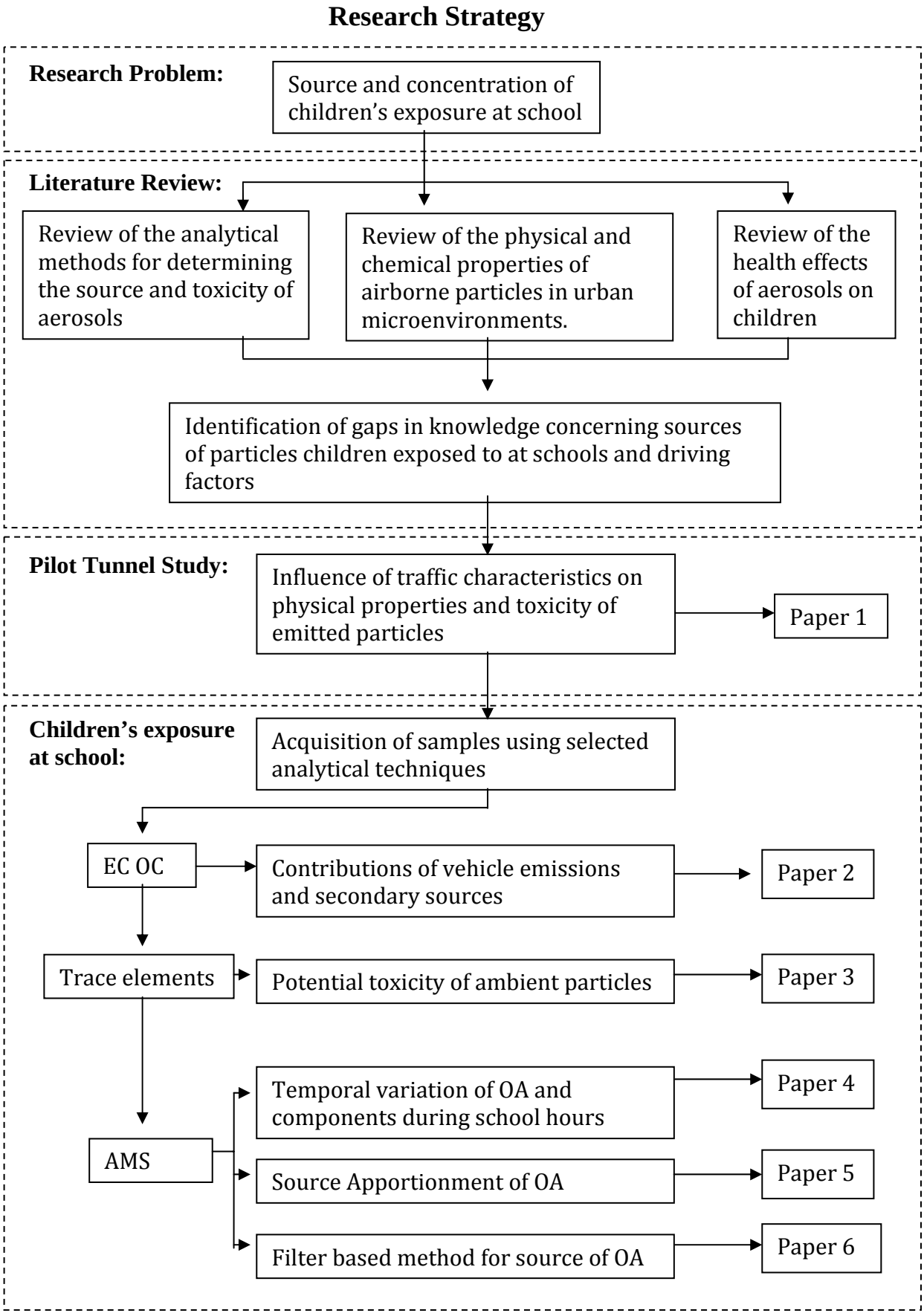

Figure 1-1: Flow diagram of the research process undertaken for this thesis.

The review of the literature revealed limited knowledge of children's exposure at urban schools, so the physical and chemical properties of fine particles were investigated at 25 schools within the Brisbane Metropolitan area. Chemical characterization of airborne fine particles by means of elemental carbon (EC), organic carbon (OC), trace elements and aerosol mass spectrometry were found in the literature to be an effective method for identifying the sources in urban environments. Thus, filter and aerosol mass spectrometry sampling was performed at the participating schools. Filter samples were taken at an outdoor location within each school that was determined to give the best overall exposure. Filters were taken on the same school days for one week at each school and sampled both PM_1 (mass concentration of particles with an aerodynamic diameter less than 1 μm) and $PM_{2.5}$ fractions (Papers 2, 3 and 6). The aerosol mass spectrometer sampled ambient air at 5 of the schools continuously for 2-3 weeks from an empty classroom nearby the outdoor filter sampling location (Papers 4-6).

All of the analytical techniques in this thesis were applied to the filters collected at the schools. EC and OC analysis was performed on the $PM_{2.5}$ samples according to the IMPROVE protocol on a thermal/optical transmittance carbon analyser (Paper 2). PM_1 samples were analysed for the trace elemental composition by Ion Beam analysis at the Australian Nuclear Science and Technology Organisation, Sydney (Paper 3). An Aerodyne time-of-flight aerosol mass spectrometer was used in this thesis. The high temporal resolution afforded by the AMS allowed for the variation in concentrations of OA and its source components at school to determine what children were exposed to during school hours (Papers 4 and 5). As the AMS only sampled at a subset of the participating schools, a novel methodology for the analysis

of OA collected on filters by AMS was validated. Thus it was subsequently applied to PM_1 filters samples from the remaining schools for source identification (Paper 6).

Advanced multivariate data analysis techniques were employed throughout this thesis in order to disentangle the multiple source contributions at both the pilot and schools study. On such techniques was principal component analysis (PCA), applied in papers 1, 2 and 3 to find the contributing sources and the relationships between the measured parameters and contributing factors. A particular focus was organic aerosols as it is frequently the largest component in urban environments and source apportionment was determined using positive matrix factorisation (PMF) (Paper 5). The PMF-derived source profiles were compared using cluster analysis. Another data analysis method employed in papers 4 and 6 to determine the sources of OA was tracer ions. These are specific m/z ions that have been shown to be surrogates for various OA components and enabled their relative contributions to be determined.

Overall, this research project resulted in the generation of six papers that have been published or submitted for publication as detailed in the next section.

1.4 LINKAGE OF PAPERS

The six papers each address one or more of the earlier outlined aims that seek to address the gaps in knowledge set out in Section 1.2. The first paper was a pilot study examining the relationships between traffic characteristics and physical and toxicity of particle emissions. This study indicated the significant parameters for assessing the children's exposure at school to vehicle emissions in the subsequent papers. The sources of the aerosols that children are exposed to at school were

investigated using a variety of analytical techniques and advanced data analysis techniques to probe different aspects of children's exposure. Thus a more complete picture of the contributing sources and the driving factors was achieved. While each paper investigated different facets of children's exposure at school, there were a number of similar findings through the papers, as demonstrated below in the main results and conclusions from each paper.

1.4.1 Concentration and oxidative potential of on-road particle emissions and their relationship with traffic composition: Relevance to exposure assessment

Aim: To determine the relationships between traffic composition and the physical characteristics and oxidative potential of vehicle emissions

On-road particle number count, fine particle mass ($PM_{2.5}$), CO, CO_2 and for the first time, particle associated reactive oxygen species (ROS) were measured using vehicle-based mobile sampling in a tunnel and an above-ground road. The profile of particle number and $PM_{2.5}$ concentration in the tunnel demonstrated relationships with both road gradient and tunnel ventilation. ROS levels in the tunnel were found to be high compared to an open road with similar traffic characteristics, which was attributed to the substantial difference in estimated emission dilution ratios on the two roadways. Overall, levels of pollutants and ROS were generally better correlated with total traffic count, rather than the traffic composition (i.e. diesel and gasoline-powered vehicles).

This study demonstrated that for exposure assessment to vehicle emissions, the total vehicle counts is a key parameter, not just heavy-duty vehicles as previously thought when considering the potential health effects.

1.4.2 Characterisation of carbonaceous aerosols at urban schools to determine the source of children's exposure

Aim: To determine the source of ambient carbonaceous aerosols in urban schools and the contributing factors to the observed concentrations

The concentration of organic carbon (OC) and elemental carbon (EC) was analysed at 25 schools in Brisbane, Australia. The concentration of primary and secondary OC was quantified using the EC tracer method. Both primary and secondary sources were present at the schools with secondary OC accounting for the majority of the OC. Multivariate techniques were able to distinguish the contribution of vehicle emissions and SOA at the schools from the urban background, two sources that contributed to higher exposure. At the schools, the concentration of vehicle emissions was primarily dependent on the total traffic counts on surrounding roads, with the wind direction relative to the surrounding roads the second most important factor. Schools with elevated SOC concentrations were found to be correlated with solar radiation levels indicating influence from photochemical SOA formation. The largest group of schools had concentrations that were indicative of the urban background.

While local meteorology affected the measured concentrations, overall the range of concentrations measured at these schools can be considered as representative of children's exposure to vehicle emissions and SOA at schools with similar traffic conditions.

1.4.3 Elemental composition of ambient fine particles in urban schools: sources of children's exposure

Aim: To assess the source contributions and potential toxicity of PM_1 at schools based upon the elemental composition.

Trace elemental composition of the PM_1 was analysed at 24 urban schools to determine the sources and toxicity. Five types of sources were identified using principal component analysis, which included secondary sulphate, biomass burning, vehicle, shipping and industrial emissions. Comparison of the concentrations of from this study to previous work on the elemental composition of the $PM_{2.5}$ in suburban and roadside site in Brisbane [33] revealed that the anthropogenic elements (V, Cr, Ni, Cu, Zn and Pb) were generally in the PM_1 fraction.

Thus as the toxic heavy metals were found predominantly in the PM_1 fraction it points to PM_1 being a potentially better parameter for investigating the health effects of airborne particles.

1.4.4 Aerosol Mass Spectrometric analysis of the chemical composition of non-refractory PM1 samples from school environments in Brisbane, Australia

Aim: To quantify the diurnal variation in the composition of organic aerosols during school hours.

An Aerodyne aerosol mass spectrometer sampled the non-refractory PM_1 (NR-PM_1) at five urban schools in Brisbane to assess the composition of organic aerosols during school hours. At each school the organic fraction comprised the majority of NR-PM_1 with secondary organic aerosols as the main constitute. At two of the schools, a

significant source of the organic aerosol (OA) was slightly aged vehicle emissions from nearby highways. More aged and oxidised OA was observed at three schools, which also recorded strong biomass burning influences. The diurnal cycle of OA concentration varied between schools but was generally found to be at a minimum during school hours. SOA were the major organic component that school children were exposed to within school hours. School drop off and pick up times represented the times of maximum exposure to primary OA for school children at school.

As a general conclusion from this study, unless a school is located near one or more major roads, children are predominantly exposed to regional secondary OA as opposed to local emissions during schools hours in urban environments.

1.4.5 First measurements of source apportionment of organic aerosols in the Southern Hemisphere.

Aim: Source apportionment of OA at multiple sites within a city to analyse the mass spectral variability in source profiles

PMF was applied to the AMS OA data to apportion the sources at 5 schools. The number of source factors identified at the sites varied from 2-4 and included contributions from HOA, biomass burning OA (BBOA) and OOA and its components. The main component at all of the sites was OOA, which accounted for 62-73% of the total OA mass. Similarities between the PMF derived sources at the sites were compared using cluster analysis and were grouped into primary OA (POA) and SOA. The POA cluster generally contained the HOA and BBOA factors whereas the SOA cluster included the OOA factors. The cluster analysis results indicated that the distinction between the OOA components differed between the schools, and was

only useful for distinguishing the OOA at a particular site. Within the POA cluster, the HOA factors were very similar between the sites, and the main source was vehicle emissions from surrounding roads. BBOA was identified during at three locations sampled during winter when controlled burning is prevalent.

Thus cluster analysis was able to give meaningful groups of the different PMF derived factors. In addition, the apparent lack of spatial variation indicates that PMF-derived factors from a receptor site is applicable across an urban area

1.4.6 Analysis of organic aerosols collected on filters by Aerosol Mass Spectrometry for source identification

Aim: Determine the source of OA in urban schools using a novel method for the analysis of filters by aerosol mass spectrometry

An AMS was deployed at 5 urban schools to determine the sources of the organic aerosols at the schools directly. PM_1 aerosols were also collected on filters at these and 20 other urban schools. The filters were extracted with water and the extract run through a nebulizer to generate the aerosols, which were analysed by an AMS. The mass spectra from the samples collected on filters at the 5 schools were found to have excellent correlations with those obtained directly by AMS, with r^2 ranging from 0.89 to 0.98. Filter recoveries varied between the schools from 40 -115%, possibly indicating that this method provides qualitative rather than quantitative information. The stability of the organic aerosols on Teflon filters was demonstrated by analysing samples stored for up to two years. Application of the procedure to the remaining 20 schools showed that secondary organic aerosols were the main source of aerosols at the majority of the schools.

Overall, this procedure provides accurate representation of the mass spectra of ambient organic aerosols and could facilitate rapid data acquisition at multiple sites where AMS could not be deployed for logistical reasons.

1.5 IMPLICATIONS OF THE RESULTS

The research conducted as a part of this thesis has resulted in the generation of new knowledge related to the sources and potential toxicity of airborne particles at urban schools, based upon their physical and chemical characteristics. Total traffic counts rather than the traffic composition were identified in the pilot tunnel study and at the schools, as a key parameter in determining the levels and toxicity of vehicle emissions. PM_1 fraction was found to potentially have a greater toxicity than $PM_{2.5}$, suggesting it may be a better parameter to use in studies examining the health effects of airborne particles. However, further work is required to validate both of these hypotheses.

Using advanced multivariate data analysis techniques, the contributions of both vehicle emissions and secondary sources to children's exposure were shown to vary between the schools. In general, the levels of vehicle emissions at schools were principally dependent on total traffic counts on surrounding roads. Maximum exposure to vehicle emissions for children at school occurred during school drop off/pick up times and indicates where future control strategies should be focused in order to limit children's exposure.

Overall, during school hours the children were exposed predominantly to SOA as opposed to fresh vehicle emissions. The source of the SOA at the schools was found to range from slightly aged vehicle emissions to highly oxidised regional OA, however the methods employed to discriminate between the different types of SOA could be improved. Thus future work could focus on better chemical characterisation of SOA, which would allow for better classification of local and regional secondary sources. In addition, SOA is likely to have different health effects to vehicle emissions as a result of the differing chemical composition, and requires further work to specifically investigate the health effects of SOA.

The results from this thesis give a quantitative estimate of the range of concentrations of vehicle emissions and SOA that children are exposed to at urban schools with different traffic conditions. This study is part of a larger study investigating the effects of ultrafine particles from traffic emissions on children's health. Therefore the results from this thesis will be integrated with other air quality parameters measured at the participating schools to gain a holistic picture of children's exposure to vehicle emissions and other sources. This will then be evaluated, alongside health data collected from children at the tested schools, to try and quantify the health risks associated with long term exposure to vehicle emissions.

1.6 REFERENCES

1. Seinfeld, J. H.; Pandis, S. N., *Atmospheric chemistry and physics: From air pollution to climate change*. 2nd ed.; John Wiley and Sons: 2006.
2. Kanakidou, M.; Seinfeld, J. H.; Pandis, S. N.; Barnes, I.; Dentener, F. J.; Facchini, M. C.; Van Dingenen, R.; Ervens, B.; Nenes, A.; Nielsen, C. J.; Swietlicki, E.; Putaud, J. P.; Balkanski, Y.; Fuzzi, S.; Horth, J.; Moortgat, G. K.; Winterhalter, R.; Myhre, C. E. L.; Tsigaridis, K.; Vignati, E.; Stephanou, E. G.; Wilson, J., Organic aerosol and global climate modelling: a review. *Atmos. Chem. Phys.* **2005,** *5*, (4), 1053-1123.
3. Baron, P. D.; Willeke, K., *Aerosol Measurement: Principles, techniques and applications*. 2nd ed.; Wiley-Interscience: 2001.
4. Sullivan, R. C.; Prather, K. A., Recent Advances in Our Understanding of Atmospheric Chemistry and Climate Made Possible by On-Line Aerosol Analysis Instrumentation. *Anal. Chem.* **2005,** *77*, (12), 3861-3886.
5. Lee, S. C.; Cheng, Y.; Ho, K. F.; Cao, J. J.; Louie, P. K.-K.; Chow, J. C.; Watson, J. G., PM1.0 and PM2.5 Characteristics in the Roadside Environment of Hong Kong. *Aerosol Sci. Technol.* **2006,** *40*, (3), 157 - 165.
6. Morawska, L.; Ristovski, Z.; Jayaratne, E. R.; Keogh, D. U.; Ling, X., Ambient nano and ultrafine particles from motor vehicle emissions: Characteristics, ambient processing and implications on human exposure. *Atmos. Environ.* **2008,** *42*, (35), 8113-8138.
7. Thorpe, A.; Harrison, R. M., Sources and properties of non-exhaust particulate matter from road traffic: A review. *Sci. Total Environ.* **2008,** *400*, (1-3), 270-282.
8. Querol, X.; Alastuey, A.; Ruiz, C. R.; Artiñano, B.; Hansson, H. C.; Harrison, R. M.; Buringh, E.; ten Brink, H. M.; Lutz, M.; Bruckmann, P.; Straehl, P.; Schneider, J., Speciation and origin of PM10 and PM2.5 in selected European cities. *Atmos. Environ.* **2004,** *38*, (38), 6547-6555.
9. Harrison, R. M.; Jones, A. M.; Gietl, J.; Yin, J.; Green, D. C., Estimation of the Contributions of Brake Dust, Tire Wear, and Resuspension to Nonexhaust Traffic Particles Derived from Atmospheric Measurements. *Environ. Sci. Technol.* **2012,** *46*, (12), 6523-6529.
10. Kleeman, M. J.; Schauer, J. J.; Cass, G. R., Size and Composition Distribution of Fine Particulate Matter Emitted from Motor Vehicles. *Environ. Sci. Technol.* **2000,** *34*, (7), 1132-1142.
11. Minguillón, M. C.; Querol, X.; Baltensperger, U.; Prévôt, A. S. H., Fine and coarse PM composition and sources in rural and urban sites in Switzerland: Local or regional pollution? *Sci. Total Environ.* **2012,** *427–428*, (0), 191-202.
12. Robinson, A. L.; Donahue, N. M.; Shrivastava, M. K.; Weitkamp, E. A.; Sage, A. M.; Grieshop, A. P.; Lane, T. E.; Pierce, J. R.; Pandis, S. N., Rethinking organic aerosols: Semivolatile emissions and photochemical aging. *Science* **2007,** *315*, 1259-1262.
13. Jimenez, J. L.; Canagaratna, M. R.; Donahue, N. M.; Prevot, A. S. H.; Zhang, Q.; Kroll, J. H.; DeCarlo, P. F.; Allan, J. D.; Coe, H.; Ng, N. L.; Aiken, A. C.; Docherty, K. S.; Ulbrich, I. M.; Grieshop, A. P.; Robinson, A. L.; Duplissy, J.; Smith, J. D.; Wilson, K. R.; Lanz, V. A.; Hueglin, C.; Sun, Y. L.; Tian, J.; Laaksonen, A.; Raatikainen, T.; Rautiainen, J.; Vaattovaara, P.; ehn, M.; Kulmala, M.; Tomlinson, J.; Collins, D. R.; Cubison, M. J.; Dunlea, E. J.; Huffman, A.; Onasch, T. B.; Alfarra, M. R.; Williams, P. I.; Bower, K. N.; Kondo, Y.; Schneider,

J.; Drewnick, F.; Borrmann, S.; Weimer, S.; Demerjian, K. L.; Salcedo, D.; Cottrell, L.; Griffin, R.; Takami, A.; Miyoshi, T.; Hatakeyama, S.; Jayne, J. T.; Herndon, S. C.; Trimborn, A.; Williams, L. R.; Wood, E. C.; Middlebrook, A.; Kolb, C. E.; Baltensperger, U.; Worsnop, D. R., Evolution of Organic Aerosols in the Atmosphere *Science* **2009,** *326*, 1525-1529.
14. Goldstein, A. H.; Galbally, I. E., Known and unexplored organic constituents in the Earth's atmosphere. *Environ. Sci. Technol.* **2007,** *41*, (5), 1514-1521.
15. Lanz, V. A.; Alfarra, M. R.; Baltensperger, U.; Buchmann, B.; Hueglin, C.; Prévôt, A. S. H., Source apportionment of submicron organic aerosols at an urban site by factor analytical modelling of aerosol mass spectra. *Atmos. Chem. Phys.* **2007,** *7*, (6), 1503-1522.
16. Ng, N. L.; Canagaratna, M. R.; Zhang, Q.; Jimenez, J. L.; Tian, J.; Ulbrich, I. M.; Kroll, J. H.; Docherty, K. S.; Chhabra, P. S.; Bahreini, R.; Murphy, S. M.; Seinfeld, J. H.; Hildebrandt, L.; Donahue, N. M.; DeCarlo, P. F.; Lanz, V. A.; Prévôt, A. S. H.; Dinar, E.; Rudich, Y.; Worsnop, D. R., Organic aerosol components observed in Northern Hemispheric datasets from Aerosol Mass Spectrometry. *Atmos. Chem. Phys.* **2010,** *10*, (10), 4625-4641.
17. Spracklen, D. V.; Jimenez, J. L.; Carslaw, K. S.; Worsnop, D. R.; Evans, M. J.; Mann, G. W.; Zhang, Q.; Canagaratna, M. R.; Allan, J.; Coe, H.; McFiggans, G.; Rap, A.; Forster, P., Aerosol mass spectrometer constraint on the global secondary organic aerosol budget. *Atmos. Chem. Phys.* **2011,** *11*, (23), 12109-12136.
18. Stone, R., Counting the cost of London's killer smog. *Science* **2002,** *298*, (5601), 2106-7.
19. Bell, M.; Davis, D.; Fletcher, T., A Retrospective Assessment of Mortality from the London Smog Episode of 1952: The Role of Influenza and Pollution. In *Urban Ecology*, Marzluff, J.; Shulenberger, E.; Endlicher, W.; Alberti, M.; Bradley, G.; Ryan, C.; Simon, U.; ZumBrunnen, C., Eds. Springer US: 2008; pp 263-268.
20. Brook, R. D.; Rajagopalan, S.; Pope, C. A.; Brook, J. R.; Bhatnagar, A.; Diez-Roux, A. V.; Holguin, F.; Hong, Y.; Luepker, R. V.; Mittleman, M. A.; Peters, A.; Siscovick, D.; Smith, S. C.; Whitsel, L.; Kaufman, J. D., Particulate Matter Air Pollution and Cardiovascular Disease: An Update to the Scientific Statement From the American Heart Association. *Circulation* **2010,** *121*, (21), 2331-2378.
21. Pope, C.; Burnett, R. T.; Thun, M. J.; Calle, E. E.; Krewski, D.; Ito, K.; Thurston, G. D., Lung cancer, cardiopulmonary mortality, and long-term exposure to fine particulate air pollution. *J. Am. Med. Assoc.* **2002,** *287*, (9), 1132-1141.
22. Beddows, D. C. S.; Dall'Osto, M.; Harrison, R. M., Cluster Analysis of Rural, Urban, and Curbside Atmospheric Particle Size Data. *Environ. Sci. Technol.* **2009,** *43*, (13), 4694-4700.
23. Kreyling, W.; Semmler-behnke, M.; Moller, W., Ultrafine particle-lung interactions: Does size matter? *J. Aerosol Med.* **2006,** *19*, (1), 74-83.
24. Donaldson, K.; Brown, D.; Clouter, A.; Duffin, R.; MacNee, W.; Renwick, L.; Tran, L.; Stone, V., The pulmonary toxicology of ultrafine particles. *J. Aerosol Med.* **2002,** *15*, (2), 213-220.
25. Knaapen, A.; Shi, T.; Borm, P.; Schins, R., Soluble metals as well as the insoluble particle fraction are involved in cellular DNA damage induced by particulate matter. *Mol. Cell. Biochem.* **2002,** *234-235*, (1), 317.
26. Harrison, R. M.; Smith, D. J. T.; Kibble, A. J., What is responsible for the carcinogenicity of PM2.5? *Occup. Environ. Med.* **2004,** *61*, (10), 799-805.

27. Lippmann, M.; Chen, L.-C., Health effects of concentrated ambient air particulate matter (CAPs) and its components. *Crit. Rev. Toxicol.* **2009,** *39*, (10), 865-913.
28. Chen, L. C.; Lippmann, M., Effects of Metals within Ambient Air Particulate Matter (PM) on Human Health. *Inhal. Toxicol.* **2009,** *21*, (1), 1-31.
29. Rückerl, R.; Schneider, A.; Breitner, S.; Cyrys, J.; Peters, A., Health effects of particulate air pollution: A review of epidemiological evidence. *Inhal. Toxicol.* **2011,** *23*, (10), 555-592.
30. Gehring, U.; Wijga, A.; Brauer, M.; Fischer, P.; de Jongste, J.; Kerkhof, M.; Oldenwening, M.; Smit, H.; Brunekreef, B., Traffic-related Air Pollution and the Development of Asthma and Allergies during the First 8 Years of Life. *Am. J. Resp. Crit. Care* **2010,** *181*, (6), 596-603.
31. Ryan, P. H.; Bernstein, D. I.; Lockey, J.; Reponen, T.; Levin, L.; Grinshpun, S.; Villareal, M.; Khurana Hershey, G. K.; Burkle, J.; LeMasters, G., Exposure to Traffic-related Particles and Endotoxin during Infancy Is Associated with Wheezing at Age 3 Years. *Am. J. Resp. Crit. Care* **2009,** *180*, (11), 1068-1075.
32. Mejía, J. F.; Choy, S. L.; Mengersen, K.; Morawska, L., Methodology for assessing exposure and impacts of air pollutants in school children: Data collection, analysis and health effects – A literature review. *Atmos. Environ.* **2011,** *45*, (4), 813-823.
33. Friend, A. J.; Ayoko, G. A.; Stelcer, E.; Cohen, D., Source apportionment of PM2.5 at two receptor sites in Brisbane, Australia. *Environ. Chem.* **2011,** *8*, (6), 569-580.

Chapter 2. Literature Review

2.1 INTRODUCTION

Atmospheric particles are a complex mixture of chemical compounds with a size range across several orders of magnitude ranging from 10 nm to larger than 10 μm in diameter [1]. As a result, the size of airborne particles is conventionally grouped into coarse, fine, ultrafine and nano particle size fractions based on the particles aerodynamic diameter (D_p). These fractions are defined as: the coarse fraction is 2.5 μm < 10μm, the fine fraction is < 2.5 μm, ultrafine are < 0.1 μm and nanoparticles are < 50 nm. This convention for the names of particle size fractions is followed throughout this chapter unless otherwise noted. Particles with different size fractions might differ not only in size and morphology but also in sources, formation mechanisms and chemical and physical properties [2].

Ambient particles are produced by both anthropogenic and natural sources, resulting in a high chemical complexity of ambient particles. The chemical compounds present include both inorganic and organic compounds such as metals, elemental carbon and ions such as sulphate, ammonium and nitrate and numerous organic compounds. In an urban environment, organic aerosols are frequently one of the largest components of fine particles accounting for up to 90% of the PM_1 (D_p < 1 μm) [3] and references therein). The number of organic compounds present in the atmosphere has been estimated to be between 10^4 and 10^5 and as such the chemical composition of the organic particles in urban areas is poorly understood [4]. Common primary sources of ambient particles in urban areas include industrial, biomass burning and vehicle emissions.

Vehicle emissions have been shown to be a major source of pollution in urban environments (See e.g. [5-7]) and there are growing concerns over the adverse effects of vehicle emissions to the air quality of urban environments. As a consequence, vehicle emissions are a feature of this review. Thomas and Morawska [8] found for that the main contributors to PM_{10} ($D_p < 10$ μm) mass in urban air in Brisbane were elements of natural origin. In the $PM_{2.5}$ ($D_p < 2.5$ μm) the elements found were mostly anthropogenic in origin with by far the biggest source being vehicle emissions. The majority of vehicle exhaust emissions are in the fine fraction (see e.g. [9-11]), an observation that has important implications for assessing the exposure to vehicle emissions.

A popular method for investigating the physical and chemical characteristics of vehicle emissions is to conduct measurements in road tunnels and this approach has both advantages and disadvantages. In road tunnels, the vehicle emissions sampled undergo 'real world' dilution and are considered representative of freeway emissions. Vehicle flows and traffic composition can be precisely defined in a tunnel making it possible to quantitatively determine the average of the local fleet and the contribution of heavy-duty vehicles (HDV) and light duty vehicles (LDV) [12]. This review will highlight previous research in quantifying the particle emissions from vehicles by size fraction and by vehicle type.

Particulate phase vehicle emissions are composed mainly of carbonaceous aerosols [11] which can be differentiated into either elemental carbon (EC) or organic carbon (OC) [13]. EC is formed by incomplete combustion of fuel and is similar to pure

graphite but with a more complex three-dimensional structure that is mostly carbon [14]. EC is emitted from primary sources only and is not formed in the atmosphere, with diesel engines being one of the main sources of EC in urban areas [15]. OC in vehicle emissions is a complex mixture of hundreds of organic compounds which have not all been identified [16]. OC is emitted by both primary sources such as vehicles and also formed in the atmosphere by the reaction of gaseous organic compounds [17]. Therefore the ratio of OC to EC can be used to identify and quantify the source contribution to carbonaceous aerosols in the atmosphere. As will also be shown in this review, the ratio of OC/EC is particularly useful in source identification and apportionment of vehicle emissions and secondary organic aerosols in urban atmospheres.

Other than organic species, there are trace elements present in the atmosphere from a variety of anthropogenic and biogenic sources. Though these elements are present at only trace amounts, the particle elemental composition is useful for source identification as there are characteristic elements associated with the different sources. For example, vehicles emission contain a wide range of trace metals as a result of both exhaust and non-exhaust process such as vehicle wear and these include S, V, Mn, Fe, Ni, Cu, Zn, Sb, Ba and Pb [18, 19]. However there are limitations to using the trace elemental composition of ambient aerosols to determine the source identification and contribution due to traffic emissions and other sources due to their multiple anthropogenic and natural sources [19]. However, this review will show that the careful analysis of the ambient trace elemental composition can reveal information on the contributions by vehicles and other sources in urban environments.

One of the more significant advances in aerosol science in the past 20 years has been the development of aerosol mass spectrometers [20]. An aerosol mass spectrometer analyses the particle size and chemical composition of aerosols in situ at the sampling site with a high temporal resolution [21]. As such, this chapter will demonstrate how aerosol mass spectrometers are a powerful tool for investigating the sources of fine particles, particularly organic aerosols in urban environments. Aerosol mass spectrometers have been used extensively in the analysis of organic aerosols and this review will outline the successful techniques' employed for the source apportionment of secondary organic aerosols, vehicle emissions and biomass burning.

Finally, a brief review of the potential health effects of ambient particles and how the detrimental respiratory, cardiovascular and neurological effects are related to both the size and chemical composition is presented. One measure of the toxicity of the airborne particles is concentration of reactive oxygen species (ROS) which act as a measure of the oxidative potential. ROS cause oxidative stress on cellular material and consequently the health effects of airborne particles are thought to be due at least in part to the ROS [22] and are covered in this review. A number of elements emitted by vehicles, such as Pb, Mn, and Ni are considered toxic by the U.S.A. Environment Protection Agency (EPA) [23] and are thus also potentially contributing to the toxicity of airborne particles [24] however their role is not fully understood. The size of the airborne particles is thought to play a key role in the health effects, with smaller particle being more toxic than larger particles as they can penetrate deeper into the lungs [25]. Children are more susceptible to the detrimental respiratory and

neurological effects of airborne particles and research detailing the link is featured, particularly relating to traffic related air pollution in urban areas.

2.2 MEASUREMENTS OF VEHICLE EMISSIONS IN ROAD TUNNELS

Two main methods that have been employed in the literature to investigate vehicle emissions are measurements with a dynamometer and in a tunnel (e.g. [26]). Dynamometer studies can be carried out using different driving cycles under controlled engine load and speed conditions and so can offer accurate measurements of characteristics of vehicle exhaust emissions. However, normally only a small number of vehicles are tested on a dynamometer study as they are time-consuming and costly to conduct. In contrast, measurements in tunnels provide opportunities to measure the average of emission profiles of thousands of vehicles and are measured under real world dilution with minimal interference from other sources. Unlike dynamometer studies, which generally focus on just exhaust emissions, particles sampled in tunnel studies capture not just tailpipe emissions but the full range of vehicle emissions, including tyre and brake wear. Although tunnel measurements do not measure emissions over a full engine cycle, they are considered characteristic of freeway emissions [12]. This is also a disadvantage of tunnel studies as it is difficult to generalize the data to other driving conditions. Therefore tunnel studies offer several advantages over dynamometer studies.

Tunnel studies can provide comparable results to a dynamometer studies provided they are carefully designed, as demonstrated by Jamriska et al. [26]. Jamriska et al. [26] studied bus emissions in a tunnel and found that the particle number and mass emission factors were in reasonable agreement with a dynamometer study on a sample of buses from the same fleet. As a tunnel study is cheaper and simpler to

undertake compared to a dynamometer study, they have become a preferred method to measure vehicle emissions [27]. This section will examine previous measurements using road tunnels, to determine particle number and mass emissions from vehicles and the driving factors. Measurements of elemental carbon, organic carbon and trace elements emissions from vehicles using road tunnels will be covered in Sections 2.3.2 and 2.4.1.

2.2.1 Particle number concentration

Due to the lack of dilution, the particle number concentration (PNC) within a road tunnel can be an order of magnitude greater compared to an open road carrying a similar traffic volume [28]. The M5 east tunnel in Sydney has reported some of the highest average PNC in tunnels at $6.0x10^{6}$ particles cm^{-3} [28]. By comparison, Gidhagen et al. [29] noted an average of $7.6x10^{5}$ particles cm^{-3} in a Swedish tunnel and Kirchstetter et al. [30] found an average $4.0x10^{5}$ particles cm^{-3} in the Caldecott tunnel, San Francisco. Thus the wide range of PNC reported in the literature indicates that there are a number of factors driving the number concentration of particles emitted by vehicles.

A significant parameter in determining PNC is traffic composition. Recently, HDV traffic volume was shown to be a better predictor of ultrafine PNC compared to gasoline vehicles in the M5 east tunnel [28]. Similarly in the Caldecott tunnel, heavy duty diesel vehicles (HDDV) was found to emit 15-20 times the number of particles compared to LDV [30]. PNC was determined by size fraction in the Caldecott tunnel and it was found that HDV emit more larger particles than LDV, by a factor of 10 for particles larger than 180 nm [31]. Gighagen et al. [29] constructed a model of particle number concentrations in a tunnel in Sweden and found a larger contribution

from LDV compared to results by Kirchstetter et al. [30] with the variation explained by vehicle speed dependent factors. Therefore, while the traffic composition can be an important variable in determining the PNC, it is not the only one and its contribution to the air quality in tunnels is still uncertain.

In addition to the traffic composition, the gradient of the road will also affect the PNC in a tunnel. In the only study to date to have measured this effect, the ascending bore of a tunnel had a higher mean particle number concentration compared to the descending bore [32]. In both bores of this tunnel, the PNC profiles had a decrease for the first 200m followed by a constant increase towards the exit. Gouriou et al. [32] suggested that this dip was due to the piston effect, whereby vehicles entering the tunnel bringing fresh air with them that diluted the emissions. Thus the gradient of the road may be a significant determinant of on-road PNC however this is yet to be fully explored.

2.2.2 Particle mass concentrations

In the same respect as PNC, the concentration of particles by mass emitted by a fleet of vehicles is also affected by the traffic composition and tunnel gradient. $PM_{2.5}$ mass concentration is found to be mainly controlled by vehicle fleet composition, changes in the number of diesel vehicle having the biggest impact [33, 34]. To illustrate this, Table 2-1 lists the $PM_{2.5}$ mass emission factors calculated from various tunnels studies around the world with varying proportions of HDV. From Table 2-1, HDV have been found to emit far more $PM_{2.5}$ mass compared to LDV as Grieshop et al. [35] found that HDDV emitted 25-40 times more $PM_{2.5}$ mass compared to LDV, for example. In road tunnels with a similar HDV percentage and traffic count, the emission factors for $PM_{2.5}$ mass were found to be similar (Table 2-1) [23, 27].

Table 2-1: Comparison of tunnel mean particle mass and HDV and LDV $PM_{2.5}$ emission factors (mg veh^{-1} km^{-1}) for tunnel sites around the world.
[a] Represents $PM_{1.9}$,[b, c] values for descending and ascending bores, respectively. N/A – not available.

Tunnel Location	Reference	% HDV	Tunnel Mean	HDV	LDV
Shing Mun, Hong Kong	[34]	30 - 60	131 ± 37	257±31	167
Howell, Milwaukee	[23]	1.5 - 9.4	33 ± 5	N/A	N/A
Caldecott, San Francisco	[37]	N/A	N/A	430 ± 79[a]	4[a]
Woolloongabba, Brisbane	[26]	100	N/A	267 ± 207	N/A
Zhujiang, Guangzhou	[33]	19.8	110 ± 4	267 ± 56	52 ± 15
Chung-Liao, Taiwan	[27]	8	38 ± 11	N/A	N/A
Kaisermuhlen, Vienna	[38]	9.6	26 ± 10	N/A	N/A
Squirrel Hill, Pittsburgh	[35]	19 ± 2	158 ± 29	N/A	N/A
Hsuehshan Tunnel, Taiwan	[36]	0	45 ± 22[b] 62 ± 23[c]		2 ± 2[b] 4 ± 3[c]

The diurnal variation of $PM_{2.5}$ mass and diesel vehicle has been shown to be similar [34] which is a further indication of the large impact that diesel vehicles have on

particle mass concentrations. $PM_{2.5}$ mass concentrations are also affected by the road gradient, as shown in one study (Table 2-1) where the ascending bore had a higher overall mass concentration and twice the calculated emission factors compared to the descending section [36]. Therefore it can be concluded that the main contributor to the $PM_{2.5}$ mass concentration encountered in a tunnel is the traffic composition, specifically the proportion of HDV and the gradient of a road.

In the Caldecott tunnel, San Francisco there have been a series of studies that looked at the emission factors for HDV and LDV and the results are summarised in Table 2-2 to illustrate the change over time in vehicle emissions. $PM_{2.5}$ mass emissions have dropped by 37% for LDV and 60% for HDV between the work reported by Kirchstetter et al. [30] and Geller et al. [31]. This decrease could be attributed to more fuel efficient engines across the fleet and the use of more efficient diesel engine emission controls [31]. In contrast to the decrease found for the particle mass emissions the PNC emission were found to increase by a factor of 540% for LDV and 30% for HDV. As newer engines emit less carbonaceous particulate matter, there is less surface area for the semi-volatile compounds emitted to condense on. This results in an excess of semi-volatile material that condenses homogeneously, producing large numbers of nanoparticles. However the main reason was likely to be the introduction of catalytic after treatment devices which are known to increase nucleation [31]. Thus from these two case studies, it can be seen that vehicle emissions in terms of particle number and mass concentration have changed over time as a result of changing engine technologies indicating the need for continuing measurements to stay up to date on vehicle emissions.

Table 2-2: Comparison of emission factors for $PM_{2.5}$ mass and particle number per kg of fuel burned in the Caldecott tunnel (Adapted from Geller et al. [31]).
[a] Represents $PM_{1.9}$. N/A – not available.

Vehicle Type	Reference	$PM_{2.5}$ (mg kg^{-1})	Particle number (# kg^{-1})
LDV	[30]	110 ± 10	(4.6±0.7) $x10^{14}$
LDV	[37]	70 ± 50 [a]	N/A
LDV	[31]	70 ± 20	(2.5±1.4) $x10^{15}$
HDV	[30]	$2.5x10^{3}$ ± 200	(6.3±1.9) $x10^{15}$
HDV	[37]	$1.285x10^{3}$ ± 200 [a]	N/A
HDV	[31]	$1.02x10^{3}$ ± 40	(8.2±2.5) $x10^{15}$

2.2.3 On-road studies on open road

There have been studies that have measured on-road, and in real time, pollutant concentrations using a mobile laboratory and a brief review is included here as a comparison to the tunnel work. In one study, the on-road concentration ranged from 10^4 and 10^6 particles cm^{-3} [39], with the freeways having the highest ultrafine PNC, which can be an order of magnitude higher than ambient [40, 41]. Average on-road concentrations of PNC and $PM_{2.5}$ mass on freeways and residential streets vary according to location, road type and truck traffic volumes [40]. The main driving factor for the PNC on the freeways was the number of HDV [41], as the concentration increased as HDV traffic increased [39, 40]. On the arterial roads it was the proximity to LDV undergoing hard acceleration that seemed to be the main factor for the PNC encountered [41]. In contrast to PNC, the $PM_{2.5}$ mass showed less variation according to location and road type but was impacted more by specific encounters with high emitting vehicles [40]. Vehicle speed has also been shown to

contribute to increased emissions, with higher vehicle speeds found to increase the PNC [39]. From these case studies using on-road measurements, the traffic composition, specifically HDV count has been shown to be significant factor in determining the on-road particle concentrations.

2.3 REACTIVE OXYGEN SPECIES

Reactive oxygen species (ROS) refers to free radicals such as hydroxyl ($OH^{\cdot}$), peroxyl ($HOO^{\cdot}$, $ROO^{\cdot}$), ions such as superoxide ($O_2^{-\cdot}$), peroxynitrite ($ONOO^{-}$) and molecules such as hydrogen peroxide (H_2O_2) and hydroperoxides (ROOH). The precursors to ROS include carbon-centred radicals can also be considered as ROS [42]. While there is still some debate over exactly which chemical components in particles are responsible for the generation of ROS, it has been shown that transition metals such as nickel, copper, chromium, vanadium and especially iron [43, 44] are involved. Pro-oxidative hydrocarbons such as polycyclic aromatic hydrocarbons and quinones are also thought to be involved in producing ROS in particles [45]. Recent attention has turned to particle associated ROS in ambient particles owing to their potential health effects.

The adverse health effects of airborne particles are generally thought to be a result of the particles containing or generating ROS and causing oxidative stress at the deposition site [22, 45, 46]. An important factor in determining the ROS levels is the particle size, with ambient ultrafine particles found to have higher ROS activity compared to fine and coarse particles [45]. Particle size is also relevant to the amount of oxidative stress generated, with smaller particles being able to penetrate further into the tissue. The result of the oxidative stress caused by ROS in airborne particulate matter can cause damage to cellular proteins, lipids, and DNA [22]. As

such chemical methods have been developed for detecting ROS, with the two main methods utilised in the study of vehicle emissions; the BPEAnitprobe and the DiThioThreitol (DTT) assay discussed in more detail in the following two sections.

2.3.1 BPEAnit probe

The BPEAnit probe is a profluorescent nitroxide probe for detection of particle based ROS [42, 47]. This probe contains 9,10-bis(phenylethynyl)anthracene (BPEA) fluorophore covalently linked to a 5-membered nitroxide-containing ring and has been given the acronym BPEAnit [47]. When this compound undergoes reduction or oxidation it becomes fluorescent and the fluorescent spectrum can be analysed to determine the concentration of ROS.

Dynamometer studies have utilised the BPEAnit probe to determine the parameters affecting the concentration of ROS emitted from diesel engines [48-50]. Diesel engine type and diesel fuel composition had more impact on the emitted ROS levels than the engine load and speed [49]. However, the engine load will effect particle associated ROS concentrations, with increasing concentrations observed with decreasing engine load [50]. The injection system used in a diesel engine has a marked effect on ROS concentrations, with the common rail injection resulting in 16 fold increase compared to a direct injection run on ultra-low sulphur diesel (ULSD) [49].

Recent research has focused on the affect of the diesel fuel composition on the oxidative potential of diesel emissions. For a direct injection system, significant differences were noticed in the emitted ROS levels between ULSD, a synthetic diesel blend, a 20% biodiesel blend made with cooking oil (B20) [49]. ULSD had the

lowest emitted ROS levels followed by the synthetic diesel with the B20 fuel having twice the concentration compared to ULSD. For the same direct injection engine as in Surawski et al. [49], the type of feedstock (soy, tallow and canola) in the biodiesel however has been observed to have little effect on the ROS concentration relative to ULSD [48]. However, increasing the percentage of all three feed stocks in the biodiesel from 20% to 80% resulted in around a 9-fold increase in ROS emissions [48]. This trend was also observed for a similar diesel engine fitted with ethanol fumigation technology, with the increasing levels of ethanol fumigation resulting in increased levels of particle related ROS [50]. Therefore, these studies have shown that the particle associated ROS levels in diesel exhaust are dependent on a number of parameters related to the type of engine and fuel.

2.3.2 DTT assay

Another analytical technique that has been used to measure the ROS of vehicle particulate emissions is the dithiothreitol (DTT) assay developed and described by Kumagai et al. [51]. In this assay the DTT acts a reducing agent in a similar fashion to biological reductants like glutathione due to the presence of thiol functional groups. The decay rate of DTT in aqueous solutions has been correlated with the levels of oxidative stress in cellular systems. After the reaction is completed the resultant solution is analysed using ultraviolet-visible absorption spectrometry. This assay is a simple and biologically relevant technique for measuring the toxicity of particles due to its redox activity [52]. However it is an indirect technique for measuring ROS concentrations unlike the BPEAnit probe. The DTT assay has been utilised to analyse the redox activity of vehicle emissions in measurements on a dynamometer [53-55] and to assess the health risks related to ambient particle exposure [56, 57].

2.3.2.1 ***Ambient measurements of redox activity using DTT assay***

The redox activity of ambient particles was analyzed at urban sites within the Los Angeles basin to determine the characteristics of redox activity in ambient particles [56, 57]. ROS levels were found to vary across the ultrafine (D_p <150 nm), fine and coarse fractions, with the highest redox activity found in the ultrafine particles [56]. Verma et al. [57] examined quais-ultrafine particle (D_p <250 nm) and found that as the particles were heated from 50 to 200°C the DTT activity of the particles was observed to decrease, with a 66% decrease in DTT activity at 200°C compared to the ambient temperature. Organic carbon and polycyclic aromatic hydrocarbon content of the ambient particles was highly correlated with redox activity of the particles [56, 57]. Atmospheric aging will also affect the ROS activity as McWhinney et al. [52] demonstrated that the redox activities of engine exhaust particles increased as the particles are oxidized. Thus, in ambient particles the smaller particles (D_p <250 nm) have highest redox activity, with the semi-volatile component comprising a significant fraction of the oxidative potential of the ambient particles [57].

2.3.2.2 ***Dynamometer measurements of redox activity using DTT assay***

Diesel and gasoline vehicles were tested using a dynamometer to examine the redox activity of the emitted particles, and gasoline exhaust particles had the highest redox activity by mass compared to the diesel [53]. This result from Geller et al. [53] is consistent with observations in the gasoline only bore of the Caldecott tunnel which had the higher oxidative potential compared to the mixed bore [56]. However, diesel vehicles have a higher overall ROS activity compared to gasoline vehicles when the ROS activity is expressed in terms of kilometers driven [53, 54]. Therefore the relative contribution of gasoline or diesel vehicles to the oxidative potential is yet to

be fully elucidated and can vary depending on the other factors such as engine technology.

Diesel vehicles fitted with after treatment devices have a reduced overall oxidative potential of exhaust compared to diesel and gasoline vehicles, with the level of reduction varying from 60 to 98% depending on the device installed [55]. However the oxidative potential by mass in diesel vehicles with after treatment devices has been shown to be higher by a factor of three compared to diesel vehicles without one [53]. The redox activity was significantly less for thermally denuded particles in the exhaust of vehicles fitted with after treatment devices but this trend was not observed in vehicles without after treatment devices. Therefore, this indicates that the semi-volatile particles are more oxidative in nature than refractory particles [55] in agreement with the findings of Verma et al. [57]. This raises the possibility that reducing the particle mass emissions may not result in completely eliminating the adverse health effects [53].

The chemical composition of engine particle emissions and its relationship with redox activity has been examined on a dynamometer. Cheung et al. [54] found that polycyclic aromatic hydrocarbons (PAH) were strongly correlated with DTT consumption rates while soluble Fe was also highly correlated with ROS particulate activity. Geller et al. [53] also found a strong correlation with redox activity and PAH as well as EC, and OC, which is in agreement with ambient measurements conducted by Ntziachristos et al. [56] and Verma et al. [57]. Chemical tracers for lubricating oil emissions, which included Zn, P, Ca and hopanes were found to be highly correlated with distance based DTT consumption rates [54]. Therefore, the

incomplete combustion of lubricating oil has potentially an important role in the overall toxicity of particles from vehicle emissions [54]. The studies highlighted in this section have demonstrated that vehicles emit ROS and this may account for its toxicity. The concentration of ROS that is emitted by vehicles is dependent on a number of factors, and has yet to be fully explained. In particular, measurements of ROS from vehicles under real world dilution conditions and the influence of traffic composition on ambient concentrations have not been fully answered.

2.4 ELEMENTAL CARBON AND ORGANIC CARBON

2.4.1 Definition of Organic Carbon (OC)

The OC component comprises a mixture of non-volatile and semi-volatile organic compounds at various levels of oxidation comprises. OC is emitted by a wide range of sources, which can either be primary sources such as vehicle emissions or formed by secondary atmospheric processes. As such, OC can be defined as either primary organic carbon (POC) or secondary organic carbon (SOC) by the following equation:

$$OC = POC + SOC$$

POC refers to OC that is released directly either by biogenic (bush fires) or anthropogenic sources (vehicle emissions, domestic heating). SOC is formed either by the condensation of semi-volatile primary gaseous organic compounds or the condensation of the low-volatile products from the photo-oxidation of volatile organic compounds [59]. Organic particles formed by atmospheric photo-oxidation are referred to as secondary organic aerosol (SOA) which differs slightly from SOC. As the OC is defined by a mass of carbon, to get an estimate of the mass of organic aerosols (OA) the OC must be multiplied by a factor to account for average

molecular mass per carbon weight of the organic aerosols to obtain the mass of particular organic compounds [61]. The mass of organic aerosol is calculated from the OC by multiplying by a factor which accounts for the presence of oxygen and hydrogen atoms. After reviewing several datasets from the USA, Turpin and Lim [61], determined that a factor of 1.6±0.2 was realistic for urban locations. As noted by Keywood et al. [62] the factor may be location specific and there is a significant level of uncertainty in the correct value for this factor. Therefore SOA refers to the mass and are calculated by multiplying the concentration of SOC by this factor.

In the atmosphere, the number of VOCs has been estimated to be between 10^4 to 10^5 [4] and each VOC can undergo multiple oxidations to produce a range of products that might result in the formation of secondary organic aerosols (SOA) [62]. When considering this level of complexity, it is perhaps not unexpected that the processes which govern SOA formation are poorly understood. However one notable aspect of SOA is that as different sources of OA age in the atmosphere, they become more alike in their properties [63].

2.4.1.1 ***Definition of Elemental Carbon (EC)***

In the atmosphere, the EC component is a mixture of compounds that cover a combustion continuum ranging from slightly charred material to highly condensed refractory soot-EC [64] and references therein). EC has a range of different chemical compositions, morphology, size and optical properties that reflect the difference in origin and atmospheric aging. The vast majority of EC is due to incomplete combustion of primary sources that can either be anthropogenic (vehicle) or biogenic (bushfires). Carbonaceous material in the atmosphere formed by incomplete combustion can also be referred to as black carbon (BC). The terms BC and EC were used interchangeably in the past however they do not describe the same properties of

airborne particles. The convention currently adopted is to define BC as optically measured light absorbing carbon whereas EC is defined as refractory carbon measured by oxidation using thermal/optical carbon analysers [65]. Importantly significant relationships between BC and EC for consistent measurement techniques and sources [66] have been shown, as discussed in Section 2.4.2.3. Whereas EC is only from primary sources, OC can have both primary and secondary sources and this is a critical parameter for the identification of the source of carbonaceous aerosols, as discussed further in Section 2.4.3.

2.4.2 EC and OC analytical methodology

2.4.2.1 ***Analysis protocols***

Carbonaceous particles are most frequently defined as OC and EC by thermal optical analysis. Thermal optical analysis involves a two phase heating process of a section of the quartz fibre filter [67]; firstly in an oxygen free, helium environment followed by 2% O_2 environment. There are two main operation protocols in use in the literature to define the temperature evolution, and these are the Interagency Monitoring of Protected Visual Environments (IMPROVE) protocol [68] and the National Institute of Occupational Health and Safety (NIOSH) 5040 thermal evaluation protocol [69]. Initially, the NIOSH protocol was intended for the analysis of vehicle pollution while the IMPROVE protocol was meant for ambient environmental pollution [13]. As a result there are significant differences in the results for OC and EC from these two protocols, which are discussed below.

The definition of the split between OC and EC is the point during analysis where the light transmittance or reflectance of the sample returns to the initial condition [65]. OC is thus defined as the carbon released in the oxygen free atmosphere plus the

pyrolysed carbon, while the EC is the carbon emitted after the laser transmittance or reflectance returns to the initial condition. There are eight carbon fractions defined by temperature, oxidation atmosphere and He-Ne laser light reflectance in the IMPROVE database [13, 68, 70]. These eight fractions are grouped into EC; which is light absorbing fractions, whilst the light non-absorbing fractions are defined as the OC. The eight carbon fractions defined by the IMPROVE protocol are OC1 - OC4, pyrolysed carbon (PC) and EC1 - EC3. In Table 2-3, the temperature of each of the fractions for the IMPROVE protocol are listed. The PC fraction is there to differentiate between OC compounds that have pyrolysed or charred to form an EC-like material. This charred OC is thought be chemically and optically similar to EC and so is corrected using an optical laser. This is done to correctly assign the charred compounds to OC fraction to ensure the correct OC/EC split and assumes that all the charred material is OC and therefore evolved before the EC fractions [67].

Table 2-3: IMPROVE temperatures used in the analysis of each OC and EC fraction

Fraction	*OC1*	*OC2*	*OC3*	*OC4*	*EC1*	*EC2*	*EC3*
Temperature (°C)	120	250	450	550	550	700	850

The NIOSH thermal protocol uses the same thermal evolution as IMPROVE except for differences in the temperature and optical protocols. Between the methods, the two main differences are hold times for each fraction and the peak temperature for the oxygen free heating stage [65]. The NIOSH method uses a higher temperature (850°C compared to 550°C) for the OC4 fraction and fixed hold times while the IMPROVE method hold times vary depending on the carbon evolution for each heating stage. Therefore in practice the two protocols report significant differences in the split between OC and EC [71], with the NIOSH protocol reporting lower concentrations of EC compared to the IMPROVE protocol [13]. This should be

considered when comparing results, as it will impact the OC/EC ratio as determined by the two protocols.

2.4.2.2 ***Comparison between NIOSH and IMPROVE protocols***

Unfortunately, it has been established that there is no simple relationship between these two protocols [13]. However, both methods give reasonably similar results for TC concentration for a variety of different samples [13, 71, 72]. For example, the TC from airborne particles in an urban tunnel, was not significantly different [72], and no significant difference in TC concentration has been reported for samples from cook stove emissions, diesel exhaust, rural and urban ambient particles [67]. These studies [67, 72] have demonstrated that as the TC concentrations are similar between protocols, the main difference in the two techniques is the split of OC and EC resulting in differing OC and EC concentrations and OC/EC ratios.

EC and OC concentrations of urban ambient $PM_{2.5}$ samples were measured by both NIOSH and IMPROVE methods and were found to give different readings at each sampling site for EC and OC [73]. The NIOSH method recorded lower EC concentrations and higher OC concentrations and the differences were attributed to greater influence of charring organic vapour, absorbed on the quartz fibre filters. However, the impact of the charred materials on the OC and EC fractions is not well understood and additional research is needed to determine which compounds are susceptible to charring and its effect as well, as better optical characterisation between charred OC and EC [67].

Further comparison work on the NIOSH and IMPROVE protocols was carried out by Khan et al. [67] on a variety of samples that included diesel exhaust, cook stove

aerosols and ambient rural and urban environments. In general, it was found that the average OC/EC ratio for each sample type was lower when measured by the IMPROVE protocol compared to the results by the NIOSH analysis. No significant difference between the rural and cook stove samples was found between the two protocols. In contrast, there were significant differences for diesel exhaust and urban samples, with the OC/EC ratio for diesel exhaust being 0.46 and 1.54 for the IMPROVE and NIOSH protocol, respectively. Ancelet et al. [72] also observed a difference in the OC/EC ratio for vehicle emissions between the NIOSH and IMPROVE protocols, at 1.7 and 1.0, respectively. These results demonstrate that there is a temperature influence on the OC/EC ratio, as the higher ratios as determined by NIOSH are due to the methods having a higher temperature organic step. This step is known to include some EC, therefore increasing the concentration of carbon attributed to OC [13]. Overall, the results from the two protocols are not directly comparable and errors in source identification can occur if results from the different methods are incorporated. In addition, these studies highlight that there is no analysis protocol that is more suitable for the analysis of all aerosol sample types.

2.4.2.3 ***Comparison of elemental carbon and black carbon***

As EC and BC in airborne particles are both formed by incomplete combustion, studies have demonstrated that there is a relationships between BC and EC for consistent measurement techniques and sources [66]. In a comparative study throughout Asia the correlations of BC and EC concentration has been found to vary from country to country [66], due to differences in contributions from various sources such as biomass burning and vehicles emissions. Quincey at al. [74] found reasonable agreement between BC and EC for rural and urban ambient samples in the United Kingdom, however the manual thermo-optical methods may under read

EC (and hence over read OC) when compared to automatic optical methods for BC. This effect was more significant at a rural site, where the concentrations are lower, than a roadside site with higher concentrations. In an urban tunnel, a site dominated by one source, Ancelet et al. [72] found that the BC concentrations were well correlated with the EC concentrations as determined by both the NIOSH and IMPROVE (r^2 of 0.96 and 0.69, respectively). Therefore, the better correlations between BC and EC have been found in locations where there were fewer different potential sources of EC and BC.

2.4.3 Identification of the sources of EC and OC

As discussed previously, EC is predominantly from primary sources whereas OC may come directly from primary sources and also SOA which are formed in the atmosphere from VOC [75]. In an urban environment the main primary source of EC and OC is generally vehicle emissions, but can include sources such as biomass burning [62] and references therein). Vehicle emissions are mostly carbonaceous in nature with EC frequently the largest component due to the incomplete combustion of fuel [11, 15]. Therefore, EC has been used as a marker for vehicle emissions and in particular, diesel emissions as gasoline cars emit a smaller fraction of EC compared to TC than diesel vehicles [65]. Overall, OC emissions from vehicles have been shown to be more variable than other emitted compounds [35] and so EC has been used as a chemical marker for vehicle emissions, particularly diesel emissions, in urban environments.

2.4.3.1 ***EC and OC as a tracer for traffic emissions***

In urban environments, the spatial variation of the concentration of EC and OC would suggest that vehicle emissions are the main primary source of EC and OC. The concentration of EC has been observed to increase from rural to urban

background, urban centre and kerbside measurements as would be expected due to contribution of anthropogenic sources [76]. The same trend was observed for OC but the greater difference between rural and kerbside was seen for EC [76]. Across the three European cities also showed higher OC and EC values were in the vicinity of roads, with higher levels observed in Amsterdam (3.9–6.7 and 1.7–1.9 μg m^{-3}, respectively) and Barcelona (3.6–6.9 and 1.5–2.6 μg m^{-3}) than in Ghent (2.7–5.4 and 0.8–1.2 μg m^{-3}) [77]. The OC concentration was found to depend not on the region in Europe but rather the vicinity of local sources, and the EC concentration was dependent mostly on traffic levels at the site. This was also observed in a study in Berlin which showed that the EC levels correlated with traffic volume [78]. The diurnal variation in EC concentration further supports traffic emissions as the source, as the EC concentration was strongly correlated with morning rush hour in two American cities [79].

Additionally, BC has been found to be a better marker than other frequently used markers for traffic emissions such as particle mass and NO_2 ([80] and references therein). These studies in this section point to vehicle emissions as being the sole source of elevated concentrations in urban areas. However, EC is not unique to diesel emissions and there are other ambient sources of EC, such as biomass burning and coal burning, and these will affect any source identification that attempts to use EC concentration solely. In addition the fraction of EC is dependent on the measurement technique. Therefore EC alone cannot be used as a chemical marker for traffic emissions unless there are no other significant sources of EC, such as biomass burning, or the influence of these additional sources have been accounted for [65].

*2.4.3.2 **Source identification using ratio of OC to EC***

Based upon the assumption that all of the EC is from primary sources and that the OC can be from either primary or secondary sources, the ratio of OC to EC can be used for source identification. As such the OC/EC ratio can be of more value than the concentrations of OC and EC in determining the source of the carbonaceous aerosols. In an urban environment there can be multiple sources of carbonaceous aerosols and these sources can be distinguished based upon the OC/EC ratio. Vehicle emissions have been shown to have a low ratio, with diesel vehicles having a lower ratio than gasoline vehicles. Direct measurements of diesel exhaust emissions has found a ratio of 0.8 [81] and 0.46 ± 0.22 [67] while for gasoline exhaust emissions the ratio has been shown to be higher at 2.2 [81]. In general, in an urban environment an OC/EC ratio of about 1 or less would show that vehicle emissions are a significant source [2, 82]. However the OC/EC ratio at an urban roadside location in Japan has been shown to vary from 1.55 to 2.28 depending on the season for $PM_{2.5}$ [83].

Tunnel studies around the world have shown that the OC/EC ratio will vary according to traffic composition and count [72] with a range from 0.44 to 1.4 (see Table 2-5). This variation in the OC/EC ratio as a result of these variables can make it difficult to identify vehicle emissions based purely on the OC/EC ratio.

In an urban environment, an OC/EC ratio of around 1 indicates that vehicle emissions are the main source, and so an OC/EC ratio that is higher than 2 points to an increased contribution from SOA [79, 84, 85]. This is complicated by other sources of carbonaceous aerosols that have ratios greater than 2 such as coal combustion and paved road dust, which can have an OC/EC ratio of 12 [14] and 13.1 [15], respectively. Biomass burning OC/EC ratios have been reported to range from

1 to 15, with a mean of 6 in Europe [86], with domestic heating having a lower ratio (4.2) compared to forest fires (14) [87]. In Australia, bushfires in the state of Victoria were reported to have a ratio of 7.64±1.27 [62]. The large range of OC/EC ratios that have been reported for biomass burning limits its use in source identification, unless the ratio is derived locally. The OC/EC ratio for urban environments has been observed to vary seasonally, which can aid the identification of the contribution of biomass burning, for example if domestic heating is prevalent in winter [88]. Therefore when the OC/EC ratio is greater than 2 the source of the carbonaceous aerosols is not readily discernible from the ratio alone; however there are methods to distinguish primary and secondary sources. The following sections will highlight some recent efforts in the literature of using the OC and EC concentration and OC/EC ratio to identify vehicle emissions and SOA in both tunnel and urban environments.

2.4.4 Road tunnel measurements of OC and EC

Road tunnels are ideal places to determine the vehicle emission rates/factors of EC and OC as there is little interference from other sources and the vehicle exhaust are subject to real world dilution conditions. Road tunnels have been shown to have elevated concentrations of EC and OC in the $PM_{2.5}$fraction, such as the Chung-Liao tunnel, China, where the EC and OC concentrations from 150 m outside of the tunnel to the centre both increased by a factor of about 2.6 [27]. Emission factors and OC/EC ratios determined in tunnel studies are an average of the local fleet and so can be used to aid the source apportionment of vehicle emissions and influence of vehicle type. In one study, the OC and EC emission factors were found to depend on the fleet composition, with both emission factors significantly higher during period dominated

by HDDV [35] highlighting how tunnel measurements can allow for the differentiating between vehicle type.

The Caldecott tunnel, San Francisco can allow for the determination of emission factors as LDV are only allowed in bore 1, while bore 2 has a mixture of LDV and HDV. Allen et al. [37] analysed the OC and EC content of the PM_{10} and $PM_{1.9}$ fractions and found significantly higher concentrations of EC and OC in bore 2 in both fractions. Based on the results from both bores emission factors were estimated for HDV and LDV, shown in Table 2-4. For both fractions carbonaceous aerosols were the major component of the HDV and LDV emissions, with EC the largest contributor in HDV and OC the largest contributor in LDV emissions. This reflected in the OC/EC ratio, which in the $PM_{1.9}$ was 0.63 for HDV and 2.6 for LDV.

Table 2-4: Calculated emission factors (mg / kg of C) by vehicle type for Caldecott tunnel.

	HDV	**LDV**
PM_{10} EC	714.4 ± 8.2	40.5 ± 8.3
PM_{10} OM	1278 ± 54	49.9 ± 1.3
$PM_{1.9}$ EC	788 ± 332	15 ± 71
$PM_{1.9}$ OM	495 ± 105	39 ± 22

In contrast to previous studies [35, 37], more OC than EC was observed in both the PM_{10} and $PM_{2.5}$ fraction in two tunnels in Milwaukee with the average OC/EC ratio being 3.22 ± 0.04 and 2.27 ± 0.06 for PM_{10} and $PM_{2.5}$ respectively [23]. The $PM_{2.5}$ OC/EC ratio in one of the tunnels highlighted the impact of small decreases in HDV traffic from 7% on the weekdays to 2% on the weekend, resulting in corresponding increase in OC/EC from 1.35 ± 0.01 to 5.6 ± 0.01. This increase in OC/EC ratio

illustrates the significant contribution of HDV to EC ambient concentrations. He et al. [33] also observed that the variations in the emission factors for $PM_{2.5}$ mass, EC and OA were related to the traffic composition. HDV had higher emission factors for $PM_{2.5}$ mass, EC and OA than LDV [33], which further highlights that HDV is the main source of $PM_{2.5}$ emissions.

Road tunnel measurements have been conducted to determine the OC/EC ratio for vehicle emissions in a number of studies around the world. OC/EC ratios in tunnels have been found to vary from location to location, with the OC/EC ratio determined in various studies around the world listed in Table 2-5. One of the main reasons for the differences in the observed ratio is as a result of differences in the fleet composition in the tunnels. The tunnels with the lowest OC/EC ratio, the Zhujiang and Chung-Liao, have a high fraction of HDV at 20% and 8% respectively (Table 2-5). Therefore the low ratios observed in these studies, indicate that HDV were the dominant source of $PM_{2.5}$ emissions in the tunnel [27, 33]. The higher ratio observed at the Mt Victoria tunnel, is attributed to the low percentage of HDV at 2% [72]. In addition, the Mt Victoria tunnel had lower concentrations of OC and EC at 21.7 and 21.3 $\mu g\ m^{-3}$ compared to 53 and 94 $\mu g\ m^{-3}$, respectively in the Zhujing tunnel. This was attributed to lower traffic flows in the Mt Victoria tunnel as well as the lower proportion of HDV [72]. Therefore the OC/EC ratio is more dependent on the traffic composition while the concentration of EC and OC is dependent on the traffic flows in a tunnel environment.

Table 2-5: OC/EC ratios for $PM_{2.5}$ determined by the IMPROVE protocol in various locations in the world.

Location	*OC/EC*	*Reference*
Melbourne, Australia	0.84	[62]
Mt Victoria tunnel, New Zealand	1.4	[72]
Xueshan tunnel, Taiwan	1.26	[82]
Zhujing tunnel, China	0.49 ± 0.04	[33]
Zhujing tunnel China	0.56	[89]
Sepulveda tunnel, Los Angeles	0.76	[90]
Chung-Liao tunnel, China	0.44	[27]
Shing Mun tunnel, Hong Kong	0.6 ± 0.2	[91]

Measurements in tunnels of different particle size fractions have found variations in the EC and OC concentration based on size. In the Chung-Liao tunnel, the concentration of EC and OC was found to be higher in the $PM_{2.5}$ compared to the $PM_{2.5-10}$ fraction [27]. In another tunnel in China, the concentration of EC and OC in $PM_{2.5}$ were found to be higher than that in the $PM_{0.1}$ [82]. A lower ratio was observed for the $PM_{0.1}$ (0.64), which would suggest that the diesel emissions are mainly in this size fraction [82]. Therefore, it would appear from these studies that the EC and OC from vehicle emissions are found predominantly in the finer particles.

2.4.5 Urban measurements of EC and OC

In cities around the world the concentration of OC and EC varies, though in general the OC/EC ratios fall between 2 and 4, as can be seen in Figure 2-1. Rural sites generally have a higher ratio when compared to urban sites (see e.g. [67]).

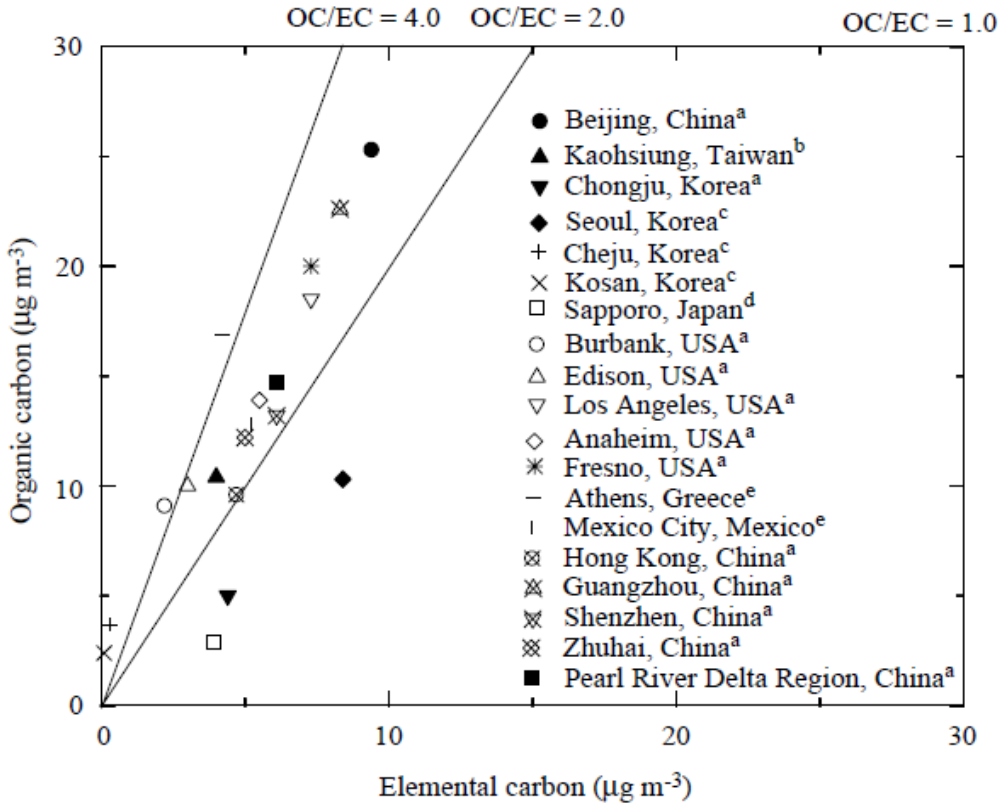

Figure 2-1: Average $PM_{2.5}$ OC vs. average $PM_{2.5}$ EC for different urban areas in China, Korea, Japan, USA, Greece and Mexico.
Measurement method: a, thermal/optical reflectance (TOR); b, element analyzer; c, thermal manganese dioxide oxidation (TMO); d, Combustion method (at 8501C and 3001C); e, thermal optical transmission (TOT). (Reprinted from [93] with permission from Elsevier)

There have been numerous studies in urban environments worldwide that have analysed the EC and OC concentration and its ratio to identify the sources, such as vehicle emissions. The influence of vehicle emissions can be determined in urban environments by the OC/EC ratio, as roadside sites generally have a lower ratio than background locations. This was observed in London where Jones and Harrison [76] found the OC/EC ratio at a background site to be 2.09, whereas at a roadside site it was 0.88. Hong Kong is one of the most densely populated cities in the world with a large number of vehicles on a small road network [75]. Consequently, vehicles are

considered to be one of the major contributors to air pollution in Hong Kong and is thus a good location to observe the impact of traffic emissions on levels of ambient OC and EC [75].

2.4.5.1 ***Contribution of traffic emissions to ambient EC and OC in urban areas***

Investigations into the spatial variation of chemical composition of $PM_{2.5}$ across a roadside, urban, tunnel and rural background sites in Hong Kong found that carbonaceous aerosols were the largest source of the $PM_{2.5}$ mass [91, 92]. Across these three different types of sites in Hong Kong - tunnel, roadside and background, the contribution of EC to the total $PM_{2.5}$ mass at 51, 36 and 15%, respectively. In contrast the OA is a more even fraction of the total $PM_{2.5}$ mass at 31, 32 and 33% at the tunnel, roadside and background sites, respectively. Thus vehicle emissions were the main source of EC, illustrated by the highest EC concentrations of 114±40 μg m^{-3} that were observed at the tunnel site compared to 7.3±3 μg m^{-3} at the background site [91]. At three roadside sites in Hong Kong, the EC concentrations were 44±21, 28±3 and 20±4.3 μg m^{-3}, which correlated well with the fraction of diesel vehicles at those sites at 80%, 51% and 38%, respectively. The calculated emission rates further highlight the contribution of diesel vehicles, accounting for 51 and 26% of the $PM_{2.5}$ EC and OC emissions, respectively [91].

OC/EC ratios ranged from 0.6±0.2, 0.9±0.4, 0.8±0.1 and 1.9±0.7 at the tunnel, two roadside locations and background site, respectively in Hong Kong [91]. That the highest ratio was observed at the background site indicates that the source of the OC was not just from vehicle emissions but a variety sources including SOA. In a separate study in Hong Kong, Louie et al. [92] reported that the OC/EC ratio was approximately 0.8 at a roadside site and was noticeably higher at an urban and rural

background site at 1.6 and 2.6 respectively. Therefore, the least influence of vehicle exhaust was at the background sites and that it was more influenced by SOA and aged aerosols from regional sources such as coal power stations. Ternary diagrams showed the EC measurements clustered towards the roadside site, which suggested a correlation between EC concentration and traffic density, with the caveat that over 60% of Hong Kong fleet was diesel based at the time of sampling [92].

Roadside measurements of $PM_{2.5}$ OC and EC in Hong Kong were carried out in order to assess the contribution of vehicle emissions [75]. The average OC and EC concentrations were 16.7 and 17.1 μg m^{-3}, which are higher than corresponding ambient concentration observed at Hong Kong of 9.6 and 4.7 μg m^{-3} [93] implicating vehicle emissions as the main source of carbonaceous aerosols at the roadside location. Further confirmation was observed in the OC/EC ratios, varying from 0.8 to 1.6 with an average of 1.0. OC/EC ratios also exhibited a diurnal variation with a higher ratio observed at night corresponding with less diesel vehicle activity. Additional roadside measurements of the EC and OC in both the $PM_{2.5}$ and PM_1 fractions was conducted by Lee et al. [2] and found that carbonaceous aerosols were the main species, at around 45% in both fractions. EC and OC for both PM_1 and $PM_{2.5}$ followed similar patterns irrespective of the seasonal variation and regional pollution. This indicates that both the fractions of carbonaceous aerosols were from similar sources, most likely vehicles emissions. Average OC/EC ratio for PM_1 and $PM_{2.5}$ was 0.8 and 1.0; further proof that vehicle emissions were the main source of carbonaceous aerosols. The $PM_{2.5}$ ratio is somewhat lower than observed by Cao et al. [93], as Lee et al. [2] sampled 2-3 m from the roadside compared to over 30 m by Cao et al. [93].

The $PM_{2.5}$ concentrations of OC and EC were measured across 4 cities in Pearl River Delta Region, China, with the average OC and EC concentrations of 14.7±11.9 and 6.1±4 μg m^{-3} in the region [93]. A strong correlation was observed between EC and OC in the four cities, indicating a common source that was likely vehicle emissions. Average OC/EC was 2.4, with the highest ratio (3.3) observed at the background site and the lowest ratio (1.7) was observed at the site near a major road. Thus the OC/EC ratio is able to determine the influence of vehicle emissions, with vehicle emissions dominating only near roads.

Elsewhere in the world, the contribution of OC and EC from vehicle emissions has been studied. Emission factors for OC and EC were determined for two freeways in Los Angeles, the CA-110 where only LDV are allowed and the I-710 which averages about 20% HDV [19]. Average OC and EC factors for the fine particles at the CA-100 were 105.5 ± 22.1 and 20.5 ± 4.9 mg kg^{-1} of fuel burned and for the I-710 they were 205.9 ± 48.8 and 110.1 ± 13.7 9 mg kg^{-1} of fuel burned, respectively. Based on these emission factors, HDV were calculated to have the highest emission factors for both OC and EC. An OC/EC ratio of 5.2 at CA-100 and 1.9 at I-710 also demonstrates the major contribution of diesel vehicles to ambient EC concentrations. Emission factors for EC and OC determined by Ning et al. [19] for the I-710 are within realistic agreement to those obtained by Grieshop et al. [35] in a tunnel with similar HDV content. As these studies have shown, traffic emissions can be a significant source of OC and EC in urban environments, particularly in Hong Kong due to high traffic density.

2.4.5.2 ***Contribution of SOA in urban areas***

In cities where traffic emissions are not as dominant as they are in Hong Kong, secondary sources of carbonaceous aerosols are an important source and this section will illustrate how the influence of SOA can be identified using the OC/EC ratio. OC/EC ratio varies considerably across cities, as shown in Figure 1 and differing levels of SOA are a major reason for this. In a study in the United Kingdom, Jones and Harrison [76] demonstrated in urban areas that non-traffic sources of OC are the major source of OC, and can be either primary or secondary. In the same study, traffic emissions were found to be the main source of EC and as such the lowest OC/EC ratio was observed at the roadside site when compared to the urban centre and urban background sites [76]. A high correlation between OC and EC was also observed at the roadside site unlike at the urban background sites. Thus this work by Jones and Harrison [76] highlights that the influence of traffic emissions will vary depending on the proximity to local sources and that the OC/EC ratio can be sensitive to this variation.

A number of studies have used the OC/EC ratio to indicate the presence of SOA formation in urban areas. Characterization of the OC and EC component of the $PM_{2.5}$ in Milan, Italy, gave results outside this range shown in Figure 2-1 with an OC/EC ratio of 6.5 and 10.2 in summer and winter respectively, for urban background aerosols [84, 88]. Tunnel measurements were conducted to estimate the OC/EC ratio for vehicle emissions in Milan, and were found to be 1.34. Therefore, Giugliano et al. [84] proposed that, particularly in the summer where there was no other major source, the high OC/EC ratio observed at the urban background site could be attributed to SOA formation. Viana et al. [77] compared the daily OC/EC ratio to seasonal means, with days with significantly higher ratios attributed mostly to the

formation of SOA, though occasionally long range transport of carbonaceous aerosols was also contributing. High OC/EC ratios were also observed in Rochester and Philadelphia, USA, with a mean of 23.6 ± 19.8 and 18.7 ± 10.2, respectively, which suggested that a high proportion of SOA was present at these sites [79]. By simply using the OC/EC ratio, as shown by these examples, it can indicate the presence of SOA but does not allow for quantitative analysis on the levels of SOA. Using a technique known as the EC tracer method can estimate quantitatively the SOA levels in urban environments.

2.4.6 Estimation of SOC levels by EC tracer method

As there are no direct analytical techniques available, particulate POC and SOC has been tricky to separate and quantify. Therefore, in order to determine the levels of POC in ambient particles indirect methods have been employed. One such method is known as the EC tracer method, which works on the assumption that all EC emitted is from a primary or combustions source [94-96]. OC can either be emitted from a primary source or be the result of secondary processes. Therefore Turpin and Huntzicker [96] proposed the following equation for determining the amount of SOC:

$$SOC = OC_{total} - EC \times (OC/EC_{pri})$$

Where OC/EC_{pri} refers to OC/EC ratio from primary sources, which will vary depending on the source. Castro et al. [94] proposed that the OC/EC_{pri} could be replaced by an OC/EC minimum ratio (OC/EC_{min}) if all the OC and EC are exclusively from a primary source. Therefore a minimum OC/EC ratio can be determined which reflects the primary source if the primary OC and EC are generally

from the same source. Any OC that is above this minimum ratio is assumed to be secondary in nature [97] and so provides an estimation of SOC levels present. The minimum ratio should be determined on days when photochemistry is at a minimum, so that SOA production is minimal [95]. Consequently only POC would be included in the determination of the OC/EC_{min}. The EC tracer method has been shown to give a useful estimation of SOC levels provided the correct OC/EC_{min} is used [98]. In the literature, the methods for determining the OC/EC_{min} have varied and will be discussed below, with the OC/EC_{min} determined in the studies summarised in Table 2-6.

Table 2-6: OC/EC_{min} results for $PM_{2.5}$ at various urban locations.

OC/EC_{min}	**Location**	**Location type**	**Sample Interval**	**Reference**
1.2	Budapest	Kerbside	12 hr	[99]
0.9	Beijing	Urban	24 hr	[100]
2.6 + 0.3	Pittsburgh	Urban background	4-6 hr	[95]
2.07 + 0.01	Pittsburgh	Urban background	4 hr	[101]
0.65	Birmingham	Urban	24hr	[97]
0.37	Birmingham	Kerbside	24hr	[97]
2.248 + 0.242	Melbourne	Urban background	24hr	[62]

2.4.6.1 ***Methods for establishing the OC/EC_{min}***

Castro et al. [94], and Harrison and Yin [97] used a graphical method to OC/EC_{min} to characterise SOC levels at a rural and urban locations in Europe. To determine the OC/EC_{min} , the OC concentration was plotted as function of EC and the lower limit of the data points are taken to signify a constant mixture of OC and EC or the

OC/EC_{min} [97]. At an urban background site in Birmingham the OC/EC_{min} for PM_{10} was found to be consistent over time at 1.1 [94] and 0.99 [97]. This was despite using different analytical procedures which would suggest that the correct OC/EC_{min} was determined. The OC/EC_{min} was found to be higher at rural sites compared to the urban sites, which show the difference in source contribution [94, 97].

Another method used to establish the OC/EC_{min} was to selectively choose sampling days that would be expected to have the lowest levels of SOA formation [62, 95]. Sampling days that were affected by significant rainfall were not used for calculating OC/EC_{min} as the rain would wash away the aged aerosols, adding potential bias to the calculation. The next step was to remove days where there was high photochemical activity and hence a high likelihood of SOA formation. This was done by considering the ozone concentration and days with a maximum concentration of ozone, higher than the 90^{th} percentile, were removed [62]. Finally, sampling days when primary emissions were the main source of carbonaceous particles were determined. This was done by using tracer gases for combustion process, CO and NO, and sampling days with a high concentration of CO and NO ($>80^{th}$ percentile) where chosen if the ozone concentrations were at a minimum. These sampling days were then assumed to be representative of primary emissions and the OC/EC_{min} was calculated by linear regression between the OC and EC concentrations.

Cabada et al. [95] at an urban site found the OC/EC_{min} for $PM_{2.5}$ to vary from 0.9 to 3.1 with an intercept value ranging from 0.3 to 1.2 $\mu g\ C\ m^{-3}$ where the intercept value corresponds to the contribution of non combustion related OC present. The range is due to the varying length of sampling times, with the 24 hour resolution

samples generally recording higher ratio and intercepts than those obtained from some samples with higher time resolutions. This was thought to be due to the ability of the higher time resolution samples to accurately separate between secondary and primary OC [95]. Keywood et al. [62] measured daily $PM_{2.5}$ samples and calculated an OC/EC_{min} for days at an urban site dominated by vehicle emissions to be 2.248 with an intercept value of 0.242.

Alternatively, Lonati et al. [88] used the OC/EC ratio observed at a tunnel site (0.67) in the same area as an estimation for their OC/EC_{min} as representative of the assumed main primary source, traffic emissions. However for winter this OC/EC_{min} would not be representative as the main primary sources would be both traffic and domestic heating. Thus, Lonati et al. [88] applied the criteria outlined earlier by Cadada et al [95] for determining sampling days where primary emissions are dominant. The OC/EC ratio that was determined was 9.5, which was thought to be too high for primary emissions and may be due to SOA formation occurring in cold temperatures. It could also be due to the high atmospheric stability that is characteristic in winter in Milan and which would lead to high residence times of OA in the atmosphere. This shows that a subset of ambient data may not be suitable for OC/EC_{min} estimation in winter samples and therefore limited the application of the EC tracer method to winter samples in this study.

*2.4.6.2 **Issues with the EC tracer methods***

A major weakness with the EC tracer method is that it assumes that the OC/EC_{min} and non combustion related OC are constant throughout the sampling period. These two parameters would be expected to change as a result of variations in meteorological sources and this can lead to significant errors in the calculation of

SOC [95]. Plaza et al. [59] captured this variation by collecting hourly samples of OC and EC using a semi-continuous thermal analyser. This would allow for better differentiation between secondary and primary OC compared to daily samples, enabling the diurnal evolution of the carbonaceous aerosols to be captured, particularly in peak emissions periods. To calculate the primary traffic related OC/EC_{min} Plaza et al. [59] used times of rapidly increasing EC concentrations to better determine the minimum ratio as opposed to daily averaged samples in the previous examples. In addition, the background contribution to OC and EC concentration was subtracted to properly estimate the OC/EC_{min} and only the most obvious EC peaks were chosen. The range of estimated OC/EC_{min} varied from 0.2 to 1.24, with an average of 0.59, for the morning and evening rush hours. This is at the lower end of the ratios determined by other studies, as shown in Table 6. Seasonal variation was found for the OC/EC_{min} with a lower average value for autumn-winter compared to spring-summer, thought to be due to the different ambient temperatures [59].

The ability of OC/EC_{min} to represent the ratio of OC and EC aerosols from fossil fuel combustion was assessed using long term monitoring of $PM_{2.5}$ across Europe with a constant analytical method [58]. OC/EC_{min} over Europe was shown to be consistent in these urban background areas during the long term monitoring, as shown in Figure 2-2, with an OC/EC_{min} of 0.7 for $PM_{2.5}$. This suggested that it was correctly determining the ratio for primary OC and EC and so was effective at differentiating between POC and SOC. However when compared to measurements conducted in a road tunnel and for kerbside measurements, these urban background ratios are higher than the environments which are dominated by fresh vehicle emissions. Pio et al.

[58] found the OC/EC_{min} for a $PM_{2.5}$ ranged from 0.29-0.37, while for kerbside measurements it was 0.3. This lower OC/EC_{min} for roadside measurements compared to urban was also observed by Harrison and Yin [97]. Therefore these results would indicate that OC/EC_{min} values determined in an urban environment are higher than the actual OC/EC_{pri} with added OC. This extra OC is most likely to be SOC and due to the consistency of the OC/EC_{min} across a range of urban areas, it would appear that there is consistent contribution of other OC sources apart from traffic emissions [58].

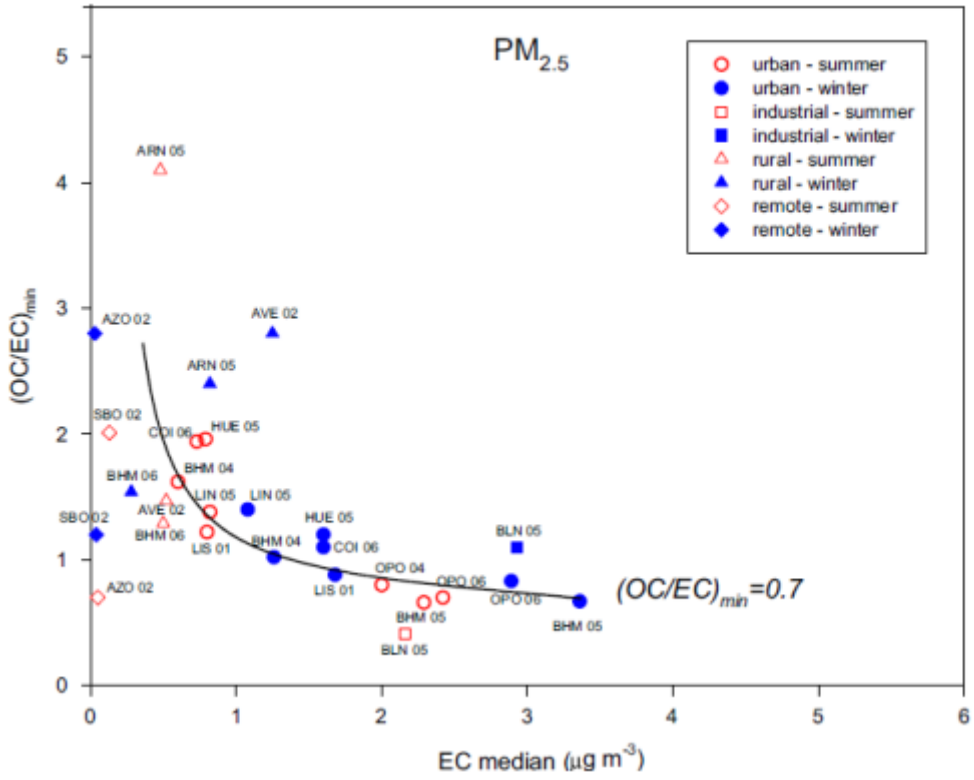

Figure 2-2: OC/EC_{min} for $PM_{2.5}$ fraction across Europe. (Reprinted from [58] with permission from Elsevier).

Pio et al. [58] could not find the cause of the additional OC but suggested that it may be due to gas to particle condensation of freshly emitted volatile organic compounds and their oxidation products. This suggests that tunnel measurements would enable more accurate determination of OC/EC_{min} for vehicle emissions than ambient sampling in urban environments.

2.4.6.3 ***SOC levels in urban areas estimated by EC tracer method***

At a number of the cities in Europe, North America, Australia and Asia the concentration of SOC has been determined using the EC tracer method and shown to exhibit a large variation. In the fine fraction, the SOA levels varied from an annual median concentration of 1.1 μg m^{-3} or 13% of total mass in Melbourne, Australia [62] while Polidori et al. [101] found in Pittsburgh, USA that the annual average for SOA was 0.92 μg m^{-3}, which was 33% of the particulate OC. Higher levels have been observed elsewhere, such as in Taiwan where the SOC accounted for half the total OC concentration [17] and in Milan during summer, the average SOA concentration was 6.1 ug m^{-3}, about 84% of the TC mass [88].

A seasonal variation in SOC levels has been observed with the lowest levels in winter (17%) with the highest levels in summer (78%) at an urban site in Portugal [94]. A clear seasonal variation was observed by Plaza et al. [59] as well, with the daily SOC levels in summer ranging from 80 to 92% while in winter it was from 70 to 84%. The higher levels in summer were mostly attributed to an increase in photochemical activity, although biogenic SOA could also have been contributing. In contrast to the European studies, a different seasonal variation was observed in Melbourne, with the maximum concentrations occurring in autumn and winter and the lowest during summer [62]. Keywood et al. [62] thought that this was due to the formation of pollution inversions, which meant that the particles emitted by domestic wood heaters were allowed to accumulate. Another time that significantly high SOA concentrations were obtained was when bushfire smoke affected the local air shed. Like in Melbourne, in Beijing winter levels of SOC were also observed to be higher compared to summer also attributed to increased levels of combustion for domestic heating [100]. However, in Beijing coal is the main fuel, which would have increased

the levels of VOC in the atmosphere and points to the burning of coal as an important source of OA in Beijing [100]. Thus the concentration of SOC in urban areas can exhibit a seasonal variation that is dependent on local sources and meteorology.

SOA concentrations in urban environments do not always exhibit a strong seasonal trend, such as in Pittsburgh, where the summer and winter means were 1.3 and 1.44 μg C m^{-3}, respectively [101]. Regional transport of aged aerosols as opposed to local photochemical formation was the likely cause of the winter presence of SOA. This indicates a potential weakness of the EC tracer method particularly for locations that can be affected by significant regional transport of biomass burning. Harrison and Yin [97] observed a strong seasonality for POC that is similar to EC, with higher concentrations in winter compared to summer. However, like Polidori et al. [101] there was the seasonal pattern in SOC levels was less marked, with higher average concentration in winter than summer. Harrison and Yin [97] hypothesised that long-range transport and temperature were the main influences on SOC concentrations, due to the nitrate levels having a similar seasonality. The lack of influence from wood burning may have also been a reason for the observed lack of seasonality for SOC.

Cabada et al. [95] explored the diurnal cycle of SOA to investigate the influence of local and regional sources. A minimum concentration was observed in the early morning (6am till 9am), with the concentration increasing as photochemical reactions increased during the day to a maximum in the mid afternoon (3pm). The lowest levels of SOA formation corresponded with the ozone concentrations at their lowest, and were generally from 4am till 8am. Cabada et al. [95] suggested that for their data

a significant amount of the SOA at night and late afternoon was due to long range transport pointing to the sources of SOA differing during the day.

2.4.7 Source identification using the OC and EC fractions

2.4.7.1 ***Identification of diesel and gasoline emissions using the eight carbon fractions***

The eight carbon fractions as described by the IMPROVE protocols can be used to improve source identification. In urban environments, the OC fractions have been found to be correlated with NO_x, suggesting a combustion source [102]. When looking in particular at vehicle emissions, the OC and EC fractions can be used to differentiate between gasoline and diesel as they have been found to have different profile of carbon fraction [73, 103]. Diesel vehicle source profiles have more EC fractions compared to gasoline vehicle profiles, as demonstrated by Han et al. [64] who measured the EC fraction for standard reference diesel soot and found that it was mainly in the EC2 fraction. Gasoline vehicle source profiles are generally higher in the OC fractions and however it has a higher degree of variation in the source profiles when compared to diesel emissions [73].

The OC and EC fractions of the $PM_{2.5}$, as defined by the IMPROVE protocol, at roadside locations that were dominated by different sources (diesel, gasoline and LPG) in Hong Kong [75] gave different carbon profiles. The main fraction present in diesel vehicle exhaust was EC2 and OC2 whereas LPG and gasoline exhaust had similar carbon profiles, with the OC3 and OC2 as the largest fractions. These source profiles of carbon fraction were in agreement with samples taken directly from vehicle tailpipes [15]. In measurements conducted in a road tunnel, the dominant fraction in the fine particles was EC1 while for the nanoparticles the main fraction was EC2, which was attributed to metal catalysis of soot oxidation of the smaller

particles [82]. Using Positive Matrix Factorisation (PMF) to extract the profiles for diesel and gasoline vehicles for fine particles, the profiles for both types had high peaks for OC1-OC4 and EC1. Differences in the profiles were observed, with diesel profile having a higher EC2 while the gasoline profile had higher peaks for OC4 and PC [82].

In contrast to the Chinese studies [75, 82], studies which were conducted in the USA derived different source profiles using PMF [73, 103]. At a rural site, a gasoline and diesel source were identified characterized by high concentration of OC, specifically OC3 and OC4, and large amounts of EC1, respectively [104]. Similar source profiles were determined by Sahu et al. [73], where the diesel source profiles had high OC2 and EC1 while the gasoline vehicles had high concentrations of OC3 and OC4. Therefore it can be seen that carbon fractions derived by IMPROVE protocol can improve the identification of vehicle emissions, though there is not yet a consensus on profiles for gasoline or diesel vehicles though results are promising. The large variation found for gasoline profiles in particular hinders using the OC and EC fractions for source identification and requires further work to determine source profiles.

2.4.7.2 ***Identification of the source of EC using its fractions***

2.4.7.2.1 Char-EC and Soot-EC

EC can be defined as either char-EC or soot-EC, which have different physical, chemical and light absorbing properties ([105] and references therein). Soot-EC are generally submicron particles with a distinct physical morphology while char-EC retains the morphology of the parent material with a wide range of particle diameters, mostly from 1-100 μm. Char-EC absorbs light mainly in the Ultra-Violet spectrum

while soot-EC absorbs light strongly across the spectrum pointing to differing impacts on the environment.

The IMPROVE protocol was able to distinguish between char-EC and soot-EC for standard reference materials [64]. Char-EC reference materials, which were wood charred materials, were observed to show high EC1 with little of the other EC fractions. Soot-EC standard reference materials, which included diesel soot and n-hexane soot, evolved mainly in EC2 and EC3 fractions [64]. Therefore for the IMPROVE protocol Han et al. [64] defined char-EC as EC1-PC and soot-EC as EC2 and EC3.

In a tunnel environment, the concentration of char-EC was higher in the fine fraction whereas for the $PM_{0.1}$ fraction the soot-EC was the dominant form [82]. Han et al. [64] also observed that char-EC was found more in the fine fraction while the soot-EC was in the ultrafine particles. For fine particles char-EC was well correlated with EC, with a similar correlation for soot-EC and EC for $PM_{0.1}$, suggesting that the EC was char-EC and soot-EC for $PM_{2.5}$ and $PM_{0.1}$, respectively. In urban location within Japan, almost all of the EC in fine fraction was char-EC, while the char-EC accounted for only 40-50% of the ultrafine fraction EC [102]. Therefore these studies, suggest that the composition of EC changes with size as a result of different sources.

In Xi'an, China the char-EC, EC, OC and TC in the $PM_{2.5}$ fraction showed a marked seasonal variation, with low concentration in summer and high concentrations in winter [105]. This peak in winter was attributed to coal combustion associated with

winter heating in this city. The same trend was not observed for OC/EC ratio indicating that the OC/EC ratio was more affected by secondary sources, making it less suitable for the identification of primary sources. In contrast, soot-EC was found to exhibit little seasonal variation and was thus more indicative of a background EC. Seasonal variation in the concentration of fine and ultrafine soot-EC and char-EC was observed in Japan [102]. Kim et al. [102] found for both size fractions the concentration peaked in winter, also suggesting a combustion source related to home heating. The exception was the concentration of soot-EC in the fine fraction which peaked in summer and may have been due to long-range transport. The similar variation of soot-EC and char-EC in ultrafine particles suggests vehicle emissions as a source [102], thus the soot-EC and char-EC can differentiate between the different sources of EC.

2.4.7.2.2 Source identification using the ratio of Char-EC to Soot EC

Analysis of $PM_{2.5}$ carbonaceous aerosol data in China showed that char-EC/soot-EC can be a more effective source indicator than OC/EC as the OC/EC is more affected by formation of SOA, which can bias the OC/EC ratio [105, 106]. As char-EC and soot-EC are mainly produced by combustion process, the char-EC/soot-EC ratio is affected mostly by emission sources, meaning it can be a more effective source indicator. Han et al. [106] observed a weak correlation between OC/EC ratio and char-EC/soot-EC indicating different sources were affecting the two ratios. Across 14 cities in China, the char-EC/soot-EC ratio showed winter maximums and summer minimums, which are consistent with the increased contributions due to fuel burning for heating [106]. The high ratios that were observed in winter and autumn in China meant it can also be used for indentifying fuel combustion sources, and the char-EC/soot-EC ratio for various combustions sources are given in Table 2-7. In general,

motor vehicle exhaust has a char-EC/soot-EC ratio below 1, while higher ratios indicate the presence of biomass burning and coal combustion [106], similar to that for OC/EC. Differences observed in the OC/EC and char-EC/soot-EC ratios for the fine and ultrafine particles can also point to differences in the age of the particles. The carbonaceous component of fine particles are thought more to be due to regional transport, while the ultrafine particles are the results of local emissions [102].

Table 2-7: Char-EC/soot-EC ratios for various combustion sources.

Combustion Source	*Char-EC/Soot-EC*	*Reference*
Coal	1.5 – 3.0	[14]
	1.31	[107]
Vehicle emission	0.6	[107]
	0.3-0.7	[75]
Biomass burning	11.6	[14]
	22	[107]

Most of the research on using the char-EC/soot-EC have been mainly carried out in China [14, 75, 105, 106], where the concentrations of char-EC and soot-EC are remarkably large, due to widespread biomass and coal burning. Therefore Kim et al. [102] compared the OC/EC ratio to char-EC/soot-EC ratio in Japan where vehicle emissions are predominant over coal and biomass burning. The results from Kim et al. [102] suggested that char-EC/soot-EC ratio could be used for source identification becuase they are comparable with results from the studies conducted in China [106]; however the characteristic ratio of char-EC/soot-EC would vary depending on the location.

2.4.8 Identification of sources in urban schools using EC and OC

There have been few studies on the outdoor OC and EC levels in schools, with research focused in the USA. Recent studies in schools in the greater Cincinnati area [108, 109] have highlighted the effect of diesel school buses on the air quality in the

schools. Li et al. [109] performed simultaneous measurement of EC at a school opposite a bus depot and a control site from 6 am till 9 am weekdays, in winter and summer. EC concentrations were found to be three times greater at the school site compared to the test site, with no seasonal variation observed. This would suggest that school bus emissions have a significant impact on the air quality at the school studied.

The link between school bus emissions on air quality in urban schools has been further studied in schools in New York City [110, 111]. In New York City urban or inner city schools had higher concentrations than a suburban school located in the same city [110]. At urban schools hourly levels of BC were found to be more correlated with diesel traffic levels than the $PM_{2.5}$ mass, which suggests that BC is a more specific marker for diesel emissions [110]. Furthermore, at these schools the BC levels were correlated with diesel vehicle traffic whereas total traffic counts was not associated with BC levels [110]. In another study in New York City one of the main contributors to the variability in BC concentrations was found to be trucks and buses idling in the street outside the schools [111], more so than other traffic variables at the school such as traffic count and composition. In addition, meteorological factors such as wind speed and direction were other factors that were associated with BC and $PM_{2.5}$ levels [110]. These studies in New York City further highlight the significant contribution made by HDV, in particular school buses, to children's exposure to vehicle emissions in urban schools.

Hochstetler et al. [108] found that the highest EC, OC and $PM_{2.5}$ mass concentrations were observed at the school with the highest bus and car counts. OC accounted for a

large fraction of the outdoor ambient $PM_{2.5}$ in the schools tested, with OC daily values ranging from 3.1 - 13.2 μg m^{-3} and daily EC values ranging from 0.06 - 2.7 μg m^{-3}. OC levels were slightly lower but comparable to another study in the Cincinnati metropolitan area [112], whereas the EC levels were markedly lower and Hochstetler et al. [108] were unable to determine the cause of the EC decrease. From these limited number of studies it can be seen that traffic composition and count has an effect on the air quality in the schools and the EC levels in schools can differ from the local environment. However as the research has been conducted in the USA, where schools are extensively serviced by school buses, the results from these studies may not be as applicable to schools in other locations where the school traffic is different.

2.5 TRACE ELEMENTAL COMPOSITION OF AEROSOLS

2.5.1 Introduction

Ambient particles, particularly in urban environments have a complex trace elemental composition from a variety of sources. Though trace metals can constitute as low as 1% of the total particulate mass [38], the elemental composition is still useful for the identification of the sources of airborne particulate matter. There are characteristic elements that have been associated with various sources such industry (Cr, Cd, Zn), secondary sulphate (S), biomass burning (K), marine (Na, Cl) and vehicle emissions (see Table 2-8). In urban environments, traffic emission is a significant source of a number of toxic metals such as Pb, Ni, V, Sb, and other transition metals (See Section 2.5.2) and the composition of these elements in exhausts varies depending on the vehicular processes. While a reduction in vehicle exhaust emissions as a result of environmental regulation has been achieved, it has not been complemented by a reduction in non-exhaust traffic emissions [113].

Table 2-8: Summary of the vehicle source of traffic related elements

Element	Vehicle Source	Reference
Ba	Brake wear	[119]
Br	Fuel	[120]
Ca	Lubricating oil	[19]
Cu	Brake wear	[18]
Fe	Engine, Tyre, and Brake wear, Tailpipe emissions	[23]
Mg	Lubricating oil	[19]
Mn	Brake wear	[18]
Mo	Lubricating oil,	[19]
	Auto catalyst	[35]
Ni	Oil	[117]
Pb	Fuel, Motor Oil, Brake wear	[23]
S	Diesel fuel, Lube oil	[19]
Sb	Brake wear	[18]
V	Oil	[117]
Zn	Tyre and Brake Wear,	[18]
	Motor oil	[23]

Non-exhaust traffic emissions, which includes brake, tyre and road wear and road dust resuspension, can now contribute equal proportion of the PM_{10} concentration in roadside air (See e.g. [114]). It has been predicted that the contribution of non-exhaust emission will steadily increase to 80-90% in central Europe by the 2020 [115].

Harrison et al. [116] found that most trace elements in roadside aerosols are from vehicle wear products as opposed to exhaust emissions. Thus the analysis of the trace elemental composition of airborne particulate matter will shed light on this increasingly important emission source. However, since the removal of leaded petrol,

no trace metals have been found to be a clear marker for vehicle emissions in general and organic compounds may prove to be better source tracers [116]. Nevertheless, as the studies considered in this section of the review show, rather than use a single element as a tracer, there are groups of elements that can be associated with traffic emissions to aid source apportionment. In addition, some elements have been found to be associated with particular vehicular abrasion processes, and can shed light on the contribution of these specific non-exhaust traffic emissions.

The use of trace elements remains problematic as there are sometimes multiple sources, both anthropogenic and biogenic, for elements such as Mg, S, Ca and Fe, that are associated with vehicle emissions [19]. It is also further complicated by the fact that road dust composition varies considerably from location to location. Additionally, the composition of brake pads and tyres differs greatly depending on the manufacturer, making it difficult to generalise across the entire fleet in a given location. He et al. [33] noted there was a large variation between their results in China and other results from the USA, thus highlighting the need for local elemental emission factors, as they can vary significantly from location to location. Without knowing the local emissions factors it can make the source apportionment and the health effects of the local airborne particles difficult to determine. Trace elemental compositional information is still useful in determining the impact of traffic emissions, particularly with other complementary information. Elemental composition of aerosols provides important data on the potential toxicity of urban particulate matter, particularly with regard to the heavy metals present.

2.5.2 Elements commonly associated with vehicles emissions

There are a number of elements that are commonly associated with traffic emissions and these are Mg, S, Ca, V, Mn, Fe, Ni, Cu, Zn, Mo, Ba, Sb and Pb. The vehicular source of these elements are summarised in Table 2-8. Lead is emitted from fuel and motor oil combustion and brake wear [23]. Magnesium, S, Ca, and Mo are lubricating oil additives [19] while S also is emitted from combustion of S containing fuels, particularly diesel [19]. Molybdenum is also a component of automotive catalysts [35]. Iron is emitted from engine, tyre and brake wear and tailpipe emissions [23]. Zinc is often used as a marker for tyre wear [18] but can also be brake wear as well as being a motor oil additive [23]. Manganese, Cu, Sb and Ba are from brake wear and Cu and Sb have been suggested as possible tracers for brake wear [18]. Vanadium and Ni are found in crude oil and so are emitted from combustion of fuel and oil [117]. Platinum group metals such as Pt, Pd and Rh have also been attributed to vehicle emissions in countries where catalytic convertors are present in vehicle exhaust systems [118].

2.5.3 Particle size, elemental composition and its relationships with source

Airborne particles in urban environments will vary depending on the source, as demonstrated by Perez et al. [121], who observed a clear division between elements in the PM_1 and PM_{1-10} fraction related to their source. The contribution of crustal material decreases with particle size, in one study accounting for 17%, 4% and 1% of the total particulate matter concentration in the PM_{10}, $PM_{2.5}$ and PM_1 fractions, respectively [122]. Traffic emissions are generally related to the finer particles and in particular are correlated with PM_1 [2, 121]. In Hong Kong, around 70% of the $PM_{2.5}$ mass at a roadside location was PM_1 and it was proposed as an indicator for vehicle

emissions [2]. At this roadside location in Hong Kong vehicle emissions were found to be the largest contributor to the PM_1 [123].

PM_{10} and PM_1 mass concentration in a rural and urban site in Switzerland was found to be similar across the seasons except for the PM_1 winter concentrations, though the variation was correlated [124]. The main point of difference between the two size fractions at the Swiss sites was in the trace elemental composition. At an urban background site in Barcelona a clear division related to their source was observed between elements in the PM_1 and PM_{1-10} fraction [121]. In general, the coarse fraction contained crustal elements and some vehicle wear products whereas the finer particles are more related to vehicle exhaust emissions. These two papers, [121, 124] will be used as case studies to look at the difference in elemental composition of coarse and fine particles in urban environments.

2.5.3.1 ***Comparison of coarse and fine particle fractions in two case studies***

In the larger particle size fractions, the elements present are generally from crustal material in the majority of urban environments. In Switzerland, crustal matter associated elements, Li, Ti, Sr, La, and Nd were found preferentially in the PM_{10} fraction [124] as was the case at Barcelona where Li, P, Ti, Rb, Sr, La and Ce were found more in the PM_{1-10} fraction [121]. Elements further related to vehicle wear were also observed in the coarse fraction at these two sites and included Cr, Mn, Cu, Zn, Co, Se, Sn, Sb, Ba, Tl and Bi [121, 124]. This therefore indicates that dust resuspension and vehicle abrasion products are also contributing to the coarse particles present in urban environments.

Elements present in the smaller particle size fraction are more related to combustion processes as opposed to mechanical processes. Elements that were mainly found in the PM_1 fraction in Switzerland were As, Cd and Pb, and these were identified as being from high temperature anthropogenic processes [124]. Industrial emission related elements such as As, Cd, Pb and U and fossil fuel combustion associated elements, Ni and V were predominately in the PM_1 fraction in Barcelona [121]. Therefore at these sites the composition of the airborne particulate matter was highly affected by vehicle emissions, with exhaust emissions contributing to the PM_1 and dust resuspension and abrasion products to the larger size fraction.

2.5.4 Identification of vehicle emissions using tracer elements

2.5.4.1 ***Lead***

Recent research has focused on finding an elemental tracer for vehicle emissions in urban environments to aid source apportionment over other potential sources of trace elements in airborne particulate matter. Lead has traditionally been used as a tracer for vehicle emissions owing to the use of leaded petrol. Cohen et al. [125] showed that a Pb/Br ratio of 2 to 5 was characteristic of the emissions from vehicles on leaded petrol. However the removal of leaded petrol has reduced the suitability of Pb as a tracer for vehicle emissions. Harrison et al. [116] noted this when comparing the results from the 2003 study to an earlier study in the same location [126]. In the earlier study Pb was identified as clear tracer element for vehicle emissions, yet in the later study there were no trace metals identified as potential tracers to replace Pb. Lead continues to be associated with vehicle emissions in urban environments in many studies (See e.g. [112, 127, 128]) in spite of the worldwide removal of leaded petrol. There are a few other potential sources of Pb in urban environments and so it is likely that lead particles are present in the road dust from earlier emissions. In

addition, Radhi et al. [129] identified the influence of vehicle emissions in Australian mineral dust samples as Pb and Br were well correlated and had a ratio of 4.2, well within the expected range for vehicle emissions. Therefore, while Pb is still indicative of vehicle emissions, it is no longer a clear tracer for vehicle exhaust emissions and organic compounds are likely to be of more use [116]. The trace elemental composition can however shed light on the influence of non-exhaust vehicle emissions from brake and tyre wear as discussed in the next sections.

2.5.4.2 ***Brake wear elements: antimony, barium and copper***

Brake wear emissions in particular have been shown to be the most promising in the use of tracer elements for vehicle emissions. Iron, Cu, Ba and Sb were strongly correlated and had the same size distribution at a roadside urban background location [119], suggesting a similar traffic related source for these elements. These elements have been associated with brake wear emissions before [130] and considering the lack of other potential sources of Ba, Geitl et al. [119] proposed using Ba as a quantitative tracer for brake wear emissions in urban environments. Thorpe and Harrison [18], in a review of the literature of laboratory and field studies on vehicle abrasion emissions, suggested Cu and Sb as suitable tracers for brake wear particles. In Tokyo elevated concentrations of Sb in the PM_2 fraction was determined to be from brake wear particles, based on the morphology of ambient Sb rich particles matching that of particles from actual brake wear particles [131]. Thorpe and Harrison [18] suggested a diagnostic ratio of 5 for Cu/Sb to indicate the contribution of brake wear particles as opposed to crustal material. Caution is needed though in assigning these as tracer elements for brake pads, as the elemental composition of brake pads differs significantly across the globe [132].

2.5.4.3 ***Zinc***

Zinc has been proposed as a tracer element for tyre wear, owing to the high concentration of Zn in tyres, with studies showing an association between Zn and tyre wear ([18] and references therein). Zinc is not only emitted in tyre wear, but has also been observed in brake wear and exhaust emissions, somewhat limiting Zn use a tracer for tyre wear [18, 133]. However, using a chemical mass balance model, Schauer et al. [133] found that most of the Zn emitted from vehicle was likely due to tyre wear. Industrial emissions are another atmospheric source of Zn and the ratio between Cu/Zn has been shown to enable differentiation between vehicle and industrial emissions [134]. With vehicle emissions, the Cu/Zn is low, at 0.21 ± 0.15 and 0.01 ± 0.003 for gasoline and diesel vehicles, respectively [135]. Industrial sources have a higher ratio around 1 and as such can distinguish between the sources (see [134] and references therein).

2.5.4.4 ***Issues related to tracer elements for vehicle emissions***

Thorpe and Harrison [18] also concluded that no other elements are suitable tracers for other non-exhaust vehicle emissions in an urban environment due to the interaction of the various sources; for example brake wear particles mixing with resuspended road dust. Resuspended road dust is therefore very difficult to identify based on the elements present due to the contribution of multiple source to the particles on roads. Methods other than tracer elements should be employed to determine the contribution from the resuspension of road dust [136].

Source identification based solely on the ratio of one element to another carries considerable ambiguity, owing to possibility of more than one source for a given element. Therefore a holistic approach is required when identifying the source of trace elements by examining related groups of elements and the size of the particles

with reference to local composition (i.e. crustal material). The trace elemental composition of the airborne particles is still useful in source identification and apportionment of traffic emissions, as will be shown in the following sections.

2.5.5 Source apportionment using trace elemental composition

*2.5.5.1 **Road tunnel measurements***

Road tunnels are good places to measure trace element emissions from vehicles as the tunnel can concentrate the emissions making detection easier. As vehicles are the primary source in a tunnel it can make source identification and apportionment straightforward as well. In one study in the Zhujiang tunnel, China the five most abundant elements in order were Fe, Ca, Na, Mg, and K and these accounted for 93% of the total mass of trace elements [33]. These five elements correlated well with each other but not with EC pointing to a common origin not related to vehicle exhaust emissions but rather resuspended road dust. This study [33] highlights that the size of the particles is a relevant parameter to consider when identifying the source of the elements in traffic emissions.

The most abundant elements, in the PM_{10} mass in a tunnel in Milwaukee were Fe, Ca, Si, Na, Mg and K, which represented 94% of the total mass of metal emissions. These elements are major components of crustal material and soil and so were attributed to these sources [23]. In the $PM_{2.5}$ there were significant correlations found between Si, Ca, Cu, Sb and Ba indicating that brake wear is an important source. There was little correlation between Sb and Zn in the fine fraction, which suggests that Zn did not come from brake wear. Pb was found mostly in the $PM_{2.5\text{-}10}$ fraction, which suggests that the Pb mainly came from the resuspension of road dust. Size distribution analysis revealed that Pb, Ca, Fe and Cu were observed to have modes

less than 0.1 μm, which indicates that these metals are emitted by combustion processes [23]. In the fine fraction S, V, Co, Cu, Sr and Sb were found to have higher concentration in the centre of the Chung-Liao tunnel compared to 150m from the entrance of the tunnel [27], indicating that these elements were emitted from vehicles. Fine particle metal emissions in a road tunnel were found to consist mainly of Mg, Al, Ca, Zn and Fe [35] with concentrations of Li, Ti, Mn, Cu, Ga, Sr, Mo, Sb, Cs, Ba and Ce found at concentrations that were significantly above background levels. Overall, as demonstrated by Handler et al. [38] the emissions of coarse particles in a tunnel are largely due to resuspended road dust and brake wear, whereas particles in the fine fraction were mainly a result of combustion processes.

Tunnel measurements have been conducted to investigate the effect of traffic composition, with good correlations between the percentage of HDV and the emission factors of Cu, Fe and Ba in the tunnel [38]. In contrast to the results by Handler et al. [38], Ba as well as V, Br and Sb were shown to have higher emission rates for gasoline and LPG vehicles compared to diesel emissions, therefore indicating that these elements may be markers for gasoline and LPG vehicles [91]. Diesel emissions showed higher emissions for all other elements measured, such as S, Mg, Al, Ca, Ti, Cr, Mn, Ni, Cu, Zn and Pb. In the Caldecott tunnel where the contribution of HDV can be determined, Allen et al. [37] found that Mg, Al, Cr and Zn were significant trace metals in the HDV fleet emissions.

Grieshop et al. [35] found that Mg, Ca, Zn, Mo, Sb and to a lesser degree Fe emissions all showed significant variation within the sampling period and therefore seemed to be affected by fleet composition. Mg, Ca, Mn and Zn emissions were higher in the sampling period that was dominated by HDDV and thus could be

associated with HDDV. Cu, Sb and Ba emissions were also observed to be significantly higher in morning rush hour period, this can be attributed to brake wear as vehicle speed was more variable, indicating that more braking was occurring. The Mo emission rate was significantly higher during the midday sampling period when there was more LDV traffic than other periods. In general it was found that diesel emissions, particularly HDV are the largest emitters of trace metals compared to light duty gasoline vehicles.

2.5.5.2 ***Trace elemental composition at roadside locations***

Analysis of the elemental composition and concentration of particulate matter sampled beside urban roads gives information on the contribution of trace elements from vehicle emissions to ambient concentrations. Typically a roadside location will be enriched with vehicle emissions making it easier to detect the elements that are associated with vehicle emissions and aid the source identification at other locations within that urban environment (See e.g. [137]).

Investigations into the spatial and temporal variation in the elemental composition of ambient fine particles were performed using three sites that were from increasing distance (<150 m) from the heavily trafficked New Jersey Turnpike [138]. Concentrations of Al, Cr, Fe, Cu, Cd and Pb, were found to decrease with distance from the highway. In contrast Sc, V, Mn, Co, Ni, Zn and Sb, which were found to increase in concentration over distance from the road. Xia and Gao [138] proposed that the reason for the non-crustal elements (V, Co, Ni, Zn and Sb) having a positive correlation with distance was that these elements were enriched in the ultrafine fraction and so would have longer residence times in the atmosphere, resulting in the higher concentrations at the furthest site. A similar seasonal variation in elemental

concentration was observed at all three sites. Concentrations of all of the elements measured were found to be higher on the weekdays as opposed to weekends suggesting that traffic volume affected the concentration of all elements, due to higher concentrations during times of higher traffic flows, namely weekdays [138]. Wind direction and speed was found to influence the spatial and temporal concentration of the elements, with wind speed in particular showing a negative correlation with elemental concentrations.

At an urban roadside location in the PM_{10} fraction Cu, Zn, Mo, Ba and Pb had significant correlations with NO_x and PNC, tracers for vehicle emissions, indicating a traffic source for these elements [116]. Cadmium, Cs, Pb and Bi were found to be more abundant in the $PM_{0.2\text{-}0.1}$ fraction and so may be from vehicle emissions. Correlations for Ba and Pb were improved when the $PM_{0.2}$ concentrations were used, suggesting traffic emissions as the source. Nickel, Zn and Se were evenly distributed through the different particles sizes (from PM_{10} to $PM_{0.2}$) indicating a range of sources. For Cu and Mo the correlation coefficient scores decreased as the particle size became smaller, which indicated traffic-generated resuspended dust particles. Ca was correlated with methylphenanthrenes in the finer fractions, a tracer compound (that also correlated with NOx and PNC) for diesel emissions, which suggested that there was a combustion/exhaust emission for Ca. This study observed differences in elemental composition across the particle size fractions indicating that the different vehicular sources of elements have different particle size emissions.

2.5.5.2.1 Differences in elemental composition by particle size fraction

Trace metal concentrations in nanoparticles, ultrafine, fine, and coarse particles sampled near a busy road in Taiwan were investigated using Principal Component

Analysis (PCA) to determine the source contribution to each fraction [127]. Differences were found across the size fractions with resuspended road dust the largest source for coarse particles while for fine, ultrafine and nanoparticles it was vehicle emissions. Nanoparticles were found to have a higher content of traffic related elements Ni, Cu, Zn, Cd, Ba and Pb. Zinc, Ba and Pb showed very high correlations with each other in the fine, ultrafine and nanoparticles and so it was proposed that these three metals were from traffic emissions [127]. At this location the concentration of V, Zn, Ag, Cd, Sb, Ba and Pb, in nanoparticles was found to be strongly associated with diesel fuel, whereas Mn, Cu and Sr in ultrafine particles were more associated with gasoline emissions [127].

At a roadside site in Hong Kong three groups of elements were identified. The first group mainly had a coarse size distribution (PM_{10-1}) and were attributed to natural sources such as crustal elements (Mg, Al, Si, Ca and Ti) and sea salt (Na and Cl) [139]. Another group was mainly in the PM_1 fraction and consisted of S, Cu, Zn, As, Se, Cd, Ba and Pb, elements that have been associated with vehicle emissions. Three elements, K, V and Ni were found to have both fine and coarse modes and K was likely from both anthropogenic and soil sources. Nickel and V were found to have similar size distribution indicating a similar source, which was suggested as ship emissions [139]. As demonstrated by these studies and similar to the road tunnel studies in the previous Section 2.5.5.1, finer particles are more related to vehicle emissions whereas the coarser particles contain crustal elements which are related to resuspended road dust, and are a challenging source to identify.

2.5.5.2.2 Contribution of resuspended road dust

At a roadside site the contribution of resuspended road dust can be determined as it would be one of the main sources of crustal material. Roadside measurements in an urban centre in India revealed that the PM_{10} fraction was composed of mainly soil crustal elements (74%) that included Al, Ca, Fe and Mg, likely due to resuspension of road dust. Ten percent of the PM10 was made up of elements associated with vehicle emissions and included V, Mn, Ni, Cu, Zn and Pb [140]. At a roadside site in Birmingham the elements that appeared mainly in the course particle fraction (PM_{2-10}) were Mg, Fe, Cu, Sr, Mo, Ba and Ce [116]. The source of these elements was crustal however Ca and Mo may have had an anthropogenic source owing to their predominant presence in the fine fraction [116].

In London, resuspended road dust was found to contribute 20-22% of the total PM_{10} concentration, while 19% was attributed to coarse sized abrasion sources, with the remaining 60% from vehicle exhaust and fine particle abrasion sources [136]. A number of factors have been shown to affect the scale of resuspended road dust and include HDV traffic count, wind speed and rainfall ([136] and references therein). Thorpe et al. [136] found that in a busy London street HDV count was the most influential factor on the resuspension of road dust. A weaker association with wind speed was also observed, which led Thorpe et al. [136] to suggest a two-step process where initially the traffic generated particles from turbulence and tyre shear, and then these particles are kept airborne by high wind speeds. No clear influence from rainfall was observed by Thorpe et al. [136], unlike that for Omstedt et al. [141] who noted variation in the PM_{10} concentration as a function of the wetness of the road. Thus the levels resuspended road dust is affected by traffic composition along with

the elemental composition, as demonstrated by the studies in Los Angeles in the next section.

2.5.5.2.3 Effect of traffic composition in selected Los Angeles case studies

A number of studies have been conducted near two Los Angeles freeways, the I-710 and route 110 as they have differing traffic composition. The I-710 is main traffic corridor for the port of Los Angeles and consequently has a high heavy-duty diesel fraction at 20% whereas sections of the route 110 are restricted to LDV traffic only. Fine and ultrafine (D_p < 180 nm) particles near the I-710 freeway was characterized for trace metals with the most abundant being S, Na and Fe [142]. Crustal enrichment factors (EF) were calculated for this site and an urban background site and revealed that for both size fractions very high EF for S, Cu, Zn, Mo, Sn, Sb, Ba and Pb were found at both sites implicating vehicle emissions as the source. Phosphorus, Ca, Fe, Cu, Mo and Sb were shown to have higher EF at the freeway site compared to the background site and therefore show possible enrichment from the freeway emissions. Of these elements P, Ca and Mo are associated with lubricating oil, while Fe, Cu and Ba are associated with brake wear [142] indicating the possible vehicular source.

Ning et al. [19] found higher emission factors for Cu and Ba on CA-110 (LDV only) freeway, a similar result to Ntziachristos et al. [142]. The highest emission factors were found for S, Ca and Fe, which represented the majority of the elemental contribution to the airborne particles. Iron and Ca are major components of crustal material and therefore the high levels of these elements were attributed to the resuspension of road dust. The S emission factor was much higher at the I-710 site (20% HDV) due to the higher levels of S in diesel fuel. Ning et al. [19] determined

emission factors for the I-710 that were in realistic agreement to those obtained by Grieshop et al. [35] in a tunnel with similar HDV content.

On-road sampling of the elemental concentration of $PM_{2.5}$ was done on the I-710 and CA-110 freeways [143], where previous roadside measurements have been conducted [19, 142]. Higher levels of Ba were observed on the I-710 while higher levels of Cu were observed on the CA-110. This would suggest that HDV are heavy emitters of Ba while LDV are the main source of Cu. The trace element EF were found to be higher on-road when compared to the near roadside measurements done previously [19], in particular for Mg, K, Ca, Mn, Fe, Cu, Zn, Mo and Ba [143]. Liacos et al. [143] suggested that roadside sampling is therefore underestimating the concentration of trace elements emitted by vehicles by exhaust and non-exhaust pathways.

2.5.5.3 ***Comparison between Roadside and Urban environments***

Typically in an urban environment, as would be expected, roadside locations have a higher concentration of elements than background sites. A concentration gradient for a particular element from a roadside location to an urban background site can give an indication that traffic emissions are a source of that element. This has been observed in a number of studies for both crustal and anthropogenic elements and so can give an indication of the source whether it is traffic emissions or resuspension of road dust [137, 139]. Concentrations of most of the crustal and anthropogenic element were higher at a roadside compared to a suburban site in Hong Kong. In particular, Cr, Fe, Co, Cu, As and Ba were found to have a concentration twice that of the urban background, suggesting a vehicular source for these elements [139].

Analysis of the PM_{10} fraction in Barcelona was conducted to determine the roadside enrichment of trace elements from roadside to urban background sites [144]. Elements that are tracers of traffic emissions, such as Cr, Fe, Cu, Sn, Sb and Ba demonstrated the highest enrichments at greater than 70%, while Cd and Zn showed lower roadside enrichments. Cobalt, As and Bi showed unexpected roadside enrichments of 23%, 47% and 78%, respectively suggesting a traffic link, though the vehicular source is uncertain [144]. Crustal material elements such as Ca, Ti, Ga, Sr, La and Ce showed a roadside enrichment of 30-40% as a result of road dust resuspension. As demonstrated by this study, the comparison between roadside and urban elemental composition can distinguish between the vehicle emissions and resuspended road dust and is further explored in the next two sections.

2.5.5.3.1 Contribution of vehicle emissions

A gradient in the urban Cu concentration was observed in the PM_{10} fraction in Zurich and Amsterdam, with the highest concentration observed at a kerbside location which gradually decreased to urban background level [145]. The same concentration gradient for Cu was not seen in the $PM_{2.5}$ fraction in these two cities, suggesting that the Cu is found in the $PM_{2.5-10}$ fraction. Cu was also seen to have an increasing concentration from rural to suburban to roadside sites in Switzerland, along with Ca, Mn, Fe, Mo, Rh, Sb, Ba, La, Ce and Pb most likely due to vehicle emissions [137]. At a roadside site in London the roadside concentration of Fe, Cu, Sb and Ba, were found to be four times that of the urban background [113], which would indicate a traffic source for these elements. In addition, at the roadside and urban background site Fe, Cu, Sb and Ba were all strongly correlated and had the same size distribution, which would further suggest a similar traffic related source for Fe, Cu, Ba and Sb [113, 119]. This roadside site was beside an intersection where there is heavy stop

start traffic., Combined with elemental composition of brake pads containing Fe, Cu, Sb and Ba, this would strongly suggest brake wear as the source [113, 119].

In several cities in the Netherlands, the elemental concentration of PM_{10} for several busy urban streets and background locations was compared and it was found that Cu, Cr and Fe were consistently elevated in the street locations [80]. The contrast was higher than that for crustal elements Al, Si and Ti, which therefore indicates a traffic source, likely non-exhaust emissions. The elevation of Cr was unexpected as there is no clear vehicle source for Cr, but it was also found to be highly correlated with tracers for traffic like NO_x, BC, Cu and Fe, further suggesting traffic as the source [80]. The elemental concentration $PM_{2.5}$ fraction, with the exception of Ni, S and V, were generally lower than in the PM_{10} fraction with only Cu and Fe consistently higher at street location in the $PM_{2.5}$ fraction. The contrast in Cr, Fe and Cu concentrations was similar to the high contrast for particle number and BC concentration, suggesting that non-exhaust emissions were a significant source of traffic emissions, along with direct tailpipe emissions.

2.5.5.3.2 Resuspended road dust

In addition to direct vehicle emissions, resuspended road dust also makes a significant contribution to ambient particulate matter pollution. At a roadside site, the highest concentrations of the crustal related elements were observed in the $PM_{2.5-10}$ fraction and were attributed to the contribution from resuspended road dust [137]. Amato et al. [146] was able to characterise the contribution of resuspended road dust to total traffic emission using PMF and a prior knowledge of the chemical nature of this source. PMF analysis revealed that resuspended road dust contributed to 37%, 15% and 3% to the total traffic emissions for PM_{10}, $PM_{2.5}$ and PM_1, respectively.

This therefore shows that the resuspended road dust contributed mainly to the coarser size fractions as opposed to exhaust emissions, which are generally associated with the finer fractions.

2.5.6 Urban trace elemental composition and concentration

The trace elemental composition and concentration in urban environment will vary depending on the nature of the sources present, and as such will vary across locations. This section will review studies conducted in urban environments grouped by location to assess the contributions and relative importance of traffic emissions and other sources to the elemental composition of airborne particles around the world.

2.5.6.1 ***North and South America***

Los Angeles is a city where vehicle emissions are a major source of fine particulate matter [147], and there have been many studies investigating the impact of vehicle emissions, as seen in the previous section 2.5.5.2.2 [19, 142, 143]. Singh et al. [148] in a study of the size distribution of trace elements at an urban site influenced by both industrial and traffic emissions, also observed traffic emission to be one of the main sources of $PM_{2.5}$. In the $PM_{2.5}$ mode, three groups of highly correlated elements [148] were observed. Titanium, Mn, Fe, Zn and Pb was the first group and as Pb was shown in a previous study to be predominantly from vehicle emissions [149] along with the differing size distributions, the likely source was road dust resuspension. In addition, Sn and Ba were found to be correlated with Pb. Therefore, they were also attributed to vehicle emissions while correlations between Ni and Cr pointed to an industrial influence in the $PM_{2.5}$ fraction. The elements found in the $PM_{2.5}$ fraction all had diurnal patterns that peaked in the early morning, followed by a steady decrease during the day [148]. Peak traffic corresponded with this morning peak concentration

and was subsequently attributed to vehicle emissions; with the steady decrease resulting from the dispersion of the fine particles by the increasing wind speed. Crustal elements, Al, Si, K and Ca were found mainly in the coarse mode ($PM_{2.5-10}$). Thus, at this site the main source of the trace elements in the $PM_{2.5}$ was anthropogenic: namely industrial and vehicle emissions.

At six sites within Los Angeles, the elemental composition and concentration of fine particles was analysed, with a focus on the port area [150]. Crustal enrichment factors (EF) were calculated similarly to Nztiachristos et al. [142] and minimal spatial variation was observed with fine particles having the highest overall EF compared to the larger size fractions. Elements previously associated with vehicle emissions such as S, Cu, Zn, Mo, Cd, Sb and Pb recorded the highest EF in the $PM_{2.5}$ mode. Concentrations of Cu, Sb and Ba were highly correlated across all size ranges indicating brake wear as the source of these elements. Nickel and V were also highly correlated and were attributed to shipping emissions, as the concentration of V decreased with distance from the port. The observed high levels of enrichment factors indicate that vehicle emissions were the main source of trace elements and in general for fine particles across Los Angeles [150].

Similarly, the $PM_{2.5}$ mass concentrations had a low spatial variations across rural, suburban, city centre and roadside sites in the Cincinnati metropolitan area [112]. In contrast, the elemental concentrations showed high spatial variation, especially for Mn, Ni, Zn and Pb, which had the highest concentration near a major highway indicating that these elements came from local sources, likely traffic. However, traffic intensity and meteorological parameters were found to have no significant

influence on elemental concentrations, which may have been due to the low variation in traffic volumes in the city [112].

The influence of traffic volume on the concentration of elements in PM_{10} was investigated in Rio de Janeiro, Brazil at five sites within the city with varying traffic intensities [118]. As expected, vehicle emissions were found to be a significant source of particulate matter at all sites based on the elemental composition. The background site was found to have the lowest concentrations, while the highest concentrations was found at the two sites with high traffic levels. Molybdenum, Rh, Pd, Sb and Pb were detected at all sites and these were attributed to the deterioration of catalytic convertors and to brake and engine wear, respectively [118]. This study highlights the importance of vehicle wear particles to the emissions of vehicles.

The trace elemental composition of three particle size fractions, nano (D_p 57-100 nm), fine (D_p 100-1000 nm) and coarse (D_p 1-10 μm) were compared at an urban location in Ottawa, Canada [151]. Particle mass was found to be concentrated in the coarse fraction, while the elements were found to be mainly in the finer fractions. Vanadium, Mn, Ni, Cu, Zn, Se and Cd were predominantly found in nanoparticles while the fine fraction had a different composition and contained primarily Mo, Fe, Sr, Sn, Sb, Ba and Pb. Many of these elements have been associated previously with vehicle emissions, and based on the particle size, vehicle emissions were suggested as the main source of the fine particulate matter at this site [151]. From these case studies in urban environments within North and South America, it can be seen that vehicle emissions were the main source based upon the trace elemental composition.

This is however, not necessarily true for other locations in the world as shown in the next section on European studies.

2.5.6.2 ***Europe***

There currently exists a large body of research on the trace elemental composition of urban particulate matter and its source identification and apportionment in Europe. As with the American studies from the previous section, differences in the trace elemental composition are apparent not just from country to country but also within a country. This was demonstrated in one study comprising of six urban centres in Spain, where there were significant differences in the elemental composition and concentration across the six centres unlike the particle mass concentrations [152]. There were three pollution sources identified; traffic, industrial and crustal with two cities, Barcelona and Alcobendas, were found to have a strong traffic influence due to high PM_{10} concentration of traffic related elements such as V, Mn, Ni, Cu, Zn, As, Cd, Sb, Ba and Pb. Crustal elements were also high in Barcelona indicating that resuspension of road dust was important. Combined with traffic emissions, road dust gave the highest average PM_{10} elemental composition levels in Spain. Overall this study demonstrates that the trace elemental composition is a better indicator than particle mass for determining the source contributions in urban environments [152]. The ability of the elemental composition to distinguish sources is further developed in this section by looking at the difference between size fractions in selected urban locations.

For example in Switzerland, the trace elemental composition of the $PM_{2.5}$ and $PM_{2.5-10}$ fraction at a rural, near city, suburban and roadside sites were found to differ based on the source [124, 137]. At all of the sites the $PM_{2.5}$ fraction contained mostly

elements associated with anthropogenic emissions, including road traffic markers Pb and Cd, while the $PM_{2.5-10}$ fraction was mostly crustal elements, such as Mg, Al, Ca and Fe [137]. In Barcelona, detected elements were also mainly from anthropogenic sources, with the most common elements being Ti, V, Mn, Cu, Zn and Pb. In Barcelona V, Ni and Cd were found mostly in the PM_1 fraction while crustal elements consisted of Li, Ti, Ga and Sr in the PM_{10} [153], highlighting that anthropogenic source emitted metals are generally in the finer fractions.

More detailed analysis of the source contribution was conducted in a later study at an urban background site in Switzerland [154]. The main elements present were Fe, Cu, Zn, Sb and Ba the $PM_{2.5-10}$ size fraction indicated that the largest source of metals was traffic predominately from vehicle abrasion products. Only two other factors were found for the $PM_{10-2.5}$, which were apportioned to the contributions from mineral dust and de-icing salt. Overall, traffic accounted for 28%, 9% and 2% of the trace elemental mass of $PM_{10-2.5}$, $PM_{2.5-1}$ and $PM_{1-0.1}$, respectively [154]. An industrial factor was present in the two smaller size fractions, which accounted for 2% in each fraction and that was characterised by Pb and Zn. These two factors were also seen in the $PM_{2.5-1}$ but not in the $PM_{1-0.1}$ size highlighting that the $PM_{2.5-1}$ fraction was the crossover between coarse mineral particles and the finer emissions particles.

The sources of the smaller particles, ultrafine ($PM_{0.5}$) and fine particles ($PM_{1.5-3.0}$) in Birmingham, UK were investigated [132]. In the fine fraction ($PM_{1.5-3.0}$), Mn, Fe, Cu and Ba were highly correlated and Birmili et al. [132] proposed that the source was brake wear emissions as these elements are all found in the chemical makeup of

European brake pads. The $PM_{1.5-3.0}$ fraction was predominantly composed of Na^+, Mg^{2+}, Ca^{2+}, Al, Fe, and Ba; this would indicate a mechanical or crustal source. Significant correlations in the coarse fraction were observed for Na^+, Mg^{2+} and Cl^-, which indicates a sea spray source, and also for Mn, Fe, Cu and Ba that indicates a vehicle emissions source [132]. In the $PM_{0.5}$ fraction Cd and Pb had the highest concentration, indicating a possible combustion or industrial source. In general, elements from anthropogenic sources, which can include vehicle emissions and industrial emissions, are predominantly found in the smaller particles size whereas crustal sources elements are in the larger particles. More detailed particle size analysis can reveal information on the vehicular process source, as demonstrated by Birmili et al. [132], who found brake wear emissions in a specific size fraction.

2.5.6.2.1 Temporal trends in elemental composition in European studies

The large number of studies conducted in Europe has allowed the long-term temporal variations in source contributions to be examined. Therefore this section focuses on the changes to vehicle emissions, as this has been found to show the most temporal variation, as demonstrated in the contribution of vehicle emissions to urban centres in Switzerland. Minguillon et al. [124] found that the PM_{10} trace elemental concentration at the urban site (Zurich) were similar to earlier studies [137, 155] apart from lower concentrations Zn, Cd and Pb, and increased levels of Sb. The decrease in Zn and Pb concentrations suggests an overall decrease in vehicle emissions over time. However, the increase in Sb points to an increased contribution from brake wear particles.

Differences in source contribution to the heavy metals between the $PM_{2.5}$ and PM_1 fractions was analysed for an industrial area of an Italian city [156, 157]. All of the

heavy metals, except Mn, were found to have high crustal enrichment factors in the $PM_{2.5}$, which would suggest an anthropogenic source [157]. Concentrations of the heavy metals in the $PM_{2.5}$ were influenced by wind speed, which is consistent with a stationary source. Two source profiles for the heavy metals in the $PM_{2.5}$ fraction were identified, and the included crustal elements (Fe and Mn) and elements related to industrial emissions (Cr, Ni and Cu) [157]. The second source was likely traffic and was characterised by Zn, Cd and Pb. In the PM_1 fraction, three likely sources of the trace elements were identified, which were crustal (Na, Mg, Al, K, Ti and Fe), industrial (Ca, Cr, Ni, Cu and Cd) and traffic emissions (Mn, Zn and Pb) [156]. Comparisons between the traffic sources from Ragosta et al. [157] and Caggiano et al. [156] are limited due to the 5 year difference in sampling time but it was noteworthy that the Pb and Zn are associated with traffic in both size fractions.

The temporal variation of the trace metal concentration of airborne particles at an urban background site in Barcelona was examined [153]. A seasonal variation was observed in the daily average concentrations of all trace elements in the fine and coarse fractions, with higher concentrations observed in winter. The cause of the seasonal variations was the stagnant weather conditions common during winter in Barcelona resulting in higher concentrations [153]. The exception was Ni and V, which were observed to have higher concentrations during summer, particularly in the finer fractions. Nickel and V have previously been associated with oil combustion [117] and it was proposed that the source was regional dispersal of fuel oil combustion from industrial smokestacks and shipping emissions [153]. Thus any seasonal variation is related more to the corresponding weather conditions as opposed to changes in emission patterns.

Some studies have examined the trace metal concentration with an hourly resolution in urban centres [153, 154]. In the $PM_{10-2.5}$ fraction, Fe, Cu, Sn and Sb had a diurnal pattern similar to that of peak traffic times in Zurich [154]. Similarly in Barcelona, a classic double peak rush hour pattern was observed for Cu, Sb, Sn and Ba, which was most prominent in the coarser fractions (PM_{10}) [153], suggesting a traffic related source for these elements in urban areas. Moreno et al. [153] observed little daily variation for Cu and Sb in the PM_1 fraction indicating that mechanical abrasion and road dust resuspension were the main emission processes for these metals. Manganese, Ni and Cr showed only a morning peak, which was attributed to industrial sources outside of the city brought in by overnight land breezes, which are common to Barcelona [153]. Therefore additional sources can overlay the traffic influence in a city brought on the by the air movements controlled by the microclimate particular to that city. Overall, the long term the element composition of vehicle emissions have changed as a result of changing vehicle technologies and this is likely to continue to be the case. Therefore, continued research on composition of airborne particles is necessary to keep abreast of the changing role of vehicle emission and other sources.

2.5.6.3 ***Elemental composition in Asian countries***

Vehicle emissions are one of the major sources of airborne particulate matter in Hong Kong, owing to the large number of vehicles on a small road network [75]. As a result, much of the research on elemental composition of particulate matter in Hong Kong has focused on roadside and tunnel location to characterise this important source [91, 139]. Hong Kong is also therefore an ideal location to study the influence of different types of vehicles, where Cheng et al. [91] calculated chemically

speciated emission factors for $PM_{2.5}$ by vehicle type across different microenvironments. Diesel vehicles were found to have higher speciated emissions factors compared to gasoline and LPG engines for all the trace elements in the $PM_{2.5}$ expect for V, Br, Sb and Ba. The majority of the on-road $PM_{2.5}$ emission for diesel and gasoline vehicles was carbonaceous, while trace elements made up 9% and 10% of the average emissions, respectively. Little variation in the elemental concentration has been observed between an urban site and rural site in Hong Kong with the strongest urban influence shown for Mn, Fe, Cu and Zn [92].

Other cities in Asia have also been shown to have a strong influence from vehicle emissions based upon the trace elemental composition, such as Kuala Lumpur [158]. In the $PM_{2.5}$, fraction PMF analysis showed that the main source was vehicle emissions. The first factor was attributed to two stroke engines, and was characterised by high loading of BC, Fe and Zn and also P, S, Mn and Br. The second factor contained high levels of BC, Al, Si, S, Ca, Fe and Br and this was attributed to motor vehicle emissions [158]. These two factors explained almost 68% of the $PM_{2.5}$ mass which indicates that traffic emissions were the main source of fine particle in this city.

In China, the influence of vehicle emissions in urban environments is not as strong as in the rest of the world. In Shanghai specially and China generally, the major source of heavy metals in $PM_{2.5}$ such as As, Cd, Sb and Pb was not traffic emissions but rather stationary coal-related industrial sources [159]. This is further illustrated by the observation that at a roadside site in Shanghai, the Pb and CO concentration was not found to be correlated so vehicle emissions were not the source, rather other

sources such as industrial emissions were important [160]. PMF analysis of $PM_{2.5}$ chemical composition in Beijing revealed that vehicle emissions and industrial emissions had small contributions, both at 6% to the total mass [161]. The largest source was found to be coal combustion (19%) [161], in agreement with other studies conducted in Beijing [162]. In general there is limited information on the chemical composition of particulate matter, particularly relating it to size distribution for China [162].

2.5.6.4 ***Elemental composition of Australian urban centres***

In Australia, there have been several studies investigating the elemental composition of fine particles in the major urban centres. The chemical composition of $PM_{2.5}$ in four Australian cities; Adelaide, Brisbane, Melbourne and Sydney was analysed to establish the different source contributions [163]. PMF was applied to determine the source profiles and eight factors which included crustal, marine, aged sea salt, secondary sulphate, nitrates, motor vehicle, other combustion and industry were identified. These factors can be considered to be representative of the emissions sources found in Australian cities. Across all of the cities, the motor vehicle factor was characterised by BC, Fe, Cu and Zn. A seasonal variation was observed in the contribution of sources to $PM_{2.5}$ where crustal and combustion sources were higher in winter then summer, attributed to decreased efficiency of vehicle engines and more frequent temperature inversions. Contributions of marine aerosols, secondary sulphates and industry were higher in summer due to stronger sea breezes, increased photochemistry and higher energy demand in summer. In addition to the seasonal variation observed in Chan et al [162], the temporal variation of sources over an extended period has been studied.

One such study involved the long term monitoring of the elemental composition of $PM_{2.5}$ at an urban location in Sydney [164]. PMF analysis on the elemental data revealed two factors that were attributed to vehicle emissions. The first vehicle factor had high loadings of H, BC, Zn, Br and Pb, and was attributed to vehicle emissions prior to the phase out of leaded petrol in 2001. The second vehicle factor had BC, Fe and H and was suggested to be typical of modern vehicles since 2001 [164]. PMF source contributions to overall mass over time showed a decrease in contribution from the first vehicle factor till the phase out, while the second factor contribution increased towards the end of the sampling. In Brisbane, Friend et al. [165] also observed a similar trend, where the phasing out of leaded petrol resulted in significant reduction in pollution level, probably due to lower levels of Pb and Br. Overall, the vehicle emissions demonstrated the most temporal change in these studies [164, 165], and the influence of vehicle emissions and other sources to the airborne particles has been further studied in Brisbane.

2.5.6.4.1 Trace elemental composition of ambient particles in Brisbane

There have been a number of studies into the elemental composition of particulate matter in Brisbane. Chan et al. [166] studied the elemental composition of PM_{10} and $PM_{2.5}$ and determined that crustal matter, marine aerosols, industrial dust and vehicle emissions were the main sources. At a suburban site sea salt and crustal components were identified as the main constituents of the course fraction while EC, organics, Pb, Br and sulphate were the major components in the fine fraction. In the absence of a dominant local source, such as road traffic, the PM_{10} elemental components from anthropogenic sources (such as EC, OM, Pb) at the suburban site had similar levels to the heavy industrial and light industrial/commercial sites. Therefore it was concluded by Chan et al. [166] that most anthropogenic emissions are evenly and

widely distributed across Brisbane and elements related to anthropogenic source were more in the fine fraction.

Further work on the source contributions to the $PM_{2.5}$ fraction in Brisbane found that most of the elements detected in the $PM_{2.5}$ fraction at a city centre site are anthropogenic and included Al, Si, V, Cr, Mn, Fe, Co, Cu, Zn, Sr, Mo, Br, Cd and Sn [8, 134]. Elements associated with vehicle emissions, Ca, Cr, Fe, Ni, Zn, Ba and Pb had higher concentrations in the sub-micrometer (D_p of 0.008 to 0.36 μm) particles compared to $PM_{2.5}$ fraction, indicating vehicle emissions as a major source [8]. In the later study by Lim et al. [134], $PM_{2.5}$ elemental concentration were higher compared to results from Thomas and Morawska [8] and this was attributed to an increase in road traffic beside the city centre site. Lim et al. [134] also found that the city centre site was the most polluted and had higher concentrations of Al, V, Mn, Zr, Sr and Mo in the fine fraction compared to a roadside site. In contrast, the roadside site, which had a strong influence from traffic and local industry, was observed to have higher concentrations of Mg, Co, Cu, Zn and Sn. It is clear from these three studies [8, 134, 166] that vehicle emissions are a significant source of the elemental composition of the Brisbane air shed. However, more advanced data analysis techniques were needed to fully elucidate the source contributions.

In addition to Chan et al. [163], more recent studies have applied the receptor model PMF to elemental composition of urban in Brisbane in order to improve the source apportionment. At a suburban site and a roadside site, analysis of the elemental composition by PMF extracted six and five sources, respectively [128]. At the suburban the largest contributor was found to be biomass burning which accounted

for 43.3% of the fine particles, with H, S, K and EC as the dominant species [128]. Other sources identified were soil (Al, Si, K, Ca, Ti and Fe), railways (Fe, EC, Zn and H) and aged (S, Na, EC) and fresh sea salt (Na and Cl). Vehicle emissions were found to contribute 2% of the $PM_{2.5}$ and was characterised by high concentrations of EC, Zn, Br, Pb and H and the low contribution of vehicle emissions at this suburban site was likely due to the fact that sampling site was not situated close to a main road [128].

At the roadside site, the most significant source was secondary sulphate, with sea salt, soil, and biomass burning also having similar profiles to those reported for the suburban site [128]. The roadside site was found to have a higher contribution from vehicle emissions, at around 30%, due to its closer proximity to roads, and the vehicle source was characterised by BC and Fe. As expected, the motor vehicle source was found to have the highest concentrations on weekdays compared to weekends at both sites and had a seasonal trend with higher concentrations in winter. Therefore, in Brisbane there are a number of sources contributing to the elemental load of $PM_{2.5}$ and these can be distinguished based upon their unique profiles. Depending on the proximity of a sampling site to surrounding roads, vehicle emissions can be a significant source, which has important implications when considering the concentrations at urban microenvironments such as schools.

2.5.7 Trace elemental composition of airborne particles in urban schools

As with EC and OC (see Section 2.4.8), there have been relatively few studies on the elemental composition of airborne particles and their contributing factors in schools. Two recent studies [108, 109], have looked at the effect of diesel bus emissions on the chemical composition of the outdoor ambient $PM_{2.5}$ mass in Cincinnati, USA. At

a school site affected by diesel bus emissions, there were elevated concentration of Ti, Mn, Fe, Cu, As and Pb compared to a control site, leading Li et al. [109] to suggest that these elements were related to bus emissions. In a separate study at four urban schools, Hochstetler et al. [108] focused on the $PM_{2.5}$ concentrations of traffic emissions related elements; Si, S, Ti, Mn, Fe, Cu, Zn, Br and Pb. Significant correlations between all of these elements with the exception of S were observed, and the lack of correlation of S with the other elements hypothesized to be due to the source of S being regional coal combustion [112]. As a result of the substantial number of correlations and moderate to high value of the correlation coefficients between these elements, traffic emissions were deemed to be a prominent source at the schools [108]. These two studies from Cincinnati illustrate that vehicle emissions particularly from school buses, can be a significant source of the outdoor trace elements present at schools.

The outdoor concentration of trace elements of $PM_{2.5}$ was also measured in Swedish schools in three urban locations, city centre, suburban and background [167]. Little difference was observed in the outdoor concentration of elements for the city centre and suburban schools, with the main elements found being S, K, Ca, Fe and Zn. The background schools had lower concentrations of many of the elements, notably for Ca, Ti, Mn, Fe and Cu, and this was attributed to the lower population density which resulted in lower traffic intensity [167]. In all schools, significant correlations were found among Cu, Zn and NO_2, indicating a traffic source for these two elements. This study by Molnar et al. [167] showed that vehicle emissions could affect the composition of airborne particulate matter in school regardless of their location within a city, but the concentrations may vary due to varying traffic intensity.

Overall, the limited studies in school environments mean there are significant gaps in knowledge related to the effect of traffic composition, especially for schools that are not serviced by school buses like the USA. As the studies to date have focused on $PM_{2.5}$, the size distribution of elements needs attention, especially in the light of recent literature that have found increased harmful health effects related to ultrafine particles. This will aid the toxicity assessment of elements in the smaller particles.

2.6 AEROSOL MASS SPECTROMETRY

2.6.1 Introduction

The high chemical complexity and size range exhibited by the airborne particulate matter, together with the rapid changes in particle chemistry and size that occurs in the atmosphere makes investigating the chemical and physical properties of atmospheric particles challenging. Aerosol mass spectrometers are able to address this issue due to their ability to analyse on-line the physical and chemical properties of aerosols with the high temporal resolution required. To achieve this, a typical aerosol mass spectrometer contains both a particle sizing section and mass spectrometer (MS) for the chemical analysis of the particles. In this respect, aerosol mass spectrometers are arguably the most significant development in aerosol measurements in the past 20 years [20].

There are two main classes of aerosol mass spectrometers, which are classified according to their ionization and vaporization technique. Thermal vaporization followed by electron ionization and laser vaporization and ionization are the two techniques, which are employed in the two commercially available instruments. One is the Aerodyne aerosol mass spectrometer (AMS) which uses thermal vaporization/electron ionization and can either have a quadrupole MS (Q-AMS)

[168] or a time of flight MS (TOF-AMS) [169]. The other is the TSI aerosol time of flight mass spectrometer (ATOFMS) [170], also available as an ultrafine ATOFMS (UF-ATOFMS) [171] which has better detection of smaller particles in the ultrafine range. Both of the TSI instruments use time of flight MS technique.

The different aerosol mass spectrometry techniques have different capabilities due to their different ionization techniques but can give complementary, though not necessarily the same, information on airborne particles. Thermal vaporization/electron ionization system can only analyse non-refractory chemical species but allows for quantifiable analysis. Laser ionization systems are designed to measure single particle spectra and are as such unable to give quantifiable results. However this system is able to analyse essentially all the chemical components of the particles. Both of these aerosol mass spectrometers have been applied successfully in the source identification of ambient particles. The focus will be on the AMS for this chapter as this was the aerosol mass spectrometer used in the current research. In the next section a description of the Aerodyne AMS instrument and its various models is given, followed by its application to the source identification and apportionment of organic aerosol, which are frequently the largest component of urban ambient particulates ([3] and references therein).

2.6.2 Description of Aerodyne Aerosol Mass Spectrometers

There are three versions of the Aerodyne aerosol mass spectrometer (AMS) that differ in the type of mass spectrometer used. The first developed AMS used a quadrupole mass spectrometer (Q-AMS) followed by versions with a compact time of flight mass spectrometer (TOF-AMS) and lastly a high resolution time of flight mass spectrometer (HR-TOF-AMS) described in detail by Jayne et al. [168],

Drewnick et al. [169] and DeCarlo et al. [172], respectively. A brief description of the three AMS follows.

*2.6.2.1 **Common aspects to all three AMS versions***

As illustrated in Figure 2-3 an AMS has three main sections, the aerosol sampling chamber, the particle sizing chamber and the particle composition detector chamber [168]. The aerosol sampling chamber comprises of a sub-micron inlet which samples the aerosol particles through a critical orifice at a flow rate of 1.4 cm^3 s^{-1}. Sampled aerosols are then passed through an aerodynamic lens system [173, 174], which focuses the particles into a narrow beam before they are transferred to the sizing chamber. Computational fluid dynamics simulations showed that the AMS inlet

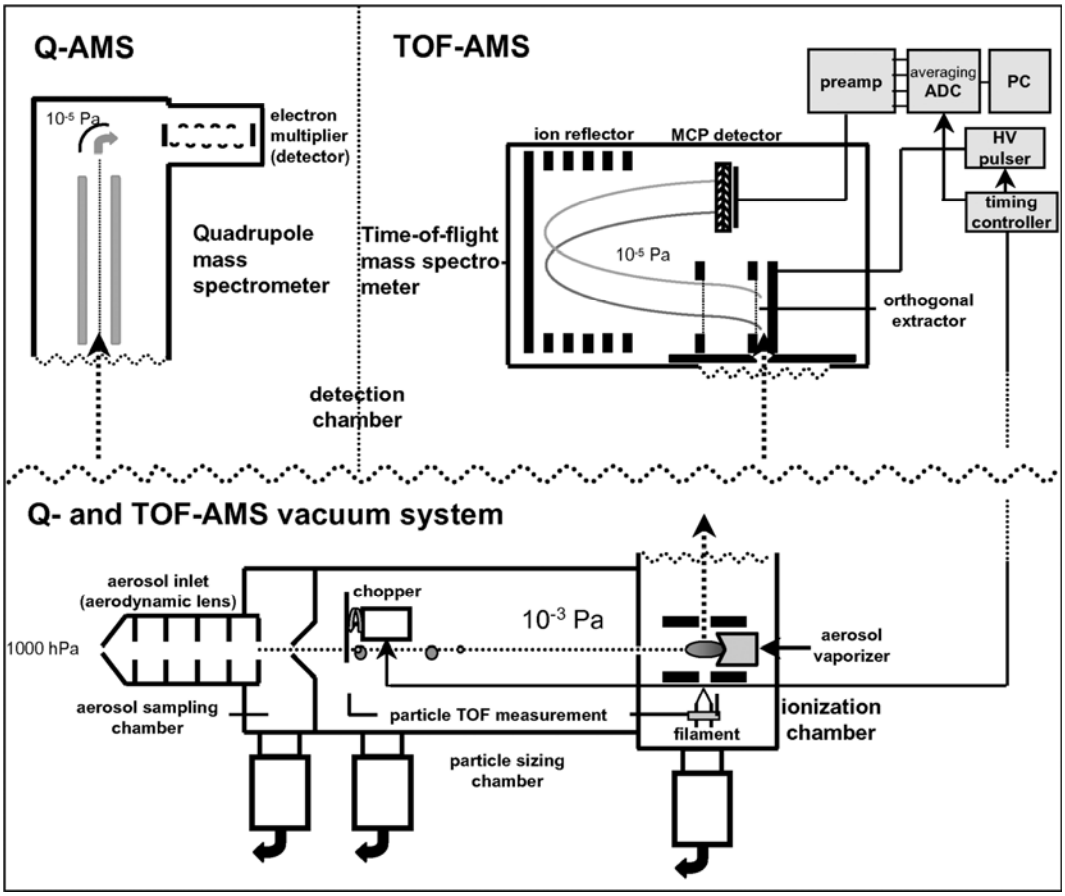

Figure 2-3: Schematic showing the Aerodyne aerosol mass spectrometer. The lower part shows the aerosol inlet and sizing regions that are identical to both designs. The upper part shows the mass analysers for the Q-MS on the left and TOF-MS on the right. (Reprinted from [175] with permission from Taylor and Francis).

system has 100% transmission efficiency to the detector for spherical particles in the aerodynamic range of 70-500 nm and considerable transmission for particles 30 – 70 nm and 500 nm – 2.5 μm. Non-spherical particles may have lower transmission efficiencies [168]. The transmission curve was verified experimentally by Jayne et al [168] for particles 100 nm to 1 μm in size. Thus the aerodynamic lens system is designed to sample the majority of the ambient atmospheric accumulation mode particles for analysis in the particle size chamber [21].

When the focused particle beam enters the particle sizing chamber, the particles are accelerated by gas expansion under vacuum to a terminal velocity related to their vacuum aerodynamic diameter. These particle velocities are determined by measuring the particle flight times between a mechanical chopper and the vaporizer surface [168] and the time of flight measurement is dependent on a fast particle vaporisation to the detector at the mass spectrometer scheme. The focused particle beam is regulated by a rotating chopper which operates in three modes: open mode which allows all of the particles through; closed mode which completely blocks the beam or chopped mode. Chopped mode regulates the transmission of the beam with a 1- 4% duty cycle that is determined by the chopper slit width and this mode is used to measure particle flight times before vaporization and detection [21].

Detection of the particles is achieved by directing the particle beam onto a resistively heated tungsten surface under high vacuum typically heated to 600°C. This is the optimum temperature for detecting the non refractory organic aerosols and major inorganic salts such as $(NH_4)_2SO_4$ and NH_4NO_3 generally found in ambient air [21]. Upon impact these components are vaporized and then the vapour undergoes

ionization by electron impact [168]. The resulting ions are guided into the mass spectrometer for detection.

2.6.2.2 ***Quadrupole AMS***

In the original AMS (Q-AMS), the ions are guided continuously into a quadrupole mass spectrometer (Q-MS) which selects ions according to the mass to charge ratio (m/z) [168]. In the MS (Mass Spectrum) mode of operation, a continuous mass spectrum is obtained without size information. The chopper is used to alternatively block or not block the particle beam allowing the background spectra to be recorded when the beam is blocked and the background spectra are subtracted from the open chopper mode to get the particle mass spectra [176]. The Q-AMS is only able to detect selected m/z in a given chopper cycle in the P-TOF (Particle Time-of-Flight) mode but obtains a particle size distribution for each of the selected m/z. Therefore these modes of the Q-AMS are only able to provide averaged information for the sampled aerosols and are improved upon by the TOF-AMS.

2.6.2.3 ***Time-of-flight AMS***

The Aerodyne time of flight aerosol mass spectrometer (TOF-AMS) employs the same aerosol sampling, particle sizing and vaporisation/ionisation equipment as the Q-AMS but it uses a time of flight mass spectrometer (TOF-MS) instead of a Q-MS [169]. A detailed description of the TOF-MS employed is described in Steiner et al. [177]. Briefly the ions are transferred continuously to the source region for the TOF-MS and are accelerated orthogonally to their flight direction into the mass spectrometer by a pulsed electric field to the detector. Unlike the Q-MS, a TOF-MS is not a scanning instrument. Therefore, it is able to measure a complete mass spectrum for each copper cycle [169].

The addition of the TOF-MS improves the sensitivity and time resolution to enable single particle chemical characterisation. In the TOF-MS a complete mass spectrum is acquired in 12 μs while for the Q-MS it takes 300 ms as each m/z is detected one at a time. There are three mode of operation for the TOF-AMS, the MS mode, the P-TOF mode, and the SP-TOF (Single Particle Time of-Flight) mode [169]. MS and P-TOF modes have the same function as for the Q-AMS except that the P-TOF mode can record a complete average size distributed mass spectrum for each chopper cycle. While in the SP-TOF mode, size dependent single particle mass spectra are obtained. Overall, the TOF-AMS offers improved performance with comparable results. When operated under well calibrated conditions and at the same location, the Q-AMS and the TOF-AMS have been shown to agree quantitatively [175]. Very good correlations with relatively narrow ranges were obtained for the comparison of the individual species concentrations. The exception was the organics, which had a broader correlation but this was attributed to the ability of the TOF-MS to detect all particles reaching the vaporiser, with some larger particles not detected by the Q-AMS skewing the data. Average size distributions of the individual species demonstrated good agreement between the instruments with the difference in calculated mode diameters being attributed to the increased sensitivity of the TOF-AMS [175]. Overall, the TOF-AMS was been shown to have improved sensitivity in measuring the particle size and chemical composition, which was extended by the next model.

2.6.2.4 ***High resolution TOF-AMS***

A later model of TOF-AMS utilised a high resolution orthogonal time of flight mass spectrometer (HR-TOF-AMS) with the increased mass resolution of the mass spectrometer further improving the chemical characterisation [172]. A HR-TOF-

AMS has two ion optical modes of operation for the mass spectrometer, v-mode and w-mode. In the v-mode the ions undergo single refection before reaching the detector while in the w-mode the ions have a flight path twice as long as v-mode as they have a second reflection before hitting the detector. Increasing the flight path will increase the mass resolution but it will reduce the total signal as fewer ions reach the detector. Consequently, the v-mode is more sensitive but w-mode gives higher mass resolution [172]. The main benefit of HR-TOF-AMS is that it can distinguish between organic ions at the same m/z and also differentiate between fragments enabling better chemical characterization, particularly for the largest and most complex component, the organic aerosols.

2.6.3 AMS analysis of organic aerosols

Organic aerosol (OA) is frequently the largest component of the non-refractory PM_1 (NR-PM_1) in many field studies, particularly for urban environments ([3] and references therein). The OA fraction of ambient air is a highly complex and poorly understood component and as such makes analysis of the compounds present and its characteristics difficult [4, 178]. Due to the nature of the mass spectra data provided by the AMS, individual organic compounds that are present in the OA are difficult to determine [21].

Gas phase reactions transform the OA component, making it a highly dynamic and complex system, as the OA is actually an intermediate between the gas phase precursors and products [3]. Hence recent efforts have focused on deconvoluting the organic aerosols spectra from an AMS in order to determine the type of OA present to aid source identification and apportionment. OA can be distinguished, based upon the source, as either primary or secondary OA. Primary OA (POA) is emitted directly

from sources, such as vehicle emissions and biomass burning while secondary OA (SOA) is formed by reactions of volatile organic compounds occurring in the atmosphere. SOA is the dominant component of the OA in urban environments [179, 180]; however modelling based upon traditional SOA formation precursors such as aromatics cannot account for the high levels of SOA observed in urban environments, particularly in summer [181].

POA are not static once emitted to the atmosphere, due to their semi volatile nature they undergo substantial photochemical oxidation to become very similar to SOA in short timeframes [181]. Thus oxidised POA contribute to the overall SOA load observed in urban environments and accounts for the high levels of SOA observed [3, 181]. As will be shown through this section, as the SOA ages the more chemically similar the SOA becomes. Therefore the OA is an intermediate between primary emissions of reduced organic species to the highly oxidised gaseous species (CO and CO_2) [3]. The ability to distinguish between the sources of OA is critical in enabling the understanding of the OA and this section outlines the efforts to develop methods to describe the source of the OA spectra in the literature. In a later section, the application of these methods in source identification and apportionment of OA in urban environments is discussed.

2.6.3.1 ***Distinction between primary and secondary sources of OA***

Organic mass spectra from an AMS was first split into two components by Zhang et al. [182] using an algorithm based upon certain m/z ions previously shown to be tracers for combustion and oxygenated organic aerosol. The first component was named hydrocarbon-like organic aerosol (HOA) due to similarities to the AMS spectra of hydrocarbon mixtures while the second component was called oxygenated

organic aerosol (OOA) due to the high oxygen content [182]. These two components explained 99% of the total OA, demonstrating that the algorithm was successful in quantifying the OA in that study [182]. Importantly, the use of these two components was a chemically meaningful method to describe the OA and is each discussed in detail below.

An earlier study [183] had shown the m/z 44 ion to be prominent in the mass spectra of highly oxidised organic particles, suggesting the possibility of its use as a tracer. The m/z 44 ion is due to the CO_2^+ ion and is likely due to the fragmentation of dicarboxylic acids, which are present in highly oxidised OA. Zhang et al. [182] observed that the levels of m/z 44 ion was correlated with the concentration of sulphates ($r^2 = 0.75$) and combined with the m/z 44 ion being found mostly in the larger particles strongly suggest the use of the m/z 44 ion as a tracer for oxidised OA. To describe these oxidised OA, the broader term of oxygenated organic aerosols (OOA) was employed by Zhang et al. [182] instead of SOA as there are sources for OOA other than secondary processes, for example vehicle emissions, which will emit OOA but at a small fraction of the overall OA. Another potential source of OOA is biomass burning and this influence is discussed later. OOA spectra was found to resemble that of aged aerosols in an urban/rural setting and also that of fulvic and humic acid, a class of highly oxidised OA which are considered models for aged and oxidised OA [182]. In addition, a good correlation was observed between OOA and sulphate, indicating that at least in this study OOA was a good surrogate for SOA [182].

For HOA, the m/z 57 ion is the tracer ion as it is one of the more prominent ions in the hydrocarbon series observed in previous studies of combustion exhaust aerosols [184, 185]. The m/z 57 ion was chosen over m/z 55 and 43, other ions prominent in the AMS spectra of combustion aerosols, due to lack of potential contamination from other oxygenated organic fragments, $C_3H_3O^+$ and $C_2H_3O^+$, respectively, limiting their usefulness as tracers for HOA. Good correlations with CO, NO_x and EC, which are known combustion tracers and the m/z 57 ion compared to the m/z 55 and 43, was a added confirmation for m/z 57 as a tracer for HOA [182]. The HOA is also considered to be a representative of primary OA (POA), as the spectra for HOA was found to closely resemble that of urban vehicle emissions [183], lubricating oil and diesel emissions [185]. In addition, the m/z 57 ion was found to be prominent in the ultrafine mode, further evidencing that it is due to primary sources, namely vehicle emissions. However, this work only demonstrates the qualitative worth of using single tracer ions for determining the components of OA, and more advanced data analysis techniques were needed for quantitative analysis.

*2.6.3.2 **Use of Positive Matrix Factorisation for determining the sources of OA***

A multiple component analysis technique, PMF, has been successfully applied for the quantitative analysis of the organic spectral data from an AMS (See e.g. [179, 180]). PMF is a technique widely used in the study of atmospheric particles (See review by Reff et al. [186]). It was developed by Paatero and Tapper [187] as a receptor modelling technique that determines the identity and contributions of sources based on the principles of factor analysis [186]. Two aspects of PMF make it suitable for environmental samples: there is a non-negativity constraint and it incorporates point-to-point uncertainty of the data point into the model. The advantage of using PMF over the methodology of Zhang et al. [182] is that it

requires no prior knowledge of the sources and provides quantitative analysis of the source contributions. However, the correct number of factors in the analysis by PMF is chosen by the user and this is the most subjective part of the process. Consequently, Zhang et al. [188] and Ulbirch et al. [180] recently proposed a methodology for selecting the correct number of factors for AMS OA data.

Lanz et al. [179] and Ulbrich et al. [180] analysed data from an urban background site in Switzerland and the USA, respectively, and compared the solutions with two to seven factors to determine the correct number of sources. In both studies, the two factor solution gave a HOA and OOA factor which were very similar to that of Zhang et al. [182]. With the addition of more factors, the HOA factor mass spectra was unchanged, whereas the OOA factor mass spectra and contribution changed with the number of factors as new factors were being extracted from the OOA component. Thus depending on the dataset, the two factor solution either overestimated or underestimated the amount of OOA [179, 180]. Furthermore, the OOA component/s cannot necessarily be taken solely as SOA because oxidised organic aerosols from primary sources are contributing to the OOA; however this does not reduce the ability of PMF to identify the sources.

More of the variability in the OA can be extracted using PMF and this has enhanced the source apportionment. This is evidenced in the case of OOA. Both Lanz et al. [179] and Ulbrich et al. [180] were able to determine two OOA components: one which was highly oxidised and therefore aged, and the other which was less aged due to its low volatility and did not match any previous reference spectra for SOA. Overall, the number of factors thought to best represent the data differed between the

studies, however the overall split between POA and SOA was similar between the studies at about one and two-thirds, respectively [179, 180]. Therefore, the number and type of sources factors for the OA in urban will differ and so identifying correct factors that best represents the data should be supported with external measurements.

Selected factors should be supported by correlations between external measurements to confirm source the proposed solutions. For example, in many studies the HOA component has been correlated with primary tracers such as CO and NO_x (See e.g. [179, 180, 182]) and consequently confirms that it is from POA. The OOA component has been correlated with secondary species, such as ozone and sulphate, in several studies pointing to it being SOA (e.g. [179, 182]). Another primary source, biomass burning OA (BBOA) has been found to correlate with biomass burning tracers acetonitrile and levoglucosan [189]. Overall, the source identification of the PMF derived factors from AMS OA mass spectra requires confirmation from external measurements due to the spectral variability of the OA types.

While the use of PMF has allowed the identification of more distinct OA types and sources, and resulted in better modelling of POA and SOA, there are limitations to its application owing to the dynamic and complex nature of OA in the atmosphere. For example, Mohr et al. [190] observed that vehicle emissions, plastic burning and meat cooking are likely to be pulled out as one HOA factor in ambient measurements due to similarities in their mass spectral profiles with unit mass resolution data. The use of a HR-TOF-AMS can aid in the distinguishing these and other primary sources, due to the larger difference in the high resolution mass spectra [191]. However, overall data with unit mass resolution is somewhat limited to identifying broad

classes of sources. In addition, a bilinear PMF model, with constant mass spectra, aids in the qualitative evaluation of the levels of oxidation but is overall a generalization due to the dynamic nature of the OA. Thus, unique constant mass spectra that are used to describe the variability in the OA by PMF may be more accurately described as points on a continuum rather than distinct components [192]. This is best illustrated in the continuum of oxidation of the OA that has been observed from fresh SOA to the aged OOA, and is demonstrated through the elemental analysis of OA.

2.6.3.3 ***Elemental composition of OA***

High resolution electron ionisation mass spectra from a HR-TOF-AMS is able to determine the elemental composition (H, C, N, O) for organic species, with an error of about 30% for individual species [193]. The O/C, H/C and N/C ratios of the total organic aerosols in ambient air can therefore be quantified using a HR-TOF-AMS [194]. However, the Q-AMS and c-TOF-AMS are not able to determine the elemental ratios directly as they have a unit mass resolution of the mass spectrum. An approximation of the O/C ratio for the unit mass resolution AMS data was presented by Aiken et al. [194] and was based upon the m/z 44 ion acting as a surrogate for the O/C ratio. This was possible as significant correlation ($r^2 = 0.84$) was observed in HR-TOF-AMS data between the f_{44} (where the f_{44} refers to the ratio of m/z 44 ion to the total organic mass) and the O/C ratio [194]. An approximation of the H/C ratio for unit mass resolution AMS data was developed by Ng et al. [195] and this was based upon the m/z 43 ion in SOA/OOA component datasets. In a similar method to that of Aiken et al. [194], the f_{43} (calculated similarly to the f_{44}) and the H/C ratio determined with HR-TOF-AMS data, was found to be related. This parameterisation however was found to be only valid for OOA components and not

for primary OA components such as HOA and BBOA where the $f_{44} < 0.05$ and hence require a separate parameterisation [195]. Therefore, the f_{43} can be considered a tracer for the H/C ratio but only for datasets with dominant OOA component such as urban environments. The different elemental ratios have been used as a reference enabling the comparison of sources from different locations.

Of particular interest is the O/C ratio as it gives an indication of the oxidation levels of the OA. The O/C ratio from laboratory experiments of specific sources of OA are summarised in Table 2-9. The vehicle emissions were observed to have the lowest ratios, whilst SOA had the higher ratios. BBOA and paper burning have a similar ratio to that of the chamber SOA studies. Chirico et al. [196] observed that after 5 hours of oxidation the O/C ratio for the POA from diesel exhaust increased from 0.21-0.37. Thus the O/C ratio can aid the source identification of primary and secondary OA from ambient datasets.

The elemental ratios, O/C and H/C, can also add weight to the identification of the source profiles determined using PMF. Ng et al. [197] compared datasets from 43 campaigns across the Northern Hemisphere and found that there was a clear distinction in the O/C values between the three main PMF factors, HOA, SV-OOA and LV-OOA at most of the sites. The HOA factor was found to have an O/C ratio less than 0.2 at the sites where it was identified. LV-OOA had the highest O/C ratio at 0.73 ± 0.14 while the SV-OOA factor had a ratio of 0.35 ± 0.14 across all sites. For the two OOA factors, the wide range in the O/C ratios is indicative of the continuum of the OOA properties in ambient aerosols [197] and as expected, the O/C

ratio has been observed to increase with SOA formation as a result of photochemical aging [194].

Table 2-9: O/C ratios from laboratory experiments on various sources of OA. Note that the chamber SOA experiments represent the values from a range of precursor compounds

Source of OA	O/C ratio	Reference
POA – diesel	0.03	[194]
POA – diesel	0.03	[190]
POA – diesel	0.1-0.19	[196]
POA - gasoline	0.04	[190]
POA - gasoline	0.04	[194]
BBOA	0.3-0.4	[194]
Paper burning	0.31	[190]
Meat cooking	0.11-0.14	[190]
Chamber - SOA	0.27-0.43	[194]

.

Table 2-10 summarises the O/C ratios for specific urban campaigns and they fall within the ranges observed by Ng et al. [197]. The two OOA factors identified by Huang et al [191] had similar O/C ratio which suggested that the differences in the mass spectra for these two OOA factors was related to the volatility or oxidation levels. Rather, it was found that the OOA factors correlated with meteorological changes and this was likely due to the difference in the background OOA compositions from different source regions [191]. Another source not previously mentioned that was identified in two of the studies listed in Table 2-10 was a cooking OA (COA) factor, which generally has O/C ratio that is in between that of HOA and SV-OOA and this suggested that it was a different source [198]. The COA factor is

spectrally similar to HOA, making it difficult to disentangle the two factors and is discussed further in Section 2.6.4.4.2. Therefore, the O/C ratio from ambient urban datasets is a useful tool in determining the age and source of the OA, but cannot always distinguish between the OOA types. Thus it should be used in conjunction with other analyses. However, the similarities observed in the O/C ratio across the different PMF derived OA sources led to the proposed standard mass spectra for the different sources.

Table 2-10: O/C ratios for the PMF derived factors at urban locations.
*Huang et al [191] identified two distinct OOA factors but did not call them SV-OOA and LV-OOA rather OOA-1 and OOA-2 as they were unlike the LV-OOA and SV-OOA standard spectra.

Location	HOA	COA	SV-OOA	LV-OOA	Reference
Mexico City	0.1	-	0.52	0.83	[194]
Northern Hemisphere	<0.2	-	0.35±0.14	0.73±0.14	[197]
New York	0.06	0.18	0.38	0.63	[198]
Beijing	0.17	0.11	0.47*	0.48*	[191]
PRD Region, China	0.11		0.45	0.59	[199]

2.6.3.4 ***Standardisation of the OA source components***

The PMF derived factors from the OA component of AMS data was found to have similarities across many studies, as shown in the previous section by the elemental ratios [197]. Therefore attempts have been made to determine standard spectra and a means of comparing the results from various studies. As discussed previously, the organic fraction from AMS datasets can be easily separated into HOA and OOA, with the OOA in many cases split further in two factors based upon the volatility and

oxidation levels, LV-OOA and SV-OOA [3]. However it is important to note here that the assignment of the LV-OOA and SV-OOA is not definitive and the components may have different composition at each site [197]. That is, in general the more oxidised component at site is referred to as the LV-OOA component for that location regardless of the actual level of oxidation. In addition, within the SV-OOA and LV-OOA factors there is some overlap between these subtypes and so there is a continuum in the properties in terms of oxidation and volatility in the OOA, which can make the comparison between sites difficult.

One standardised tool for comparing and distinguishing between the OA subtypes is the triangle graph developed by Ng et al. [197]. The OA subtypes are characterised by the two more dominant oxygen ions in the mass spectra, the m/z 44 (mostly CO_2^+) and m/z 43 ($C_2H_3O^+$ for OOA data and $C_3H_7^+$ in HOA data). Signal intensities of these two ions are determined by the ratio of the m/z 43 and 44 ions to the total organic signal, known as f_{43} and f_{44}, respectively. Differences in the f_{44} are used to classify the OA components and when the f_{44} is plotted against the f_{43}, the OA subtypes fall within a distinct triangle region on the plot, hence why it is known as the triangle graph. The triangle plot from Ng et al. [195] is shown in Figure 2-4 and gives the results from 43 ambient measurements and selected laboratory measurements. From Figure 2-4, the LV-OOA components are clustered at the top of the triangle space while the SV-OOA and HOA components occupy the bottom section of the triangle. The triangle on the graph is only meant to be a visual guide, yet it highlights some of the properties of the OA in the atmosphere. The base of the triangle shows that there is a wide range of precursor compounds in the atmosphere that undergo oxidation, while the fact that the data narrows up the f_{44} scale indicates

that the further it is oxidised the more similar OOA becomes.. Therefore the higher up a species is in the triangle the more aged and similar the OOA become regardless of the source. HOA are clustered on the base of the triangle, due to lack of oxidation, which distinguishes it from the OOA. The shaded area on Figure 2-4 represents where the laboratory data on SOA formation lies, and shows that generally the laboratory data are underestimating the oxidation of aged OA in the ambient atmosphere.

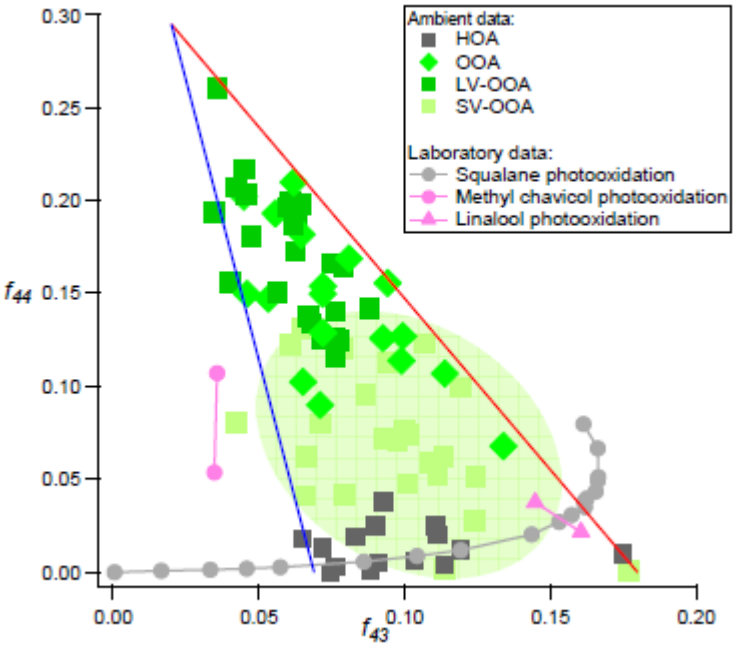

Figure 2-4: The triangle plot, with f_{43} and f_{44} plotted.
The triangle space is only a guide to show the trend as the OOA is oxidised.
(Reprinted from [195], under Creative Commons license 3)

The triangle plot that was developed by Ng et al. [197] was tested by chamber experiments via the oxidation of common SOA precursor compounds [200]. Overall, the study found that differences in the oxidative conditions had little effect on the mass spectra of the SOA as measured by the AMS. For example, the SOA generated under high and low NO_x conditions occupied similar areas of the triangle space.

Chhabra et al. [200] also observed that as the SOA was aged in the chamber it migrated to the top of the triangle along a path that was dependent on the precursor, with increasing carboxylic acid content and decreasing mass spectrum variability. In general, Chhabra et al. [200] were able to recreate the triangular space determined by Ng et al. [197] for ambient OOA in chamber experiments using a finite number of SOA precursors. This supports the hypothesis that increasing f_{44} values corresponds to increasing oxidation of the SOA and that it become spectrally similar with atmospheric aging. The similarities of the different OA components demonstrated by the triangle plot enabled the standard mass spectral profiles derived by PMF to be proposed

2.6.3.5 ***Standard spectra of the OA source components***

The organic component of 15 urban AMS datasets was analysed by PMF in order to determine a standard mass spectra for the different components: HOA, OOA, LV-OOA, SV-OOA and BBOA [201]. HOA and OOA components were identified at all 15 sites, while a BBOA factor was only identified at two of the sites. At six of the sites the OOA was able to be further deconvolved into the LV-OOA and SV-OOA. While the mass spectra for each of the components showed variation from site to site, they were found to be qualitatively similar. Figure 2-5 displays the average of each mass spectrum for the different components and this can be considered as a standard profile for each OA component [201]. In the HOA standard profile, the main features are the alkyl fragment signatures, which include the $C_nH_{2n+1}^+$ (m/z 29, 43, 57, 71 etc) and $C_nH_{2n-1}^+$ ion series (m/z 27, 41, 55, 69 etc). HOA standard profile correlated more with the mass spectra of POA sources such as lubricating oil, diesel fuel, diesel exhaust and cooking aerosols, rather than reference SOA or BBOA [201] and is

therefore likely to be a mixture of these anthropogenic combustions sources in the ambient atmosphere.

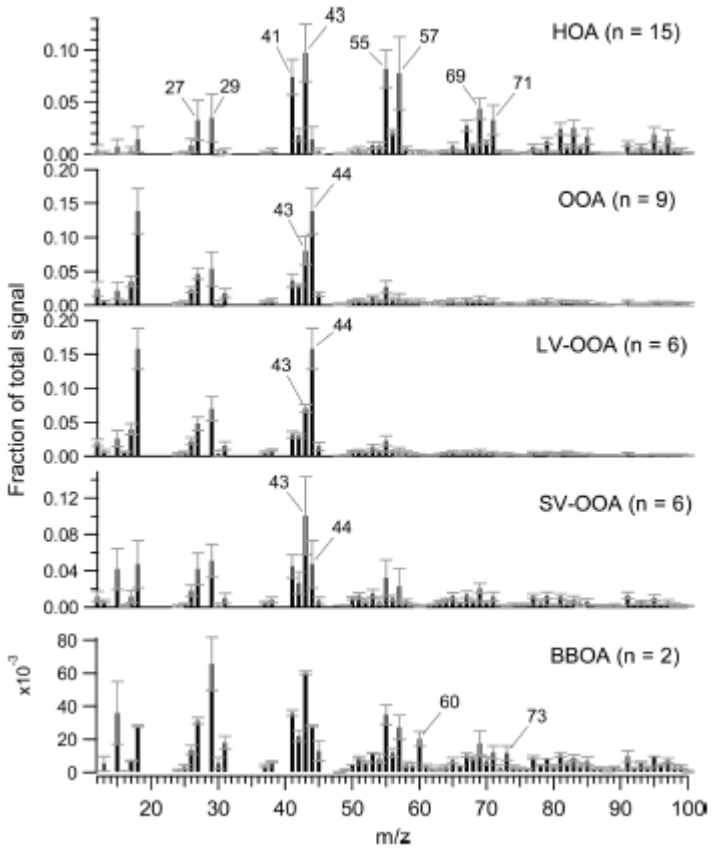

Figure 2-5: Standard spectra for the different OA components as determined by PMF analysis of 15 urban datasets.

(Reprinted (adapted) with permission from [201]. Copyright 2011 American Chemical Society.)

For all of the OOA mass spectra, the characteristic feature is the intensity of the m/z 44 ion (CO_2^+) peak which is used to distinguish between the SV-OOA and LV-OOA. The m/z 44 ion in the LV-OOA spectra has a greater intensity than the SV-OOA spectra and it is therefore more oxidised. At the sites where only one OOA component was identified, the mass spectra were more similar to the LV-OOA than the SV-OOA, and thus representative of more aged OA. Furthermore, the standard

LV-OOA and OOA spectra are considered indicative of SOA as they were more strongly correlated with the reference SOA than the POA sources and BBOA [201].

The SV-OOA standard profile was found to have a similar correlation with most of the previously mentioned reference mass spectra, but the best correlation was observed with the mass spectrum of fresher biogenic SOA [201]. On the other hand, the mass spectral profile of BBOA was distinguished by the presence of the m/z 60 ($C_2H_4O_2^+$) and 73 ($C_3H_5O_2^+$), which are the fragments ions known to be produced by levoglucosan, a tracer for biomass burning [201]. As expected for different primary sources, it was also noted that the BBOA profile was more oxidised than HOA,. Moreover, the BBOA profile was found to correlate well with the reference BBOA spectrum and not the POA and SOA references [201]. Nevertheless, the high spectral variability in the SV-OOA and BBOA spectrums can hinder the use of standard profiles in source apportionment for these two components. Overall, the standard profiles for the different OA components established by Ng et al. [201] in this study can be used to identify the sources of the OA in the ambient atmosphere.

2.6.3.6 ***Tracer ions for the different OA source components***

With the establishment of standard profiles for HOA, OOA and BBOA ions that could be used as tracers for these components were investigated by Ng et al. [201]. The tracer ions used are ions that are characteristic to each profile and whose signal intensity strongly correlates with the total concentration of that particular component, even if it is only a small part of the overall signal. In the HOA mass spectrum, the m/z 57 ion, though it did not have the strongest signal, was found to be more pronounced in the HOA profile than in the OOA and BBOA profiles and was therefore chosen as the HOA tracer ion. The most prominent ion in the OOA profile

was the m/z 44 ion; coupled with the low signal in the HOA profile, it was used as a tracer ion for OOA. For BBOA, the m/z 60 ion was more pronounced when compared to the HOA and OOA spectra and can thus be considered as a tracer ion for BBOA [201]. Thus suitable tracer ions were identified for the HOA, OOA and BBOA components and were then analysed to determine their suitability for quantitative analysis.

Quantitative analysis based upon the tracer ions required a scaling factor for each ion based upon the correlation of the time series of the PMF determined concentrations of the components and the corresponding tracer ions [201]. Thus the total OOA concentration was estimated from the m/z 44 ion concentration whereas the HOA concentration was could not be determined just from the m/z 57 concentration, as high resolution spectral analysis of ambient OA at this m/z revealed two responsible fragments [189]. The main fragment was from $C_4H_9^+$, which is part of the hydrocarbon series and HOA, but it also contains a significant contribution from $C_3H_5O^+$, an oxygenated fragment from OOA. Ng et al. [201] determined the following linear relationships for estimating the concentration of HOA and OOA from the tracer ions:

$HOA = 13.4(C_{57} - 0.1 \times C_{44})$

$OOA = 6.6 \times C_{44}$

where C_i is the mass concentration of the tracer ion i.

The estimated concentration was found to be within ±30% of the PMF results at most of the sites. Time series of the tracer ion estimates correlated with the time series from the PMF analysis, with an r^2 of 0.67 to 0.97 [201]. Therefore, the tracer ions

gave a reasonable estimate of the concentrations of the HOA and OOA components based upon the determined linear relationship. (Ng et al. [201] did not attempt this method for the BBOA components as it was only identified at two of the sites and but has been studied elsewhere in the literature.)

The use of the m/z 60 ion as a tracer for biomass burning was further investigated by Cubison et al. [202] by comparing data with insignificant biomass burning and data from biomass burning plumes. In urban datasets with negligible biomass burning present, a background level of the m/z 60 ion was of 0.3 ± 0.06% was established for the total OA mass, and this represented the contribution to the m/z 60 from non-biomass burning sources [202]. Therefore any urban OA with m/z 60 signal over this background is affected by biomass burning. Photochemical aging of BBOA was investigated by plotting f_{44} and f_{60}, in a similar fashion to the triangle plot described in an earlier section. The f_{44} axis represents the oxidation level of the OA, whilst the f_{60} signifies the influence of biomass burning and hence the age of the BBOA. Figure 2-6 shows the general trends observed by Cubison et al. [202] in the oxidation levels from urban/biogenic data and biomass burning plume data. Urban and biogenic datasets had a uniform f_{60} value around that of the background level irrespective of the f_{44} value. BBOA data exhibited a decreasing f_{60} value as the f_{44} increases, indicating that as the BBOA becomes more aged, the m/z 60 ion signal decreases. However, even aged BBOA retains the m/z 60 signature, indicating its usefulness as a tracer.

Overall, the analysis methods for OA described in this section; PMF, elemental ratios and tracer ions are useful methods for identifying and quantifying the various OA

components. As such they have been applied to both laboratory and ambient measurements to further our understanding of OA. The next section details of recent efforts from the literature in describing the OA and the causal factors to the observed composition and load.

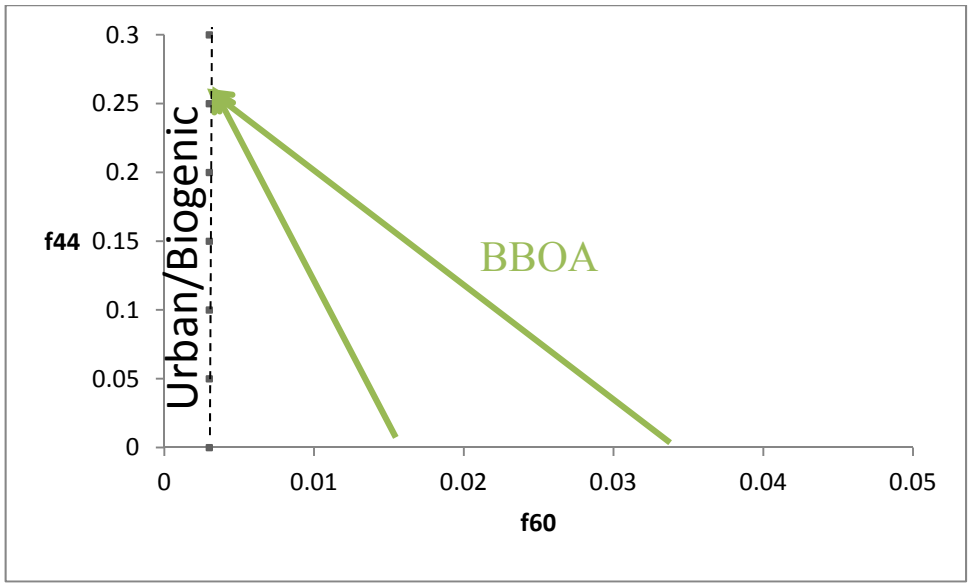

Figure 2-6: Schematic diagram of the trends for urban OA and BBOA plumes on the f_{60} and f_{44} plot. Solid black line represents the background level.
Adapted from Cubison et al. [202].

2.6.4 Source Apportionment of OA using AMS

2.6.4.1 ***Chamber studies of the oxidation of OA***

Chamber experiments with traditional SOA precursors do not produce OA that match the mass spectra of the aged OA or accounts for the levels of SOA observed in field studies [203]. To account for this difference Robinson et al. [181] proposed that the difference was due to the photo-oxidation of POA occurring urban atmosphere. To test this hypothesis aerosol mass spectrometry was used to characterise the photo-oxidation of diesel exhaust, as a surrogate for POA, in an environmental chamber and to assess the contribution of POA to the levels of SOA found in ambient air [181, 196, 203]. As expected, the POA mass spectra were dominated by alkyl fragment ion

series with an O/C ratio of 0.1-0.19 and was found to be independent of the engine conditions [196].

When the diesel exhaust emissions were subjected to photochemical oxidation, SOA formation was observed to start quickly, after 15 minutes, and the oxidation continued throughout the 5 hour experiments [196, 203]. Rising levels of POA oxidation were distinguished by an increasing ratio of the m/z 44 to m/z 43 ion [203] and also by an increased m/z 44 ion signal and a corresponding decrease of the m/z 57 ion [196]. In the study by Chirico et al. [196] after 5 hours of aging approximately 80% of the total OA was secondary, with an O/C ratio of 0.21-0.37, indicating the increased level of oxidation [196]. Sage et al. [203] found that 40% of the OA was SOA after 5 hours of oxidation and that the mass spectrum of the resultant SOA in the chamber closely matched that of OOA from previous field studies. Overall, the mass spectrum of the total OA was starting to appear like the ambient aged organic aerosol observed in field studies suggesting the oxidation of the POA could continue longer than 5 hours.

These results show that a large amount of SOA is formed by the oxidation of POA from diesel exhausts [181, 203]. In addition, these experiments illustrate how quickly the oxidation can occur, with it starting to appear like ambient OOA spectra after only a few hours and would suggest that the majority of OA in urban environments should be secondary since the POA under goes rapid photo oxidation, especially during summer [181]. As will be shown in later sections, this is in agreement with field studies, which have shown that SOA is the dominant type of OA in urban environments. However, in close proximity to vehicle traffic, it would still be

expected that primary emissions comprise the majority of the ambient OA, and this is investigated in the next section on roadside measurements with an AMS.

2.6.4.2 ***Roadside measurements of OA***

Deployment of an AMS at a roadside site allows for the characterisation of vehicle emissions and its contribution to ambient particles. The high temporal resolution of the AMS can capture the variation in chemical composition of airborne particles as a result of vehicle emissions to determine the driving factors. A HR-TOF-AMS along with gaseous and BC monitors were deployed in a Swiss tunnel to determine the chemical composition of mixed fleet emissions [204]. A distinctive diurnal pattern marked by peaks during morning and afternoon rush hours on weekdays was observed for the concentrations of all measured chemical species as expected for an environment dominated by vehicle emissions. OA and BC were the major chemical species in the tunnel with the highest concentrations observed on weekdays, when HDV traffic was more frequent (11 ± 4%). Whereas on weekends when the average traffic density was similar to weekdays but with lower percentage of HDV (0.6%), the average mass loadings of OA and BC decreased by a factor of 3 and 2, respectively. OA mass spectra in the tunnel was highly correlated with POA mass spectra from a light duty diesel vehicle with a speed similar to the average vehicle speed in the tunnel [204]. Overall, this study demonstrates that the OA in the tunnel resembled HOA, further indicating it can be used as a surrogate for fresh vehicle emissions to assess its variation near roadways.

A HR-TOF-AMS was deployed near a main highway in New York in order to characterise the variation in chemical composition and size distribution of the NR-PM_1 [205]. Overall the main influence of traffic on the NR-PM_1 was on the organic

component whereas the inorganic species (sulphates, ammonium and nitrates) showed little variation due to traffic. For the organic species the observed size distribution was bimodal, with peaks in the ultrafine (120 nm) and accumulation mode (550 nm). Inorganic species were found mainly in the accumulation mode that was also centred on 550 nm. These size distribution suggest that there is a mixture of fresh traffic emissions and a larger mode of more aged, secondary particles [205]. The chemical composition and size distribution of the OA was analysed to distinguish the sources of the OA. In the ultrafine mode, the OA was found to contain mostly HOA, which further suggests that this mode is due to fresh traffic emissions. OOA and sulphate showed a similar size distribution suggesting that they are secondary in nature and internally mixed [205]. Thus near a highway, vehicle emissions were the main influence on the OA present, particularly for the smaller particles. However this influence quickly diminishes as demonstrated by the next study.

The spatial variation in the levels of HOA and OOA downwind from a major freeway was determined with an AMS to assess the reach of vehicle emissions [206]. HOA reached background levels about 300 m from the highway, and had a similar spatial variation as CO_2 consistent with the HOA having a road source and that the gradient is due to dilution. In contrast, the OOA was not observed to have any spatial variation indicating that the OOA was aged OA. Near a highway, the ambient concentration of OA may be dominated by vehicle emissions, but this study showed that even as close 200m, the ratio of OA from vehicles can be the same as from ambient OA [206], which has implications for the exposure assessment of people to vehicle emissions. Therefore, this result highlights the need for techniques that can

deconvolve the OA into its components in order to fully appreciate the contribution from the different sources involved. This is particularly true for sites where the SOA concentrations are high and may mask the contribution of combustions sources to the total OA mass concentration. Another method for capturing vehicle emissions in ambient conditions is on-road mobile measurements.

*2.6.4.3 **Mobile measurements of vehicle emissions with an AMS***

Using a mobile laboratory equipped with an AMS allows vehicle emissions to be studied within seconds of their emissions under real world conditions. On-road measurements have shown that vehicle emissions levels are half those determined by dynamometer studies [206] and so on road measurements provide a more accurate picture of the contribution of vehicle emissions. Canagaratna et al. [185] conducted one such study with a Q-AMS on diesel buses emissions in New York City. Particles emitted by the diesel buses had a mass spectrum very similar to that for lubricating oil [207] as shown in Figure 2-7. Average size distributions for the total organic and sulphate had very similar shapes, both showing a small mode peaking at 100 nm and a larger mode that peaked at 550 nm [185]. This similarity in size distributions suggested that these two species are internally mixed within the exhaust aerosols. Traffic counts correlated with a small organic mode at 100 nm, indicating that this is a signature of aerosol from vehicles [185]. Overall, the non refractory organic component of diesel exhaust composed mainly of lubricating oil, along with a small contribution from sulphuric acid.

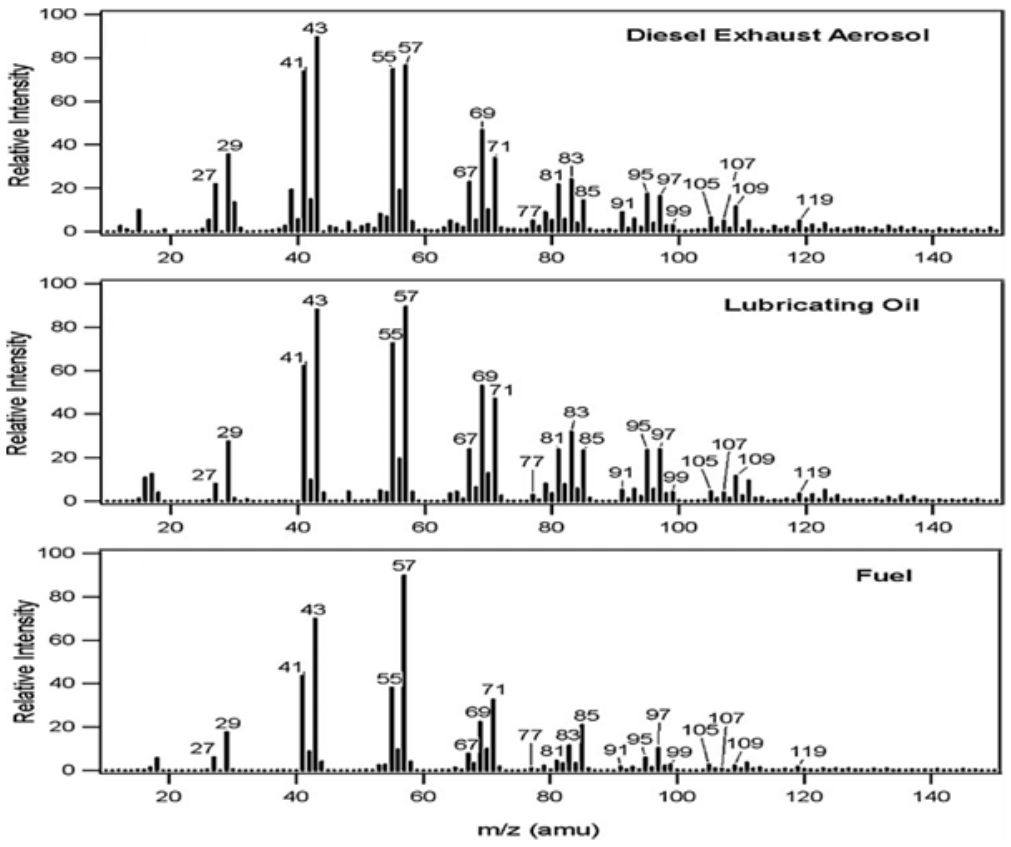

Figure 2-7: Comparison of Q-AMS mass spectra of diesel bus exhaust, pure lubricant oil and pure diesel fuel aerosols. The diesel bus spectrum is an average of the chase events in the study and the lubricant oil and diesel fuel spectra were obtained from laboratory aerosols. (Reprinted from [185] with permission from Taylor and Francis).

Further work on the emissions of HDDV was carried out with a mobile laboratory containing a Q-AMS, with data also gathered data on the motorway, inner city roads and rural roads when not chasing HDDV [208]. HDDV chasing events were characterised by having the highest PNC, comprising of mostly particles less than 200 nm which were mainly organic carbon plus a small amount of sulphate. Mass concentration of sulphate was found to be independent of measurement location and was thus likely not due to traffic emissions. Overall, the results from this work indicated that particles centred around 100 nm consisting of soot coated in organic were the main contribution from traffic, and these particles had the highest concentrations on the inner city roads [208].

Mobile measurements with an AMS have also been used to study the spatial variation in source contributions to the OA around a Zurich, Switzerland [209]. Three sources were identified for the OA using PMF, which were OOA, wood burning OA (WBOA) and HOA, and OOA was the largest organic fraction, followed by WBOA and HOA. As the study was conducted in winter, the OOA did not separate into the low and semi volatile fractions commonly seen in urban environments due to the small diurnal variations in temperature. Further analysis of the OA on the triangle plot from Ng et al. [197] revealed that the oxygenated organic fraction in Zurich was moderately aged OA [209]. Local traffic emissions were the source of the HOA and contributed to high concentrations of OA along major roads however the WBOA was found to be a more significant primary source in winter than traffic. The WBOA factor had the same contribution to the total OA for the urban background measurements (34%) as it did for on-road measurements (32%) suggesting that the WBOA source as either from regional sources or well mixed local sources [209].

This research which was conducted by Mohr et al. [209] highlighted the benefit of mobile measurements as it can distinguish between local and regional sources and provide information on the spatial distribution of different OA components around a city. However, there is limited information in the literature on the spatial variability of AMS OA source factors in urban areas and the impact of the local sources. As will be illustrated in the next section the majority of urban measurements with an AMS are located at one site in the city, thus providing limited information on spatial variation. Conversely, the work done thus far has focused on the physical and chemical properties for the source identification and apportionment in urban areas.

*2.6.4.4 **Source apportionment of OA in urban environments***

There exists a large body of research on the sources of OA in urban environments in the Northern Hemisphere [197] as OA is frequently the largest component of the NR-PM_1 in urban environments around the world, for example; Los Angeles [192], PRD region of China [199] and central Europe [210]. OA has been correlated with total particle mass, indicating that OA can be a key driver in the overall levels of pollution [199]. While the total OA diurnal pattern can display little variation, the diurnal variation of the OA components will typically show clear trends that are related to their source (See e.g. [199]). As discussed previously, these PMF-derived sources can include HOA, COA, BBOA, OOA and its subtypes, LV-OOA and SVOOA. The next sections will consider each of these components separately as there have been found many similarities between urban sites overall. In central Europe, the main influences on the differences in the composition of NR-PM_1 was the season (summer or winter) and the location of the site as opposed to the type of site (i.e. urban or rural) [210]. The composition of OA in selected urban areas is listed in Table 2-11, and on average the POA and SOA accounts for 1/3 and 2/3 of the total OA. The exception are observed generally in winter, when BBOA due to heating is more pronounced [7]. The size of the organic particles is also related to the source. This is considered in the next section followed by discussion on the different POA and SOA in urban areas.

2.6.4.4.1 Size distributions of OA and its relationships with sources

In urban environments a bimodal size distribution is often observed in the organic particulate matter [183, 213]. The larger mode, known as the accumulation mode, peaks between 200- 500 nm and consists of highly oxidised organic particles and inorganic species such as sulphates, ammonium and nitrate [183, 213].

Table 2-11: Percentage contributions for the various OA factors in selected urban areas.
Note [*]denotes LV-OOA, [**]denotes SV-OOA, - source factor not found. [^]Allan et al [7] did not describe this factor as BBOA as there was no peak m/z 60 ion but at m/z 73, rather as solid fuel OA as there was influence from burning of coal and other fuels related to heating.

Location	HOA (%)	OOA (%)	BBOA (%)	COA (%)	Reference
Manchester, UK	35	28	18[^]	19	[7]
London, UK	23	28	19[^]	30	[7]
Los Angeles, USA	15	55[*] + 30[**]	-	-	[192]
New York, USA	14	34[*] + 30[**]	-	16	[198]
Las Vegas, USA	26	26[*] + 34[**]	12	-	[211]
Beijing, China	18	58	-	24	[191]
PRD region, China	30	19[*] + 28[**]	24	-	[199]
Zurich, Switzerland	22	60	17	-	[154]
Barcelona, Spain	16	28[*] + 27[**]	11	17	[212]

This accumulation mode has been found to increase during photo-chemically active periods and was likely internally mixed aged aerosol [213]. The smaller mode, composed of mainly organics, peaked at around 100-150 nm and correlated well with NO_x and CO, tracer gases for vehicle emissions [213]. During morning rush hour, the concentration in the smaller mode has also been observed to peak [183]. Particles observed in this mode composed of a mixture of n-alkanes, branched alkanes, cycloalkanes and aromatics with a mass spectra similar to lubricating oil and diesel exhaust aerosols [185, 214]. This indicates that the source of these smaller particles is vehicle related [183]. Thus the size of the particles is related to the source, as further demonstrated using the OA components. OOA was found mainly in the accumulation mode that was centred on 550 nm, and had a similar size distribution to the inorganic species. In contrast, HOA had a distinct distribution that was broader, with around 30% by mass in the ultrafine mode [98].

2.6.4.5 ***Primary sources of OA in urban areas***

Primary sources of OA in urban areas include vehicle emissions, cooking and biomass burning. As discussed previously, these primary sources are likely to be extracted as one component, HOA [190]. For example, the HOA component can include a contribution from COA as demonstrated by the high O/C ratio due to the mass spectrum similarities [189, 199]. However, HOA, COA and BBOA sources of urban OA have been extracted successfully in many studies as will be demonstrated in the next sections.

2.6.4.5.1 Hydrocarbon-like OA in urban atmospheres

HOA is generally considered as a surrogate for vehicle emissions, as has been demonstrated in previous sections detailing roadside and chamber studies. This has also been found in many urban studies where the HOA concentration has been correlated with combustion tracers BC, CO, NO_x and EC [98, 154, 191]. The diurnal pattern of HOA in urban areas further supports vehicle emissions as the source, that can either follow the peak traffic with morning and afternoon peaks [154] or consists of a large morning peak which then decreased during the day as the boundary layer rose [7, 98]. The HOA from urban studies typically dominated by hydrocarbon peaks and so exhibits mass spectral similarities to vehicle emissions ([7] and references therein). HOA are generally the largest primary source of OA in urban areas however cooking emissions are increasingly being found to be as a significant source as vehicle emissions (see Table 2-11).

2.6.4.5.2 Cooking OA in urban atmospheres

Cooking aerosols are increasingly being recognised as an important source of OA in urban areas and have been reported in a number of recent studies (See e.g. [7, 191, 198]). As shown in Table 2-11, COA and HOA can have similar contributions to the total OA, highlighting how COA is potentially a significant primary source of OA in

urban environments. For unit mass resolution AMS data, COA and HOA are spectrally similar [190], the likely reason for it being detected in only a small number of studies despite the potential significant contribution of cooking emissions in urban areas. The use of HR-TOF-AMS has been more effective at distinguishing COA and HOA and has facilitated further understanding on the characteristics of COA.

The most distinguishing characteristic of COA in urban areas is its diurnal cycle with peaks that occur at the main cooking periods, which will vary depending on local customs but are generally in early afternoon and evening [191, 212]. The diurnal cycle of COA is thus distinct from HOA, which has peaks that generally follow rush hour traffic, and so the diurnal cycle is useful for source identification.

In addition, the O/C ratio as shown in Tables 2-9 and 2-10 can be used to differentiate between HOA and COA, with COA having a higher ratio due to the presence of oxygenated fatty acids. The mass spectrum of HOA and COA can be discriminated based upon key ions m/z 55 and 57 [198, 212]. In COA the signal intensity for the m/z 55 ion is stronger than the m/z 57 ion, in contrast to HOA where the two ions are about equal intensity, thus enabling the mass spectra to be differentiated [198]. Mohr et al. [212] further developed the use of the m/z 55 ion for distinguishing COA and demonstrated that the m/z 55 ion can be used as a tracer for COA based upon high resolution mass spectrum. COA are increasingly being found to be a significant source of POA in urban areas with the development of higher resolution AMS, along with another primary source, biomass burning.

2.6.4.5.3 Biomass burning OA in urban atmospheres

In urban areas, another primary source of OA that is frequently identified is BBOA as shown in Table 2-11. BBOA is distinguished based upon the m/z 60 and 70 ions,

attributed to the fragmentation of levoglucosan as discussed in detail in Sections 2.6.3.5 and 2.6.3.6 and as such correlates well with concentrations of levoglucosan and acetonitrile [189]. The sources of BBOA in urban areas are domestic heating, particularly in winter [210] and nearby forest fires [189]. OA from forest fires are generally aged. Therefore, it contains a strong signal at m/z 44 ion [202]. Whereas when fresh local emissions are the source of the BBOA, it is evidenced by the higher levels of m/z 60 ion [154]. BBOA is commonly observed in winter due to the influence of domestic heating; hence it displays a temporal variation and depending on the fuel used for heating it is also location dependent.

When domestic heating is the source of BBOA in urban areas, a distinctive diurnal cycle is often observed, with a large peak observed in evening around 8-9 pm [211]. However the OA from domestic heating is not always due to wood burning, as a domestic burning source has been identified, which lacked signal at m/z 60 but was present at m/z 73 [7]. Therefore Allan et al. [7] did not attribute the source to solely wood burning, rather suggested it contained emissions from coal and other solid fuel burning.

Thus there are three main primary sources of OA in urban environments. A nitrogen enriched OA source, which may be the result of industrial emissions has also been identified in only a limited number of studies accounting for only a small fraction (6-9% of total OA) [189, 198]. Thus this source factor is likely to be found at only certain locations. However, overall POA are not the dominant source of OA in urban areas, as shown by Table 2-11, rather it is secondary sources of OA and are the topic of the next section.

2.6.4.6 ***Secondary sources of OA in urban environments***

As shown by Table 2-11, in urban areas, OOA are the largest component of the OA, indicating that secondary sources are the main source of OA. Thus in urban areas the OOA can be considered as SOA as correlates with secondary species such as sulphate, nitrate and ozone [98, 189, 192]. As discussed previously, OOA can split into two subtypes: SV-OOA and LV-OOA both of which have been observed in urban atmospheres (See Table 2-11). The chemical composition of the LV-OOA and SV-OOA was examined by filter analysis during periods of high LV-OOA and SV-OOA concentration and this revealed a complex mixture of chemicals [192], with carboxylic acids as the main group in both LV-OOA and SV-OOA and phthalic acid across all periods. Shorter chain (C4-9) dicarboxylic acids characterised the LV-OOA periods and also contained notable amounts of nitrate and sulphate-substituted organics [192]. Thus the main functional groups present in the two OOA subtypes is similar, but are generally separated based upon their level of oxidation with the LV-OOA more oxidised. For all of the summer campaigns the OOA was split into the SV-OOA and LV-OOA fractions and Lanz et al. [210] proposed that the driving force for the separation of OOA into SV-OOA and LV-OOA could be the diurnal variation of temperature in the summer season.

The diurnal variation observed for OOA and or its subtypes offers clues to the source of the OOA. When the OOA has little diurnal variation the source is more regional OA [98]. Whereas a more distinct diurnal variation is often observed for SV-OOA, characterised by a peak in the mid-afternoon due to photochemical formation of SOA [192, 199]. Correlation with ozone are often observed during cases like this [192] further indicating SOA formation. Therefore the diurnal variation of the OOA subtypes can give clues to the sources.

However, OOA cannot always be conveniently split based upon the level of oxidation, as was observed by Huang et al. [191] in Beijing. Two OOA factors were determined by PMF which had similar O/C and H/C ratios but there were sufficient differences in the mass spectra and time series to justify two OOA factors. Huang et al. [191] proposed that the two OOA factors represent background OOA from two different source regions, to account for the difference in the mass spectra with similar oxidation levels. This was confirmed by back trajectory analysis which showed the two OOA factors coming in from different source regions during sampling. Therefore the terms LV-OOA and SV-OOA were not the most accurate description of the OOA subtypes and other terminology may be more appropriate.

Generally, when two OOA subtypes are identified differences in the volatilities of the sub-types are identified, usually by correlation analysis with less volatile ammonium sulphate and semi-volatile ammonium nitrate, the terminology LV-OOA and SV-OOA are sufficient [188]. However, in some studies, there have been two OOA factors identified that have had different O:C ratios but were not found to differ in volatility ([188] and references therein). In these situations, Zhang et al. [188] suggested that it is more appropriate to label the factors as more-oxygenated OOA (MO-OOA) and less-oxygenated (LO-OOA). Overall, as demonstrated with the triangle plot in Section 2.6.3.4, the source factors LV-OOA and SV-OOA or MO-OOA and LO-OOA are relative to each location and so are not always directly comparable.

In conclusion, as illustrated in the preceding sections, by utilising the advanced data analysis techniques available for the organic fraction, along with the development of suitable reference spectra for the organic components, aerosol mass spectrometry is therefore a useful tool for determining the source contributions in urban areas. The high temporal resolution afforded by the AMS also improves the source apportionment and enables more accurate source exposure estimates to be performed. This makes the AMS ideal for the characterisation of people's actual exposure to vehicle emissions and SOA in a specific urban microenvironment and the temporal variation as a result of local sources. One such microenvironment is urban schools, and is the topic of the next section.

2.6.5 Source contribution to the OA in urban schools

The use of AMS to study the source contributions that children are exposed in a school environment has been very limited. Brown et al. [211] employed a HR-TOF-AMS at an elementary school in Las Vegas near a major freeway to study the sources of OA present. OA concentration was found to be similar in both conditions that were downwind and upwind, relative to the freeway. This was in contrast to BC, CO, and NO_x tracers for primary emissions, which were on average twice as much in downwind conditions. OA had a distinct diurnal pattern with the highest concentration in the evening and also a peak during the morning peak traffic.

Brown et al. [211] employed PMF and was able to identify and apportion four factors in the OA, which were HOA, LV-OOA, SV-OOA and BBOA. HOA comprised on average 24% of the total OA and the concentration was found to increase to 40% during conditions downwind from the freeway. Also present alongside the POA was a background of OOA, with LV-OOA and SV-OOA accounting for an average of

29% and 34%, respectively. BBOA was found to peak in the evening as a result of residential heating. The paper by Brown et al. [211] highlights the potential exposure for school children to vehicle emissions in urban schools and that the levels will vary throughout the day, potentially leading to different levels of exposures during school hours. An AMS with its high temporal resolution can address the issue of children's exposure during school hours and the variation to get a better understanding of what children are actually exposed to.

2.7 HEALTH CONCERNS OF AIRBORNE PARTICLES

Airborne particles are known to be a serious health hazard and both the size and chemical composition of airborne particles have been shown to influence the toxicological effects [22, 215]. Exposure to airborne particles has been associated with harmful health effects to the respiratory [216], cardiovascular [217] and neurological systems [218]. Particle size is thought to affect the toxicity, as smaller particles can reach deeper into the respiratory system, with a clear relationship demonstrated between $PM_{2.5}$ exposure and adverse health effects [216, 217]. The chemical composition of particles is also considered to affect the toxicity, yet the relative effect of both the size and composition is still under debate [24, 219].

Ambient particles of different size have been associated with a variety of health effects, such as in a recent epidemiological study carried out in London, the coarser and nano-particles were more associated with respiratory and cardiovascular disease, respectively ([220] and references therein). Ultrafine and nano-particles are thought to be the most dangerous particle size fraction as the smaller size enables the particles to be deposited deeper into the lungs at greater numbers than larger particles [25, 221, 222]. In addition ultrafine and nano-particles are able to migrate into the

bloodstream, unlike larger particles, potentially affecting other large organs such as the heart and brain [223]. Nano-particles are known to cause a greater inflammatory response in the lungs than larger particles of the same material [224-226]. One suggested reason why nano-particles have an increased toxicity than larger particles is the higher surface area to mass ratio of nano-particles [225]. The surface chemistry of the nano-particles is important as the higher surface area enables it to absorb a greater fraction of possibly toxic chemicals onto their surface [25, 226, 227].

Currently there is a need for a better understanding of which chemical components are having the greatest effect on the toxicity of airborne particles [22, 24, 228]. As discussed previously in Section 2.3, ROS are thought to play a key role in particulate matter toxicity [22, 229]. Trace metals frequently found in ambient particle such as Fe, Cu, Ni, V, Zn and Co could be responsible for generating ROS upon contact with cellular material [229]. The trace elemental composition in urban areas also includes other toxic and carcinogenic compounds such as polycyclic aromatic hydrocarbons (PAH), Pb, Cd, Cr and As (See e.g. [127, 227]) which may also affect the toxicity. This was highlighted in one study, where ambient concentrations of known carcinogens (PAH, Cr, Ni and As) may have accounted for the observed association between long term $PM_{2.5}$ exposure and lung cancer [24]. In a recent review Chen and Lippmann [229] found evidence which suggests that ambient V, Ni, Zn and Pb had harmful health effects. Most of the evidence on the toxicity of the chemical components is based on ambient concentration as opposed to actual exposure, leading to considerable uncertainty on the causality. The low ambient concentrations of these toxic compounds also raise doubts as to whether the biological plausibility of the chemical components has a direct effect [229]. Therefore, as noted by Harrison

et al. [24], ambient particles may be a toxin in its own right, and the chemical composition may not matter, though more recent work would suggest otherwise [229].

As shown throughout this chapter, vehicle emissions are the largest contributor to air pollution in urban areas, and as such many studies have focused on the affect of vehicle emissions on human health. Systemic health effects of diesel emissions are generally thought to be as a result of the ultrafine particles [221], as will be shown in the following sections. This section seeks to highlight some of the potential health issues associated with exposure to vehicle emissions with the focus on children's health.

2.7.1 Respiratory effects on children

It is intuitive that air pollution would adversely affect the lungs and there is a growing body of evidence suggesting that children's exposure to traffic emissions has a detrimental effect on their respiratory health. Due to their immature respiratory systems and faster breathing rates, children are particularly at risk from harmful health effects of vehicle emissions [223, 230]. Genetic variation in children can also increase their risk from traffic emissions [231]. Traffic related pollution was measured in schools along a busy traffic corridor in San Francisco, and data about children's respiratory health in those schools was also collected, over a 12 month period [232]. Kim et al. [232] found significant increases in the odds of bronchitis symptoms and physician-diagnosed asthma in neighbourhoods with higher concentrations of traffic pollutants. Therefore this study found clear associations between traffic related pollution and asthma and bronchitis symptoms in an area with good regional air quality. Hospitalization rates for children with respiratory disease

across six Californian counties were studied and compared with air quality data for these counties [233]. Associations between hospital admission for childhood respiratory disease, especially pneumonia and exposure to $PM_{2.5}$ and it components, EC, OC, nitrate and sulphate was observed. As EC is a marker for vehicle emissions Ostro et al. [233] pointed out that small reductions in their ambient concentrations would have a noticeable effect on childhood respiratory morbidity.

Traffic related air pollution and its influence on the development of asthma in children in the first 8 years of life was studied in the Netherlands [234]. Gehring et al. [234] found a correlation between the levels of traffic related pollution at the birth address and the incidence and prevalence of asthma, and asthma related symptoms. This association was shown to be stronger for children who had not moved since birth [234]. In a study of children aged 10 to 18 years old found a positive association between traffic pollution and the onset of asthma [235]. Thus the long term exposure to traffic emission has been attributed to development of asthma in children up to the age of 18 years old.

Gauderman et al. [236] found that residential proximity to freeway traffic was associated with substantial deficits in lung function in 10 to 18 year old children. This conclusion was found to be independent of regional air quality, which suggests that children near freeways (<500m) are at risk even in areas with low levels of air pollution [236]. Ryan et al. [237] found that risk of wheezing in infants (<1 year old) was related to the type and distance from traffic where they lived. The highest prevalence of wheezing was among infants who lived less than 100m from stop and go bus and diesel traffic. In contrast to the results from Gauderman et al. [236],

infants less than 400m from high volume moving traffic did not have higher prevalence of wheezing [237], suggesting a complex relationship between exposure to traffic emissions and health effects. Exposure to traffic emissions in the first 12 months has been significantly associated with significant levels of wheezing at 36 months of age [238]. These studies indicate that for children there is long term health effects to the respiratory system related to exposure to traffic emissions, however the relationship is complex.

2.7.2 Cardiovascular effects

The most significant health risk attributable to ambient particles is actually to the cardiovascular as opposed to the respiratory system [223]. Short and long term exposure to ambient particles can adversely affect the cardiovascular systems [217, 239]. People with pre existing heart disease have increased risk to acute exacerbation on days with high concentrations of ambient particles [239]. In Beijing, short term exposure to airborne particles led to an increased risk of cardiovascular mortality with a two day delay, in addition the strongest association found was for submicron particle number concentration [240].

Long term exposure to ambient fine particles results in an increased risk of coronary heart disease over a person's lifetime [217, 241]. In a recent review, Mills et al. [241] implicated combustion derived nanoparticles as the main driver for adverse cardiovascular health effects. However a reduction in the concentration of ambient particles in a time span of a few years leads to a decrease in cardiovascular mortality, providing incentive for pollution reduction schemes [217]. Overall, the American Heart Association recently concluded that a causal relationship exists between exposure to ambient $PM_{2.5}$ and cardiovascular morbidity and mortality [217].

There is little information in the literature on the effects of airborne particles on children's cardiovascular health [242]. As such, Gao et al. [242] investigated the effects of airborne particles on children's cardio-respiratory fitness, as it is a good indicator for cardiovascular health later in life [243]. Gao et al. [242] concluded that long term exposure to higher concentrations of ambient particles led to a decrease in cardio-respiratory fitness. This was found to be independent of the children's physical activity levels as the benefits of physical exercise were negated by the increased pollutants inhaled during exercise. In general, exposure to airborne particles has been shown detrimentally affect cardiovascular health, with recent research suggesting for children exposure can lead to long term affects.

2.7.3 Neurological effects on children

Recent research in Mexico City has shown detrimental effects on the brains of children who are living in a highly polluted urban environment. Clinically healthy children living in a highly polluted urban environment exhibited deficits in fluid cognition, memory and executive functions compared to children living in a less polluted urban environment [244]. Also those children living in the highly polluted environment had white lesions on the prefrontal cortex and this could have contributed to their cognitive dysfunction. Similar lesions are observed in elderly patients with Alzheimer's disease. Calderon-Garciduenas et al. [244] suggested that ultrafine particles reaching the frontal cortex are likely to be causing the neuroinflammation.

Records of healthy children who lived in Mexico City and died suddenly were investigated to study the effect of long term exposure to high air pollution on their

brains [218]. Exposure to significant concentration of ultrafine particles and $PM_{2.5}$ was found to cause neuroinflammation and an altered brain innate immune response. Deposits of amyloid-beta and alpha-synuclein, proteins that are markers for Alzheimer's and Parkinson's disease, were also discovered on the children's brains. Therefore, Calderon-Garciduenas et al. [218] proposed that the neuroinflammation occurring as a result of exposure to air pollution might have a causative role in both Alzheimer's and Parkinson's disease and that long term exposure will result in higher risk for the development of these two diseases. The results from these two studies point to ambient particles affecting children's neurological function.

This section has highlighted some of detrimental health effects that have been associated with long-term exposure to airborne particles. In particular, for children detrimental health effects to the respiratory system have been associated with long-term exposure to vehicle emissions, with recent work also demonstrating influences on cardio-vascular and neurological function in children. The cause of these toxicological effects is thought to be related to the size and chemical composition of the ambient particles, however the relative contributions are unclear and the focus of current research.

2.8 REFERENCES

1. Sullivan, R. C.; Prather, K. A., Recent Advances in Our Understanding of Atmospheric Chemistry and Climate Made Possible by On-Line Aerosol Analysis Instrumentation. *Anal. Chem.* **2005,** *77*, (12), 3861-3886.
2. Lee, S. C.; Cheng, Y.; Ho, K. F.; Cao, J. J.; Louie, P. K.-K.; Chow, J. C.; Watson, J. G., PM1.0 and PM2.5 Characteristics in the Roadside Environment of Hong Kong. *Aerosol Sci. Technol.* **2006,** *40*, (3), 157 - 165.
3. Jimenez, J. L.; Canagaratna, M. R.; Donahue, N. M.; Prevot, A. S. H.; Zhang, Q.; Kroll, J. H.; DeCarlo, P. F.; Allan, J. D.; Coe, H.; Ng, N. L.; Aiken, A. C.; Docherty, K. S.; Ulbrich, I. M.; Grieshop, A. P.; Robinson, A. L.; Duplissy, J.; Smith, J. D.; Wilson, K. R.; Lanz, V. A.; Hueglin, C.; Sun, Y. L.; Tian, J.; Laaksonen, A.; Raatikainen, T.; Rautiainen, J.; Vaattovaara, P.; ehn, M.; Kulmala, M.; Tomlinson, J.; Collins, D. R.; Cubison, M. J.; Dunlea, E. J.; Huffman, A.; Onasch, T. B.; Alfarra, M. R.; Williams, P. I.; Bower, K. N.; Kondo, Y.; Schneider, J.; Drewnick, F.; Borrmann, S.; Weimer, S.; Demerjian, K. L.; Salcedo, D.; Cottrell, L.; Griffin, R.; Takami, A.; Miyoshi, T.; Hatakeyama, S.; Jayne, J. T.; Herndon, S. C.; Trimborn, A.; Williams, L. R.; Wood, E. C.; Middlebrook, A.; Kolb, C. E.; Baltensperger, U.; Worsnop, D. R., Evolution of Organic Aerosols in the Atmosphere *Science* **2009,** *326*, 1525-1529.
4. Goldstein, A. H.; Galbally, I. E., Known and unexplored organic constituents in the Earth's atmosphere. *Environ. Sci. Technol.* **2007,** *41*, (5), 1514-1521.
5. Morawska, L.; Ristovski, Z.; Jayaratne, E. R.; Keogh, D. U.; Ling, X., Ambient nano and ultrafine particles from motor vehicle emissions: Characteristics, ambient processing and implications on human exposure. *Atmos. Environ.* **2008,** *42*, (35), 8113-8138.
6. Toner, S. M.; Shields, L. G.; Sodeman, D. A.; Prather, K. A., Using mass spectral source signatures to apportion exhaust particles from gasoline and diesel powered vehicles in a freeway study using UF-ATOFMS. *Atmos. Environ.* **2008,** *42*, (3), 568-581.
7. Allan, J. D.; Williams, P. I.; Morgan, W. T.; Martin, C. L.; Flynn, J. L.; Nemitz, E.; Phillips, G. J.; Gallagher, M. W.; Coe, H., Contributions from transport, solid fuel burning and cooking to primary organic aerosols in two UK cities. *Atmos. Chem. Phys.* **2010,** *10*, (2), 647-668.
8. Thomas, S.; Morawska, L., Size-selected particles in an urban atmosphere of Brisbane, Australia. *Atmos. Environ.* **2002,** *36*, (26), 4277-4288.
9. Shi, J. P.; Harrison, R. M., Investigation of Ultrafine Particle Formation during Diesel Exhaust Dilution. *Environ. Sci. Technol.* **1999,** *33*, (21), 3730-3736.
10. Kittelson, D., Engines and Nanoparticles: A reveiw. *J. Aerosol Sci.* **1998,** *29*, (5/6), 575-588.
11. Kleeman, M. J.; Schauer, J. J.; Cass, G. R., Size and Composition Distribution of Fine Particulate Matter Emitted from Motor Vehicles. *Environ. Sci. Technol.* **2000,** *34*, (7), 1132-1142.
12. Phuleria, H. C.; Geller, M. D.; Fine, P. M.; Sioutas, C., Size-Resolved Emissions of Organic Tracers from Light- and Heavy-Duty Vehicles Measured in a California Roadway Tunnel. *Environ. Sci. Technol.* **2006,** *40*, (13), 4109-4118.
13. Chow, J. C.; Watson, J. G.; Crow, D.; Lowenthal, D. H.; Merrifield, T., Comparison of IMPROVE and NIOSH Carbon Measurements. *Aerosol Sci. Technol.* **2001,** *34*, (1), 23 - 34.

14. Cao, J. J.; Wu, F.; Chow, J. C.; Lee, S. C.; Li, Y.; Chen, S. W.; An, Z. S.; Fung, K. K.; Watson, J. G.; Zhu, C. S.; Liu, S. X., Characterization and source apportionment of atmospheric organic and elemental carbon during fall and winter of 2003 in Xi'an, China. *Atmos. Chem. Phys.* **2005,** *5*, (11), 3127-3137.
15. Watson, J. G.; Chow, J. C.; Lowenthal, D. H.; Pritchett, L. C.; Frazier, C. A.; Neuroth, G. R.; Robbins, R., Differences in the carbon composition of source profiles for diesel and gasoline-powered vehicles. *Atmos. Environ.* **1994,** *28*, (15), 2493-2505.
16. Watson, J. G., Visibility: science and regulation. *J. Air Waste Manag. Assoc.* **2002,** *52*, (6), 628-713.
17. Chu, C.-C.; Fang, G.-C.; Lee, S.-C.; Lin, I.-C., Characteristics of Carbonaceous Aerosol at a Near–Highway-Traffic Sampling Site During Spring 2006. *Environ. Foren.* **2008,** *9*, (4), 283 - 289.
18. Thorpe, A.; Harrison, R. M., Sources and properties of non-exhaust particulate matter from road traffic: A review. *Sci. Total Environ.* **2008,** *400*, (1-3), 270-282.
19. Ning, Z.; Polidori, A.; Schauer, J. J.; Sioutas, C., Emission factors of PM species based on freeway measurements and comparison with tunnel and dynamometer studies. *Atmos. Environ.* **2008,** *42*, (13), 3099-3114.
20. McMurry, P. H., A review of atmospheric aerosol measurements. *Atmos. Environ.* **2000,** *34*, (12-14), 1959-1999.
21. Canagaratna, M. R.; Jayne, J. T.; Jimenez, J. L.; Allan, J. D.; Alfarra, M. R.; Zhang, Q.; Onasch, T. B.; Drewnick, F.; Coe, H.; Middlebrook, A.; Delia, A.; Williams, L. R.; Trimborn, A. M.; Northway, M. J.; DeCarlo, P. F.; Kolb, C. E.; Davidovits, P.; Worsnop, D. R., Chemical and microphysical characterization of ambient aerosols with the Aerodyne aerosol mass spectrometer. *Mass Spectrom. Rev.* **2007,** *26*, 185-222.
22. Nel, A., Air Pollution-Related Illness: Effects of Particles. *Science* **2005,** *308*, (5723), 804-806.
23. Lough, G. C.; Schauer, J. J.; Park, J.-S.; Shafer, M. M.; DeMinter, J. T.; Weinstein, J. P., Emissions of Metals Associated with Motor Vehicle Roadways. *Environ. Sci. Technol.* **2005,** *39*, (3), 826-836.
24. Harrison, R. M.; Smith, D. J. T.; Kibble, A. J., What is responsible for the carcinogenicity of PM2.5? *Occup. Environ. Med.* **2004,** *61*, (10), 799-805.
25. Oberdörster, G.; Oberdörster, E.; Oberdörster, J., Nanotoxicology: An Emerging Discipline Evolving from Studies of Ultrafine Particles. *Environ. Health Persp.* **2005,** *113*, (7), 823-839.
26. Jamriska, M.; Morawska, L.; Thomas, S.; He, C., Diesel Bus Emissions Measured in a Tunnel Study. *Environ. Sci. Technol.* **2004,** *38*, (24), 6701-6709.
27. Hung-Lung, C.; Yao-Sheng, H., Particulate matter emissions from on-road vehicles in a freeway tunnel study. *Atmos. Environ.* **2009,** *43*, (26), 4014-4022.
28. Knibbs, L. D.; de Dear, R. J.; Morawska, L.; Mengersen, K. L., On-road ultrafine particle concentration in the M5 East road tunnel, Sydney, Australia. *Atmos. Environ.* **2009,** *43*, (22-23), 3510-3519.
29. Gidhagen, L.; Johansson, C.; Ström, J.; Kristensson, A.; Swietlicki, E.; Pirjola, L.; Hansson, H. C., Model simulation of ultrafine particles inside a road tunnel. *Atmos. Environ.* **2003,** *37*, (15), 2023-2036.
30. Kirchstetter, T. W.; Harley, R. A.; Kreisberg, N. M.; Stolzenburg, M. R.; Hering, S. V., On-road measurement of fine particle and nitrogen oxide emissions

from light- and heavy-duty motor vehicles. *Atmos. Environ.* **1999,** *33*, (18), 2955-2968.
31. Geller, M. D.; Sardar, S. B.; Phuleria, H.; Fine, P. M.; Sioutas, C., Measurements of Particle Number and Mass Concentrations and Size Distributions in a Tunnel Environment. *Environ. Sci. Technol.* **2005,** *39*, (22), 8653-8663.
32. Gouriou, F.; Morin, J. P.; Weill, M. E., On-road measurements of particle number concentrations and size distributions in urban and tunnel environments. *Atmos. Environ.* **2004,** *38*, (18), 2831-2840.
33. He, L.-Y.; Hu, M.; Zhang, Y.-H.; Huang, X.-F.; Yao, T.-T., Fine Particle Emissions from On-Road Vehicles in the Zhujiang Tunnel, China. *Environ. Sci. Technol.* **2008,** *42*, (12), 4461-4466.
34. Cheng, Y.; Lee, S. C.; Ho, K. F.; Louie, P. K. K., On-road particulate matter (PM2.5) and gaseous emissions in the Shing Mun Tunnel, Hong Kong. *Atmos. Environ.* **2006,** *40*, (23), 4235-4245.
35. Grieshop, A. P.; Lipsky, E. M.; Pekney, N. J.; Takahama, S.; Robinson, A. L., Fine particle emission factors from vehicles in a highway tunnel: Effects of fleet composition and season. *Atmos. Environ.* **2006,** *40*, (Supplement 2), 287-298.
36. Chang, S.-C.; Lin, T.-H.; Lee, C.-T., On-road emission factors from light-duty vehicles measured in Hsuehshan Tunnel (12.9 km), the longest tunnel in Asia. *Environ. Monit. Assess.* **2009,** *153*, (1), 187-200.
37. Allen, J. O.; Mayo, P. R.; Hughes, L. S.; Salmon, L. G.; Cass, G. R., Emissions of Size-Segregated Aerosols from On-Road Vehicles in the Caldecott Tunnel. *Environ. Sci. Technol.* **2001,** *35*, (21), 4189-4197.
38. Handler, M.; Puls, C.; Zbiral, J.; Marr, I.; Puxbaum, H.; Limbeck, A., Size and composition of particulate emissions from motor vehicles in the Kaisermühlen-Tunnel, Vienna. *Atmos. Environ.* **2008,** *42*, (9), 2173-2186.
39. Kittelson, D. B.; Watts, W. F.; Johnson, J. P., Nanoparticle emissions on Minnesota highways. *Atmos. Environ.* **2004,** *38*, (1), 9-19.
40. Westerdahl, D.; Fruin, S.; Sax, T.; Fine, P. M.; Sioutas, C., Mobile platform measurements of ultrafine particles and associated pollutant concentrations on freeways and residential streets in Los Angeles. *Atmos. Environ.* **2005,** *39*, (20), 3597-3610.
41. Fruin, S.; Westerdahl, D.; Sax, T.; Sioutas, C.; Fine, P. M., Measurements and predictors of on-road ultrafine particle concentrations and associated pollutants in Los Angeles. *Atmos. Environ.* **2008,** *42*, (2), 207-219.
42. Miljevic, B.; Fairfull-Smith, K. E.; Bottle, S. E.; Ristovski, Z. D., The application of profluorescent nitroxides to detect reactive oxygen species derived from combustion-generated particulate matter: Cigarette smoke - A case study. *Atmos. Environ.* **2010,** *44*, (18), 2224-2230.
43. Valavanidis, A.; Salika, A.; Theodoropoulou, A., Generation of hydroxyl radicals by urban suspended particulate air matter. The role of iron ions. *Atmos. Environ.* **2000,** *34*, (15), 2379-2386.
44. Knaapen, A.; Shi, T.; Borm, P.; Schins, R., Soluble metals as well as the insoluble particle fraction are involved in cellular DNA damage induced by particulate matter. *Molec. Cell. Biochem.* **2002,** *234-235*, (1), 317.
45. Li, N.; Alam, J.; Venkatesan, M. I.; Eiguren-Fernandez, A.; Schmitz, D.; Di Stefano, E.; Slaughter, N.; Killeen, E.; Wang, X.; Huang, A.; Wang, M.; Miguel, A. H.; Cho, A.; Sioutas, C.; Nel, A. E., Nrf2 Is a Key Transcription Factor That Regulates Antioxidant Defense in Macrophages and Epithelial Cells: Protecting

against the Proinflammatory and Oxidizing Effects of Diesel Exhaust Chemicals. *J. Immunol.* **2004,** *173*, (5), 3467-3481.
46. Dellinger, B.; Pryor, W. A.; Cueto, R.; Squadrito, G. L.; Hegde, V.; Deutsch, W. A., Role of Free Radicals in the Toxicity of Airborne Fine Particulate Matter. *Chem. Res. Toxicol.* **2001,** *14*, (10), 1371-1377.
47. Fairfull-Smith, K. E.; Bottle, S. E., The Synthesis and Physical Properties of Novel Polyaromatic Profluorescent Isoindoline Nitroxide Probes. *Eur. J. Org. Chem.* **2008,** *2008*, (32), 5391-5400.
48. Surawski, N. C.; Miljevic, B.; Ayoko, G. A.; Elbagir, S.; Stevanovic, S.; Fairfull-Smith, K. E.; Bottle, S. E.; Ristovski, Z. D., Physicochemical Characterization of Particulate Emissions from a Compression Ignition Engine: The Influence of Biodiesel Feedstock. *Environ. Sci. Technol.* **2011,** *45*, (24), 10337-10343.
49. Surawski, N. C.; Miljevic, B.; Ayoko, G. A.; Roberts, B. A.; Elbagir, S.; Fairfull-Smith, K. E.; Bottle, S. E.; Ristovski, Z. D., Physicochemical Characterization of Particulate Emissions from a Compression Ignition Engine Employing Two Injection Technologies and Three Fuels. *Environ. Sci. Technol.* **2011,** *45*, (13), 5498-5505.
50. Surawski, N. C.; Miljevic, B.; Roberts, B. A.; Modini, R. L.; Situ, R.; Brown, R. J.; Bottle, S. E.; Ristovski, Z. D., Particle Emissions, Volatility, and Toxicity from an Ethanol Fumigated Compression Ignition Engine. *Environ. Sci. Technol.* **2009,** *44*, (1), 229-235.
51. Kumagai, Y.; Koide, S.; Taguchi, K.; Endo, A.; Nakai, Y.; Yoshikawa, T.; Shimojo, N., Oxidation of Proximal Protein Sulfhydryls by Phenanthraquinone, a Component of Diesel Exhaust Particles. *Chem. Res. Toxicol.* **2002,** *15*, (4), 483-489.
52. McWhinney, R. D.; Gao, S. S.; Zhou, S.; Abbatt, J. P. D., Evaluation of the Effects of Ozone Oxidation on Redox-Cycling Activity of Two-Stroke Engine Exhaust Particles. *Environ. Sci. Technol.* **2011,** *45*, (6), 2131-2136.
53. Geller, M. D.; Ntziachristos, L.; Mamakos, A.; Samaras, Z.; Schmitz, D. A.; Froines, J. R.; Sioutas, C., Physicochemical and redox characteristics of particulate matter (PM) emitted from gasoline and diesel passenger cars. *Atmos. Environ.* **2006,** *40*, (36), 6988-7004.
54. Cheung, K. L.; Ntziachristos, L.; Tzamkiozis, T.; Schauer, J. J.; Samaras, Z.; Moore, K. F.; Sioutas, C., Emissions of Particulate Trace Elements, Metals and Organic Species from Gasoline, Diesel, and Biodiesel Passenger Vehicles and Their Relation to Oxidative Potential. *Aerosol Sci. Technol.* **2010,** *44*, (7), 500 - 513.
55. Biswas, S.; Verma, V.; Schauer, J. J.; Cassee, F. R.; Cho, A. K.; Sioutas, C., Oxidative Potential of Semi-Volatile and Non Volatile Particulate Matter (PM) from Heavy-Duty Vehicles Retrofitted with Emission Control Technologies. *Environ. Sci. Technol.* **2009,** *43*, (10), 3905-3912.
56. Ntziachristos, L.; Froines, J.; Cho, A.; Sioutas, C., Relationship between redox activity and chemical speciation of size-fractionated particulate matter. *Particle Fibre Toxicol.* **2007,** *4*, (1), 5.
57. Verma, V.; Pakbin, P.; Cheung, K. L.; Cho, A. K.; Schauer, J. J.; Shafer, M. M.; Kleinman, M. T.; Sioutas, C., Physicochemical and oxidative characteristics of semi-volatile components of quasi-ultrafine particles in an urban atmosphere. *Atmos. Environ.* **2011,** *45*, (4), 1025-1033.
58. Pio, C.; Cerqueira, M.; Harrison, R. M.; Nunes, T.; Mirante, F.; Alves, C.; Oliveira, C.; Sanchez de la Campa, A.; Artíñano, B.; Matos, M., OC/EC ratio

observations in Europe: Re-thinking the approach for apportionment between primary and secondary organic carbon. *Atmos. Environ.* **2011,** *45*, (34), 6121-6132.
59. Plaza, J.; Artíñano, B.; Salvador, P.; Gómez-Moreno, F. J.; Pujadas, M.; Pio, C. A., Short-term secondary organic carbon estimations with a modified OC/EC primary ratio method at a suburban site in Madrid (Spain). *Atmos. Environ.* **2011,** *45*, (15), 2496-2506.
60. Chuang, P. Y.; Duvall, R. M.; Bae, M. S.; Jefferson, A.; Schauer, J. J.; Yang, H.; Yu, J. Z.; Kim, J., Observations of elemental carbon and absorption during ACE-Asia and implications for aerosol radiative properties and climate forcing. *J. Geophys. Res.* **2003,** *108*, (D23), 8634-8643.
61. Turpin, B. J.; Lim, H.-J., Species Contributions to PM2.5 Mass Concentrations: Revisiting Common Assumptions for Estimating Organic Mass. *Aerosol Sci. Technol.* **2001,** *35*, (1), 602 - 610.
62. Keywood, M.; Guyes, H.; Selleck, P.; Gillett, R., Quantification of secondary organic aerosol in an Australian urban location. *Environ. Chem.* **2011,** *8*, (2), 115-126.
63. Andreae, M. O., A new look at aging aerosols. *Science* **2009,** *326*, 1493-1494.
64. Han, Y.; Cao, J.; Chow, J. C.; Watson, J. G.; An, Z.; Jin, Z.; Fung, K.; Liu, S., Evaluation of the thermal/optical reflectance method for discrimination between char- and soot-EC. *Chemosphere* **2007,** *69*, (4), 569-574.
65. Schauer, J. J., Evaluation of elemental carbon as a marker for diesel particulate matter. *J. Exposure Anal. Environ. Epidemiol.* **2003,** *13*, (6), 443.
66. Salako, G. O.; Hopke, P. K.; Cohen, D. D.; Begum, B. A.; Biswas, S. K.; Pandit, G. G.; Chung, Y.; Rahman, S. A.; Hamzah, M. S.; Davy, P. K.; Markwitz, A.; Shagjjamba, D.; Lodoysamba, S.; Wimolwattanapun, W.; Bunprapob, S., Exploring the Variation between EC and BC in a Variety of Locations. *Aerosol Air Qual. Res.* **2012,** *12*, (1), 1-7.
67. Khan, B.; Hays, M. D.; Geron, C.; Jetter, J., Differences in the OC/EC Ratios that Characterize Ambient and Source Aerosols due to Thermal-Optical Analysis. *Aerosol Sci. Technol.* **2011,** *46*, (2), 127-137.
68. Chow, J. C.; Watson, J. G.; Pritchett, L. C.; Pierson, W. R.; Frazier, C. A.; Purcell, R. G., The DRI thermal/optical reflectance carbon analysis system: description, evaluation and applications in U.S. air quality studies. *Atmos. Environ.* **1993,** *27A*, 1185-201.
69. Birch, M. E.; Cary, R. A., Elemental carbon-based method for monitoring occupational exposure to particulate diesel exhaust. *Aerosol Sci. Technol.* **1996,** *25*, 221-241.
70. Eldred, R. A.; Cahill, T. A.; Flocchini, R. G., Composition of PM2.5 and PM10 aerosols in the IMPROVE network. *J. Air Waste Manag. Assoc.* **1997,** *47*, 194-203.
71. Bae, M.-S.; Schauer, J. J.; Turner, J. R.; Hopke, P. K., Seasonal variations of elemental carbon in urban aerosols as measured by two common thermal-optical carbon methods. *Sci. Total Environ.* **2009,** *407*, (18), 5176-5183.
72. Ancelet, T.; Davy, P. K.; Trompetter, W. J.; Markwitz, A.; Weatherburn, D. C., Carbonaceous aerosols in an urban tunnel. *Atmos. Environ.* **2011,** *45*, (26), 4463-4469.
73. Sahu, M.; Hu, S.; Ryan, P. H.; Le Masters, G.; Grinshpun, S. A.; Chow, J. C.; Biswas, P., Chemical compositions and source identification of PM2.5 aerosols for

estimation of a diesel source surrogate. *Sci. Total Environ.* **2011,** *409*, (13), 2642-2651.
74. Quincey, P.; Butterfield, D.; Green, D.; Coyle, M.; Cape, J. N., An evaluation of measurement methods for organic, elemental and black carbon in ambient air monitoring sites. *Atmos. Environ.* **2009,** *43*, (32), 5085-5091.
75. Cao, J. J.; Lee, S. C.; Ho, K. F.; Fung, K.; Chow, J. C.; Watson, J. G., Characterization of Roadside Fine Particulate Carbon and its Eight Fraction in Hong Kong. *Aerosol Air Qual Res.* **2006,** *6*, (2), 106-122.
76. Jones, A. M.; Harrison, R. M., Interpretation of particulate elemental and organic carbon concentrations at rural, urban and kerbside sites. *Atmos. Environ.* **2005,** *39*, (37), 7114-7126.
77. Viana, M.; Maenhaut, W.; ten Brink, H. M.; Chi, X.; Weijers, E.; Querol, X.; Alastuey, A.; Mikuska, P.; Vecera, Z., Comparative analysis of organic and elemental carbon concentrations in carbonaceous aerosols in three European cities. *Atmos. Environ.* **2007,** *41*, (28), 5972-5983.
78. Fromme, H.; Lahrz, T.; Hainsch, A.; Oddoy, A.; Piloty, M.; Rüden, H., Elemental carbon and respirable particulate matter in the indoor air of apartments and nursery schools and ambient air in Berlin (Germany). *Indoor Air* **2005,** *15*, (5), 335-341.
79. Jeong, C.-H.; Lee, D.-W.; Kim, E.; Hopke, P. K., Measurement of real-time PM2.5 mass, sulfate, and carbonaceous aerosols at the multiple monitoring sites. *Atmos. Environ.* **2004,** *38*, (31), 5247-5256.
80. Boogaard, H.; Kos, G. P. A.; Weijers, E. P.; Janssen, N. A. H.; Fischer, P. H.; van der Zee, S. C.; de Hartog, J. J.; Hoek, G., Contrast in air pollution components between major streets and background locations: Particulate matter mass, black carbon, elemental composition, nitrogen oxide and ultrafine particle number. *Atmos. Environ.* **2011,** *45*, (3), 650-658.
81. Hildemann, L. M.; Markowski, G. R.; Cass, G. R., Chemical composition of emissions from urban sources of fine organic aerosol. *Environ. Sci. Technol.* **1991,** *25*, 744-59.
82. Zhu, C.-S.; Chen, C.-C.; Cao, J.-J.; Tsai, C.-J.; Chou, C. C. K.; Liu, S.-C.; Roam, G.-D., Characterization of carbon fractions for atmospheric fine particles and nanoparticles in a highway tunnel. *Atmos. Environ.* **2010,** *44*, (23), 2668-2673.
83. Kim, K. H.; Sekiguchi, K.; Kudo, S.; Sakamoto, K., Characteristics of Atmospheric Elemental Carbon (Char and Soot) in Ultrafine and Fine Particles in a Roadside Environment, Japan. *Aerosol Air Qual. Res.* **2011,** *11*, (1), 1-12.
84. Giugliano, M.; Lonati, G.; Butelli, P.; Romele, L.; Tardivo, R.; Grosso, M., Fine particulate (PM2.5-PM1) at urban sites with different traffic exposure. *Atmos. Environ.* **2005,** *39*, (13), 2421-2431.
85. Chow, J. C.; Watson, J. G.; Lu, Z.; Lowenthal, D. H.; Frazier, C. A.; Solomon, P. A.; Thuillier, R. H.; Magliano, K., Descriptive analysis of PM2.5 and PM10 at regionally representative locations during SJVAQS/AUSPEX. *Atmos. Environ.* **1996,** *30*, (12), 2079-2112.
86. Gelencsér, A.; May, B.; Simpson, D.; Sánchez-Ochoa, A.; Kasper-Giebl, A.; Puxbaum, H.; Caseiro, A.; Pio, C.; Legrand, M., Source apportionment of PM2.5 organic aerosol over Europe: Primary/secondary, natural/anthropogenic, and fossil/biogenic origin. *J. Geophys. Res.* **2007,** *112*, (D23), D23S04.
87. Watson, J. G.; Chow, J. C.; Houck, J. E., PM2.5 chemical source profiles for vehicle exhaust, vegetative burning, geological material, and coal burning in Northwestern Colorado during 1995. *Chemosphere* **2001,** *43*, (8), 1141-1151.

88. Lonati, G.; Ozgen, S.; Giugliano, M., Primary and secondary carbonaceous species in PM2.5 samples in Milan (Italy). *Atmos Environ.* **2007,** *41*, (22), 4599-4610.
89. Huang, X.-F.; Yu, J. Z.; He, L.-Y.; Hu, M., Size Distribution Characteristics of Elemental Carbon Emitted from Chinese Vehicles: Results of a Tunnel Study and Atmospheric Implications. *Environ Sci. Technol.* **2006,** *40*, (17), 5355-5360.
90. Gillies, J. A.; Gertler, A. W.; Sagebiel, J. C.; Dippel, W. A., On-Road Particulate Matter (PM2.5 and PM10) Emissions in the Sepulveda Tunnel, Los Angeles, California. *Environ. Sci. Technol.* **2001,** *35*, (6), 1054-1063.
91. Cheng, Y.; Lee, S. C.; Ho, K. F.; Chow, J. C.; Watson, J. G.; Louie, P. K. K.; Cao, J. J.; Hai, X., Chemically-speciated on-road PM2.5 motor vehicle emission factors in Hong Kong. *Sci. Total Environ.* **2010,** *408*, (7), 1621-1627.
92. Louie, P. K. K.; Chow, J. C.; Chen, L. W. A.; Watson, J. G.; Leung, G.; Sin, D. W. M., PM2.5 chemical composition in Hong Kong: urban and regional variations. *Sci. Total Environ.* **2005,** *338*, (3), 267-281.
93. Cao, J. J.; Lee, S. C.; Ho, K. F.; Zhang, X. Y.; Zou, S. C.; Fung, K.; Chow, J. C.; Watson, J. G., Characteristics of carbonaceous aerosol in Pearl River Delta Region, China during 2001 winter period. *Atmos. Environ* **2003,** *37*, (11), 1451-1460.
94. Castro, L. M.; Pio, C. A.; Harrison, R. M.; Smith, D. J. T., Carbonaceous aerosol in urban and rural European atmospheres: estimation of secondary organic carbon concentrations. *Atmos. Environ.* **1999,** *33*, (17), 2771-2781.
95. Cabada, J. C.; Pandis, S. N.; Subramanian, R.; Robinson, A. L.; Polidori, A.; Turpin, B., Estimating the Secondary Organic Aerosol Contribution to PM2.5 Using the EC Tracer Method Special Issue of Aerosol Science and Technology on Findings from the Fine Particulate Matter Supersites Program. *Aerosol Sci Technol.* **2004,** *38*, (sup1), 140-155.
96. Turpin, B. J.; Huntzicker, J. J., Identification of secondary organic aerosol episodes and quantitation of primary and secondary organic aerosol concentrations during SCAQS. *Atmos. Environ.* **1995,** *29*, (23), 3527-3544.
97. Harrison, R. M.; Yin, J., Sources and processes affecting carbonaceous aerosol in central England. *Atmos Environ* **2008,** *42*, (7), 1413-1423.
98. Zhang, Q.; Worsnop, D. R.; Canagaratna, M. R.; Jimenez, J. L., Hydrocarbon-like and oxygenated organic aerosols in Pittsburgh: insights into sources and processes of organic aerosols. *Atmos. Chem. Phys.* **2005,** *5*, (12), 3289-3311.
99. Salma, I.; Chi, X.; Maenhaut, W., Elemental and organic carbon in urban canyon and background environments in Budapest, Hungary. *Atmos. Environ.* **2004,** *38*, (1), 27-36.
100. Dan, M.; Zhuang, G.; Li, X.; Tao, H.; Zhuang, Y., The characteristics of carbonaceous species and their sources in PM2.5 in Beijing. *Atmos. Environ.* **2004,** *38*, (21), 3443-3452.
101. Polidori, A.; Turpin, B. J.; Lim, H.-J.; Cabada, J. C.; Subramanian, R.; Pandis, S. N.; Robinson, A. L., Local and Regional Secondary Organic Aerosol: Insights from a Year of Semi-Continuous Carbon Measurements at Pittsburgh. *Aerosol Sci. Technol.* **2006,** *40*, (10), 861-872.
102. Kim, K. H.; Sekiguchi, K.; Furuuchi, M.; Sakamoto, K., Seasonal variation of carbonaceous and ionic components in ultrafine and fine particles in an urban area of Japan. *Atmos. Environ.* **2011,** *45*, (8), 1581-1590.

103. Kim, E.; Hopke, P. K.; Edgerton, E. S., Improving source identification of Atlanta aerosol using temperature resolved carbon fractions in positive matrix factorization. *Atmos. Environ.* **2004,** *38*, (20), 3349-3362.
104. Kim, E.; Hopke, P. K., Improving source identification of fine particles in a rural northeastern U.S. aarea utilizing temperature-resolved carbon fractions. *J. Geophys. Res.* **2004,** *109*, (D09204).
105. Han, Y. M.; Cao, J. J.; Lee, S. C.; Ho, K. F.; An, Z. S., Different characteristics of char and soot in the atmosphere and their ratio as an indicator for source identification in Xi'an, China. *Atmos. Chem. Phys.* **2010,** *10*, (2), 595-607.
106. Han, Y. M.; Lee, S. C.; Cao, J. J.; Ho, K. F.; An, Z. S., Spatial distribution and seasonal variation of char-EC and soot-EC in the atmosphere over China. *Atmos Environ.* **2009,** *43*, (38), 6066-6073.
107. Chow, J. C.; Watson, J. G.; Kuhns, H.; Etyemezian, V.; Lowenthal, D. H.; Crow, D.; Kohl, S. D.; Engelbrecht, J. P.; Green, M. C., Source profiles for industrial, mobile, and area sources in the Big Bend Regional Aerosol Visibility and Observational study. *Chemosphere* **2004,** *54*, (2), 185-208.
108. Hochstetler, H. A.; Yermakov, M.; Reponen, T.; Ryan, P. H.; Grinshpun, S. A., Aerosol particles generated by diesel-powered school buses at urban schools as a source of children's exposure. *Atmos. Environ.* **2011,** *45*, 1444-1453.
109. Li, C.; Nguyen, Q.; Ryan, P. H.; LeMasters, G. K.; Spitz, H.; Lobaugh, M.; Glover, S.; Grinshpun, S. A., School bus pollution and changes in the air quality at schools: a case study. *J. Environ. Monitor.* **2009,** *11*, (5), 1037-1042.
110. Patel, M. M.; Chillrud, S. N.; Correa, J. C.; Feinberg, M.; Hazi, Y.; Deepti, K. C.; Prakash, S.; Ross, J. M.; Levy, D.; Kinney, P. L., Spatial and temporal variations in traffic-related particulate matter at New York City high schools. *Atmos. Environ.* **2009,** *43*, (32), 4975-4981.
111. Richmond-Bryant, J.; Bukiewicz, L.; Kalin, R.; Galarraga, C.; Mirer, F., A multi-site analysis of the association between black carbon concentrations and vehicular idling, traffic, background pollution, and meteorology during school dismissals. *Sci. Total Environ.* **2011,** *409*, (11), 2085-2093.
112. Martuzevicius, D.; Grinshpun, S. A.; Reponen, T.; Górny, R. L.; Shukla, R.; Lockey, J.; Hu, S.; McDonald, R.; Biswas, P.; Kliucininkas, L.; LeMasters, G., Spatial and temporal variations of PM2.5 concentration and composition throughout an urban area with high freeway density--the Greater Cincinnati study. *Atmos. Environ.* **2004,** *38*, (8), 1091-1105.
113. Harrison, R. M.; Jones, A. M.; Gietl, J.; Yin, J.; Green, D. C., Estimation of the Contributions of Brake Dust, Tire Wear, and Resuspension to Nonexhaust Traffic Particles Derived from Atmospheric Measurements. *Environ. Sci. Technol.* **2012,** *46*, (12), 6523-6529.
114. Harrison, R. M.; Yin, J.; Mark, D.; Stedman, J.; Appleby, R. S.; Booker, J.; Moorcroft, S., Studies of the coarse particle (2.5–10μm) component in UK urban atmospheres. *Atmos. Environ.* **2001,** *35*, (21), 3667-3679.
115. Rexeis, M.; Hausberger, S., Trend of vehicle emission levels until 2020 – Prognosis based on current vehicle measurements and future emission legislation. *Atmos. Environ.* **2009,** *43*, (31), 4689-4698.
116. Harrison, R. M.; Tilling, R.; Callén Romero, M. S.; Harrad, S.; Jarvis, K., A study of trace metals and polycyclic aromatic hydrocarbons in the roadside environment. *Atmos. Environ.* **2003,** *37*, (17), 2391-2402.
117. Moreno, T.; Querol, X.; Alastuey, A.; de la Rosa, J.; Sánchez de la Campa, A. M.; Minguillón, M.; Pandolfi, M.; González-Castanedo, Y.; Monfort, E.; Gibbons,

W., Variations in vanadium, nickel and lanthanoid element concentrations in urban air. *Sci. Total Environ.* **2010,** *408*, (20), 4569-4579.
118. da Silva, L. I. D.; de Souza Sarkis, J. E.; Zotin, F. M. Z.; Carneiro, M. C.; Neto, A. A.; da Silva, A. d. S. A. G.; Cardoso, M. J. B.; Monteiro, M. I. C., Traffic and catalytic converter – Related atmospheric contamination in the metropolitan region of the city of Rio de Janeiro, Brazil. *Chemosphere* **2008,** *71*, (4), 677-684.
119. Gietl, J. K.; Lawrence, R.; Thorpe, A. J.; Harrison, R. M., Identification of brake wear particles and derivation of a quantitative tracer for brake dust at a major road. *Atmos. Environ.* **2010,** *44*, (2), 141-146.
120. Huang, X.; Olmez, I.; Aras, N. K.; Gordon, G. E., Emissions of trace elements from motor vehicles: Potential marker elements and source composition profile. *Atmos. Environ.* **1994,** *28*, (8), 1385-1391.
121. Pérez, N.; Pey, J.; Cusack, M.; Reche, C.; Querol, X.; Alastuey, A.; Viana, M., Variability of Particle Number, Black Carbon, and PM10, PM2.5, and PM1 Levels and Speciation: Influence of Road Traffic Emissions on Urban Air Quality. *Aerosol Sci. Technol.* **2010,** *44*, (7), 487-499.
122. Ariola, V.; D'Alessandro, A.; Lucarelli, F.; Marcazzan, G.; Mazzei, F.; Nava, S.; Garcia-Orellana, I.; Prati, P.; Valli, G.; Vecchi, R.; Zucchiatti, A., Elemental characterization of PM10, PM2.5 and PM1 in the town of Genoa (Italy). *Chemosphere* **2006,** *62*, (2), 226-232.
123. Cheng, Y.; Zou, S. C.; Lee, S. C.; Chow, J. C.; Ho, K. F.; Watson, J. G.; Han, Y. M.; Zhang, R. J.; Zhang, F.; Yau, P. S.; Huang, Y.; Bai, Y.; Wu, W. J., Characteristics and source apportionment of PM1 emissions at a roadside station. *J. Hazard. Mater.* **2011,** *195*, (0), 82-91.
124. Minguillón, M. C.; Querol, X.; Baltensperger, U.; Prévôt, A. S. H., Fine and coarse PM composition and sources in rural and urban sites in Switzerland: Local or regional pollution? *Sci. Total Environ.* **2012,** *427–428*, (0), 191-202.
125. Cohen, D. D., Characterisation of atmospheric fine particles using IBA techniques. *Nucl. Inst Meth B* **1998,** *14*, (22), 136-138.
126. Harrison, R. M.; Smith, D. J. T.; Luhana, L., Source Apportionment of Atmospheric Polycyclic Aromatic Hydrocarbons Collected from an Urban Location in Birmingham, U.K. *Environ. Sci. Technol.* **1996,** *30*, (3), 825-832.
127. Lin, C.-C.; Chen, S.-J.; Huang, K.-L.; Hwang, W.-I.; Chang-Chien, G.-P.; Lin, W.-Y., Characteristics of Metals in Nano/Ultrafine/Fine/Coarse Particles Collected Beside a Heavily Trafficked Road. *Environ. Sci. Technol.* **2005,** *39*, (21), 8113-8122.
128. Friend, A. J.; Ayoko, G. A.; Stelcer, E.; Cohen, D., Source apportionment of PM2.5 at two receptor sites in Brisbane, Australia. *Environ. Chem.* **2011,** *8*, (6), 569-580.
129. Radhi, M.; Box, M. A.; Box, G. P.; Keywood, M. D.; Cohen, D. D.; Stelcer, E.; Mitchell, R. M., Size-resolved chemical composition of Australian dust aerosol during winter. *Environ. Chem.* **2011,** *8*, (3), 248-262.
130. Iijima, A.; Sato, K.; Yano, K.; Tago, H.; Kato, M.; Kimura, H.; Furuta, N., Particle size and composition distribution analysis of automotive brake abrasion dusts for the evaluation of antimony sources of airborne particulate matter. *Atmos. Environ.* **2007,** *41*, (23), 4908-4919.
131. Furuta, N.; Iijima, A.; Kambe, A.; Sakai, K.; Sato, K., Concentrations, enrichment and predominant sources of Sb and other trace elements in size classified airborne particulate matter collected in Tokyo from 1995 to 2004. *J. Environ. Monitor.* **2005,** *7*, (12), 1155-1161.

132. Birmili, W.; Allen, A. G.; Bary, F.; Harrison, R. M., Trace Metal Concentrations and Water Solubility in Size-Fractionated Atmospheric Particles and Influence of Road Traffic. *Environ. Sci. Technol.* **2006,** *40*, (4), 1144-1153.
133. Schauer, J. J.; Lough, G. C.; Shafer, M. M.; Christensen, W. F.; Arndt, M. F.; DeMinter, J. T.; Park, J.-S., Characterization of metals emitted from motor vehicles. *Research Report, Health Effects Institute* **2006**.
134. Lim, M. C. H.; Ayoko, G. A.; Morawska, L., Characterization of elemental and polycyclic aromatic hydrocarbon compositions of urban air in Brisbane. *Atmos. Environ.* **2005,** *39*, (3), 463-476.
135. Cadle, S. H.; Mulawa, P. A.; Hunsanger, E. C.; Nelson, K.; Ragazzi, R. A.; Barrett, R.; Gallagher, G. L.; Lawson, D. R.; Knapp, K. T.; Snow, R., Composition of Light-Duty Motor Vehicle Exhaust Particulate Matter in the Denver, Colorado Area. *Environ. Sci. Technol.* **1999,** *33*, (14), 2328-2339.
136. Thorpe, A. J.; Harrison, R. M.; Boulter, P. G.; McCrae, I. S., Estimation of particle resuspension source strength on a major London Road. *Atmos. Environ.* **2007,** *41*, (37), 8007-8020.
137. Hueglin, C.; Gehrig, R.; Baltensperger, U.; Gysel, M.; Monn, C.; Vonmont, H., Chemical characterisation of PM2.5, PM10 and coarse particles at urban, near-city and rural sites in Switzerland. *Atmos. Environ.* **2005,** *39*, (4), 637-651.
138. Xia, L.; Gao, Y., Characterization of trace elements in PM2.5 aerosols in the vicinity of highways in northeast New Jersey in the U.S. east coast. *Atmos. Pollut. Res.* **2011,** *2*, 34-44.
139. Cheng, Y.; Lee, S. C.; Cao, J.; Ho, K. F.; Chow, J. C.; Watson, J. G.; Ao, C. H., Elemental composition of airborne aerosols at a traffic site and a suburban site in Hong Kong. *Int. J. Environ. Pollut.* **2009,** *36*, (1), 166-179.
140. Srimuruganandam, B.; Shiva Nagendra, S. M., Characteristics of particulate matter and heterogeneous traffic in the urban area of India. *Atmos. Environ.* **2011,** *45*, (18), 3091-3102.
141. Omstedt, G.; Bringfelt, B.; Johansson, C., A model for vehicle-induced non-tailpipe emissions of particles along Swedish roads. *Atmos. Environ.* **2005,** *39*, (33), 6088-6097.
142. Ntziachristos, L.; Ning, Z.; Geller, M. D.; Sheesley, R. J.; Schauer, J. J.; Sioutas, C., Fine, ultrafine and nanoparticle trace element compositions near a major freeway with a high heavy-duty diesel fraction. *Atmos. Environ.* **2007,** *41*, (27), 5684-5696.
143. Liacos, J. W.; Kam, W.; Delfino, R. J.; Schauer, J. J.; Sioutas, C., Characterization of organic, metal and trace element PM2.5 species and derivation of freeway-based emission rates in Los Angeles, CA. *Sci. Total Environ.* **2012,** *435–436*, (0), 159-166.
144. Amato, F.; Viana, M.; Richard, A.; Furger, M.; Prévôt, A. S. H.; Nava, S.; Lucarelli, F.; Bukowiecki, N.; Alastuey, A.; Reche, C.; Moreno, T.; Pandolfi, M.; Pey, J.; Querol, X., Size and time-resolved roadside enrichment of atmospheric particulate pollutants. *Atmos. Chem. Phys.* **2011,** *11*, (6), 2917-2931.
145. Denier van der Gon, H. A. C.; Hulskotte, J. H. J.; Visschedijk, A. J. H.; Schaap, M., A revised estimate of copper emissions from road transport in UNECE-Europe and its impact on predicted copper concentrations. *Atmos. Environ.* **2007,** *41*, (38), 8697-8710.
146. Amato, F.; Pandolfi, M.; Escrig, A.; Querol, X.; Alastuey, A.; Pey, J.; Perez, N.; Hopke, P. K., Quantifying road dust resuspension in urban environment by

Multilinear Engine: A comparison with PMF2. *Atmos. Environ.* **2009,** *43*, (17), 2770-2780.
147. Minguillón, M. C.; Arhami, M.; Schauer, J. J.; Sioutas, C., Seasonal and spatial variations of sources of fine and quasi-ultrafine particulate matter in neighborhoods near the Los Angeles–Long Beach harbor. *Atmos. Environ.* **2008,** *42*, (32), 7317-7328.
148. Singh, M.; Jaques, P. A.; Sioutas, C., Size distribution and diurnal characteristics of particle-bound metals in source and receptor sites of the Los Angeles Basin. *Atmos Environ.* **2002,** *36*, (10), 1675-1689
149. Lankey, R. L.; Davidson, C. I.; McMichael, F. C., Mass Balance for Lead in the California South Coast Air Basin: An Update. *Environ. Res.* **1998,** *78*, (2), 86-93.
150. Arhami, M.; Sillanpää, M.; Hu, S.; Olson, M. R.; Schauer, J. J.; Sioutas, C., Size-Segregated Inorganic and Organic Components of PM in the Communities of the Los Angeles Harbor. *Aerosol Sci. Technol.* **2009,** *43*, (2), 145-160.
151. Niu, J.; Rasmussen, P.; Hassan, N.; Vincent, R., Concentration Distribution and Bioaccessibility of Trace Elements in Nano and Fine Urban Airborne Particulate Matter: Influence of Particle Size. *Water Air Soil Poll.* **2010,** *213*, (1), 211-225.
152. Moreno, T.; Querol, X.; Alastuey, A.; Viana, M.; Salvador, P.; Sánchez de la Campa, A.; Artiñano, B.; de la Rosa, J.; Gibbons, W., Variations in atmospheric PM trace metal content in Spanish towns: Illustrating the chemical complexity of the inorganic urban aerosol cocktail. *Atmos. Environ.* **2006,** *40*, (35), 6791-6803.
153. Moreno, T.; Querol, X.; Alastuey, A.; Reche, C.; Cusack, M.; Amato, F.; Pandolfi, M.; Pey, J.; Richard, A.; Prévôt, A. S. H.; Furger, M.; Gibbons, W., Variations in time and space of trace metal aerosol concentrations in urban areas and their surroundings. *Atmos. Chem. Phys.* **2011,** *11*, (17), 9415-9430.
154. Richard, A.; Gianini, M. F. D.; Mohr, C.; Furger, M.; Bukowiecki, N.; Minguillón, M. C.; Lienemann, P.; Flechsig, U.; Appel, K.; DeCarlo, P. F.; Heringa, M. F.; Chirico, R.; Baltensperger, U.; Prévôt, A. S. H., Source apportionment of size and time resolved trace elements and organic aerosols from an urban courtyard site in Switzerland. *Atmos. Chem. Phys.* **2011,** *11*, (17), 8945-8963.
155. Gehrig, R.; Hill, M.; Lienemann, P.; Zwicky, C. N.; Bukowiecki, N.; Weingartner, E.; Baltensperger, U.; Buchmann, B., Contribution of railway traffic to local PM10 concentrations in Switzerland. *Atmos. Environ.* **2007,** *41*, (5), 923-933.
156. Caggiano, R.; Macchiato, M.; Trippetta, S., Levels, chemical composition and sources of fine aerosol particles (PM1) in an area of the Mediterranean basin. *Sci. Total Environ.* **2010,** *408*, (4), 884-895.
157. Ragosta, M.; Caggiano, R.; Macchiato, M.; Sabia, S.; Trippetta, S., Trace elements in daily collected aerosol: Level characterization and source identification in a four-year study. *Atmos. Res.* **2008,** *89*, (1–2), 206-217.
158. Rahman, S. A.; Hamzah, M. S.; Wood, A. K.; Elias, M. S.; Salim, N. A. A.; Sanuri, E., Sources apportionment of fine and coarse aerosol in Klang Valley, Kuala Lumpur using positive matrix factorization. *Atmos. Poll. Res.* **2011,** *2*, 197-206.
159. Chen, J.; Tan, M.; Li, Y.; Zheng, J.; Zhang, Y.; Shan, Z.; Zhang, G.; Li, Y., Characteristics of trace elements and lead isotope ratios in PM2.5 from four sites in Shanghai. *J. Hazard. Mater.* **2008,** *156*, (1–3), 36-43.
160. Ye, B.; Ji, X.; Yang, H.; Yao, X.; Chan, C. K.; Cadle, S. H.; Chan, T.; Mulawa, P. A., Concentration and chemical composition of PM2.5 in Shanghai for a 1-year period. *Atmos. Environ.* **2003,** *37*, (4), 499-510.

161. Song, Y.; Zhang, Y.; Xie, S.; Zeng, L.; Zheng, M.; Salmon, L. G.; Shao, M.; Slanina, S., Source apportionment of PM2.5 in Beijing by positive matrix factorization. *Atmos. Environ.* **2006,** *40*, (8), 1526-1537.
162. Chan, C. K.; Yao, X., Air pollution in mega cities in China. *Atmos. Environ.* **2008,** *42*, (1), 1-42.
163. Chan, Y.-C.; Cohen, D. D.; Hawas, O.; Stelcer, E.; Simpson, R.; Denison, L.; Wong, N.; Hodge, M.; Comino, E.; Carswell, S., Apportionment of sources of fine and coarse particles in four major Australian cities by positive matrix factorisation. *Atmos. Environ.* **2008,** *42*, (2), 374-389.
164. Cohen, D. D.; Stelcer, E.; Garton, D.; Crawford, J., Fine particle characterisation, source apportionment and long-range dust transport into the Sydney Basin: a long term study between 1998 and 2009. *Atmos. Pollut. Res.* **2011,** *2*, 182-189.
165. Friend, A. J.; Ayoko, G. A.; Elbagir, S. G., Source apportionment of fine particles at a suburban site in Queensland, Australia. *Environ. Chem.* **2011,** *8*, (2), 163-173.
166. Chan, Y. C.; Simpson, R. W.; McTainsh, G. H.; Vowles, P. D.; Cohen, D. D.; Bailey, G. M., Characterisation of chemical species in PM2.5 and PM10 aerosols in Brisbane, Australia. *Atmos. Environ.* **1997,** *31*, (22), 3773-3785.
167. Molnar, P.; Bellander, T.; Sallsten, G.; Boman, J., Indoor and outdoor concentrations of PM2.5 trace elements at homes, preschools and schools in Stockholm, Sweden. *J. Environ. Monitor.* **2007,** *9*, (4), 348-357.
168. Jayne, J. T.; Leard, D. C.; Zhang, X.; Davidovits, P.; Smith, K. A.; Kolb, C. E.; Worsnop, D. R., Development of an Aerosol Mass Spectrometer for Size and Composition Analysis of Submicron Particles. *Aerosol Sci. Technol.* **2000,** *33*, (1), 49-70.
169. Drewnick, F.; Hings, S. S.; DeCarlo, P. F.; Jayne, J. T.; Gonin, M.; Fuhrer, K.; Weimer, S.; Jimenez, J. L.; Demerjian, K. L.; Borrmann, S.; Worsnop, D. R., A New Time-of-Flight Aerosol Mass Spectrometer (TOF-AMS)—Instrument Description and First Field Deployment. *Aerosol Sci. Technol.* **2005,** *39*, (7), 637–658.
170. Gard, E.; Mayer, J. E.; Morrical, B. D.; Dienes, T.; Fergenson, D. P.; Prather, K. A., Real-Time Analysis of Individual Atmospheric Aerosol Particles: Design and Performance of a Portable ATOFMS. *Anal. Chem.* **1997,** *69*, (20), 4083-4091.
171. Su, Y.; Sipin, M. F.; Furutani, H.; Prather, K. A., Development and Characterization of an Aerosol Time-of-Flight Mass Spectrometer with Increased Detection Efficiency. *Anal. Chem.* **2003,** *76*, (3), 712-719.
172. DeCarlo, P. F.; Kimmel, J. R.; Trimborn, A.; Northway, M. J.; Jayne, J. T.; Aiken, A. C.; Gonin, M.; Fuhrer, K.; Horvath, T.; Docherty, K. S.; Worsnop, D. R.; Jimenez, J. L., Field-Deployable, High-Resolution, Time-of-Flight Aerosol Mass Spectrometer. *Anal. Chem.* **2006,** *78*, (24), 8281-8289.
173. Zhang, X.; Smith, K. A.; Worsnop, D. R.; Jimenez, J.; Jayne, J. T.; Kolb, C. E., A Numerical Characterization of Particle Beam Collimation by an Aerodynamic Lens-Nozzle System: Part I. An Individual Lens or Nozzle. *Aerosol Sci. Technol.* **2002,** *36*, (5), 617 - 631.
174. Zhang, X.; Smith, K. A.; Worsnop, D. R.; Jimenez, J. L.; Jayne, J. T.; Kolb, C. E.; Morris, J.; Davidovits, P., Numerical Characterization of Particle Beam Collimation: Part II Integrated Aerodynamic-Lens–Nozzle System. *Aerosol Sci. Technol.* **2004,** *38*, (6), 619 - 638.

175. Hings, S. S.; Walter, S.; Schneider, J.; Borrmann, S.; Drewnick, F., Comparison of a Quadrupole and a Time-of-Flight Aerosol Mass Spectrometer during the Feldberg Aerosol Characterization Experiment 2004. *Aerosol Sci. Technol.* **2007,** *41*, (7), 679 - 691.
176. Jimenez, J. L.; Jayne, J. T.; Shi, Q.; Kolb, C. E.; Worsnop, D. R.; Yourshaw, I.; Seinfeld, J. H.; Flagan, R. C.; Zhang, X.; Smith, K. A.; Morris, J. W.; Davidovits, P., Ambient aerosol sampling using the Aerodyne Aerosol Mass Spectrometer. *J. Geophys. Res.* **2003,** *108*, (D7), 8425-8438.
177. Steiner, W. E.; Clowers, B. H.; Fuhrer, K.; Gonin, M.; Matz, L. M.; Siems, W. F.; Schultz, A. J.; Jr., H. H. H., Electrospray ionization with ambient pressure ion mobility separation and mass analysis by orthogonal time-of-flight mass spectrometry. *Rapid Commun. Mass Sp.* **2001,** *15*, (23), 2221-2226.
178. De Gouw, J.; Jimenez, J. L., Organic Aerosols in the Earth's Atmosphere. *Environ. Sci. Technol.* **2009,** *43*, (20), 7614-7618.
179. Lanz, V. A.; Alfarra, M. R.; Baltensperger, U.; Buchmann, B.; Hueglin, C.; Prévôt, A. S. H., Source apportionment of submicron organic aerosols at an urban site by factor analytical modelling of aerosol mass spectra. *Atmos. Chem. Phys.* **2007,** *7*, (6), 1503-1522.
180. Ulbrich, I. M.; Canagaratna, M. R.; Zhang, Q.; Worsnop, D. R.; Jimenez, J. L., Interpretation of organic components from Positive Matrix Factorization of aerosol mass spectrometric data. *Atmos. Chem. Phys.* **2009,** *9*, (9), 2891-2918.
181. Robinson, A. L.; Donahue, N. M.; Shrivastava, M. K.; Weitkamp, E. A.; Sage, A. M.; Grieshop, A. P.; Lane, T. E.; Pierce, J. R.; Pandis, S. N., Rethinking organic aerosols: Semivolatile emissions and photochemical aging. *Science* **2007,** *315*, 1259-1262.
182. Zhang, Q.; Alfarra, M. R.; Worsnop, D. R.; Allan, J. D.; Coe, H.; Canagaratna, M. R.; Jimenez, J. L., Deconvolution and Quantification of Hydrocarbon-like and Oxygenated Organic Aerosols Based on Aerosol Mass Spectrometry. *Environ. Sci. Technol.* **2005,** *39*, (13), 4938-4952.
183. Alfarra, M. R.; Coe, H.; Allan, J. D.; Bower, K. N.; Boudries, H.; Canagaratna, M. R.; Jimenez, J. L.; Jayne, J. T.; Garforth, A. A.; Li, S.-M.; Worsnop, D. R., Characterization of urban and rural organic particulate in the Lower Fraser Valley using two Aerodyne Aerosol Mass Spectrometers. *Atmos. Environ.* **2004,** *38*, (34), 5745-5758.
184. Zhang, Q.; Stanier, C. O.; Canagaratna, M. R.; Jayne, J. T.; Worsnop, D. R.; Pandis, S. N.; Jimenez, J. L., Insights into the Chemistry of New Particle Formation and Growth Events in Pittsburgh Based on Aerosol Mass Spectrometry. *Environ. Sci. Technol.* **2004,** *38*, (18), 4797-4809.
185. Canagaratna, M. R.; Jayne, J. T.; Ghertner, D. A.; Herndon, S. C.; Shi, Q.; Jimenez, J. L.; Silva, P. J.; Williams, P.; Lanni, T.; Drewnick, F.; Demerjian, K. L.; Kolb, C. E.; Worsnop, D. R., Chase Studies of Particulate Emissions from in-use New York City Vehicles. *Aerosol Sci. Technol.* **2004,** *38*, 555-573.
186. Reff, A.; Eberly, S. I.; Bhave, P. V., Receptor Modeling of Ambient Particulate Matter Data Using Positive Matrix Factorization: Review of Existing Methods. *J. Air Waste Manag. Assoc.* **2007,** *57*, (2), 146-154.
187. Paatero, P.; Tapper, U., Positive matrix factorization: A non-negative factor model with optimal utilization of error estimates of data values. *Environmetrics* **1994,** *5*, (2), 111-126.

188. Zhang, Q.; Jimenez, J.; Canagaratna, M.; Ulbrich, I.; Ng, N.; Worsnop, D.; Sun, Y., Understanding atmospheric organic aerosols via factor analysis of aerosol mass spectrometry: a review. *Anal. Bioanal. Chem.* **2011,** *401*, (10), 3045-3067.
189. Aiken, A. C.; Salcedo, D.; Cubison, M. J.; Huffman, J. A.; DeCarlo, P. F.; Ulbrich, I. M.; Docherty, K. S.; Sueper, D.; Kimmel, J. R.; Worsnop, D. R.; Trimborn, A.; Northway, M.; Stone, E. A.; Schauer, J. J.; Volkamer, R. M.; Fortner, E.; de Foy, B.; Wang, J.; Laskin, A.; Shutthanandan, V.; Zheng, J.; Zhang, R.; Gaffney, J.; Marley, N. A.; Paredes-Miranda, G.; Arnott, W. P.; Molina, L. T.; Sosa, G.; Jimenez, J. L., Mexico City aerosol analysis during MILAGRO using high resolution aerosol mass spectrometry at the urban supersite (T0) – Part 1: Fine particle composition and organic source apportionment. *Atmos. Chem. Phys.* **2009,** *9*, (17), 6633-6653.
190. Mohr, C.; Huffman, J. A.; Cubison, M. J.; Aiken, A. C.; Docherty, K. S.; Kimmel, J. R.; Ulbrich, I. M.; Hannigan, M.; Jimenez, J. L., Characterization of Primary Organic Aerosol Emissions from Meat Cooking, Trash Burning, and Motor Vehicles with High-Resolution Aerosol Mass Spectrometry and Comparison with Ambient and Chamber Observations. *Environ. Sci. Technol.* **2009,** *43*, (7), 2443-2449.
191. Huang, X. F.; He, L. Y.; Hu, M.; Canagaratna, M. R.; Sun, Y.; Zhang, Q.; Zhu, T.; Xue, L.; Zeng, L. W.; Liu, X. G.; Zhang, Y. H.; Jayne, J. T.; Ng, N. L.; Worsnop, D. R., Highly time-resolved chemical characterization of atmospheric submicron particles during 2008 Beijing Olympic Games using an Aerodyne High-Resolution Aerosol Mass Spectrometer. *Atmos. Chem. Phys.* **2010,** *10*, (18), 8933-8945.
192. Hersey, S. P.; Craven, J. S.; Schilling, K. A.; Metcalf, A. R.; Sorooshian, A.; Chan, M. N.; Flagan, R. C.; Seinfeld, J. H., The Pasadena Aerosol Characterization Observatory (PACO): chemical and physical analysis of the Western Los Angeles basin aerosol. *Atmos. Chem. Phys.* **2011,** *11*, (15), 7417-7443.
193. Aiken, A. C.; DeCarlo, P. F.; Jimenez, J. L., Elemental Analysis of Organic Species with Electron Ionization High-Resolution Mass Spectrometry. *Anal. Chem.* **2007,** *79*, (21), 8350-8358.
194. Aiken, A. C.; DeCarlo, P. F.; Kroll, J. H.; Worsnop, D. R.; Huffman, J. A.; Docherty, K. S.; Ulbrich, I. M.; Mohr, C.; Kimmel, J. R.; Sueper, D.; Sun, Y.; Zhang, Q.; Trimborn, A.; Northway, M.; Ziemann, P. J.; Canagaratna, M. R.; Onasch, T. B.; Alfarra, M. R.; Prevot, A. S. H.; Dommen, J.; Duplissy, J.; Metzger, A.; Baltensperger, U.; Jimenez, J. L., O/C and OM/OC Ratios of Primary, Secondary, and Ambient Organic Aerosols with High-Resolution Time-of-Flight Aerosol Mass Spectrometry. *Environ. Sci. Technol.* **2008,** *42*, (12), 4478-4485.
195. Ng, N. L.; Canagaratna, M. R.; Jimenez, J. L.; Chhabra, P. S.; Seinfeld, J. H.; Worsnop, D. R., Changes in organic aerosol composition with aging inferred from aerosol mass spectra. *Atmos. Chem. Phys.* **2011,** *11*, (13), 6465-6474.
196. Chirico, R.; DeCarlo, P. F.; Heringa, M. F.; Tritscher, T.; Richter, R.; Prévôt, A. S. H.; Dommen, J.; Weingartner, E.; Wehrle, G.; Gysel, M.; Laborde, M.; Baltensperger, U., Impact of aftertreatment devices on primary emissions and secondary organic aerosol formation potential from in-use diesel vehicles: results from smog chamber experiments. *Atmos. Chem. Phys.* **2010,** *10*, (23), 11545-11563.
197. Ng, N. L.; Canagaratna, M. R.; Zhang, Q.; Jimenez, J. L.; Tian, J.; Ulbrich, I. M.; Kroll, J. H.; Docherty, K. S.; Chhabra, P. S.; Bahreini, R.; Murphy, S. M.; Seinfeld, J. H.; Hildebrandt, L.; Donahue, N. M.; DeCarlo, P. F.; Lanz, V. A.; Prévôt, A. S. H.; Dinar, E.; Rudich, Y.; Worsnop, D. R., Organic aerosol components

observed in Northern Hemispheric datasets from Aerosol Mass Spectrometry. *Atmos. Chem. Phys.* **2010,** *10*, (10), 4625-4641.
198. Sun, Y. L.; Zhang, Q.; Schwab, J. J.; Demerjian, K. L.; Chen, W. N.; Bae, M. S.; Hung, H. M.; Hogrefe, O.; Frank, B.; Rattigan, O. V.; Lin, Y. C., Characterization of the sources and processes of organic and inorganic aerosols in New York city with a high-resolution time-of-flight aerosol mass apectrometer. *Atmos. Chem. Phys.* **2011,** *11*, (4), 1581-1602.
199. He, L.-Y.; Huang, X.-F.; Xue, L.; Hu, M.; Lin, Y.; Zheng, J.; Zhang, R.; Zhang, Y.-H., Submicron aerosol analysis and organic source apportionment in an urban atmosphere in Pearl River Delta of China using high-resolution aerosol mass spectrometry. *J. Geophys. Res.* **2011,** *116*, (D12), D12304.
200. Chhabra, P. S.; Ng, N. L.; Canagaratna, M. R.; Corrigan, A. L.; Russell, L. M.; Worsnop, D. R.; Flagan, R. C.; Seinfeld, J. H., Elemental composition and oxidation of chamber organic aerosol. *Atmos. Chem. Phys.* **2011,** *11*, (17), 8827-8845.
201. Ng, N. L.; Canagaratna, M. R.; Jimenez, J. L.; Zhang, Q.; Ulbrich, I. M.; Worsnop, D. R., Real-Time Methods for Estimating Organic Component Mass Concentrations from Aerosol Mass Spectrometer Data. *Environ. Sci. Technol.* **2011,** *45*, (3), 910-916.
202. Cubison, M. J.; Ortega, A. M.; Hayes, P. L.; Farmer, D. K.; Day, D.; Lechner, M. J.; Brune, W. H.; Apel, E.; Diskin, G. S.; Fisher, J. A.; Fuelberg, H. E.; Hecobian, A.; Knapp, D. J.; Mikoviny, T.; Riemer, D.; Sachse, G. W.; Sessions, W.; Weber, R. J.; Weinheimer, A. J.; Wisthaler, A.; Jimenez, J. L., Effects of aging on organic aerosol from open biomass burning smoke in aircraft and laboratory studies. *Atmos. Chem. Phys.* **2011,** *11*, (23), 12049-12064.
203. Sage, A. M.; Weitkamp, E. A.; Robinson, A. L.; Donahue, N. M., Evolving mass spectra of the oxidized component of organic aerosol: results from aerosol mass spectrometer analyses of aged diesel emissions. *Atmos. Chem. Phys.* **2008,** *8*, (5), 1139-1152.
204. Chirico, R.; Prevot, A. S. H.; DeCarlo, P. F.; Heringa, M. F.; Richter, R.; Weingartner, E.; Baltensperger, U., Aerosol and trace gas vehicle emission factors measured in a tunnel using an Aerosol Mass Spectrometer and other on-line instrumentation. *Atmos. Environ.* **2011,** *45*, (13), 2182-2192.
205. Sun, Y. L.; Zhang, Q.; Schwab, J. J.; Chen, W. N.; Bae, M. S.; Hung, H. M.; Lin, Y. C.; Ng, N. L.; Jayne, J.; Massoli, P.; Williams, L. R.; Demerjian, K. L., Characterization of near-highway submicron aerosols in New York City with a high-resolution aerosol mass spectrometer. *Atmos. Chem. Phys.* **2012,** *12*, (4), 2215-2227.
206. Canagaratna, M. R.; Onasch, T. B.; Wood, E. C.; Herndon, S. C.; Jayne, J. T.; Cross, E. S.; Miake-Lye, R. C.; Kolb, C. E.; Worsnop, D. R., Evolution of Vehicle Exhaust Particles in the Atmosphere. *J. Air Waste Manag. Assoc.* **2010,** *60*, (10), 1192-1203.
207. Tobias, H. J.; Beving, D. E.; Ziemann, P. J.; Sakurai, H.; Zuk, M.; McMurry, P. H.; Zarling, D.; Waytulonis, R.; Kittelson, D. B., Chemical Analysis of Diesel Engine Nanoparticles Using a Nano-DMA/Thermal Desorption Particle Beam Mass Spectrometer. *Environ. Sci. Technol.* **2001,** *35*, (11), 2233-2243.
208. Schneider, J.; Kirchner, U.; Borrmann, S.; Vogt, R.; Scheer, V., In situ measurements of particle number concentration, chemically resolved size distributions and black carbon content of traffic-related emissions on German motorways, rural roads and in city traffic. *Atmos. Environ.* **2008,** *42*, (18), 4257-4268.

209. Mohr, C.; Richter, R.; DeCarlo, P. F.; Prévôt, A. S. H.; Baltensperger, U., Spatial variation of chemical composition and sources of submicron aerosol in Zurich during wintertime using mobile aerosol mass spectrometer data. *Atmos. Chem. Phys.* **2011,** *11*, (15), 7465-7482.
210. Lanz, V. A.; Prévôt, A. S. H.; Alfarra, M. R.; Weimer, S.; Mohr, C.; DeCarlo, P. F.; Gianini, M. F. D.; Hueglin, C.; Schneider, J.; Favez, O.; D'Anna, B.; George, C.; Baltensperger, U., Characterization of aerosol chemical composition with aerosol mass spectrometry in Central Europe: an overview. *Atmos. Chem. Phys.* **2010,** *10*, (21), 10453-10471.
211. Brown, S. G.; Lee, T.; Norris, G. A.; Roberts, P. T.; J. L. Collett, J.; Paatero, P.; Worsnop, D. R., Receptor modeling of near-roadway aerosol mass spectrometer data in Las Vegas, Nevada, with EPA PMF. *Atmos. Chem. Phys.* **2012,** *12*, (1), 309-325.
212. Mohr, C.; DeCarlo, P. F.; Heringa, M. F.; Chirico, R.; Slowik, J. G.; Richter, R.; Reche, C.; Alastuey, A.; Querol, X.; Seco, R.; Peñuelas, J.; Jiménez, J. L.; Crippa, M.; Zimmermann, R.; Baltensperger, U.; Prévôt, A. S. H., Identification and quantification of organic aerosol from cooking and other sources in Barcelona using aerosol mass spectrometer data. *Atmos. Chem. Phys.* **2012,** *12*, (4), 1649-1665.
213. Allan, J. D.; Alfarra, M. R.; Bower, K. N.; Williams, P. I.; Gallagher, M. W.; Jimenez, J. L.; McDonald, A. G.; Nemitz, E.; Canagaratna, M. R.; Jayne, J. T.; Coe, H.; Worsnop, D. R., Quantitative sampling using an Aerodyne aerosol mass spectrometer 2. Measurements of fine particulate chemical composition in two U.K. cities. *J. Geophys. Res.* **2003,** *108*, (D3), 4091.
214. Schneider, J.; Hock, N.; Weimer, S.; Borrmann, S.; Kirchner, U.; Vogt, R.; Scheer, V., Nucleation Particles in Diesel Exhaust: Composition Inferred from In Situ Mass Spectrometric Analysis. *Environ. Sci. Technol.* **2005,** *39*, (16), 6153-6161.
215. Heal, M. R.; Kumar, P.; Harrison, R. M., Particles, air quality, policy and health. *Chem. Soc. Rev.* **2012,** *41*, (19), 6606-6630.
216. Pope, C.; Burnett, R. T.; Thun, M. J.; Calle, E. E.; Krewski, D.; Ito, K.; Thurston, G. D., Lung cancer, cardiopulmonary mortality, and long-term exposure to fine particulate air pollution. *J.Amer. Med. Assoc.* **2002,** *287*, (9), 1132-1141.
217. Brook, R. D.; Rajagopalan, S.; Pope, C. A.; Brook, J. R.; Bhatnagar, A.; Diez-Roux, A. V.; Holguin, F.; Hong, Y.; Luepker, R. V.; Mittleman, M. A.; Peters, A.; Siscovick, D.; Smith, S. C.; Whitsel, L.; Kaufman, J. D., Particulate Matter Air Pollution and Cardiovascular Disease: An Update to the Scientific Statement From the American Heart Association. *Circulation* **2010,** *121*, (21), 2331-2378.
218. Calderón-Garcidueñas, L.; Solt, A. C.; Henríquez-Roldán, C.; Torres-Jardón, R.; Nuse, B.; Herritt, L.; Villarreal-Calderón, R.; Osnaya, N.; Stone, I.; García, R.; Brooks, D. M.; González-Maciel, A.; Reynoso-Robles, R.; Delgado-Chávez, R.; Reed, W., Long-term Air Pollution Exposure Is Associated with Neuroinflammation, an Altered Innate Immune Response, Disruption of the Blood-Brain Barrier, Ultrafine Particulate Deposition, and Accumulation of Amyloid β-42 and α-Synuclein in Children and Young Adults. *Toxicol. Pathol.* **2008,** *36*, (2), 289-310.
219. Harrison, R. M.; Yin, J., Particulate matter in the atmosphere: which particle properties are important for its effects on health? *Sci. Total Environ.* **2000,** *249*, (1–3), 85-101.
220. Beddows, D. C. S.; Dall'Osto, M.; Harrison, R. M., Cluster Analysis of Rural, Urban, and Curbside Atmospheric Particle Size Data. *Environ. Sci. Technol.* **2009,** *43*, (13), 4694-4700.

221. Sydbom, A.; Blomberg, A.; Parnia, S.; Stenfors, N.; Sandstrom, T.; Dahlen, S.-E., Health effects of diesel exhaust emissions. *Eur. Respir. J.* **2001,** *17*, 733-746.
222. Kreyling, W.; Semmler-behnke, M.; Moller, W., Ultrafine particle-lung interactions: Does size matter? *J. Aerosol Med.* **2006,** *19*, (1), 74-83.
223. Rückerl, R.; Schneider, A.; Breitner, S.; Cyrys, J.; Peters, A., Health effects of particulate air pollution: A review of epidemiological evidence. *Inhal. Toxicol.* **2011,** *23*, (10), 555-592.
224. Donaldson, K.; Li, X. Y.; MacNee, W., Ultrafine (nanometre) particle mediated lung injury. *J. Aerosol Sci.* **1998,** *29*, (5-6), 553-560.
225. Donaldson, K.; Brown, D.; Clouter, A.; Duffin, R.; MacNee, W.; Renwick, L.; Tran, L.; Stone, V., The pulmonary toxicology of ultrafine particles. *J. Aerosol Med.* **2002,** *15*, (2), 213-220.
226. Oberdörster, G., Pulmonary effects of inhaled ultrafine particles. *Int. Arch. Occ. Env. Hea.* **2000,** *74*, (1), 1-8.
227. Lin, C.-C.; Chen, S.-J.; Huang, K.-L.; Lee, W.-J.; Lin, W.-Y.; Tsai, J.-H.; Chaung, H.-C., PAHs, PAH-Induced Carcinogenic Potency, and Particle-Extract-Induced Cytotoxicity of Traffic-Related Nano/Ultrafine Particles. *Environ. Sci. Technol.* **2008,** *42*, (11), 4229-4235.
228. Lippmann, M.; Chen, L.-C., Health effects of concentrated ambient air particulate matter (CAPs) and its components. *Crit. Rev. Toxicol.* **2009,** *39*, (10), 865-913.
229. Chen, L. C.; Lippmann, M., Effects of Metals within Ambient Air Particulate Matter (PM) on Human Health. *Inhal. Toxicol.* **2009,** *21*, (1), 1-31.
230. Zhang, Q.; Zhu, Y., Measurements of ultrafine particles and other vehicular pollutants inside school buses in South Texas. *Atmos. Environ.* **2010,** *44*, (2), 253-261.
231. Kerkhof, M.; Postma, D. S.; Brunekreef, B.; Reijmerink, N. E.; Wijga, A. H.; de Jongste, J. C.; Gehring, U.; Koppelman, G. H., Toll-like receptor 2 and 4 genes influence susceptibility to adverse effects of traffic-related air pollution on childhood asthma. *Thorax* **2010,** *65*, (8), 690-697.
232. Kim, J. J.; Smorodinsky, S.; Lipsett, M.; Singer, B. C.; Hodgson, A. T.; Ostro, B., Traffic-related Air Pollution near Busy Roads: The East Bay Children's Respiratory Health Study. *Am. J. Resp.Crit. Care* **2004,** *170*, (5), 520.
233. Ostro, B.; Roth, L.; Malig, B.; Marty, M., The Effects of Fine Particle Components on Respiratory Hospital Admissions in Children. *Environ. Health Persp.* **2009,** *117*, (3), 475-480.
234. Gehring, U.; Wijga, A.; Brauer, M.; Fischer, P.; de Jongste, J.; Kerkhof, M.; Oldenwening, M.; Smit, H.; Brunekreef, B., Traffic-related Air Pollution and the Development of Asthma and Allergies during the First 8 Years of Life. *Am. J. Resp. Crit. Care* **2010,** *181*, (6), 596-603.
235. Jerrett, M.; Shankardass, K.; Berhane, K.; Gauderman, W. J.; Künzli, N.; Avol, E.; Gilliland, F.; Lurmann, F.; Molitor, J. N.; Molitor, J. T.; Thomas, D. C.; Peters, J.; McConnell, R., Traffic-related air pollution and asthma onset in children: a prospective cohort study with individual exposure measurement. *Environ. Health Persp.* **2008,** *116*, (10), 1433-1438.
236. Gauderman, W. J.; Vora, H.; McConnell, R.; Berhane, K.; Gilliland, F.; Thomas, D.; Lurmann, F.; Avol, E.; Kunzli, N.; Jerrett, M.; Peters, J., Effect of exposure to traffic on lung development from 10 to 18 years of age: a cohort study. *The Lancet* **2007,** *369*, (9561), 571-577.

237. Ryan, P. H.; Le Masters, G.; Biagini, J.; Bernstein, D.; Grinshpun, S. A.; Shukla, R.; Wilson, K.; Villareal, M.; Burkle, J.; Lockey, J., Is it traffic type, volume, or distance? Wheezing in infants living near truck and bus traffic. *J. Allergy Clin. Immunol.* **2005,** *116*, (2), 279-284.
238. Ryan, P. H.; Bernstein, D. I.; Lockey, J.; Reponen, T.; Levin, L.; Grinshpun, S.; Villareal, M.; Khurana Hershey, G. K.; Burkle, J.; LeMasters, G., Exposure to Traffic-related Particles and Endotoxin during Infancy Is Associated with Wheezing at Age 3 Years. *Am. J. Resp. Crit. Care* **2009,** *180*, (11), 1068-1075.
239. Peters, A., Particulate matter and heart disease: Evidence from epidemiological studies. *Toxicol. Appl. Pharm.* **2005,** *207*, (2, Supplement), 477-482.
240. Breitner, S.; Liu, L.; Cyrys, J.; Brüske, I.; Franck, U.; Schlink, U.; Leitte, A. M.; Herbarth, O.; Wiedensohler, A.; Wehner, B.; Hu, M.; Pan, X.-C.; Wichmann, H. E.; Peters, A., Sub-micrometer particulate air pollution and cardiovascular mortality in Beijing, China. *Sci. Total Environ.* **2011,** *409*, (24), 5196-5204.
241. Mills, N. L.; Donaldson, K.; Hadoke, P. W.; Boon, N. A.; MacNee, W.; Cassee, F. R.; Sandstrom, T.; Blomberg, A.; Newby, D. E., Adverse cardiovascular effects of air pollution. *Nat Clin Pract Cardiovasc Med* **2009,** *6*, (1), 36-44.
242. Gao, Y.; Chan, E. Y. Y.; Zhu, Y.; Wong, T. W., Adverse effect of outdoor air pollution on cardiorespiratory fitness in Chinese children. *Atmos.Environ.* **2013,** *64*, (0), 10-17.
243. Ruiz, J. R.; Castro-Piñero, J.; Artero, E. G.; Ortega, F. B.; Sjöström, M.; Suni, J.; Castillo, M. J., Predictive validity of health-related fitness in youth: a systematic review. *Brit. J. Sport Med.* **2009,** *43*, (12), 909-923.
244. Calderón-Garcidueñas, L.; Mora-Tiscareño, A.; Ontiveros, E.; Gómez-Garza, G.; Barragán-Mejía, G.; Broadway, J.; Chapman, S.; Valencia-Salazar, G.; Jewells, V.; Maronpot, R. R.; Henríquez-Roldán, C.; Pérez-Guillé, B.; Torres-Jardón, R.; Herrit, L.; Brooks, D.; Osnaya-Brizuela, N.; Monroy, M. E.; González-Maciel, A.; Reynoso-Robles, R.; Villarreal-Calderon, R.; Solt, A. C.; Engle, R. W., Air pollution, cognitive deficits and brain abnormalities: A pilot study with children and dogs. *Brain Cognition* **2008,** *68*, (2), 117-127.

Chapter 3. Concentration and Oxidative Potential of On-Road Particle Emissions and Their Relationship with Traffic Composition: Relevance to Exposure Assessment

Leigh R. Crilley[a,b], Luke D. Knibbs[a,b], Branka Miljevic[a,b], Xiaochun Cong[a,d], Kathryn E. Fairfull-Smith[c], Steve E. Bottle[c], Zoran D. Ristovski[a,b], Godwin A. Ayoko[a,b] and Lidia Morawska[a,b]

[a]International Laboratory for Air Quality and Health,
Queensland University of Technology,
Brisbane, QLD 4001, Australia.

[b]Institute of Health and Biomedical Innovation,
Queensland University of Technology,
Brisbane, QLD 4001, Australia

[c]ARC Centre of Excellence for Free Radical Chemistry and Biotechnology,
Queensland University of Technology,
Brisbane, QLD 4001, Australia

[d]Architecture Environment and Equipment Engineering,
Shandong University of Science and Technology,
Qingdao, Shandong Province, P. R. China.

(2012) *Atmospheric Environment*, **59**, 533-539.

PREFACE

This paper comprises of a pilot study aimed to investigate the effect of traffic counts and composition on the levels traffic emissions and their toxicity for the Brisbane fleet. In this paper, the on-road measurements of particle associated oxidative potential, which is a measure of toxicity, of vehicle emissions were reported under 'real world' dilution levels for the first time. A key parameter found for the toxicity of the traffic emissions was the total traffic count. Thus this parameter was investigated in subsequent research at urban schools in Brisbane (Chapters 4-8).

Statement of joint authorship of co-authors

The authors listed below have certified* that:

1. they meet the criteria for authorship in that they have participated in the conception, execution, or interpretation, of at least that part of the publication in their field of expertise;
2. they take public responsibility for their part of the publication, except for the responsible author who accepts overall responsibility for the publication;
3. there are no other authors of the publication according to these criteria;
4. potential conflicts of interest have been disclosed to (a) granting bodies, (b) the editor or publisher of journals or other publications, and (c) the head of the responsible academic unit, and
5. they agree to the use of the publication in the student's thesis and its publication on the QUT ePrints database consistent with any limitations set by publisher requirements.

In the case of this chapter:

Concentration and Oxidative Potential of On-Road Particle Emissions and Their Relationship with Traffic Composition: Relevance to Exposure Assessment, (2012) ***Atmospheric Environment,*** **59, 533-539.**

Contributor	Statement of contribution*
Leigh R. Crilley	Collected the particle data, performed the data analysis and wrote the manuscript
Luke D. Knibbs*	Assisted with the study design, collected the particle data and helped draft the manuscript
Branka Miljevic*	Performed the ROS sampling and analysis and helped draft the manuscript
Xiaochun Cong*	Collected the particle data and assisted with the data analysis
Kathryn E. Fairfull-Smith*, Steve E. Bottle*	Synthesised the BPEAnit probe
Zoran D. Ristovski*, Godwin A. Ayoko*	Assisted with the data analysis
Lidia Morawska*	Conceived the study design and assisted with analysis, data interpretation and drafting the manuscript.

Principal Supervisor Confirmation
I have sighted email or other correspondence from all Co-authors confirming their certifying authorship.

PROF GODWIN AYOKO — Name
Signature
22/11/2013 — Date

ABSTRACT

Particles emitted by vehicles are known to cause detrimental health effects, with their size and oxidative potential among the main factors responsible. Therefore, understanding the relationship between traffic composition and both the physical characteristics and oxidative potential of particles is critical. To contribute to the limited knowledge base in this area, we investigated this relationship in a 4.5 km road tunnel in Brisbane, Australia.

On-road concentrations of ultrafine particles (< 100 nm, UFPs), fine particles ($PM_{2.5}$), CO, CO_2 and particle associated reactive oxygen species (ROS) were measured using vehicle-based mobile sampling. UFPs were measured using a condensation particle counter and $PM_{2.5}$ with a DustTrak aerosol photometer. A new profluorescent nitroxide probe, BPEAnit, was used to determine ROS levels. Comparative measurements were also performed on an above-ground road to assess the role of emission dilution on the parameters measured.

The profile of UFP and $PM_{2.5}$ concentration with distance through the tunnel was determined and demonstrated relationships with both road gradient and tunnel ventilation. ROS levels in the tunnel were found to be high compared to an open road with similar traffic characteristics, which was attributed to the substantial difference in estimated emission dilution ratios on the two roadways. Principal component analysis (PCA) revealed that the levels of pollutants and ROS were generally better correlated with total traffic count, rather than the traffic composition (i.e. diesel and gasoline-powered vehicles).

A possible reason for the lack of correlation with HDV, which has previously been shown to be strongly associated with UFPs especially, was the low absolute numbers encountered during the sampling. This may have made their contribution to in-tunnel pollution largely indistinguishable from the total vehicle volume. For ROS, the stronger association observed with HDV and gasoline vehicles when combined (total traffic count) compared to when considered individually may signal a role for the interaction of their emissions as a determinant of on-road ROS in this pilot study. If further validated, this should not be overlooked in studies of on- or near-road particle exposure and its potential health effects.

KEYWORDS: Toxicity; Diesel; Gasoline; Sampling; Exposure

3.1 INTRODUCTION

Many studies have demonstrated detrimental health effects due to airborne particles, especially those in the ultrafine size range (D_p < 100 nm, UFP) [1-4]. In urban environments, vehicle emissions are the major source of UFPs [5]. The toxicity of particles emitted by vehicles is thought to be related to both their chemical composition and size [1, 6]. A well-promoted mechanism via which the chemical composition of particles may cause cellular damage is oxidative stress [2]. Therefore, characterizing and quantifying vehicle particulate emissions and their potential to cause oxidative stress under real world conditions is necessary to better appreciate their human health effects.

Many of the adverse health outcomes associated with exposure to fine (D_p < 2.5 μm, $PM_{2.5}$) and ultrafine particles have been attributed to oxidative stress caused by the

presence of reactive oxygen species (ROS) on these particles, and generation of free radicals and related ROS at their sites of deposition [2, 3, 7]. An indication of particle toxicity can be inferred by measuring particle associated ROS, which have been detected in diesel and gasoline emissions [8, 9]. However, while measurements of ROS in vehicle emissions under relatively well-controlled conditions in dynamometer studies have established their presence and variability, the relationship between vehicle emitted ROS and road and traffic parameters under real world conditions is not well defined. On-road UFP concentrations are highly dynamic, especially in tunnel environments [10], and on-road measurements can capture the characteristics of concentrations entering vehicle cabins [11, 12]. Road tunnels can be an especially high exposure microenvironment [12, 13], and are excellent locations in which to measure vehicle emissions, as the influence of meteorological conditions is minimised [10]. On-road measurements can also provide information on the influence of tunnel roadway factors, such as gradient and ventilation, on vehicle emissions [11, 14-16]. While several studies have shown that the road gradient in a tunnel can affect the concentrations of gaseous pollutants [14-16], there have only been limited on-road measurements of the effects on vehicle particle emissions [11].

This study aimed to contribute towards addressing the knowledge gaps outlined above by quantifying the effect of tunnel characteristics, namely gradient and ventilation, on particle concentrations. In addition, we aimed to assess the oxidative potential of particles present in the tunnel under real world conditions. Finally, we aimed to determine the effects of traffic number and composition on the

concentration of UFPs, $PM_{2.5}$ mass and particle associated ROS in the tunnel. Through this, we sought to better understand the physical and chemical characteristics of particles to which people are exposed in on-road microenvironments.

3.2 METHODS

3.2.1 Setting

Measurements were conducted in a recently opened (March, 2010) road tunnel in Brisbane, Australia. The tunnel runs in a north-south direction and consists of two 4.5 km unidirectional bores, each with two lanes, and with a maximum speed of 80 kmh^{-1}. The tunnel is currently Australia's longest. There are two northbound entries to the tunnel, one of which is 1.5 km along the tunnel, and a single exit at the northern portal. The southbound bore has one entry and two exits, with one exit 3 km along the tunnel and the other at the southern portal. The gradient of the tunnel roadway from the northbound entry comprises a downhill slope of 5% for 0.5 km followed by a near flat section for 1 km until the second entry point, whereupon it slopes downhill at 3.5% for 1.5 km, and finally uphill for 1.5 km at 3.5%. The opposite applies in the southbound bore. The tunnel has a longitudinal ventilation system, and no portal emissions are permitted (i.e. all air must be exhausted by one of two stacks). In the southbound bore air is extracted 0.5 km from the exit, while for the northbound section the main extraction point is located immediately adjacent to the exit. Figure 3-1 shows a schematic of the tunnel layout.

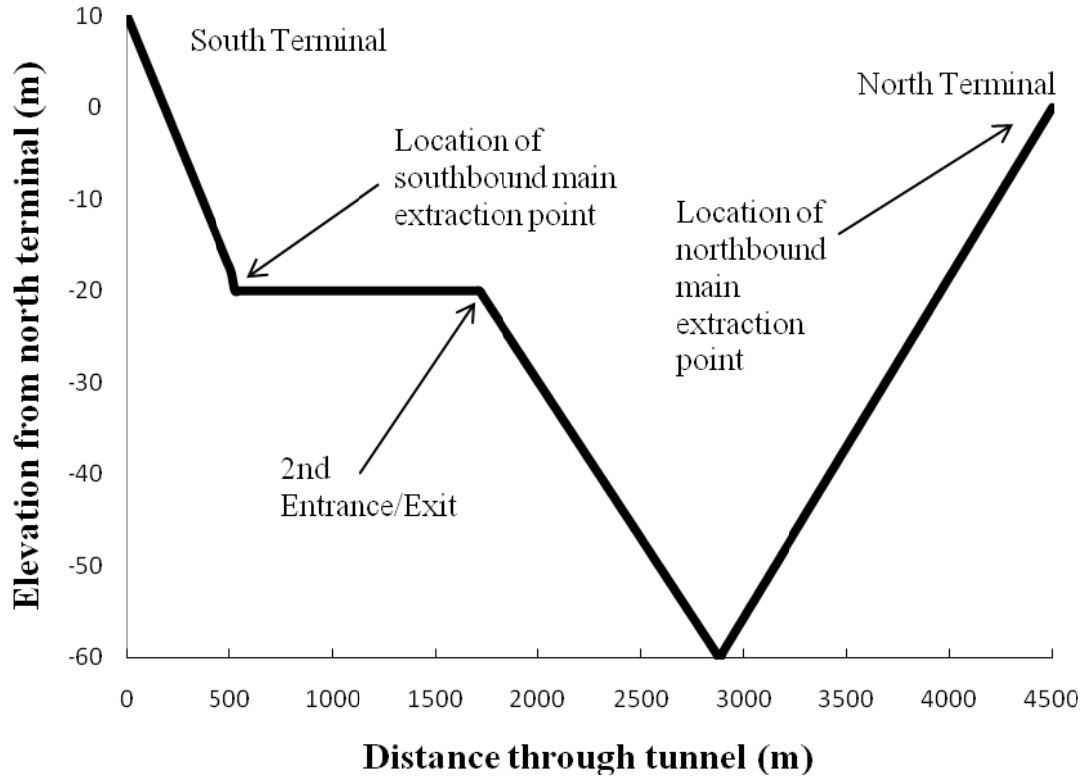

Figure 3-1: Schematic diagram of the tunnel.

3.2.2 Instrumentation

A TSI 3007 condensation particle counter (CPC) was used to measure the number concentration of particles between 10 and >1000 nm every second. In urban areas affected by vehicle emissions the great majority (85% or more) of particles in this size range are UFPs [5], and we use UFP to describe measurements made by the CPC. The 3007 CPC can detect a maximum concentration of 10^5 particles cm^{-3} before coincidence error becomes significant [17]. Accordingly, we developed a correction factor based on contemporaneous measurements with a TSI 3022A CPC, and this is described in Appendix 1. The exponential correction factor we used was very similar to that determined by Westerdahl et al. [18] based on an analogous approach, and like Westerdahl et al. [18] we applied it to all data points greater than 10^5 particles cm^{-3}.

A TSI 8520 DustTrak was fitted with a 2.5 μm impactor and measured $PM_{2.5}$ concentration every second. The DustTrak is an optical instrument, and its calibration is based on an aerosol different to that encountered on-road. As such, we used a correction factor that was based on simultaneous measurements with a tapered element oscillating microbalance (TEOM) in a Brisbane tunnel, as described by Jamriska et al. [19]. A TSI IAQ-Calc 7545 gas analyser was used to measure concentrations of CO and CO_2, in addition to temperature and relative humidity.

A new profluorescent nitroxide probe, BPEAnit**,** was used for the detection of particle based ROS as described in Miljevic et al. [20]. Briefly, the BPEAnit probe was synthesised in the laboratory by the method described by Fairfull-Smith and Bottle [21], and the aerosol was sampled through an impinger containing 20 mL of 4 μM BPEAnit solution. The flow through both impingers was 1 L min^{-1}. No cyclones or other devices were used to pre-select a specific particle size range, and the measurements were of total suspended particles entering the sample tube. For each tunnel journey, two samples were collected simultaneously; a test sample and a high efficiency particulate air (HEPA)-filtered control sample. Based on the difference in fluorescence between these, the increase due to particle associated ROS was calculated. The fluorescence of both the control and sample measurements was measured immediately after sampling with no pre-treatment using an Ocean Optics USB2000+ fibre-optic spectrometer combined with a cuvette holder and pulsed xenon lamp.

To ensure enough particle mass was collected for the BPEAnit assay, aerosol was sampled cumulatively for the 4 or 6 tunnel journeys that comprised each

measurement exercise, and this constituted one BPEAnit sample. The pump used for BPEAnit assay started operating at the entrance to the tunnel and was stopped at the exit so that only tunnel air was sampled. The assay result was determined for each sampling trip and normalised by the mass of particulate matter collected, which was approximated by integrating corrected DustTrak readings over the sampling period. For comparison, results were also expressed per volume of tunnel air sampled. The values obtained indicated the oxidative potential of particles, hereafter referred to as ROS concentrations.

3.2.3 Quality control

Quality control checks were carried out on the CPC and DustTrak daily and involved checking the flow rate and zero reading of each instrument. The flow rate of the pump used for BPEAnit assay was checked both and before and after sampling and was always within 20% of the target flow.

3.2.4 Sampling approach

The CPC and DustTrak were set up inside a vehicle and connected to a common sampling point located outside the vehicle and facing the direction of travel. A 0.8 m conductive rubber tube was used to transport particle samples to the two instruments. The sample residence time in the tube was 0.6 s, while the response times of the CPC (<9 s) [12] and DustTrak (time constant: 1s) were both sufficiently high to capture concentration fluctuations in tunnel transport microenvironments. The major respective particle loss mechanisms affecting CPC and DustTrak measurements, diffusion and antisokinetic sampling, were both negligible.

The Q-Trak probe was attached to the outside of the vehicle near the tubing inlet. The sampling inlet leading to the impingers with the BPEAnit solution sampled from

a separate tube on the rear driver side facing the direction of travel. The research vehicle used unleaded petrol and was in excellent condition. A recording of each tunnel trip was taken by a video camera mounted on the vehicle's dashboard in order to capture the traffic conditions and events encountered.

Measurements were conducted over three sampling campaigns in March (I), July (II) and August/September (III), 2010. ROS measurements were conducted during campaign III only, in order to first establish their feasibility and the concentration characteristics of particles in the tunnel during campaigns I and II. On each sampling day there were 2-3 sampling exercises and each comprised 2-3 trips through each bore. The sampling times ranged from 07:00 to 20:00 to permit measurements under a range of different traffic conditions. A total of 182 trips were performed, with 50 in campaign I, 60 in II and 72 in III, and these were evenly distributed across the two bores. The large number of tunnel trips and spread of sampling times aimed to ensure that the data was representative of general conditions in the tunnel.

All instruments were run continuously throughout leaving the Queensland University of Technology campus (located 9 km from the tunnel), performing tunnel measurements, and returning to the university. This permitted collection of additional open road data en-route to the tunnel. The same route was taken from the university to the tunnel and for the return journey, and it comprised travel on two major roads (Riverside Expressway and Innercity Bypass) with higher traffic volumes than those in the tunnel; 135,000 and 70,000 vehicles per day, respectively [22].

Open road measurements were performed in October, 2010, on a road with traffic count, composition, speed limit and flow analogous to that in the tunnel. This was

done to allow comparison of ROS concentrations under different dilution conditions to those present in the tunnel. UFP and $PM_{2.5}$ measurements were also recorded. The sampling times for the BPEAnit assay were between 16 and 24 minutes during these open road measurements, in order to match the total sampling times of 4-6 tunnel trips.

3.2.5 Data analysis

Traffic count and composition data for the tunnel were supplied at hourly resolution by its operators, River City Motorway Group. The traffic data was classified into 3 categories on the basis of length; short vehicles referred to those less than 7 m, medium vehicles defined as those between 7 and 12 m, while long vehicles were those over 12 m. The sum of medium and long vehicles was assumed to comprise diesel vehicles only, and was renamed heavy diesel vehicles (HDVs) in our analyses.

Using video recordings, tunnel trips were assigned to categories according to whether HDVs were encountered to determine their impact on the measured parameters. A simple model of UFP and $PM_{2.5}$ concentration profile in both bores was constructed for each of these scenarios (i.e. HDVs present or not) to identify the effect of traffic and tunnel characteristics. As there are four main roadway sections, each with a different gradient, individual tunnel trips were therefore divided into four corresponding sections. The slope of particle concentration profiles over distance traversed in each section was calculated. In this basic model, the median concentration profile in each section was calculated and linked to the median value at the start of the subsequent section. The first and third quartiles were also calculated in the same fashion to indicate the spread of data. This represented a ‘typical’ profile,

and the vast majority of the actual measurement profiles for northbound and southbound trips followed the trends in the calculated model.

Dilution ratio estimates corresponding to ROS measurements performed during campaign III were calculated according to the method described in Ntziachristos et al. [23] (Appendix 1). Principal component analysis (PCA) was used to identify any correlations between ROS, pollutant levels and traffic data in the campaign III data.

3.3 RESULTS AND DISCUSSION

3.3.1 Overall results

The average total vehicle counts per bore in the tunnel during campaigns I, II and III were 1728, 1029 and 1112 vehicles h^{-1}, respectively. The decrease in count after campaign I was due to the introduction of a toll. The traffic composition was similar, with short vehicles representing 79, 77 and 74.3%, medium vehicles 15.6, 17 and 19.6%, and long vehicles 5.4, 6.3 and 6.1% of the average total traffic during the 3 campaigns, respectively.

The average time taken to travel through the northbound bore was 3 min 56 s, while southbound trips took 4 min 4 s. The concentrations measured during each campaign are given in Table 3-1. No CO data was collected during campaign II due to instrument error. Data collected on above ground roads are summarised in Appendix 1.

Table 3-1: Average trip concentrations of the measured parameters during each campaign.

Campaign	*Temp. (°C)*	*Relative Humidity (%)*	*CO (ppm)*	*CO_2 (ppm)*	*UFP Number ($p\ cm^{-3}$)*	*$PM_{2.5}$ ($\mu g\ m^{-3}$)*
I	29	61	6.4	536	$1.43x10^5$	36
II	22	50	[a]	484	$1.23x10^5$	26
III	24	54	4.9	665	$1.32x10^5$	36

[a]CO data was not collected during campaign II.

3.3.2 Profile of UFP and PM2.5 concentration through the tunnel

The concentration profiles of UFP and $PM_{2.5}$ based on all southbound and northbound runs are shown in Figures 3-2 and 3-3, respectively. These all exhibited differences between the two bores that corresponded with the ascending and descending roadway sections in each. Profiles in the southbound bore were characterised by a sharp increase on the first ascending section followed by relative stability on the near-flat section. The initial sharp increase is attributed to greater vehicle engine load on ascent and an associated increase in emissions. In the final section there was a decrease in concentration that was most likely due to the tunnel ventilation system, as the main extraction point is located at the start of this section. The first quartile values in this section are negative due to the large variation observed in UFP and $PM_{2.5}$ concentrations, and the effect of this on the slope of concentration with distance.

Concentrations in the northbound bore exhibited increases throughout the entire trip, with the largest of these observed on the ascending section, and smallest on the descending section. This trend has been observed previously in terms of both UFPs [11] and $PM_{2.5}$ [14]. The ventilation extraction point at the northbound exit is sited

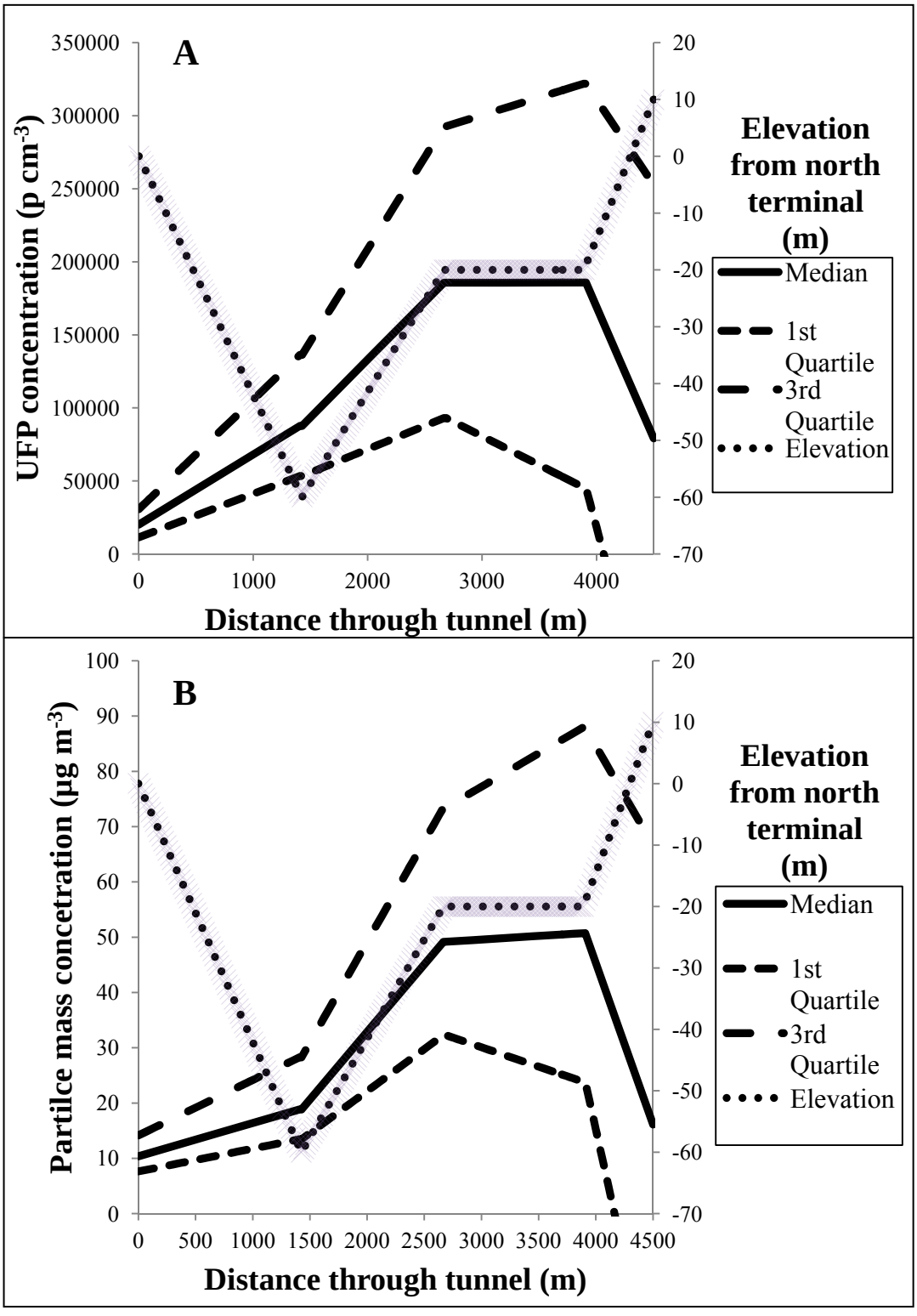

Figure 3-2: Particle number (A) and mass (B) concentration with distance through the tunnel for all southbound tunnel trips

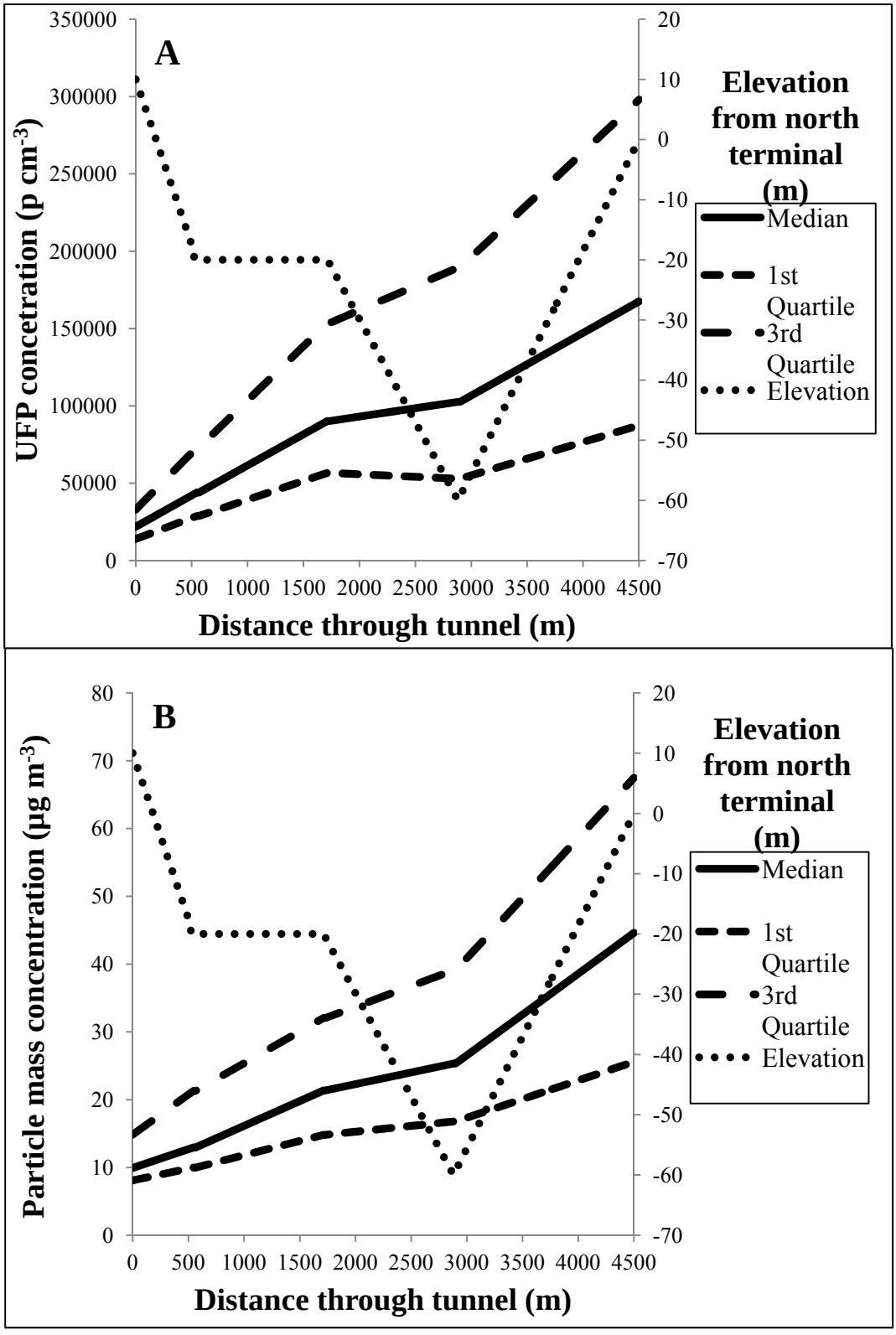

Figure 3-3: Particle number (A) and mass (B) concentration evolution by distance through the tunnel for all northbound runs.

almost at the terminal end of the bore, and its effect on the concentration profile in its vicinity is subsequently much less marked than in the southbound bore. This indicates that the location of the ventilation system had a significant effect on the pollutant levels in this tunnel. The concentration of UFPs and $PM_{2.5}$ in the tunnel was also observed to be related to the gradient in the tunnel, with a sharper increase found on the uphill sections compared to the flat and downhill sections. This implies that the gradient of the road can be used as a general predictor of the concentration profile of UFPs and $PM_{2.5}$ in the tunnel. It should also be considered that traffic speeds were relatively consistent across all sampling runs, and this minimised the effects of different engine cycles and driving conditions.

3.3.2.1 ***Influence of HDVs***

In an initial analysis we examined the correlation between on-road particle concentrations and average traffic counts and composition (i.e. HDVs and non-HDVs), as has been used successfully in previous studies [12, 24]. In contrast to these, we observed no significant correlations between on-road concentrations and HDVs. We tentatively attributed this to the one hour time resolution of the traffic data, and therefore used visual classification of the tunnel runs based on video recordings to determine the influence of HDVs. The profiles for the tunnel trips were classified according to whether HDVs were present in the immediate vicinity (i.e. visually observed) in front of the sampling vehicle; these are presented in Appendix 1. The profiles showed similar variation in the concentration for the UFP and $PM_{2.5}$ profiles when compared to those collected in the absence of HDVs. While we were able to identify HDV in the immediate vicinity of our research vehicle, there may have been some influence from HDVs that were outside our field of vision. Overall

however, HDVs and UFP and $PM_{2.5}$ concentrations were poorly correlated, and HDVs had minimal effects on concentration profiles.

The lack of readily discernible effects of HDVs is in contrast to previous studies in road tunnels, where they exerted considerable influence on UFP and $PM_{2.5}$ concentrations [12, 25, 26]. Using a similar mobile sampling approach to the present study, Knibbs et al. [12] found that hourly HDV traffic volume was a fair to very good determinant of UFP concentration in the two bores of a road tunnel in Sydney, Australia. Stationary sampling in the Caldecott tunnel, San Francisco, showed a clear increase in UFP concentration as a result of a small increase in the percentage of diesel vehicles [25, 26]. Notwithstanding any differences in the fuel used by fleets in Sydney and San Francisco, in both locations a clear influence of HDVs on UFP concentrations was observed. Although there was a large percentage of HDV (23%) in the tunnel we studied, certainly much higher than in the studies performed in San Francisco (3.8%) [25] and Sydney (7%) [12], the absolute number of HDVs we encountered was low. During sampling we observed a maximum of only a few HDVs per tunnel trip, and sometimes less. Their contribution appears to be largely indistinguishable from the contribution of the overall vehicle volume, which was predominantly comprised of gasoline vehicles.

Mobile sampling is more heavily influenced by the number and type of vehicles in the immediate vicinity of the sampling vehicle compared to stationary sampling, and this could partially explain why the presence of HDV was a poor determinant of higher concentrations in this study. The fixed sampling point approach is better

suited for the calculation of average emissions. However, of the two approaches mobile sampling is most representative of in-vehicle exposure concentrations, with the extent to which these match on-road concentrations primarily dependent on cabin ventilation rates [13]. In the absence of strong or consistent local relationships between on-road particle concentrations and other parameters, as was the case here, the simple approach to predicting on-road profiles we adopted could be combined with other modelling techniques to predict the likely range of in-cabin exposure [13].

3.3.3 Oxidative potential of particle emissions

3.3.3.1 ***General findings***

Particle associated ROS were detected during all but one of the sampling trips in the tunnel, and concentrations ranged from 0 - 1182 nmol mg^{-1} of particle mass, as shown in Table 3-2. During open road measurements we detected no particle associated ROS. Particle associated ROS in the tunnel were thus markedly elevated in all but one case compared to an open road with matched traffic and driving characteristics. On 1/9/2010, the respective concentrations of all three ROS samples were 225, 759, 1182 nmol mg^{-1} compared to the average of the other sampling days of 206 nmol mg^{-1}. The higher than average levels on that day were attributed to controlled vegetation fires in the local area. The dominance of that source was demonstrated by both UFP and $PM_{2.5}$ concentrations outside the tunnel exceeding those in it during the morning sampling exercise. In addition, wood smoke has previously been found to have high ROS content [27].

The ROS levels detected in this tunnel study are high compared to previous work [9, 28]. A recent dynamometer study using the same BPEAnit assay [9] found an ROS concentration of 50 nmol mg^{-1} in diesel exhaust from an engine running at 100%

load at 1700 rpm. This is substantially lower than ROS levels observed in the tunnel. Although dynamometer studies cannot be directly compared with on-road studies, this nonetheless indicates that diesel exhaust might not have been the predominant source of increased BPEAnit fluorescence in PM we sampled.

Table 3-2: Particle associated ROS concentrations for each sample in campaign III.

Date	Time	*ROS Concentration* (nmol mg^{-1})	(nmol m^{-3})	*Total Vehicle Count* (h^{-1})	*Traffic Composition* (% HDV)	*Dilution Ratio* (-)
23/08/2010	1000-1100	286	13	693	44	380
	1400-1500	295	12	848	29	861
1/09/2010	0700-0800	226	20	1362	15	431
	1100-1200	760	24	721	28	836
	1600-1700	1183	36	1515	25	453
10/09/2010	1200-1300	180	6	885	32	918
	1500-1600	159	6	1336	24	683
16/09/2010	0730-0830	385	8	1325	17	556
	1100-1200	212	5	774	28	856
	1600-1700	335	8	1564	23	480
23/09/2010	0900-1000	75	2	768	23	644
	1530-1630	213	6	1337	21	542
28/09/2010	1000-1100	0	0	733	25	494
	1600-1700	117	5	1444	38	-

Shaded areas represent peak traffic times in the tunnel. Traffic data is average of northbound and southbound bores.

3.3.3.2 ***Principal Component Analysis***

PCA was utilised to assess the relationships between ROS levels, traffic count, composition, and other parameters we measured in the tunnel. The resultant PCA loadings plot is shown in Figure 3-4, with 68% of total variance explained by both PC's. It indicates that, in general, the levels of pollutants were better correlated with total vehicle count rather than traffic composition. In terms of particle associated ROS, this finding may suggest that it was the combined emissions of diesel and gasoline vehicles, rather than either individually, that potentiated ROS levels we

measured in this on-road tunnel study. This effect has physio-chemical plausibility if diesel emissions provided a carbonaceous core onto which condensable gasoline emissions relatively high in ROS were absorbed. Future work will address this in greater depth.

The dithiothretiol (DTT) method has also been used to measure oxidative potential of particulate matter [28]. Though the DTT assay results are not directly comparable with those from a BPEAnit probe, relative trends can be compared. In the 1.1 km Caldecott tunnel, the highest DTT activity per particle mass was found in the bore which contained gasoline vehicles only [28]. This result is in agreement with other dynamometer studies that used the DTT assay [8, 29], which found higher ROS activity per mass of particles emitted by gasoline vehicles compared to diesel vehicles. Further to these results, our preliminary findings may suggest an interaction between diesel and gasoline emissions as a determinant of on-road ROS levels in the tunnel we studied.

3.3.3.3 ***ROS levels on an open road***

In contrast to the tunnel, sampling on an open road with similar traffic characteristics did not result in increased fluorescence of the BPEAnit probe. The ROS levels and associated oxidative potential of PM emissions were below detectable levels. This is possibly due to different dilution ratios in the two sampling environments, with tunnels characterised by low estimated dilution rations (Table 3-2) when compared to the unconstrained dilution possible on open air roadways [30]. The gas to particle partitioning of semi-volatile (organic) compounds, which has been found to contribute to oxidative potential of PM emissions [27, 30], strongly depends on dilution conditions, with lower dilution conditions favouring a higher fraction of

semi-volatile compounds in the particle phase. Biswas et al. [30] reported that PM oxidative potential measured by the DTT assay decreases with increasing dilution ratios. While we did not observe such strong correlation, possibly due to the small range of dilution ratios we encountered (500-1000), we did find relatively high ROS levels in the low dilution tunnel environment, and did not detect ROS on an open road.

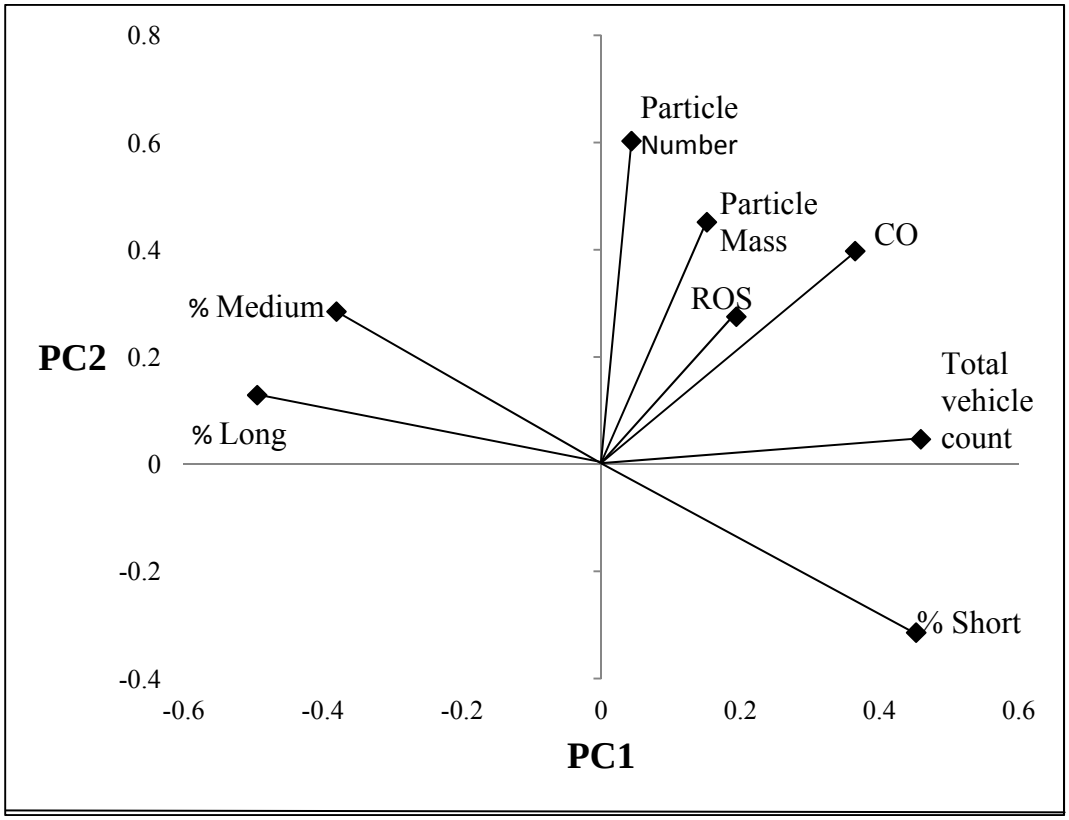

Figure 3-4: PCA loadings plot of campaign III data.

The units used for the PCA were for CO (ppm), ROS (nmol mg^{-1}), particle number (particles cm^{-1}), particle mass (μg m^{-3}) and total traffic count (vehicles h^{-1}).

3.3.3.4 ***Summary***

While we only detected ROS in the tunnel and not on an open road, the sum of our results and comparable work described above may carry implications for health risk assessment on and near roadways. Previous studies [12, 24] have shown HDV

volume to be strongly associated with on-road UFP concentrations. If, however, some other determinants, such as total traffic or gasoline vehicle volume, are consistently shown to be primarily responsible for oxidative potential of particles, then measurement, modelling and epidemiologic studies of on- and near-road exposures should also consider this.

3.4 CONCLUSIONS

Despite the absence of strong relationships between on-road particle concentrations and other parameters, we used a simple technique to estimate concentration profiles along a 4.5 km tunnel roadway. This could be combined with models for predicting in-cabin concentrations for the purposes of exposure assessment. PCA found total traffic volume was better related to UFP, $PM_{2.5}$ and ROS concentrations in the tunnel than either HDV or gasoline vehicle volume individually. ROS levels on an open road with analogous traffic volume, composition and speed were below detectable limits, which further highlights the effects of dilution on particle associated ROS. Although HDV volume is often well-correlated with UFP concentrations, if the trends observed in this and other recent studies are further validated by future work, then it should signal the need to consider total or gasoline vehicle volume (or both) as a key parameter when evaluating potential ultrafine and fine particle health effects on and near roadways.

Acknowledgements

We thank River City Motorway Group for their involvement and assistance. This project was supported by ARC Linkage Grant LP0882544 “Quantification of Traffic Generated Nano and Ultrafine Particle Dynamics and Toxicity in Transit Hubs and

Transport Corridors". LDK acknowledges an IHBI Human Health and Wellbeing Early Career Researcher Grant.

Appendix 1

Appendix 1 contains profiles of UFP and $PM_{2.5}$ concentration with and without HDVs present, dilution ratio calculations, correction factor for 3007 CPC measurements and open road particle concentrations.

3.5 REFERENCES

1. Donaldson, K.; Li, X. Y.; MacNee, W., Ultrafine (nanometre) particle mediated lung injury. *J. Aerosol Sci.* **1998,** *29*, (5-6), 553-560.
2. Nel, A., Air Pollution-Related Illness: Effects of Particles. *Science* **2005,** *308*, (5723), 804-806.
3. Li, N.; Sioutas, C.; Cho, A.; Schmitz, D.; Misra, C.; Sempf, J.; Meiying, W.; Oberley, T.; Froines, J.; Nel, A., Ultrafine Particulate Pollutants Induce Oxidative Stress and Mitochonrial Damage. *Environ. Health Persp.* **2003,** *111*, (4), 455.
4. Oberdörster, G., Pulmonary effects of inhaled ultrafine particles. *Inter. Arch. Occ. Env. Hea.* **2000,** *74*, (1), 1-8.
5. Morawska, L.; Ristovski, Z.; Jayaratne, E. R.; Keogh, D. U.; Ling, X., Ambient nano and ultrafine particles from motor vehicle emissions: Characteristics, ambient processing and implications on human exposure. *Atmos. Environ.* **2008,** *42*, (35), 8113-8138.
6. Lin, C.-C.; Chen, S.-J.; Huang, K.-L.; Lee, W.-J.; Lin, W.-Y.; Tsai, J.-H.; Chaung, H.-C., PAHs, PAH-Induced Carcinogenic Potency, and Particle-Extract-Induced Cytotoxicity of Traffic-Related Nano/Ultrafine Particles. *Environ. Sci. Technol.* **2008,** *42*, (11), 4229-4235.
7. Dellinger, B.; Pryor, W. A.; Cueto, R.; Squadrito, G. L.; Hegde, V.; Deutsch, W. A., Role of Free Radicals in the Toxicity of Airborne Fine Particulate Matter. *Chem. Res. Toxicol.* **2001,** *14*, (10), 1371-1377.
8. Cheung, K. L.; Ntziachristos, L.; Tzamkiozis, T.; Schauer, J. J.; Samaras, Z.; Moore, K. F.; Sioutas, C., Emissions of Particulate Trace Elements, Metals and Organic Species from Gasoline, Diesel, and Biodiesel Passenger Vehicles and Their Relation to Oxidative Potential. *Aerosol Sci. Technol.* **2010,** *44*, (7), 500 - 513.
9. Surawski, N. C.; Miljevic, B.; Roberts, B. A.; Modini, R. L.; Situ, R.; Brown, R. J.; Bottle, S. E.; Ristovski, Z. D., Particle Emissions, Volatility, and Toxicity from an Ethanol Fumigated Compression Ignition Engine. *Environ. Sci. Technol.* **2009,** *44*, (1), 229-235.
10. Kumar, P.; Ketzel, M.; Vardoulakis, S.; Pirjola, L.; Britter, R., Dynamics and dispersion modelling of nanoparticles from road traffic in the urban atmospheric environment—A review. *J. Aerosol Sci.* **2011,** *42*, (9), 580-603.

11. Gouriou, F.; Morin, J. P.; Weill, M. E., On-road measurements of particle number concentrations and size distributions in urban and tunnel environments. *Atmos. Environ.* **2004,** *38*, (18), 2831-2840.
12. Knibbs, L. D.; de Dear, R. J.; Morawska, L.; Mengersen, K. L., On-road ultrafine particle concentration in the M5 East road tunnel, Sydney, Australia. *Atmos. Environ.* **2009,** *43*, (22-23), 3510-3519.
13. Knibbs, L. D.; Cole-Hunter, T.; Morawska, L., A review of commuter exposure to ultrafine particles and its health effects. *Atmos. Environ.* **2011,** *45*, (16), 2611-2622.
14. Chang, S.-C.; Lin, T.-H.; Lee, C.-T., On-road emission factors from light-duty vehicles measured in Hsuehshan Tunnel (12.9 km), the longest tunnel in Asia. *Environ. Monit. Asses.* **2009,** *153*, (1), 187-200.
15. Colberg, C. A.; Tona, B.; Catone, G.; Sangiorgio, C.; Stahel, W. A.; Sturm, P.; Staehelin, J., Statistical analysis of the vehicle pollutant emissions derived from several European road tunnel studies. *Atmos. Environ.* **2005,** *39*, (13), 2499-2511.
16. John, C.; Friedrich, R.; Staehelin, J.; Schläpfer, K.; Stahel, W. A., Comparison of emission factors for road traffic from a tunnel study (Gubrist tunnel, Switzerland) and from emission modeling. *Atmos. Environ.* **1999,** *33*, (20), 3367-3376.
17. Hameri, K.; Koponen, I. K.; Aalto, P. P.; Kulmala, M., The particle detection e!ciency of the TSI-3007 condensation particle counter. *J. Aerosol Sci.* **2002,** *33*, (10), 1463-1469.
18. Westerdahl, D.; Fruin, S.; Sax, T.; Fine, P. M.; Sioutas, C., Mobile platform measurements of ultrafine particles and associated pollutant concentrations on freeways and residential streets in Los Angeles. *Atmos. Environ.* **2005,** *39*, (20), 3597-3610.
19. Jamriska, M.; Morawska, L.; Thomas, S.; He, C., Diesel Bus Emissions Measured in a Tunnel Study. *Environ. Sci. Technol.* **2004,** *38*, (24), 6701-6709.
20. Miljevic, B.; Fairfull-Smith, K. E.; Bottle, S. E.; Ristovski, Z. D., The application of profluorescent nitroxides to detect reactive oxygen species derived from combustion-generated particulate matter: Cigarette smoke - A case study. *Atmos. Environ.* **2010,** *44*, (18), 2224-2230.
21. Fairfull-Smith, K. E.; Bottle, S. E., The Synthesis and Physical Properties of Novel Polyaromatic Profluorescent Isoindoline Nitroxide Probes. *Eur. J. Org. Chem.* **2008,** *2008*, (32), 5391-5400.
22. Traffic counts highlight strong demand for Brisbane river crossings. *http://www.rivercitymotorway.com.au/userfiles/file/ASX%20Announcements/Traffic%20Counts%20011008.pdf*.
23. Ntziachristos, L.; Ning, Z.; Geller, M. D.; Sioutas, C., Particle Concentration and Characteristics near a Major Freeway with Heavy-Duty Diesel Traffic. *Environ. Sci. Technol.* **2007,** *41*, (7), 2223-2230.
24. Fruin, S.; Westerdahl, D.; Sax, T.; Sioutas, C.; Fine, P. M., Measurements and predictors of on-road ultrafine particle concentrations and associated pollutants in Los Angeles. *Atmos. Environ.* **2008,** *42*, (2), 207-219.
25. Geller, M. D.; Sardar, S. B.; Phuleria, H.; Fine, P. M.; Sioutas, C., Measurements of Particle Number and Mass Concentrations and Size Distributions in a Tunnel Environment. *Environ. Sci. Technol.* **2005,** *39*, (22), 8653-8663.
26. Kirchstetter, T. W.; Harley, R. A.; Kreisberg, N. M.; Stolzenburg, M. R.; Hering, S. V., On-road measurement of fine particle and nitrogen oxide emissions

from light- and heavy-duty motor vehicles. *Atmos. Environ.* **1999,** *33*, (18), 2955-2968.
27. Miljevic, B.; Heringa, M. F.; Keller, A.; Meyer, N. K.; Good, J.; Lauber, A.; DeCarlo, P. F.; Fairfull-Smith, K. E.; Nussbaumer, T.; Burtscher, H.; Prevot, A. S. H.; Baltensperger, U.; Bottle, S. E.; Ristovski, Z. D., Oxidative Potential of Logwood and Pellet Burning Particles Assessed by a Novel Profluorescent Nitroxide Probe. *Environ. Sci. Technol.* **2010,** *44*, (17), 6601-6607.
28. Ntziachristos, L.; Froines, J.; Cho, A.; Sioutas, C., Relationship between redox activity and chemical speciation of size-fractionated particulate matter. *Particle and Fibre Toxicology* **2007,** *4*, (1), 5.
29. Geller, M. D.; Ntziachristos, L.; Mamakos, A.; Samaras, Z.; Schmitz, D. A.; Froines, J. R.; Sioutas, C., Physicochemical and redox characteristics of particulate matter (PM) emitted from gasoline and diesel passenger cars. *Atmos. Environ.* **2006,** *40*, (36), 6988-7004.
30. Biswas, S.; Verma, V.; Schauer, J. J.; Cassee, F. R.; Cho, A. K.; Sioutas, C., Oxidative Potential of Semi-Volatile and Non Volatile Particulate Matter (PM) from Heavy-Duty Vehicles Retrofitted with Emission Control Technologies. *Environ, Sci. Technol.* **2009,** *43*, (10), 3905-3912.

Chapter 4. Characterisation of carbonaceous aerosols at urban schools to determine the sources of children's exposure

Leigh R. Crilley, Godwin A. Ayoko, Mandana Mazaheri and Lidia Morawska

International Laboratory for Air Quality and Health, Institute of Health and Biomedical Innovation, Queensland University of Technology, Brisbane, QLD, 4001, Australia.

(2013) *Atmospheric Environment*, Submitted.

PREFACE

The aim of this paper was to determine the source of ambient carbonaceous aerosols in urban schools and the contributing factors to the observed concentrations. The sampling was done concurrently at the schools along with the elemental (Chapter 5) and AMS (Chapter 6-8) analyses. Thus this chapter offers complementary information on the sources at the schools. In particular, the paper offers insights into the complete range of vehicle exhaust emissions covering both elemental and organic carbon. The contributions of primary (vehicle emissions) and secondary sources were determined along with the casual factors to high exposure schools.

Statement of joint authorship of co-authors

The authors listed below have certified* that:

1. they meet the criteria for authorship in that they have participated in the conception, execution, or interpretation, of at least that part of the publication in their field of expertise;
2. they take public responsibility for their part of the publication, except for the responsible author who accepts overall responsibility for the publication;
3. there are no other authors of the publication according to these criteria;
4. potential conflicts of interest have been disclosed to (a) granting bodies, (b) the editor or publisher of journals or other publications, and (c) the head of the responsible academic unit, and
5. they agree to the use of the publication in the student's thesis and its publication on the QUT ePrints database consistent with any limitations set by publisher requirements.

In the case of this chapter:

Characterisation of carbonaceous aerosols at urban schools to determine the sources of children's exposure, (2013) *Atmospheric Environment,* Submitted.

Contributor	Statement of contribution*
Leigh R. Crilley	Collected the samples, performed the data analysis and wrote the manuscript
Godwin A. Ayoko*	Provided overall direction for this study and assisted with the data analysis and drafting of the manuscript
Mandana Mazaheri*	Assisted with the experimental design and drafting of the manuscript
Lidia Morawska*	Designed the overall concept of the study and assisted with data interpretation and drafting the manuscript

Principal Supervisor Confirmation

I have sighted email or other correspondence from all Co-authors confirming their certifying authorship.

PROF GODWIN AYOKO _____ 22/11/2013

Name Signature Date

ABSTRACT

This comprehensive study aimed to determine the sources and driving factors of children's exposure by analysing the concentrations of organic carbon (OC) and elemental carbon (EC) at 25 schools in Brisbane, Australia. Concentrations of primary and secondary OC were quantified using the EC tracer method. The average OC/EC ratios at the schools ranged from 1.88 to 19.36, indicating that both primary and secondary sources were present, with secondary OC accounting for an average of 60%. Multivariate techniques distinguished the contribution of sources above the background and identified groups of schools with differing exposure to primary and secondary sources. Vehicle emissions were primarily dependent on total traffic counts on surrounding roads and secondly on the wind direction relative to the surrounding roads. They were also the principal source at one group of schools which had elevated concentrations of primary OC and EC, at 1.72 ± 0.31 and 1.02 ± 0.16 μg m^{-3}, respectively. Another group of schools had high average secondary OC concentrations, at 2.41 ± 0.3 μg m^{-3}, which were correlated with solar radiation levels indicting influence from photochemical SOA formation. While local meteorology affected the measured concentrations, overall the range of concentrations measured at these schools can be considered as representative of children's exposure to vehicle emissions and SOA.

KEYWORDS: Schools, Vehicle emissions, Urban, Secondary organic aerosols

4.1 INTRODUCTION

There is a growing body of evidence suggesting that children who are exposed to vehicle emissions experience a number of detrimental health effects. These include increases in wheezing for infants [1, 2], worsening of existing asthma [3], and the development of asthma in children [4, 5]. Vehicle emissions represent a significant proportion of the urban airborne particles and are mainly carbonaceous in nature [6, 7]. The carbonaceous aerosol can be defined as either elemental carbon (EC) fractions (EC1, EC2, EC3) or organic carbon (OC) fractions (OC1, OC2, OC3, OC4 and pyrolized carbon, PC) and the definition depends on the analysis method [8].

EC is soot like and originates almost exclusively from primary sources such as vehicle emissions. OC is a complex mixture of many organic compounds and the result of both primary particle emissions and secondary reactions of volatile organic compounds in the atmosphere [9]. Therefore the ratio of OC to EC can indicate whether the source of the carbonaceous aerosols is primary or secondary, with vehicle emissions typically having a ratio of around 1 to 2 ([10] and references therein). Additional insight can be gained into the source of the carbonaceous aerosol by the analysis of the OC and EC fractions [9, 11, 12]. The EC fraction can also be defined as char-EC (EC1-PC) and soot-EC (EC2+EC3) to differentiate between the sources of EC where char-EC and soot-EC are similar to wood charred materials and diesel exhaust particles, respectively [13].

Schools are an environment that can represent significant exposure of children to vehicle emissions, and schools within a city are expected to have different levels of pollutants that result from local features such as traffic characteristics, local

meteorology and geography. However there is only limited literature on children's exposure at schools [14]. In particular, school bus emissions have been found to have significant impact on the air quality at the schools, with higher concentrations of EC, BC, and OC found in schools with more buses [15-17]. However schools in Brisbane, like schools in many other locations, are not serviced by buses as in the USA and so would not be as affected by school bus emissions. Therefore the results from the schools in the aforementioned studies are less relevant to schools without school buses. So other factors would be determining children's exposure to vehicle emissions in the schools.

This study aims to further our knowledge of children's exposure to vehicle emissions by characterising the carbonaceous aerosols at a number of urban schools. The concentration of POC and SOC at each school was quantified using the EC tracer method to ascertain the contributions of primary and secondary sources to the carbonaceous particles at each school. This enabled the factors affecting the concentrations of vehicle emissions and secondary processes at the schools to be determined. The schools were ranked using Preference Ranking Organization Method for Enrichment Evaluation (PROMETHEE) according to the measured levels of OC, EC and their fractions to reveal the schools that were most affected by vehicle emissions and secondary sources. Thus the characteristics of urban schools with high concentrations of vehicle emissions were established.

4.2 METHODS

4.2.1 Sampling Sites

The 25 schools selected for this study, which will be referred to as S01 to S25, are in different suburbs in the Brisbane Metropolitan area, Australia. This study was a part of a larger project designed to study the effect of Ultrafine Particle from Traffic Emissions on Children's Health, known as UPTECH (www.ilaqh.qut.edu.au/Misc/UPTECH%20Home.htm). The sampling part of the study was conducted from October 2010 until August 2012. The schools chosen were not near any large source of air pollution other than road traffic, and were also not close to any large infrastructure projects. A site close to the middle of the school which was assumed to give the best overall exposure was chosen to conduct the measurements and sampling at each school. The inlets for the sampling were approximately 3 m off the ground and placed on the top of a trailer, which served to house all of the instruments at the site, including an automatic weather station (Monitor Sensors). As some of the schools would have been affected by local winds due to schools buildings, data from nearby weather stations was also obtained from the Bureau of Meteorology and the Queensland Department of Science, Information Technology, Innovation and the Arts. Traffic counts with five minute intervals were taken on the busiest road next to the school, referred to as the main road throughout. In addition to the total traffic count, vehicles were classified as light, medium cars, motorbikes and scooters were classified as light vehicles, light trucks with 2, 3 and 4 axels were classified as medium vehicles while long articulated trucks were classified as heavy vehicles.

4.2.2 Sampling and Analysis Methodology

The particles size sampled for EC and OC analyses were those with diameters less than 2.5 μm ($PM_{2.5}$). This was achieved using a cascade impactor supplied by Dekati, (Kangasala, Finland) set to remove particles larger than 2.5 μm. A critical orifice and needle valve was used to maintain the 20 litre per minute (lpm) flow rate required by the impactor. The particles were collected on a preloaded 37 mm quartz cassette filter (SKC). The filter samples were collected over a nine hour period from 08:00 to 17:00, each day for one week with a total of five samples collected. The sampling days at each school were typical school days with no special activities that may affect the results. The times were chosen to capture the time students spent at the school, even though not all students would be present during the whole sampling period, and will be referred to as school hours in the rest of the paper. Typical sampling volumes for the filter over the 9 hour period were 9.7 m^3. Once the sampling was completed the filters were wrapped in aluminium foil, placed in a ziplock bag and kept frozen until analysis. OC and EC analyses were conducted at Chester Labnet, Oregon, USA using the IMPROVE method on a thermal/optical transmittance carbon analyser (Sunset Laboratories) [8]. The OC and EC fractions as defined by the IMPROVE protocol were also recorded [8].

4.2.3 Quality Control

Field blanks were taken at each school. The EC and OC results were all field-blank corrected with an average of 7.4 ± 1.9 μg/filter for OC and 0 ± 1.6 μg/filter for EC. The minimum detection limit (MDL) for both OC and EC was determined from the standard deviation of several instrument blanks to be 1.6 μg/filter. All of the OC and EC results were above the MDL except for three samples from S01 that were below

the detection limit for EC. The flow rate of the impactor was checked at the beginning of each sample and was always set to within ±0.1 lpm of the target flow rate.

4.2.4 Data Analysis

To determine the levels of secondary and primary OC present at the schools the EC tracer method was used [18] to establish a minimum OC/EC ratio (OC/EC_{min}) that was representative of the main primary source. The EC tracer method has been shown to give accurate estimation of SOC levels provided the correct OC/EC_{min} is used [19]. This method assumes that there is one primary source, and due to the school selection criteria employed in this study, we expect that vehicle emissions will be the main primary source of carbonaceous aerosols at the schools, justifying the use of the EC tracer method. The OC and EC concentrations are plotted to determine the OC/EC_{min}, with points above this line taken to contain additional OC or secondary OC (SOC) [20]. Samples that were affected by significant rainfall were removed from the analysis as rain would remove aged aerosols and so bias the analysis [10]. Two clear outliers out of the 119 samples with unusually low OC values were removed before the analysis.

The multi-criteria decision making methods, Preference Ranking Organization METHods for Enrichment Evaluation (PROMETHEE) and Graphical Analysis for Interactive Assistance (GAIA) [21] were applied to the data as we were interested in comparing the schools on the basis of the carbonaceous aerosols. PROMETHEE is a non-parametric outranking method, which is useful for comparing and ranking objects based on multiple measured variables. It compares the objects (schools in this case) pair-wise in all possible combination of ways and ranks them from the most

preferred to the least preferred on the basis of the measured variables (OC, EC and OC and EC fractions, soot-EC and Char-EC in this case). The ranking procedure was described in details by Friend et al. [22]. In summary, each variable is modelled separately and this involves the application of a preference function. In addition, each variable is "minimised" when lower values are preferred or "maximised" when higher values are preferred. Of the six preference functions available in PROMETHEE, the 'V-shaped function' was chosen in the current work because it has been shown [22] to offer the best outcome for environmental work. Thus OC, EC and OC and EC fractions, soot-EC and Char-EC were "minimised" and the highest observed concentration for each variable was used as a threshold. The values of the variable for all schools were compared to this threshold and the schools compared pair-wise in all possible combinations. The comparison led to the calculation of a net outranking flow (ϕ) for each school, which was used to rank the schools from the least (with lowest (ϕ) value) to the most preferred (with highest (ϕ) value). Thus the school with the lowest overall concentrations of the various OC and EC fractions was ranked highest and vice versa. This gave an indication of the schools with comparatively low exposure. GAIA is a special form of Principal Component Analysis that incorporates the decision axis, pi, which points to the most preferred school. Both PROMETHEE and GAIA analysis were performed in this work using Visual Decision Laboratory 2000 software.

Principal component analysis (PCA) was performed using SIMCA-P modelling tool (Version 10) with the same parameters as the PROMETHEE and GAIA analysis and also included OC/EC, char-EC/soot-EC ratio, traffic and meteorological parameters.

These parameters were included in the PCA to explore the relationship of the OC and EC components with the traffic and meteorological variables at the schools. ANOVA and correlations analysis was performed using SPSS v19. Rose plots of wind speed and direction were done in IGOR Pro v6.22A.

4.3 RESULTS AND DISCUSSION

4.3.1 Meteorological conditions

The average temperature, relative humidity (RH), solar radiation and wind speed are given in Table A2-1 for each school (Appendix 2). The average results presented are for the sampling period, i.e. school hours over the five days of sampling. The wind direction data was determined with wind rose plots, given in Appendix 2 Figure A2-1, and summarised in Table A2-1. Brisbane is a subtropical city and consequently the average temperature during these measurements varied from 16.9 to 29°C. The cooler, drier and more stable weather occurs during May to October and is referred to as winter while the warmer months, November to April are more humid with higher rainfall and is referred to as summer. These seasonal characteristics are observed throughout the project, as shown in Table A2-1.

4.3.2 Traffic characteristics of the schools

The schools selected were in a variety of urban locations. Therefore there were differences in the traffic volume and composition recorded at each school as presented in Table A2-1. Schools such as S07, S09, S19 and S20 bordered major thoroughfare roads, while other schools were located on quiet suburban streets such as S01, S16 and S18. Most of the schools were in residential areas, consequently they had mostly light vehicles passing them, but some schools were located on roads that service industrial/commercial areas. Such schools (e.g S04, S06, S08, S23 and S25) had higher levels of medium and heavy vehicles.

4.3.3 Average OC and EC concentrations

As a result of the varying characteristics between the schools sampled in this study, the OC and EC concentrations differed from school to school. The OC concentration ranged from 0.21 to 5.27 μg m^{-3} while the EC concentration ranged from 0 to 2.42 μg m^{-3}. A similar study in Cincinnati schools found that the OC ranged from 3.1 to 13.2 μg m^{-3} while the EC ranged from 0.06 to 2.7 μg m^{-3} [16]. The range of OC in the Cincinnati schools was somewhat higher and could be attributed to the higher regional background concentrations. In Figure 4-1, the average OC, EC and total carbon (TC) concentrations for all schools are shown and the majority of the carbonaceous aerosol was found to be OC at all of the schools.

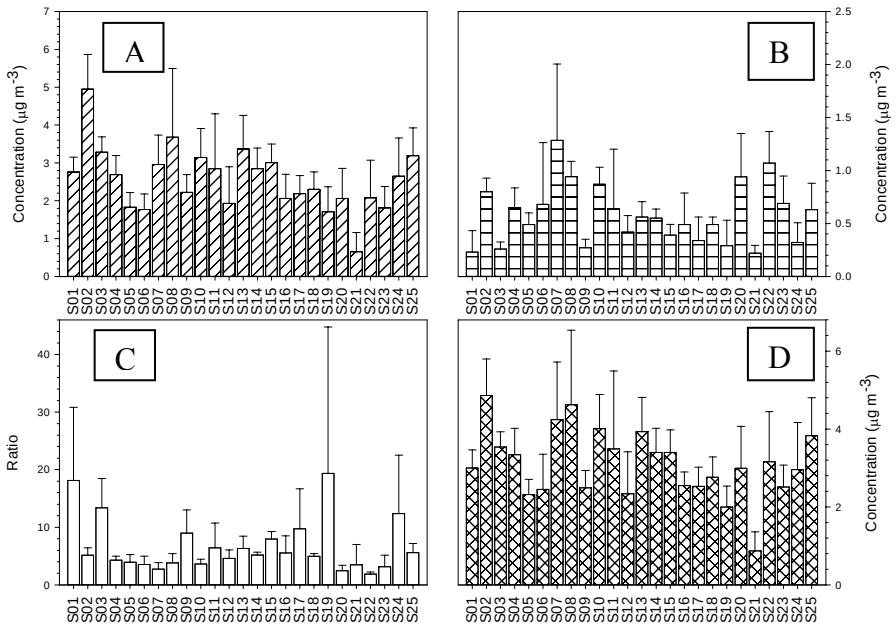

Figure 4-1: Average OC (A), EC (B), TC (D) concentrations and OC/EC (C) ratio at each school. Error bars represent one standard deviation.

As can be seen in Figure 4-1C, the average OC/EC ratio ranged from 1.88 to 19.36 at the schools studied. In an urban environment, an OC/EC ratio for $PM_{2.5}$ of around 1 has been shown to indicate that vehicle emissions are the major source [23, 24].

However, this ratio can vary depending on the traffic composition and has been observed to be as high as 2.2 at an urban roadside location [7, 25]. When the OC/EC ratio is above 2, it has been shown to indicate that secondary organic aerosols (SOA) are a significant source [26, 27], though there are other sources such as biomass burning which have a high OC/EC ([10] and references therein).

It was observed that at all the schools vehicle emissions were not the only source of carbonaceous aerosols and were influenced by SOA to varying degrees as indicated by the range of OC/EC ratios. In general, the schools that recorded the lowest OC/EC ratio (S07, S10, and S20) were beside the roads with the highest traffic counts. However there were schools, such as S09, S15, S17 and S19 that were beside equally trafficked roads and did not record a low OC/EC ratio. Therefore in addition to traffic volume there were other factors such as local meteorology that affected the levels of vehicle emissions observed at each school. It was also noted that schools with the high OC/EC ratio such as S01, S03 and S19 were generally sampled during the warmer months possibly indicating a seasonal variation in the SOA levels due to increased photochemical activity in summer. To explore these hypotheses, the levels of primary and secondary OC at the schools were investigated with the aim to improve the identification of the contributing factors.

4.3.4 Estimation of secondary and primary OC using the EC tracer method

The correlation between the OC and EC concentrations was poor (r^2 of 0.2), indicating that there were both primary and secondary sources of carbonaceous aerosols at the schools. The OC and EC concentrations were plotted (Figure A2-3, Appendix 2) and the OC/EC_{min} was determined to be

$$OC = 1.72EC + 0.017$$

The intercept value of 0.017 represents the contribution from non-combustion sources of OC such as road pavement dust, with the low value indicating that this was not a significant source at the schools [10]. The calculated OC/EC_{min} was indicative of vehicle emissions and the ratio of 1.72 was closer to the expected ratio for gasoline than diesel vehicles [28].

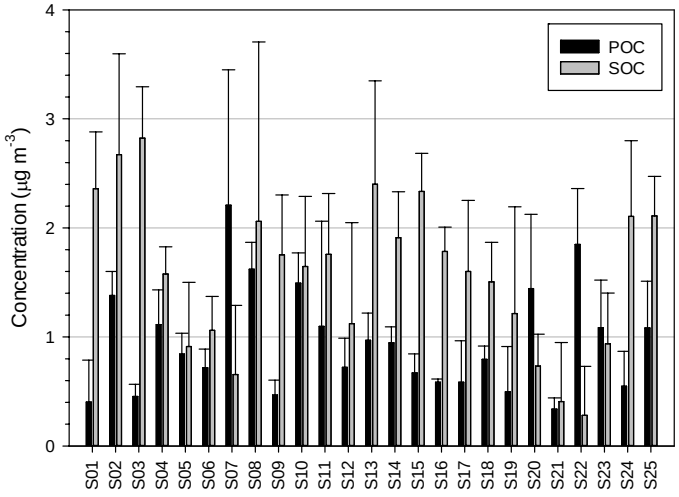

Figure 4-2: Average POC and SOC concentrations at each school.
Error bars represent one standard deviation.

In Figure 4-2 the average concentrations of primary and secondary OC at each school that were determined using the calculated OC/EC_{min} are presented. Levels of POC and SOC varied across the schools but for most of the schools there was more SOC than POC, with the average percentage of SOC to total OC (%SOC) across all of the schools being 60%. Many of the schools with high SOC concentrations were sampled in the warmer months pointing to a possible seasonal influence and are investigated further in Section 4.3.4.2.

The calculated ratio of 1.72 in this study was less than the OC/EC_{min} of 2.248EC + 0.242 reported by Keywood et al. [10] for an urban background site in Melbourne, Australia. This indicates that the vehicle emissions were contributing more to the schools, as expected as many of the schools are near major roads. The OC/EC_{min} from this study was higher than the OC/EC_{min} of 0.7 found across many sites for urban environment in Europe [29] but in the range reported by Cabada et al. [30] for results in the USA.

4.3.4.1 ***Primary sources of OC***

Only three schools (S07, S20 and S22) were dominated by POC (Figure 4-2). Schools such as S02, S07, S08, S10, S20 and S22 which had concentrations of POC greater than 1.1 $\mu g\ m^{-3}$ generally have high traffic volumes. However, there were other schools such as S09, S15 and S19, which had high traffic volumes but comparably low POC concentrations. Therefore factors other than traffic volume had affected the levels of POC in the schools. From Table A2-1, at S02, S08, S22, the wind direction was from the main road, so this was the likely source of the high levels of POC observed at these schools. Similarly, at S09 and S15 the wind direction was not from the main road during the sampling period, which explained the low levels of POC observed at these schools.

At S07 and S20 the wind direction was found not to be from the main road, and cannot account for the high POC levels observed at these schools. However, there was a high percentage of calm wind, at 40% and 25% respectively, thus the lack of dispersion as a result of the low wind speeds contributed to the high levels of POC observed at these schools. At S19, the lower POC concentrations can be due to the

possibility that a large shopping centre located between the school and main road prevented vehicle emissions from the main road from reaching the sampling site.

The effect of the wind direction on the levels of vehicle emissions was also noted in schools with low traffic counts. Thus S01, S12, S14, S21 and S24 had similar traffic counts (Table A2-1) but S01, S21 and S24 were observed to have a lower concentration of POC ($p<0.05$) compared to S12 and S14. Whereas S01, S21 and S24 had little wind blowing from the direction of the main road, S12 and S14 have higher frequencies of wind from the main road (Table A2-1). The differences in the frequencies of the wind from the main road accounted for the differences in the observed POC concentrations.

In general, schools on roads that had the highest traffic counts had the highest POC levels. The direction of wind in relation to the roads bordering the schools was the next important factor determining the levels of POC at the schools. As POC levels relate to both the traffic volume and the frequency of the wind blowing from the road, POC concentrations can be attributed predominantly to vehicle emissions. The complex relationships that determined the concentrations of vehicle emissions to which school children were exposed meant that it was necessary to employ multivariate techniques to fully determine correlations between variables and ascertain the factors that cause high exposure schools.

4.3.4.2 ***Seasonal variation***

To analyse seasonal variations in the carbonaceous aerosols at the schools, the average result for summer and winter were compared since there was an uneven

distribution and non-continuous sampling at the schools over the months. The summer and winter averages are presented in Table 4-1, compared using one-way ANOVA and were found to be significantly different ($p<0.05$) for all species except for OC. A seasonal variation in EC and OC/EC but not in OC has also been observed in other urban environments [31, 32]. The lack of seasonal variation in OC but in EC suggests that in winter primary emissions were the main source of OC and there is a complementary increase in SOC with the decrease in POC in summer. Thus secondary processes were the dominant source of OC in summer while primary emissions were the dominant source in winter.

Table 4-1: Average summer and winter concentrations (μg m^{-3}) for the various species. The uncertainty given is one standard deviation.

Species	*Summer*	*Winter*
EC	0.46 ± 0.22	0.68 ± 0.45
OC	2.69 ± 0.86	2.36 ± 1.11
POC	0.78 ± 0.37	1.11 ± 0.74
SOC	1.94 ± 0.81	1.30 ± 0.89
OC/EC	8.9 ± 9.5	4.9 ± 4.4

The lower EC and POC in summer may be due to meteorological conditions with higher wind speeds aiding the dispersion of the pollutants. Conversely the more stable weather and inversions in winter trapped the carbonaceous aerosols resulting in higher concentrations [31]. The increase in EC is not likely due to biomass burning as the analysis of the EC fractions (see Appendix 2) revealed that at the majority of the schools biomass burning was not a significant source of EC. Higher solar radiation levels were also observed in the summer months, in conjunction with the higher SOC concentrations and OC/EC ratio in summer. Average SOC concentrations at the schools were found to be somewhat correlated with the solar radiation levels ($r^2 = 0.44$, $p<0.05$). Thus, photochemical secondary organic aerosol formation could be the reason for the higher SOC levels [18, 31]. However, there

may also be higher background levels of OC during summer. The array of possible sources of carbonaceous aerosol further supported the need to apply multivariate techniques to analyse the data in order to disentangle the influence of vehicle emissions at the schools from other sources.

4.3.5 Multivariate Analysis

4.3.5.1 ***PROMETHEE ranking and GAIA***

The ranking of the schools is given in Table A2-5 (Appendix 2), with the most preferred school being S21 and the lowest ranked school being S07. In general the schools that were ranked highest had the lowest concentrations of TC and POC and so were the least affected by primary sources. Likewise, schools that were the ranked lowest had the highest levels of POC, and were the most affected by primary sources. The highest ranked schools generally had higher OC/EC ratios. Therefore they had higher contributions from SOC.

Two main groups observed in the GAIA plot (Figure A2-4, Appendix 2). These groups separated out on principal component 1 (PC1) based upon the levels of SOC and POC. The first group with negative PC1 values contained the schools that were ranked the lowest and included S07, S08, S02, S10, S11, S25, S13, S22, S20 and S14. These schools had higher concentrations of POC and were more influenced by primary source emissions (such as vehicle emissions and biomass burning) and can be considered the primary source exposure group. The second group with positive PC1 values contained the rest of the schools, see Figure A2-4. These schools have lower POC concentrations and higher OC/EC and SOC levels. Therefore they had

more influence from secondary sources and are classified as secondary source exposure schools.

4.3.5.2 ***PCA***

GAIA was used to display the PROMTHEE results visually. However PCA was also used as it enabled a more detailed analysis of the patterns in the data since more parameters such as traffic and meteorological data were used. Thus, PCA was used to explore the relationships between the contributions of vehicle emissions and other sources at the schools and traffic and meteorological factors, which enabled better identification of the contributing sources. In the loadings plot, Figure 4-3, the EC and OC/EC were found to be anti-correlated, and thus these parameters are likely to be dependent on local sources. EC is correlated with the traffic count and composition. Therefore the predominant source of EC at the schools was vehicle emissions. OC/EC was correlated with solar radiation levels. These high OC/EC ratios suggest photochemical SOA formation as a source. OC was independent of OC/EC, solar radiation, and HDV count, which meant that there was additional OC that was not related to the local sources, more likely regional OC.

The sources and factors that contributed to the carbonaceous aerosols measured at the schools were determined by considering the relationships between the schools and variables. The group of schools that were classed as primary source exposure schools could be further split into two clusters labelled 1 and 2, as indicated in the scores plot, Figure 4-4. The frequency of wind from the main road was correlated with both groups. Therefore vehicle emission was the main local source at these schools. Cluster 1, which included S07, S08, S10, S20 and S22, was correlated with EC, soot-EC, traffic counts and composition. Therefore vehicle emissions were the

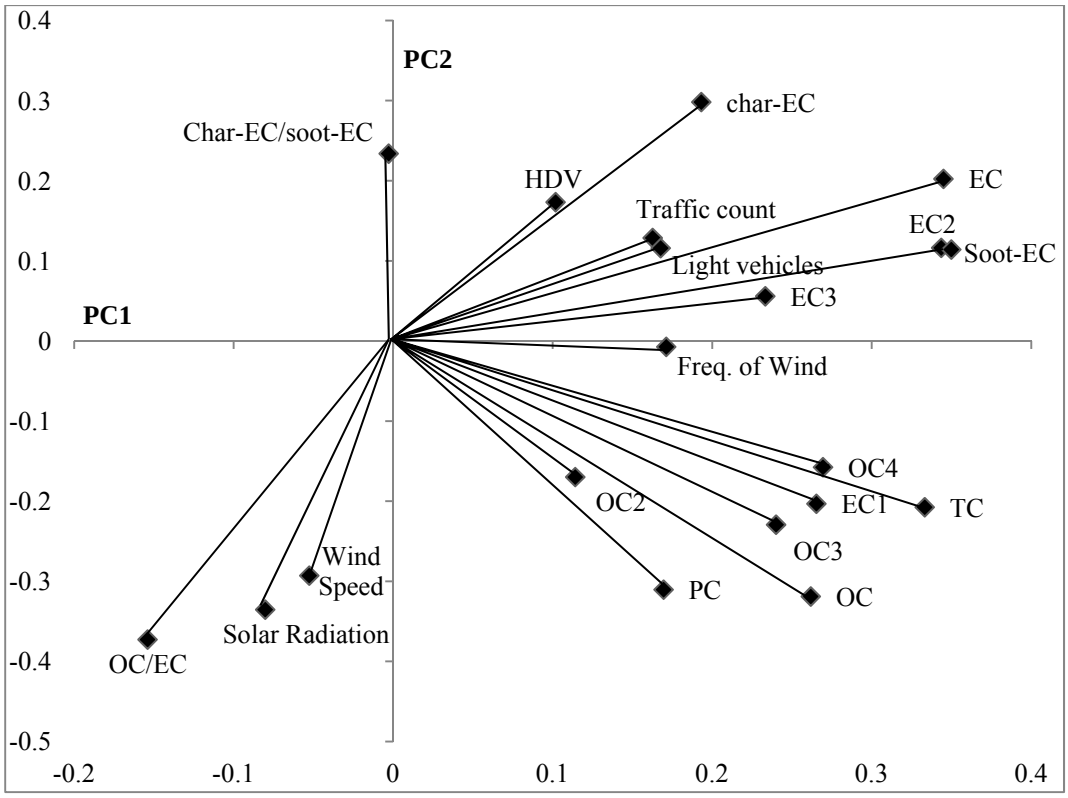

Figure 4-3: Loadings plot of the OC and EC components and traffic and weather variables.

The HDV is the sum of medium and heavy vehicles counts, and light vehicles and Traffic count referring to the hourly average counts. Freq. of wind refers to the frequency of wind from the main road as a percentage.

principal source at these schools. Cluster 2, which contained S02, S11, S13, S14 and S25 were correlated with OC and the OC fractions and had strong influence from vehicle emissions and the background. Cluster 2 was related to the OC/EC ratio but had high OC levels, suggesting a high background. Cluster 2 was also somewhat correlated to EC, traffic volume and the frequency of wind variable, so in addition to the high background present at these schools vehicle emissions contributed to the exposure. It is therefore reasonable to expect that the children were exposed to higher levels of vehicle emissions at schools in cluster 1 and 2 than at the other schools.

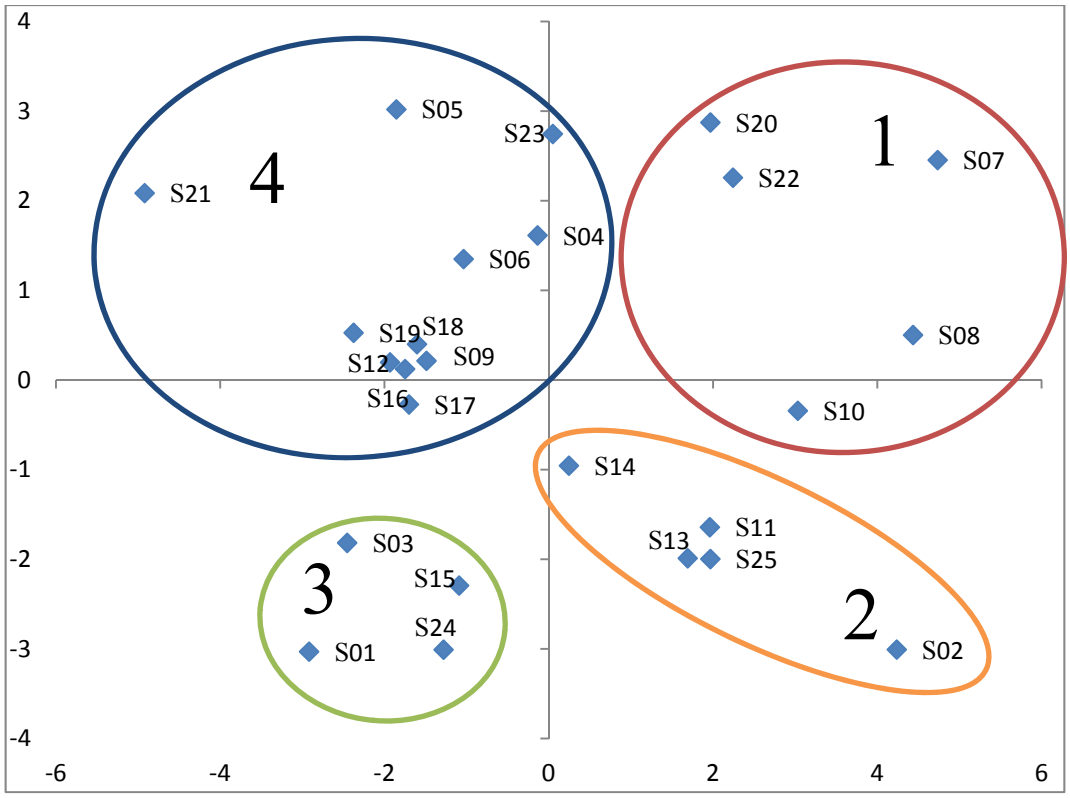

Figure 4-4: Scores plot of the schools, grouped according to source.

Schools classified as secondary source exposure schools could also be split further, based upon the influence of secondary sources, and are labelled as cluster 3 and 4 in Figure 4-4. Cluster 3 contained S01, S03, S15 and S24 and was correlated with the OC/EC and solar radiation levels, indicating the photochemical SOA formation that occurred during sampling was the principal source. As such, these schools had the highest concentration of SOC (Figure 4-2) and children experienced high exposure to SOA at these schools. Cluster 4, which was the largest and contained S04, S05, S06, S09, S12, S16, S17, S18, S19 and S23 had little influence of vehicle emissions and SOA, as there was little correlation with OC/EC, traffic counts and EC. Therefore the measured OC and EC concentrations at these schools were likely to be more indicative of the urban background in Brisbane, with little influence from local sources. The schools in Cluster 4, which covered all of the seasons and the range of observed traffic counts (Table A2-1), had the lowest exposure to vehicle emissions

and SOA with the concentrations at the schools dependent on regional sources. The cause of the decreased exposure at these schools was the meteorological conditions, specifically the solar radiation levels and wind direction relative to surrounding roads. Due to the short sampling time at the schools, the concentrations of carbonaceous aerosols quantified at each school was affected by the local meteorology, however no unusual weather patterns were encountered that would have overly affected the measured concentrations. Therefore, the range of concentrations measured for the schools in this study can be considered as representative of the children's exposure to vehicle emissions and SOA at schools with similar traffic conditions.

4.3.6 Classification of school exposure characteristics

From the multivariate analysis, the schools were divided into those with prevalent exposure to primary and secondary carbonaceous aerosols and four clusters of schools based upon the source contributions. Clusters 1, 2, 3, and 4 were named as vehicle emissions, vehicle emissions plus background, SOA plus background and background only, respectively. The distinguishing characteristics and contributing factors for the different clusters are summarized in Table 4-2 and the clusters can be classed as either primary or secondary and local or background sources to explain the difference in concentrations between schools.

The schools in clusters 1 and 2 had vehicle emissions as a major source. All of these schools were characterised by having the highest concentrations of POC and EC (Table 4-2) and are indicative of the levels of vehicle emissions that children were exposed to at schools. As vehicle emissions are local emissions we would expect that

Table 4-2: Matrix of the clusters of schools identified along with the characteristics and the contributing factors.

		Local Emissions					Background				
Primary Sources	*Name*	Vehicle emissions (cluster 1)					*Name*	Vehicle emissions + background (cluster 2)			
	Signature	High EC, POC, soot-EC, low OC/EC					*Signature*	High OC and TC			
	Average	OC/EC	POC	SOC	EC		*Average*	OC/EC	POC	SOC	EC
	(µg m^{-3})	2.97± 0.78	1.72± 0.31	1.08± 0.75	1.02± 0.16		*(µg m^{-3})*	5.73± 0.61	1.09± 0.17	2.17± 0.37	0.64± 0.1
	Factors	Traffic counts and composition Wind direction relative to road					*Factors*	Wind direction relative to road			
Secondary Sources	*Name*	Local SOA formation was not attributed at any schools					*Name*	SOA + background (cluster 3)			
							Signature	High OC/EC and SOC			
							Average	OC/EC	POC	SOC	EC
							(µg m^{-3})	11.8± 2.63	0.52± 0.12	2.41± 0.3	0.3± 0.07
							Factors	Solar radiation Wind speed			
							Name	Background only (cluster 4)			
							Signature	None			
							Average	OC/EC	POC	SOC	EC
							(µg m^{-3})	6.81± 4.93	0.74± 0.22	1.35± 0.33	0.48± 0.15
							Factors	None			

children are always exposed to high concentrations at these schools, and the converse is also applicable for schools with low POC and EC. The difference between clusters 1 and 2 schools was the background level, as illustrated by the differences in concentration of SOC and OC/EC ratios (Table 4-2), contributing to the total concentration of carbonaceous aerosols children were exposed to at these schools. The contribution of the background across the schools demonstrated a high level of variation, as illustrated in the background only schools which exhibited a wide range of OC/EC ratios, from 3.15 - 19.36. The schools with a higher SOC concentration (cluster 3) were likely as a result of local meteorology and as such children at these schools may not always be exposed to additional SOA above the background.

4.4 CONCULSIONS

This study represents the most comprehensive study to date on the EC and OC concentrations at urban schools that were affected by multiplicity of sources and factors. Multivariate techniques distinguished the contribution of sources above the background and identified groups of schools with differing exposure to primary and secondary sources. Vehicle emissions levels were primarily dependent on total traffic counts on surrounding roads and secondly on the wind direction relative to the surrounding roads, resulting in elevated concentrations of POC and EC. Influence of photochemical SOA formation was observed at certain schools, resulting in high average SOC concentrations. While local meteorology affected the measured concentrations, the range of concentrations measured at these schools can be considered as representative of children's exposure to vehicle emissions and SOA. Overall, SOC was the largest component of the carbonaceous aerosols at the majority of the schools in this study and it was outside the scope of this study to fully determine the contributing factors to SOA exposure. This could be the focus of

future work to better characterise SOA and background particles and the contribution from regional sources at schools, as SOA is likely to have different health effects from primary carbonaceous aerosols [33].

Appendix 2

Appendix 2 contains additional information on the impact of traffic at selected individual schools and analysis on the concentrations of the OC and EC fractions.

ACKNOWLEDGMENTS

We would like to thank Dr Patrick Ryan, University of Cincinnati, for his help with the EC and OC sampling design. This work was supported by the Australian Research Council (ARC), QLD Department of Transport and Main Roads (DTMR) and QLD Department of Education, Training and Employment (DETE) through Linkage Grant LP0990134. Our particular thanks go to R. Fletcher (DTMR) and B. Robertson (DETE) for their vision regarding the importance of this work. We would also like to thank Prof G. Marks, Dr P. Robinson, Prof K. Mengersen, Prof Z. Ristovski, Dr C. He, Dr G. Johnson, Dr R. Jayaratne, Dr S. Low Choy, Prof G. Williams, W. Ezz, F. Salimi, S. Clifford, M. Mokhtar, N. Mishra, R. Laiman, L. Guo, Prof C. Duchaine, Dr H. Salonen, Dr X. Ling, Dr J. Davies, Dr L. Leontjew Toms, F. Fuoco, Dr A. Cortes, Dr B. Toelle, A. Quinones, P. Kidd and E. Belousova, Dr M. Falk, Dr F. Fatokun, Dr J. Mejia, Dr D. Keogh, Prof T. Salthammer, R. Appleby and C. Labbe for their contribution to the UPTECH project.

4.5 REFERENCES

1. Ryan, P. H.; Bernstein, D. I.; Lockey, J.; Reponen, T.; Levin, L.; Grinshpun, S.; Villareal, M.; Khurana Hershey, G. K.; Burkle, J.; LeMasters, G., Exposure to

Traffic-related Particles and Endotoxin during Infancy Is Associated with Wheezing at Age 3 Years. *Am. J. Resp. Crit. Care* **2009,** *180*, (11), 1068-1075.
2. Ryan, P. H.; LeMasters, G. K.; Biswas, P.; Levin, L.; Hu, S.; Lindsey, M.; Bernstein, D. I.; Lockey, J.; Villareal, M.; Hershey, G. K. K.; Grinshpun, S. A., A comparison of proximity and land use regression traffic exposure models and wheezing in infants. *Environ. Health Persp.* **2007,** *115*, (2), 278-284.
3. Trenga, C. A.; Sullivan, J. H.; Schildcrout, J. S.; Shepherd, K. P.; Shapiro, G. G.; Liu, L. J. S.; Kaufman, J. D.; Koenig, J. Q., Effect of particulate air pollution on lung function in adult and pediatric subjects in a Seattle panel study. *Chest* **2006,** *129*, 1614-22.
4. Jerrett, M.; Shankardass, K.; Berhane, K.; Gauderman, W. J.; Künzli, N.; Avol, E.; Gilliland, F.; Lurmann, F.; Molitor, J. N.; Molitor, J. T.; Thomas, D. C.; Peters, J.; McConnell, R., Traffic-related air pollution and asthma onset in children: a prospective cohort study with individual exposure measurement. *Environ. Health Persp.* **2008,** *116*, (10), 1433-1438.
5. Gehring, U.; Wijga, A.; Brauer, M.; Fischer, P.; de Jongste, J.; Kerkhof, M.; Oldenwening, M.; Smit, H.; Brunekreef, B., Traffic-related Air Pollution and the Development of Asthma and Allergies during the First 8 Years of Life. *Am. J. Resp. Crit. Care* **2010,** *181*, (6), 596-603.
6. Kleeman, M. J.; Schauer, J. J.; Cass, G. R., Size and Composition Distribution of Fine Particulate Matter Emitted from Motor Vehicles. *Environ. Sci. Technol.* **2000,** *34*, (7), 1132-1142.
7. Ancelet, T.; Davy, P. K.; Trompetter, W. J.; Markwitz, A.; Weatherburn, D. C., Carbonaceous aerosols in an urban tunnel. *Atmos. Environ.* **2011,** *45*, (26), 4463-4469.
8. Chow, J. C.; Watson, J. G.; Crow, D.; Lowenthal, D. H.; Merrifield, T., Comparison of IMPROVE and NIOSH Carbon Measurements. *Aerosol Sci. Technol.* **2001,** *34*, (1), 23 - 34.
9. Cao, J. J.; Lee, S. C.; Ho, K. F.; Fung, K.; Chow, J. C.; Watson, J. G., Characterization of Roadside Fine Particulate Carbon and its Eight Fraction in Hong Kong. *Aerosol Air Qual. Res.* **2006,** *6*, (2), 106-122.
10. Keywood, M.; Guyes, H.; Selleck, P.; Gillett, R., Quantification of secondary organic aerosol in an Australian urban location. *Environ. Chem.* **2011,** *8*, (2), 115-126.
11. Sahu, M.; Hu, S.; Ryan, P. H.; Le Masters, G.; Grinshpun, S. A.; Chow, J. C.; Biswas, P., Chemical compositions and source identification of PM2.5 aerosols for estimation of a diesel source surrogate. *Sci. Total Environ.* **2011,** *409*, (13), 2642-2651.
12. Kim, E.; Hopke, P. K.; Edgerton, E. S., Improving source identification of Atlanta aerosol using temperature resolved carbon fractions in positive matrix factorization. *Atmos. Environ.* **2004,** *38*, (20), 3349-3362.
13. Han, Y.; Cao, J.; Chow, J. C.; Watson, J. G.; An, Z.; Jin, Z.; Fung, K.; Liu, S., Evaluation of the thermal/optical reflectance method for discrimination between char- and soot-EC. *Chemosphere* **2007,** *69*, (4), 569-574.
14. Mejía, J. F.; Choy, S. L.; Mengersen, K.; Morawska, L., Methodology for assessing exposure and impacts of air pollutants in school children: Data collection, analysis and health effects – A literature review. *Atmos. Environ.* **2011,** *45*, (4), 813-823.

15. Richmond-Bryant, J.; Bukiewicz, L.; Kalin, R.; Galarraga, C.; Mirer, F., A multi-site analysis of the association between black carbon concentrations and vehicular idling, traffic, background pollution, and meteorology during school dismissals. *Sci. Total Environ.* **2011,** *409*, (11), 2085-2093.
16. Hochstetler, H. A.; Yermakov, M.; Reponen, T.; Ryan, P. H.; Grinshpun, S. A., Aerosol particles generated by diesel-powered school buses at urban schools as a source of children's exposure. *Atmos. Environ.* **2011,** *45*, 1444-1453.
17. Li, C.; Nguyen, Q.; Ryan, P. H.; LeMasters, G. K.; Spitz, H.; Lobaugh, M.; Glover, S.; Grinshpun, S. A., School bus pollution and changes in the air quality at schools: a case study. *J. Environ. Monit.* **2009,** *11*, (5), 1037-1042.
18. Castro, L. M.; Pio, C. A.; Harrison, R. M.; Smith, D. J. T., Carbonaceous aerosol in urban and rural European atmospheres: estimation of secondary organic carbon concentrations. *Atmos. Environ.* **1999,** *33*, (17), 2771-2781.
19. Zhang, Q.; Worsnop, D. R.; Canagaratna, M. R.; Jimenez, J. L., Hydrocarbon-like and oxygenated organic aerosols in Pittsburgh: insights into sources and processes of organic aerosols. *Atmos. Chem. Phys.* **2005,** *5*, (12), 3289-3311.
20. Harrison, R. M.; Yin, J., Sources and processes affecting carbonaceous aerosol in central England. *Atmos. Environ.* **2008,** *42*, (7), 1413-1423.
21. Figueira, J.; Greco, S.; Ehrgott, M., *Multiple Criteria Decision Analysis: State of the Art Surveys*. Springer: New York, 2005.
22. Friend, A. J.; Ayoko, G. A.; Elbagir, S. G., Source apportionment of fine particles at a suburban site in Queensland, Australia. *Environ. Chem.* **2011,** *8*, (2), 163-173.
23. Lee, S. C.; Cheng, Y.; Ho, K. F.; Cao, J. J.; Louie, P. K.-K.; Chow, J. C.; Watson, J. G., PM1.0 and PM2.5 Characteristics in the Roadside Environment of Hong Kong. *Aerosol Sci. Technol.* **2006,** *40*, (3), 157 - 165.
24. Zhu, C.-S.; Chen, C.-C.; Cao, J.-J.; Tsai, C.-J.; Chou, C. C. K.; Liu, S.-C.; Roam, G.-D., Characterization of carbon fractions for atmospheric fine particles and nanoparticles in a highway tunnel. *Atmos. Environ.* **2010,** *44*, (23), 2668-2673.
25. Kim, K. H.; Sekiguchi, K.; Kudo, S.; Sakamoto, K., Characteristics of Atmospheric Elemental Carbon (Char and Soot) in Ultrafine and Fine Particles in a Roadside Environment, Japan. *Aerosol Air Qual. Res.* **2011,** *11*, (1), 1-12.
26. Chow, J. C.; Watson, J. G.; Lu, Z.; Lowenthal, D. H.; Frazier, C. A.; Solomon, P. A.; Thuillier, R. H.; Magliano, K., Descriptive analysis of PM2.5 and PM10 at regionally representative locations during SJVAQS/AUSPEX. *Atmos. Environ.* **1996,** *30*, (12), 2079-2112.
27. Giugliano, M.; Lonati, G.; Butelli, P.; Romele, L.; Tardivo, R.; Grosso, M., Fine particulate (PM2.5-PM1) at urban sites with different traffic exposure. *Atmos. Environ.* **2005,** *39*, (13), 2421-2431.
28. Allen, A. G.; Nemitz, E.; Shi, J. P.; Harrison, R. M.; Greenwood, J. C., Size distributions of trace metals in atmospheric aerosols in the United Kingdom. *Atmos. Environ.* **2001,** *35*, (27), 4581-4591.
29. Pio, C.; Cerqueira, M.; Harrison, R. M.; Nunes, T.; Mirante, F.; Alves, C.; Oliveira, C.; Sanchez de la Campa, A.; Artíñano, B.; Matos, M., OC/EC ratio observations in Europe: Re-thinking the approach for apportionment between primary and secondary organic carbon. *Atmos. Environ.* **2011,** *45*, (34), 6121-6132.
30. Cabada, J. C.; Pandis, S. N.; Subramanian, R.; Robinson, A. L.; Polidori, A.; Turpin, B., Estimating the Secondary Organic Aerosol Contribution to PM2.5 Using the EC Tracer Method Special Issue of Aerosol Science and Technology on Findings

from the Fine Particulate Matter Supersites Program. *Aerosol Sci. Technol.* **2004,** *38*, (sup1), 140-155.
31. Plaza, J.; Artíñano, B.; Salvador, P.; Gómez-Moreno, F. J.; Pujadas, M.; Pio, C. A., Short-term secondary organic carbon estimations with a modified OC/EC primary ratio method at a suburban site in Madrid (Spain). *Atmos. Environ.* **2011,** *45*, (15), 2496-2506.
32. Jones, A. M.; Harrison, R. M., Interpretation of particulate elemental and organic carbon concentrations at rural, urban and kerbside sites. *Atmos. Environ.* **2005,** *39*, (37), 7114-7126.
33. Robinson, A. L.; Donahue, N. M.; Shrivastava, M. K.; Weitkamp, E. A.; Sage, A. M.; Grieshop, A. P.; Lane, T. E.; Pierce, J. R.; Pandis, S. N., Rethinking organic aerosols: Semivolatile emissions and photochemical aging. *Science* **2007,** *315*, 1259-1262.

Chapter 5. Elemental composition of ambient fine particles in urban schools: sources of children's exposure

Leigh R. Crilley[A,B], Godwin A. Ayoko[A,B], Eduard Stelcer[C], David D. Cohen[C], Mandana Mazaheri[A,B] and Lidia Morawska[A,B]

[A] International Laboratory for Air Quality and Health, Queensland University of Technology, Brisbane, QLD, 4001, Australia.

[B] Institute of Health and Biomedical Innovation, Queensland University of Technology, Brisbane, 4059, Australia

[C] Institute for Environmental Research, Australian Nuclear Science and Technology Organisation, Locked Bag 2001, Kirrawee DC, NSW 2232, Australia.

(2013) *Science of the Total Environment,* Submitted.

PREFACE

For chapter 5 this paper seeks to assess the source contributions and potential toxicity of PM_1 at schools based upon the elemental composition. Analysis of the elemental composition offers additional information on the source contributions at urban schools compared to analysis of carbonaceous aerosols described in Chapters 4, 6-8. There were four types of sources identified based upon the trace elements, and included secondary sulphate, biomass burning, vehicle emissions and industry. Two of these sources were not identified in the other chapters, particularly the industrial sources which are more easily distinguished by elemental composition compared to organic aerosols. Non-exhaust emissions of metals (e.g. brake, tyre and engine wear) are as an important vehicular source and this contribution was captured in the paper. In addition, the size distribution of the toxic heavy metals was determined, which enabled an assessment of the potential toxicity of the PM_1 at the schools.

Statement of joint authorship of co-authors

The authors listed below have certified* that:

1. they meet the criteria for authorship in that they have participated in the conception, execution, or interpretation, of at least that part of the publication in their field of expertise;
2. they take public responsibility for their part of the publication, except for the responsible author who accepts overall responsibility for the publication;
3. there are no other authors of the publication according to these criteria;
4. potential conflicts of interest have been disclosed to (a) granting bodies, (b) the editor or publisher of journals or other publications, and (c) the head of the responsible academic unit, and
5. they agree to the use of the publication in the student's thesis and its publication on the QUT ePrints database consistent with any limitations set by publisher requirements.

In the case of this chapter:

Elemental composition of ambient fine particles in urban schools: assessment of children's exposure, (2013) *Science of the Total Environment*, Submitted.

Contributor	Statement of contribution*
Leigh R. Crilley	Collected the samples, performed the data analysis and wrote the manuscript
Godwin A. Ayoko*	Provided overall direction for this study and assisted with the data analysis and drafting of the manuscript
Eduard Stelcer*, David D. Cohen*	Performed the elemental analysis and assisted with the data analysis and manuscript
Mandana Mazaheri*	Contributed to the field measurements
Lidia Morawska*	Designed the overall concept of the study and assisted with the data interpretation and manuscript

Principal Supervisor Confirmation

I have sighted email or other correspondence from all Co-authors confirming their certifying authorship.

PROF GODWIN AYOKO — Name

Signature

22/11/2013 — Date

ABSTRACT

Currently, there is a limited understanding of the sources of ambient fine particles that contribute to the exposure of children at urban schools. Since the size and chemical composition of airborne particle are key parameters for determining the source as well as toxicity, PM_1 particles (mass concentration of particles with an aerodynamic diameter less than 1 μm) were collected at 24 urban schools in Brisbane, Australia and their elemental composition determined. Based on the elemental composition four main sources were identified; secondary sulphates, biomass burning, vehicle and industrial emissions. The largest contributing source was industrial emissions and this was considered as the main source of trace elements in the PM_1 that children were exposed to at school. PM_1 concentrations at the schools were compared to the elemental composition of the $PM_{2.5}$ particles (mass concentration of particles with an aerodynamic diameter less than 2.5 μm) from a previous study conducted at a suburban and roadside site in Brisbane. This comparison revealed that the more toxic heavy metals (V, Cr, Ni, Cu, Zn and Pb), mostly from vehicle and industrial emissions, were predominantly in the PM_1 fraction. Thus, the results from this study points to PM_1 as a potentially better particle size fraction for investigating the health effects of airborne particles.

KEYWORDS: Exposure at school, industrial emissions, PM_1 composition, health effects

5.1 INTRODUCTION

Long-term exposure to airborne particles in adults has been associated with a number of harmful effects to cardiovascular [1], and respiratory [2]. Owing to their immature immune systems and faster breathing rates, children are more susceptible to these detrimental health effects [3, 4]. In an urban environment vehicle emissions are one of the main sources of

airborne particles [5] and children's exposure to vehicle emissions has therefore been associated with a number of long-term negative health effects, including increased wheezing [6] and the development of asthma [7].

The size and chemical composition of ambient particles are important parameters in determining their toxicity [8]. A clear relationship has been established between exposure to $PM_{2.5}$ and adverse cardiovascular effects [1] and increased levels of lung cancer [2]. Thus many epidemiological studies have focused on $PM_{2.5}$ when investigating the health effects of air pollution [8]. The chemical composition of airborne particles is also thought to affect the toxicity as it contains toxic and carcinogenic compounds, such as polycyclic aromatic hydrocarbons and heavy metals [9]. In urban environments it has been observed that the majority of the toxic metals, such as V, Ni, Cu, As, Cd and Pb are in the PM_1 fraction [10, 11].

Trace metals can be used as surrogates for determining the influences of various sources (such as traffic, industrial and ship emissions), to the overall composition of the airborne particles [12, 13]. Children spend a large portion of their day at school and traffic emissions have been shown to be a prominent source at schools in urban areas, primarily due to the influence of schools buses [14]. However, not all schools are serviced by school buses. Instead, many schools are more influenced by local and school-related traffic (such as drop-off and pick up times) or other urban sources nearby. Therefore, the relative contribution of different sources at urban schools may differ from other urban environments. Overall, to date, there is limited information on the contributing sources of ambient fine particles that children are exposed to at urban schools [15].

The current study aimed to address the aforementioned gaps in knowledge in the sources of trace elements that contribute to children's exposure at schools by analysing the elemental composition of PM_1 samples obtained from various schools. To determine the size fraction of the detected elements, particularly the heavy metals, concentrations from the present study were compared to previous work on $PM_{2.5}$ composition in Brisbane. The sources of the trace elements that children were exposed to at schools, with a focus on toxic heavy metals, were identified using principal component analysis (PCA). In addition, we sought to determine the more relevant size fraction (PM_1 versus $PM_{2.5}$) for exposure assessment based upon their elemental composition.

5.2 METHOD

5.2.1 Sampling Sites and Instrumentation

The PM_1 sampling was conducted from October 2010 till August 2012 as part of a larger project known as UPTECH (www.ilaqh.qut.edu.au/Misc/UPTECH%20Home.htm) which was designed to study the effect of ultrafine particle from traffic emissions on children's health. 25 randomly selected schools within the Brisbane Metropolitan Area participated in this study and are referred to as S01 to S25. At each school a centrally located site, which was assumed to give the best overall exposure, was chosen to conduct the measurements. Inlets for the sampling were placed approximately 3 m off the ground and on top of a monitoring trailer, which served to house a TSI DustTrak DRX (model 8534) at each site and a Monitors Sensors μSmart Series weather station. The DustTrak DRX is an optical instrument that simultaneously measures the mass concentration of ambient particles across the PM_1, $PM_{2.5}$, PM_{10} and total PM fractions. Optically measured particle mass concentrations are not equivalent to gravimetric results however they are useful in this study to examine the relative

contributions of PM_1 to $PM_{2.5}$ concentrations. Particle mass concentrations for each of these size fractions were recorded and averaged every 30s by the DustTrak DRX.

Data from nearby weather stations was also obtained from the Bureau of Meteorology (BOM) and Queensland Department of Science, Information Technology, Innovation and the Arts (DSITIA) as some of the schools would have been affected by local winds due to schools buildings. Traffic counts were taken on the busiest road next the school, referred to as the main road throughout. In the traffic count cars, motorbikes and scooters were classified as light-duty vehicles. Light trucks with 2, 3 and 4 axels were classified as medium vehicles and long articulated trucks as heavy vehicles.

5.2.2 Sampling Methodology

The PM_1 particles were collected on 47 mm, 0.2 μm pore size Teflon filters (Whatman) with the filter area reduced to 25 mm to concentrate the particles, using cyclone type sampler with a flow rate of 16.7 litres per minute (lpm), maintained with critical orifices. For each sampling period two filters were collected with the flow rate split across the filters at around 5.8 lpm. The sampling period was 24 hours, from 08:00 until 08:00 the next day, Monday to Friday for one week to give a total of four samples at each school. No PM_1 samples were collected at S11 due to instrument malfunction. This sampling regime typically gave sampling volumes of 8.2 m^3. After sampling each filter was placed in a Petri dish and then sealed in a ziplock bag. Gravimetric analysis was performed on a 5 point Mettler Toledo micro balance in the Chemistry laboratories at Queensland University of Technology. Prior to weighing all filters were preconditioned at a constant temperature and humidity (25°C and 40%) for at least 24 hours.

5.2.3 Elemental Analysis

Elemental analysis was done using ion beam analysis and was performed at the Australian Nuclear Science and Technology Organisation (ANSTO) in Sydney, Australia on a STAR accelerator (2.0-MV HVEE tandetron, High Voltage Engineering Europa, Amersfoort, the Netherlands) [16] using particle induced gamma emissions (PIGE) spectroscopy and particle induced x-ray emission (PIXE) spectroscopy. These techniques can measure the following commonly occurring elements in fine particles: Na, Al, Si, P, S, Cl, K, Ca, Ti, V, Cr, Mn, Fe, Co, Ni, Cu, Zn, Br, Sr, Cd and Pb and has been described in details elsewhere [17-19]. Na was analysed by PIGE and the remaining 20 elements by PIXE.

5.2.4 Quality Control

Flow rate for the PM_1 cyclone: this was checked at the beginning of each sample and always set to within ±0.1 lpm of the desired flow rate.

Gravimetric analysis: a test filter that was given the same preconditioning treatment as the sample filters, was weighed repeatedly over the project. The standard deviation of the mean weight was 10 μg, indicating high stability of the balance.

Ion beam analysis: The average minimum detection limit (MDL) ranged from 3.3 to 40.8 ng m^{-3} as summarised in Table S1 (Supporting Information) for the PIXE elements. For Na, the PIGE analysis program could not calculate a MDL, as Na was not detected in any samples. However, previous work by Friend et al. [20] found an average MDL of 35.5, and a range of 20 to 60 ng m^{-3} for $PM_{2.5}$ sampled in Brisbane.

5.2.5 Data Analysis

Principal component analysis (PCA) and ANOVA were performed using SPSS v19. For the PCA, missing values were replaced by the mean and Varimax rotation applied to the

loadings. Only factors that had an eigenvalue above one were considered. Rose plots of wind direction and speed were calculated using IGOR Pro v6.22.

5.3 RESULTS AND DISCUSSION

5.3.1 Meteorological characteristics during sampling

The project was conducted over nearly two years with sampling covering all of the seasons, as reflected in the range of meteorological conditions recorded at the schools and listed in Table 5-1. Brisbane is a subtropical city with a low level of variation between the average daily temperatures and an average temperature ranging from 13 to 24°C across all the schools (Table 5-1). May until October is the cooler, drier period with generally more stable weather and is referred to as winter. November to April is the summer and it is warmer with higher humidity and rainfall. These weather conditions were observed throughout the project, as shown in Table 5-1. Wind rose plots were used to determine the wind direction during the sampling period, and these are given in Appendix 3, Figure A3-1, and summarised in Table 5-1.

5.3.2 Traffic characteristics of the schools

The majority of the schools were all in residential areas and had mostly light vehicles passing the schools, though schools such as S04, S06, S08, S23 and S25 were beside roads that service industrial/commercial areas and had higher levels of medium and heavy vehicles. Some schools such as S07, S09, S19 and S20 were located on busy arterial roads and others such as S01, S16 and S18 were beside quiet residential streets, as indicated by the traffic volume passing the schools.

Table 5-1: Average traffic and meteorological conditions at the schools during the sampling.

School	Date	Temp. (°C)	RH (%)	Wind speed (m s^{-1})	Prominent wind direction	Frequency of wind from main road (%)	Direction of main road	Local traffic (veh h^{-1})	% Light	% Med	% Heavy
S01	Nov-10	23	65	4.90	East	16	South	158	95.6	3.8	0.6
S02	Oct-10	22	76	3.31	East	35	East	859	95.2	4.6	0.3
S03	Nov-10	23	71	2.81	Northeast	0	Southwest	312	98.3	1.6	0.1
S04	Mar-11	23	60	1.63	East	5	West	806	87.0	7.9	2.2
S05	Mar-11	22	80	1.22	South	26	South	616	96.5	3.0	0.4
S06	May-11	15	73	3.78	West	2	East	268	87.8	8.2	2.9
S07	Jun-11	17	65	0.72	South	0	Northeast	1019	95.3	3.5	0.6
S08	Jun-11	13	69	1.11	West	19	Northwest	565	86.0	13.4	0.7
S09	Jul-11	13	65	1.91	W/SW	0	North	1164	90.7	3.6	1.8
S10	Aug-11	14	73	2.1	South	7	West	893	95.1	3.3	0.7
S12	Aug-11	15	75	0.75	West	2	South	176	97.3	2.5	0.2
S13	Oct-11	21	66	1.31	South	4	West	655	95.6	3.6	0.5
S14	Oct-11	22	74	1.09	Southeast	4	East	173	95.7	3.8	0.5
S15	Nov-11	24	65	4.13	Northeast	12	West	858	92.1	5.9	0.9
S16	Nov-11	25	75	0.96	North	40	North	46	97.8	1.6	0.4
S17	Dec-11	24	71	0.91	Southeast	15	East	757	95.3	3.0	0.6
S18	Mar-12	22	71	1.00	S/SE	0	West	35	97.9	2.1	0
S19	Mar-12	23	79	3.27	South	31	South	1093	89.9	3.2	2.0
S20	Apr-12	20	63	0.68	West	17	East	1121	96.2	2.5	0.8
S21	Jun-12	14	58	0.78	West	31	West	151	97.4	2.1	0.4
S22	Jun-12	14	66	0.64	West	1	Northwest	469	96.8	2.5	0.6
S23	Jul-12	15	60	0.66	South	40	S/SE	657	71.1	28	0.6
S24	Aug-12	15	40	2.99	West	3	North	160	97.1	2.4	0.5
S25	Aug-12	15	68	3.53	North	31	S/SW	332	92.0	6.5	1.2

5.3.3 Gravimetric analysis

The average mass of PM_1 measured on the filters across the 24 schools was 90 ± 60 μg and this equated to an average concentration of 11 ± 7 μg m^{-3}. Though the DustTrak is an optical instrument and thus the concentrations are not directly comparable to the gravimetric results, the ratios of PM_1 to $PM_{2.5}$ are expected to be the same for DustTrak and gravimetric analysis. On average, the PM_1 made up 83 ± 17% of the $PM_{2.5}$ fraction by mass, as determined by the DustTrak. Therefore the PM_1 fraction made up the majority of the $PM_{2.5}$ that children were exposed to at the schools.

5.3.4 Average elemental composition

The average concentrations and summary statistics for each element across all of the schools are presented in Table 5-2. The most abundant element at the schools was generally S. The largest source of S in Brisbane is secondary sulphates [20]. The next most abundant elements on average from Table 5-2 were Si, Ca and Fe, which along with the other elements known to be of a crustal origin such as K, Mn and Ti [20, 21] made a significant component of the total trace elements concentration of the PM_1 at the schools. Brisbane is a coastal city; therefore Cl was abundant at the schools, which was likely due to the presence of sea salt particles. However, Na was below the detection limit for all samples possibly due in part to the higher MDL of PIGE technique compared to PIXE [17] and this is discussed further in Section 5.3.7. The remaining elements, P, V, Cr, Co, Cu, Zn, Br, Cd and Pb, are related to anthropogenic sources, such as vehicle, ship and industrial emissions [12, 20] and the contributing sources are investigated further in Section 5.3.6.

Table 5-2: Summary statistics for the PM_1 concentration of the elements at all schools (ng m^{-3}).

	Average	Standard deviation	Min	Max	Median	% Detected
Na	0	0.0	0.0	0.0	0.0	0
Al	1.6	6.1	0.0	50.9	0.0	22
Si	75.8	69.2	17.9	401.4	65.7	100
P	6.3	7.1	0.0	45.6	4.4	97
S	177.9	130.1	63.5	760.1	154.1	100
Cl	21.2	28.8	0.0	166.5	11.5	99
K	8.9	9.2	0.0	51.2	6.2	98
Ca	28.9	25.5	5.0	133.9	24.7	100
Ti	2.0	2.2	0.0	13.0	1.4	84
V	0.6	1.4	0.0	10.7	0.0	33
Cr	2.8	7.0	0.0	53.1	1.0	85
Mn	4.4	6.5	0.0	55.8	2.4	97
Fe	19.1	18.3	0.0	83.9	12.4	98
Co	0.3	0.9	0.0	6.5	0.0	22
Ni	0.9	2.9	0.0	25.3	0.2	55
Cu	3.0	6.9	0.0	43.9	1.4	81
Zn	5.9	7.1	0.0	34.0	2.9	90
Br	5.6	11.6	0.0	59.5	2.8	68
Sr	10.3	27.3	0.0	191.1	3.3	61
Cd	5.5	19.1	0.0	123.8	0.0	22
Pb	10.3	27.9	0.0	238.0	3.0	68

5.3.5 School-based PM_1 elemental composition

The concentrations of the elements were compared between the schools in order to investigate the driving factors of the concentrations of heavy metals that children are exposed to at school. The average PM_1 concentrations of selected elements (S, V, Fe, Ni, Zn and Pb) are given in Figure 5-1, with Si, Cr, Cu and Br given in Figure A3-2 (Appendix 3). From Figure 5-1, except for Fe and Zn, S02 clearly had highest concentrations of all of these elements and this was likely due to the combined influence of two sources: industrial/shipping and traffic emissions. Along with the six elements from Figure 5-1, S02 also had elevated concentrations of elements such as Cr, Cu and Br (Figure A3-2) compared to the other 23 schools. The predominant wind direction at S02 was from the east (Table 5-1) and both the Port of Brisbane (approximately 10 km) and the main road lie in this direction. It is noteworthy that

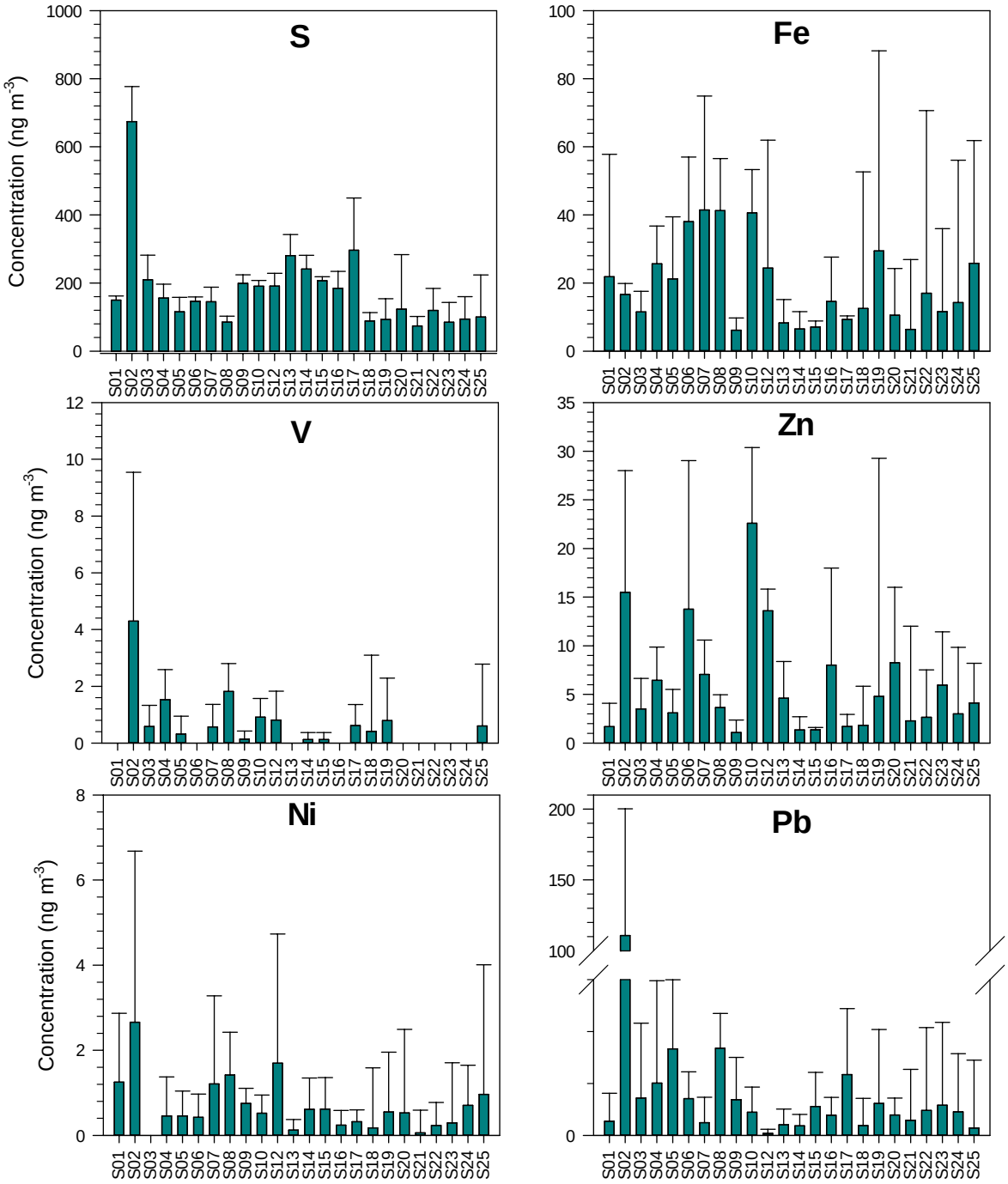

Figure 5-1: Average PM_1 concentrations at each school for selected elements. Error bars represent 1 standard deviation.

elements with elevated concentrations at S02 have previously been associated with industrial [12], shipping [13], and traffic emissions [22, 23].

S02, S04 and S17 are within similar distance to the port and during sampling the main wind direction was from the port area. These three schools recorded comparatively high concentrations of S and V (Figure 5-1), elements previously associated with shipping emissions [13], which suggests emissions from the port affected the schools. Also from Figure 5-1, the schools that recorded some of the highest concentrations of Fe, Zn and Pb (S02, S10, S19 and S20) were schools beside some of the more heavily trafficked roads (Table 5-1) implicating traffic emissions [22, 23]. However S07 and S09 had equally high traffic counts and yet recorded relatively low concentrations of these elements, which was likely due to the fact that the main wind direction was not from the main road at these schools (Table 5-1).

5.3.6 Source Identification using PCA

Overall, the PM1 elemental concentrations at the schools indicate an array of contributing sources to the elemental composition, especially for the anthropogenic elements at the schools. PCA was applied to average concentrations of all the detected elements at each school in order to determine the contributing sources and their relative importance. With all of the schools included, the number of factors was only 3 and all of the elements except for Al, Fe and Zn have high loadings in the first factor (See Table A3-3, Appendix 3). These three elements were the only elements that were not elevated at S02 compared to the rest of the schools (Figures 5-1 and A3-2), and this shows that S02 was an outlier. Therefore PCA was applied to the data without S02 and the number of factors increased to 7, explaining a total of 81% of the variance, with the results shown in Table 5-3 along with the source identification for each factor.

Table 5-3: PCA results for the schools excluding S02.

	Component						
	1	**2**	**3**	**4**	**5**	**6**	**7**
Si	***0.83***	0.31	0.04	0.32	0.12	0.23	-0.04
P	***0.87***	0.18	0.13	-0.26	-0.06	-0.07	-0.08
S	***0.94***	-0.10	-0.02	0.12	-0.17	0.05	0.10
Cl	***0.58***	0.46	0.12	-0.26	0.33	-0.19	0.10
K	0.28	-0.03	-0.04	***0.73***	-0.28	0.07	0.15
Ca	***0.82***	0.20	-0.06	0.37	-0.04	0.21	-0.01
Ti	0.29	***0.85***	0.02	0.09	0.12	-0.06	0.04
Cr	0.25	0.10	***0.87***	0.07	-0.05	-0.10	0.03
Mn	0.24	***0.65***	0.03	0.34	0.48	-0.07	0.09
Fe	-0.27	0.33	0.52	***0.62***	0.16	0.04	-0.20
Ni	-0.12	-0.05	***0.83***	0.10	0.14	-0.02	0.16
Cu	0.22	0.06	-0.02	-0.03	0.05	***0.90***	0.02
Zn	0.07	-0.13	0.31	***0.68***	0.25	-0.11	-0.23
Br	0.31	***0.54***	0.22	-0.23	0.24	-0.40	0.01
Sr	0.13	0.19	***0.60***	0.03	***0.61***	0.14	-0.06
Pb	-0.05	***0.80***	0.14	-0.14	-0.11	0.34	0.01
Al	0.22	-0.09	0.02	-0.08	-0.66	-0.17	0.11
V	-0.03	0.47	***0.62***	0.06	-0.23	0.04	-0.45
Co	0.00	0.08	0.08	-0.05	0.00	0.01	***0.91***
Cd	0.05	0.00	0.06	-0.17	***0.68***	-0.37	0.24
Variance (%)	19.6	14.4	13.3	10.1	10.0	7.3	6.4
Eiginvalue	3.93	2.88	2.67	2.02	1.99	1.46	1.28
Source	Secondary Sulphate	Vehicle emission	Ship/ Port	Biomass burning	Industry	Industry	Industry

From Table 5-3 most of the sources of the PM_1 at the schools identified were anthropogenic. Component 1 was characterised by highest loadings of S and also high loadings of Si, P, Cl and Ca, indicating secondary sulphates [20]. This component explained the most variance and was thus a significant source of the PM_1. Two oil refineries present in Brisbane emit a combined $6.7x10^6$ kg of SO_2 into the atmosphere per annum [24] and are thus contributing to the high concentrations of secondary sulphates in Brisbane.

A vehicle emission source identified in the PCA, which were characterised by Ti, Mn, Br and Pb (Component 2); these elements that have been associated with vehicle emissions ([25] and references therein). Though leaded petrol was banned in 2002 in Queensland, Pb and Br are still associated with vehicle emissions in Brisbane [20] and in other studies around the world [22, 25]. Furthermore, the ratio of the average Pb and Br concentrations at the schools was bout 2 (Table 5-2), which is characteristic of vehicle emissions [17]. In addition, Mn and Ti have also previously been associated vehicle exhaust emissions [26] and this suggests that the source of the component is vehicle exhaust emissions. This component accounted for the second highest amount of the data variance and this evidence points to vehicle emissions as a second most important anthropogenic source at the schools.

Component 3 was attributed primarily to ship emissions due to the high loadings of Ni and V, which have been previously associated with oil/combustion/shipping emissions [13]. Chromium and Sr also recorded high loadings in component 3 and have previously been associated with petrochemical [27] and cement works [28], industries present around the Port of Brisbane.

Along with high loadings of Fe and Zn, K had the highest loading in component 4. As K had the highest loadings and is also a well-known tracer for biomass burning (See e.g. [29]), component 4 was attributed to biomass burning. Zn and Fe have also previously been found in the emissions from biomass combustion [20] and as elements in the PM_1 fraction are generally related more to combustion processes than to crustal material or vehicle wear emissions [30], this observation further point to biomass burning as the source.

Components 5 to 7 were also attributed to emissions from industry. Pollution from industrial activities can be highly specific chemically [12] and this explains the number of components related to industrial sources are observed in the PCA results. Cd and Sr recorded high loadings in component 5 while component 7 was characterised by high loadings of Co; all of these elements have been previously shown to be from industrial sources [12, 28]. Co in particular has been previously attributed to industrial sources in Brisbane [31]. The main industrial areas of Brisbane are in the southwest and northeast parts and the major wind direction at schools that recorded high concentrations of Co and Cd (S03, S05, S20 and S23) was from these areas (Figure A3-1). The short sampling time at each school made identifying individual industrial sources difficult, however likely industrial sources include various metallurgical and cement plants [12, 28], all of which are present in Brisbane.

Copper, the characteristic element of component 6, has been proposed as a tracer for brake wear emissions [23]; however the lack of other metals with high loadings, such as Fe, which are also known to be from brake wear [32] suggests that the source may not be related to vehicle movement. In addition, brake wear particles are expected to be in the larger size fractions [33] while emissions from anthropogenic combustion processes, as opposed to mechanical processes, are found more in smaller sizes [30]. Therefore the source of the Cu in the PM_1 was assigned to industrial emissions, which has been observed before for fine particles in Brisbane [31] and elsewhere [12, 34]. All of the industrial sources (Components 3, 5-7) combined explained more variance that the vehicle emissions component, indicating that industrial emissions

were the largest anthropogenic source of metals in the PM_1 fraction in Brisbane. Thus industrial emissions were the main anthropogenic source of elements in the PM_1 that children were exposed to at schools.

5.3.7 Comparison to a previous Brisbane study

In Table 5-4, the PM_1 element concentrations from the schools were compared to a similar study by Friend et al. [20] on the $PM_{2.5}$ composition at a suburban and roadside site in Brisbane. The sampling by Friend et al. [20] encompassed three and one year of sampling for the suburban and roadside site respectively. Therefore they are considered as representative of the typical ambient concentrations for these types of sites in Brisbane.

Sodium was detected in the previous study (Table 5-4) as sea salt particles are generally in the coarse mode; however in the present study the sampled particles were in the PM_1 faction. Combined with the higher detection limit for Na outlined in previous sections, it is therefore not surprising that amounts of NA in the samples were not detectable.

Crustal elements (Al, Si, K, Ti and Fe) had lower concentrations in the PM_1 fraction compared to the $PM_{2.5}$ (Table 5-4). One-way ANOVA analysis of these concentrations found that compared to the $PM_{2.5}$ concentrations at the suburban site [20], Al, Si, Ti and Fe had statistically significant lower concentrations at the

Table 5-3: Comparison of the average PM_1 elemental concentrations (ng m^{-3}) at the schools (current study) to a $PM_{2.5}$ elemental concentrations (ng m^{-3}) at a suburban and roadside site in Brisbane [20].

Site	Suburban	Roadside	Schools

	Mean	Standard deviation	Mean	Standard deviation	Mean	Standard deviation
Na	330.8	237.0	332.1	181.8	0	0
Al	41.6	236.5	104.2	474.6	1.6	6.1
Si	133.4	698.1	324.7	1428.4	75.8	69.2
P	2.9	3.1	1.9	2.1	6.3	7.1
S	282.4	159.4	291.9	156.2	177.9	130.1
Cl	231.5	300.9	246.9	294.0	21.2	28.8
K	54.7	83.9	81.8	177.1	8.9	9.2
Ca	25.0	46.1	50.2	104.0	28.9	25.5
Ti	7.2	39.2	20.7	87.3	2.0	2.2
V	0.8	1.0	1.3	2.3	0.6	1.4
Cr	0.7	1.3	0.8	0.9	2.8	7.0
Mn	5.3	9.4	4.9	14.3	4.4	6.5
Fe	85.4	329.5	241.9	761.2	19.1	18.3
Co	0.7	2.3	1.3	5.2	0.3	0.9
Ni	0.5	0.6	0.4	0.3	0.9	2.9
Cu	2.0	1.9	9.9	7.7	3.0	6.9
Zn	15.5	39.5	14.2	13.1	5.9	7.1
Br	3.0	2.4	3.8	2.2	5.6	11.6
Pb	5.0	4.2	5.6	3.8	10.3	27.9

schools. Crustal elements are generally found preferentially in the larger size fractions and this would explain the lower concentrations observed at the schools [29, 30] , combined with the Fe rich nature of Australian soils [21] would partly explain why Al was not detected in every sample at the schools (Table 5-2).

On average the concentrations of P, Cr, Ni, Br and Pb in the PM_1 at the schools were found to be 2-3 times higher than those found at the roadside and suburban sites (Table 5-3) [20]. Vehicle emissions are one of the primary sources of Ni, Br and Pb in urban environments [12] and thus the higher concentrations at the schools points to a contribution from school-related traffic. However, analysis by ANOVA found that none of the higher average concentrations at the schools compared to the other sites were statistically significant ($p>0.05$).

That the PM_1 concentrations of V, Cr, Ni, Cu, Br and Pb in ther current work were similar to suburban and roadside $PM_{2.5}$ concentrations (Table 5-4), suggests that these elements were predominantly in the PM_1 fraction. Richard et al. [29] showed that the $PM_{1\text{-}2.5}$ fraction is the crossover between the coarse crustal material and particles associated with anthropogenic sources in agreement, with the results from this study.

5.3.8 Implications for investigating health effects of airborne particles

In the current study, measurements with a DustTrak determined that the majority of the $PM_{2.5}$ fraction (82%) by mass, was actually in the PM_1 where the more toxic heavy metals (e.g. V, Ni, Zn and Pb, [35]) were preferentially found. Thus based on the size and chemical composition, the PM_1 fraction may have greater detrimental health effects compared to $PM_{2.5}$. Currently the main metric for measuring the concentration of airborne particles is $PM_{2.5}$ in many epidemiological studies, as clear relationships have been established between $PM_{2.5}$ and harmful health effects (See e.g. [1]). However, the results from this study suggest that the more appropriate size fraction to use when investigating the health effects of airborne particles would be PM_1.

5.4 CONCLUSIONS

The trace elemental composition of the PM_1 was analysed at 24 urban schools to determine the sources of airborne particles children are exposed to at urban schools. The elemental composition varied from school to school as a result of differing source contributions. PCA was applied to identify these sources within Brisbane and found four types of emission sources: secondary sulphates, biomass burning, vehicle and industrial. The four sources classed as industrial were distinguished by different

elements, notably a shipping/port emission source with high loadings of V, Cr, Ni and Sr. Combined, industrial emissions, rather than vehicle emissions were the largest anthropogenic source of trace elements in the PM_1 that children were exposed to at school.

Comparison of the elemental concentrations from this study to previous work on the $PM_{2.5}$ elemental composition studies conducted in Brisbane [20] revealed that the contribution of Pb, Br and Ni had concentrations 2-3 times higher at the schools, pointing to an influence from school related traffic. However, analysis by ANOVA revealed that this difference was not statistically significant and generally elements from anthropogenic sources had similar concentrations. Therefore the anthropogenic elements, which are generally more toxic (e.g. V, Ni, Zn and Pb), were predominantly in the PM_1. As the smaller particles are thought to have a greater detrimental health effect, the results from this study point to PM_1 being a potentially better metric to use when investigating the health effects of airborne particles. Further work is required to confirm this hypothesis.

ACKNOWLEDGMENTS

This work was supported by the Australian Research Council (ARC), QLD Department of Transport and Main Roads (DTMR) and QLD Department of Education, Training and Employment (DETE) through Linkage Grant LP0990134. Our particular thanks go to R. Fletcher (DTMR) and B. Robertson (DETE) for their vision regarding the importance of this work. We would also like to thank Prof G. Marks, Dr P. Robinson, Prof K. Mengersen, Prof Z. Ristovski, Dr C. He, Dr G. Johnson, Dr R. Jayaratne, Dr S. Low Choy, Prof G. Williams, W. Ezz, F. Salimi, S.

Clifford, M. Mokhtar, N. Mishra, R. Laiman, L. Guo, Prof C. Duchaine, Dr H. Salonen, Dr X. Ling, Dr J. Davies, Dr L. Leontjew Toms, F. Fuoco, Dr A. Cortes, Dr B. Toelle, A. Quinones, P. Kidd, E. Belousova, Dr M. Falk, Dr F. Fatokun, Dr J. Mejia, Dr D. Keogh, Prof T. Salthammer, R. Appleby and C. Labbe for their contribution to the UPTECH project.

5.5 REFERENCES

1. Brook, R. D.; Rajagopalan, S.; Pope, C. A.; Brook, J. R.; Bhatnagar, A.; Diez-Roux, A. V.; Holguin, F.; Hong, Y.; Luepker, R. V.; Mittleman, M. A.; Peters, A.; Siscovick, D.; Smith, S. C.; Whitsel, L.; Kaufman, J. D.; Council on Nutrition, Metabolism, Particulate Matter Air Pollution and Cardiovascular Disease: An Update to the Scientific Statement From the American Heart Association. *Circulation* **2010,** *121*, (21), 2331-2378.
2. Pope, C.; Burnett, R. T.; Thun, M. J.; Calle, E. E.; Krewski, D.; Ito, K.; Thurston, G. D., Lung cancer, cardiopulmonary mortality, and long-term exposure to fine particulate air pollution. *J. Am. Med. Assoc* **2002,** *287*, (9), 1132-1141.
3. Zhang, Q.; Zhu, Y., Measurements of ultrafine particles and other vehicular pollutants inside school buses in South Texas. *Atmos. Environ.* **2010,** *44*, (2), 253-261.
4. Rückerl, R.; Schneider, A.; Breitner, S.; Cyrys, J.; Peters, A., Health effects of particulate air pollution: A review of epidemiological evidence. *Inhal. Toxicol* **2011,** *23*, (10), 555-592.
5. Morawska, L.; Ristovski, Z.; Jayaratne, E. R.; Keogh, D. U.; Ling, X., Ambient nano and ultrafine particles from motor vehicle emissions: Characteristics, ambient processing and implications on human exposure. *Atmos. Environ.* **2008,** *42*, (35), 8113-8138.
6. Ryan, P. H.; Bernstein, D. I.; Lockey, J.; Reponen, T.; Levin, L.; Grinshpun, S.; Villareal, M.; Khurana Hershey, G. K.; Burkle, J.; LeMasters, G., Exposure to Traffic-related Particles and Endotoxin during Infancy Is Associated with Wheezing at Age 3 Years. *Am. J. Resp. Crit. Care* **2009,** *180*, (11), 1068-1075.
7. Gehring, U.; Wijga, A.; Brauer, M.; Fischer, P.; de Jongste, J.; Kerkhof, M.; Oldenwening, M.; Smit, H.; Brunekreef, B., Traffic-related Air Pollution and the Development of Asthma and Allergies during the First 8 Years of Life. *Am. J. Resp. Crit. Care* **2010,** *181*, (6), 596-603.
8. Heal, M. R.; Kumar, P.; Harrison, R. M., Particles, air quality, policy and health. *Chem. Soc. Rev.* **2012,** *41*, (19), 6606-6630.
9. Harrison, R. M.; Smith, D. J. T.; Kibble, A. J., What is responsible for the carcinogenicity of PM2.5? *Occup. Environ. Med.* **2004,** *61*, (10), 799-805.
10. Cheng, Y.; Lee, S. C.; Cao, J.; Ho, K. F.; Chow, J. C.; Watson, J. G.; Ao, C. H., Elemental composition of airborne aerosols at a traffic site and a suburban site in Hong Kong. *Int. J. Environ. Pollut.* **2009,** *36*, (1), 166-179.
11. Moreno, T.; Querol, X.; Alastuey, A.; Reche, C.; Cusack, M.; Amato, F.; Pandolfi, M.; Pey, J.; Richard, A.; Prévôt, A. S. H.; Furger, M.; Gibbons, W.,

Variations in time and space of trace metal aerosol concentrations in urban areas and their surroundings. *Atmos. Chem. Phys.* **2011,** *11*, (17), 9415-9430.
12. Moreno, T.; Querol, X.; Alastuey, A.; Viana, M.; Salvador, P.; Sánchez de la Campa, A.; Artiñano, B.; de la Rosa, J.; Gibbons, W., Variations in atmospheric PM trace metal content in Spanish towns: Illustrating the chemical complexity of the inorganic urban aerosol cocktail. *Atmos. Environ.* **2006,** *40*, (35), 6791-6803.
13. Arhami, M.; Sillanpää, M.; Hu, S.; Olson, M. R.; Schauer, J. J.; Sioutas, C., Size-Segregated Inorganic and Organic Components of PM in the Communities of the Los Angeles Harbor. *Aerosol Sci. Technol.* **2009,** *43*, (2), 145-160.
14. Hochstetler, H. A.; Yermakov, M.; Reponen, T.; Ryan, P. H.; Grinshpun, S. A., Aerosol particles generated by diesel-powered school buses at urban schools as a source of children's exposure. *Atmos. Environ.* **2011,** *45*, 1444-1453.
15. Mejía, J. F.; Choy, S. L.; Mengersen, K.; Morawska, L., Methodology for assessing exposure and impacts of air pollutants in school children: Data collection, analysis and health effects – A literature review. *Atmos. Environ.* **2011,** *45*, (4), 813-823.
16. Cohen, D. D.; Crawford, J.; Stelcer, E.; Bac, V. T., Characterisation and source apportionment of fine particulate sources at Hanoi from 2001 to 2008. *Atmos. Environ.* **2010,** *44*, (3), 320-328.
17. Cohen, D. D., Characterisation of atmospheric fine particles using IBA techniques. *Nucl. Instrum. Meth. B* **1998,** *14*, (22), 136-138.
18. Cohen, D. D.; Bailey, G. M.; Kondepudi, R., Elemental analysis by PIXE and other IBA techniques and their application to source fingerprinting of atmospheric fine particle pollution. *Nucl. Instrum. Meth. B* **1996,** *109–110*, (0), 218-226.
19. Cohen, D. D.; Stelcer, E.; Hawas, O.; Garton, D., IBA methods for characterisation of fine particulate atmospheric pollution: a local, regional and global research problem. *Nucl. Instrum. Meth. B* **2004,** *219–220*, (0), 145-152.
20. Friend, A. J.; Ayoko, G. A.; Stelcer, E.; Cohen, D., Source apportionment of PM2.5 at two receptor sites in Brisbane, Australia. *Environ. Chem.* **2011,** *8*, (6), 569-580.
21. Radhi, M.; Box, M. A.; Box, G. P.; Keywood, M. D.; Cohen, D. D.; Stelcer, E.; Mitchell, R. M., Size-resolved chemical composition of Australian dust aerosol during winter. *Environ. Chem.* **2011,** *8*, (3), 248-262.
22. Lough, G. C.; Schauer, J. J.; Park, J.-S.; Shafer, M. M.; DeMinter, J. T.; Weinstein, J. P., Emissions of Metals Associated with Motor Vehicle Roadways. *Environ. Sci. Technol.* **2005,** *39*, (3), 826-836.
23. Thorpe, A.; Harrison, R. M., Sources and properties of non-exhaust particulate matter from road traffic: A review. *Sci. Total Environ.* **2008,** *400*, (1-3), 270-282.
24. NPI National Pollution Inventory, Australian Government Department of Sustainability, Environment, Water, Population and Communities. http://www.npi.gov.au/ (26 September 2013),
25. Lin, C.-C.; Chen, S.-J.; Huang, K.-L.; Hwang, W.-I.; Chang-Chien, G.-P.; Lin, W.-Y., Characteristics of Metals in Nano/Ultrafine/Fine/Coarse Particles Collected Beside a Heavily Trafficked Road. *Environ. Sci. Technol.* **2005,** *39*, (21), 8113-8122.
26. Wang, Y.-F.; Huang, K.-L.; Li, C.-T.; Mi, H.-H.; Luo, J.-H.; Tsai, P.-J., Emissions of fuel metals content from a diesel vehicle engine. *Atmos. Environ.* **2003,** *37*, (33), 4637-4643.

27. Singh, M.; Jaques, P. A.; Sioutas, C., Size distribution and diurnal characteristics of particle-bound metals in source and receptor sites of the Los Angeles Basin. *Atmos. Environ.* **2002,** *36*, (10), 1675-1689.
28. Widory, D.; Liu, X.; Dong, S., Isotopes as tracers of sources of lead and strontium in aerosols (TSP & PM2.5) in Beijing. *Atmos. Environ.* **2010,** *44*, (30), 3679-3687.
29. Richard, A.; Gianini, M. F. D.; Mohr, C.; Furger, M.; Bukowiecki, N.; Minguillón, M. C.; Lienemann, P.; Flechsig, U.; Appel, K.; DeCarlo, P. F.; Heringa, M. F.; Chirico, R.; Baltensperger, U.; Prévôt, A. S. H., Source apportionment of size and time resolved trace elements and organic aerosols from an urban courtyard site in Switzerland. *Atmos. Chem. Phys.* **2011,** *11*, (17), 8945-8963.
30. Minguillón, M. C.; Querol, X.; Baltensperger, U.; Prévôt, A. S. H., Fine and coarse PM composition and sources in rural and urban sites in Switzerland: Local or regional pollution? *Sci. Total Environ.* **2012,** *427–428*, (0), 191-202.
31. Lim, M. C. H.; Ayoko, G. A.; Morawska, L., Characterization of elemental and polycyclic aromatic hydrocarbon compositions of urban air in Brisbane. *Atmos. Environ.* **2005,** *39*, (3), 463-476.
32. Gietl, J. K.; Lawrence, R.; Thorpe, A. J.; Harrison, R. M., Identification of brake wear particles and derivation of a quantitative tracer for brake dust at a major road. *Atmos. Environ.* **2010,** *44*, (2), 141-146.
33. Iijima, A.; Sato, K.; Yano, K.; Tago, H.; Kato, M.; Kimura, H.; Furuta, N., Particle size and composition distribution analysis of automotive brake abrasion dusts for the evaluation of antimony sources of airborne particulate matter. *Atmos. Environ.* **2007,** *41*, (23), 4908-4919.
34. Viana, M.; Kuhlbusch, T. A. J.; Querol, X.; Alastuey, A.; Harrison, R. M.; Hopke, P. K.; Winiwarter, W.; Vallius, M.; Szidat, S.; Prévôt, A. S. H.; Hueglin, C.; Bloemen, H.; Wåhlin, P.; Vecchi, R.; Miranda, A. I.; Kasper-Giebl, A.; Maenhaut, W.; Hitzenberger, R., Source apportionment of particulate matter in Europe: A review of methods and results. *J. Aerosol Sci.* **2008,** *39*, (10), 827-849.
35. Chen, L. C.; Lippmann, M., Effects of Metals within Ambient Air Particulate Matter (PM) on Human Health. *Inhal. Toxicol.* **2009,** *21*, (1), 1-31.

Chapter 6. Aerosol Mass Spectrometric analysis of the chemical composition of non-refractory PM_1 samples from school environments in Brisbane, Australia

Leigh R. Crilley[1,2], Godwin A. Ayoko[1,2], E. Rohan Jayaratne[1,2] Farhad Salimi[1,2], and Lidia Morawska[1,2].

[1]International Laboratory for Air Quality and Health, Queensland University of Technology, Brisbane, QLD, 4001, Australia.

[2]Institute of Health and Biomedical Innovation, Queensland University of Technology, Brisbane, 4059, Australia.

(2013) *Science of the Total Environment*, **458-460**, 81-89

PREFACE

Utilising the high temporal resolution offered by AMS, chapter 6 details investigations into the composition of organic aerosols during school hours. The chemical analysis methods used in Chapters 4 and 5 required a significantly longer time resolution compared to the AMS, the diurnal variation of the organic aerosols and its components were accurately quantified in this current chapter. This allowed the concentration of vehicle emissions and secondary organic aerosols that children were actually exposed to at school as well as the influence of local and school traffic to be determined. The following two chapters (7 and 8) also examine AMS data at the schools with more focus on the source apportionment and methodology.

Statement of joint authorship of co-authors

The authors listed below have certified* that:

1. they meet the criteria for authorship in that they have participated in the conception, execution, or interpretation, of at least that part of the publication in their field of expertise;
2. they take public responsibility for their part of the publication, except for the responsible author who accepts overall responsibility for the publication;
3. there are no other authors of the publication according to these criteria;
4. potential conflicts of interest have been disclosed to (a) granting bodies, (b) the editor or publisher of journals or other publications, and (c) the head of the responsible academic unit, and
5. they agree to the use of the publication in the student's thesis and its publication on the QUT ePrints database consistent with any limitations set by publisher requirements.

In the case of this chapter:

Aerosol Mass Spectrometric analysis of the chemical composition of non-refractory PM_1 samples from school environments in Brisbane, Australia, (2013) *Science of the Total Environment,* 458-460, 81-89.

Contributor	Statement of contribution*
Leigh R. Crilley	Ran the AMS, performed the data analysis and wrote the manuscript
Godwin A. Ayoko*	Provided overall direction for this study and assisted with the data analysis and drafting of the manuscript
E. Rohan Jayaratne*	Assisted with the data analysis and manuscript
Farhad Salimi*	Collected and processed the particle number data
Lidia Morawska*	Designed the overall concept of the study and assisted with the data interpretation and manuscript

Principal Supervisor Confirmation

I have sighted email or other correspondence from all Co-authors confirming their certifying authorship.

PROF GODWIN AYOKO _____ 22/11/2013

Name Signature Date

ABSTRACT

Long-term exposure to vehicle emissions has been associated with detrimental health effects. Children are amongst the most susceptible group and schools represent an environment where they can experience significant exposure to vehicle emissions. However, there are limited studies on children's exposure to vehicle emissions in schools. The aim of this study was to quantify the concentration of organic aerosol (OA) and in particular, vehicle emissions that children are exposed to during school hours. Therefore an Aerodyne compact time-of-flight aerosol mass spectrometer (TOF-AMS) was deployed at five urban schools in Brisbane, Australia. TOF-AMS enabled the chemical composition of the non-refractory (NR-PM_1) to be analysed with a high temporal resolution to assess the concentration of vehicle emissions and other OA components during school hours. The organic fraction at each school comprised the majority of NR-PM_1. Primary emissions were found to dominate the OA at only one school which had an O:C ratio of 0.17, due to fuel powered gardening equipment used near the TOF-AMS. A significant source of the OA at two of the schools was aged vehicle emissions from nearby highways. More oxidised OA was observed at the remaining two schools, which also recorded strong biomass burning influences. In general, the diurnal cycle of the total OA concentration varied between schools and was found to be at a minimum during school hours. The major organic component that school children were exposed to during school hours was secondary OA at all schools. Peak exposure of school children to vehicle emissions occurred during school drop off and pick up times. Unless a school is located near

major roads, children are exposed predominately to regional secondary OA as opposed to local emissions during schools hours in urban environments.

KEYWORDS: Aerosol Mass Spectrometry, Schools, Organic Aerosols, Diurnal variation, Vehicle emissions

6.1 INTRODUCTION

Vehicle emissions have been associated with a number of negative health effects (See e.g. [1]). Due to their immature immune systems and faster breathing rates, children are particularly susceptible to the detrimental health effects of vehicle emissions. For example, long-term exposure to traffic emissions is thought to contribute to a range of damaging health effects to children's respiratory systems [2, 3]. Children spend a large part of the day in school and schools are a relatively controlled environment where children exposure to vehicle emissions can be monitored. Schools located within urban environments are already affected by vehicle emissions, and in addition to local traffic they have specific traffic sources related to school activities. These activities include drop off and pick up traffic and result in additional local traffic with unique characteristics such as higher proportion of idling vehicles. This would affect the levels of vehicle emissions at schools, differentiating it from other urban areas.

To date only limited literature exists on children's exposure to vehicle emissions at schools (see for example, [4]). Studies that have investigated the impact of vehicle emissions by means of chemical composition have focused on the elemental carbon and organic carbon concentrations [5, 6], and black carbon concentration [7, 8]. These studies have been conducted in schools in the USA and have found that vehicle emissions, principally school bus emissions, have an impact on the air quality

during school hours. In Brisbane, as in many other parts of the world, schools are not serviced by buses as extensively as in the USA, so the USA results may not be very relevant to the current study.

In urban environments, organic aerosols at most urban sites can be resolved into two main components based upon differences in specific key mass to charge ratios (m/z) in the mass spectrum [9]: the hydrocarbon-like organic aerosol (HOA) and oxygenated organic aerosols (OOA). The HOA component is similar to the OA emitted from vehicles with the m/z 57 ion found to be a distinctive tracer ion for HOA. However, the OOA component, characterised by the tracer ion m/z 44 [10] can be regarded as a surrogate for secondary OA. The OOA can be further resolved into two subtypes based upon the differences in the level of volatility and oxidation, these are low-volatility OOA (LV-OOA) and semi volatile OOA (SV-OOA) [11, 12]. Other organic components have also been identified in urban environments and these include biomass burning OA (BBOA). Extracting the chemical compositional information of OA from the AMS has therefore been shown to be an effective method of identifying the sources of ambient OA [11, 12].

To gain accurate information on exposure, long term measurements with a high temporal resolution are required [13]. An Aerodyne aerosol mass spectrometer (AMS) measures quantitatively, with a high temporal resolution, the chemical composition of non-refractory species of airborne particles to enable accurate exposure assessment. The organic aerosol (OA) as measured by an AMS is a complex mixture of both primary combustion sources and secondary reactions in the

atmosphere. Although the AMS is unable to single out individual organic compounds, it offers insights into the broad range of organic species in a quantitative high time resolution manner. To the authors' knowledge, the only study where an AMS has been deployed at a school was in Las Vegas [14]. However this study did not specifically look at children's exposure to vehicle emissions during school hours.

Considering the above gaps in knowledge, the present study aimed to quantify the concentration of OA that children are exposed to during school hours at urban schools by utilising the high time resolution offered by an AMS to characterise the chemical composition of the non-refractory PM_1 (NR-PM_1) fraction. Whether the OA was primary or secondary in nature at each school was determined based upon the level of oxidation. The temporal variation of the OA and its components HOA and OOA was examined, particularly during school hours, to gain an understanding of the concentration of vehicle emissions that children are actually exposed to at school. The influence of local and school specific traffic on the concentration of HOA was also explored.

6.2 METHOD

6.2.1 Study Design

Five schools, referred to as S01, S04, S11, S12 and S25, were selected for this study. These schools are located in different suburbs in the city of Brisbane, Australia. Brisbane is a subtropical city that is rapidly growing in population and in the contribution of anthropogenic sources including vehicle emissions to air pollution. The chemical sampling performed was a part of a larger project at these schools designed to study the effect of ultrafine particles from traffic emissions on children's health www.ilaqh.qut.edu.au/Misc/UPTECH%20Home.htm). Twenty-five schools

participated in this project, however an Aerodyne compact time-of-flight aerosol mass spectrometer (TOF-AMS) was run at only five schools due to various logistical reasons. Other than road traffic, the schools chosen were not near any other large source of air pollution and were also not close to any large infrastructure projects.

6.2.2 Description of the schools

A schematic diagram of each school is given in Figure 6-1A, to show the location of the roads that border the schools. Three of the schools are located in residential suburbs of Brisbane while the other schools, S01 and S11, are in the outer suburbs and have varying source influences. S01 is in the north-eastern part of the city and additional influences include the ocean 1 km to the east, and an arterial road about 300m northwest. S04 is located in the eastern suburbs and is bordered to the west by a main road (see Table 6-1). To the east of S04 lie two further sources consisting of a major highway and the Brisbane Airport, which are 500m and 1 km away, respectively. In the south of the city S11 is in a suburb surrounded by semi-rural area. S12 is in an inner northern suburb that is mainly residential and is bordered to the north by a park. S25 is found in the north-eastern suburbs with the additional sources the nearby airport and the same major highway located close to S04, about 1 km to the east. During the middle of sampling at S25 there was a large bushfire in the bushland, which lies to the west of the school.

6.2.3 Sampling Method

Details of the sampling campaigns at each school are given in Table 6-1. An automatic weather station (Monitor Sensors) was deployed at the schools to measure temperature, relative humidity (RH), solar radiation, wind speed and direction. A condensation particle counter (CPC) (TSI model 3781) was used to monitor airborne

Table 6-1: Daily average traffic and weather characteristics at each school.
The traffic composition presented is for weekdays. The temperatures, relative humidity (RH) are 24 hour averages.

	Sampling	**Traffic counts (veh hr^{-1})**		**Traffic composition (%)**			**Weather**		
	Duration	Weekday	Weekend	Light	Medium	Heavy	Temp. (°C)	RH (%)	Wind speed (km h^{-1})
S01	2 weeks	158	138	95.6	3.8	0.6	23	65	17
S04	3 weeks	806	653	87	7.9	2.2	23	71	13
S11	2 weeks	444	378	95.2	2.4	0.9	16	78	10
S12	2 weeks	176	127	97.3	2.5	0.2	15	75	12
S25	2 weeks	326	190	91.8	6.5	1.3	16	58	14

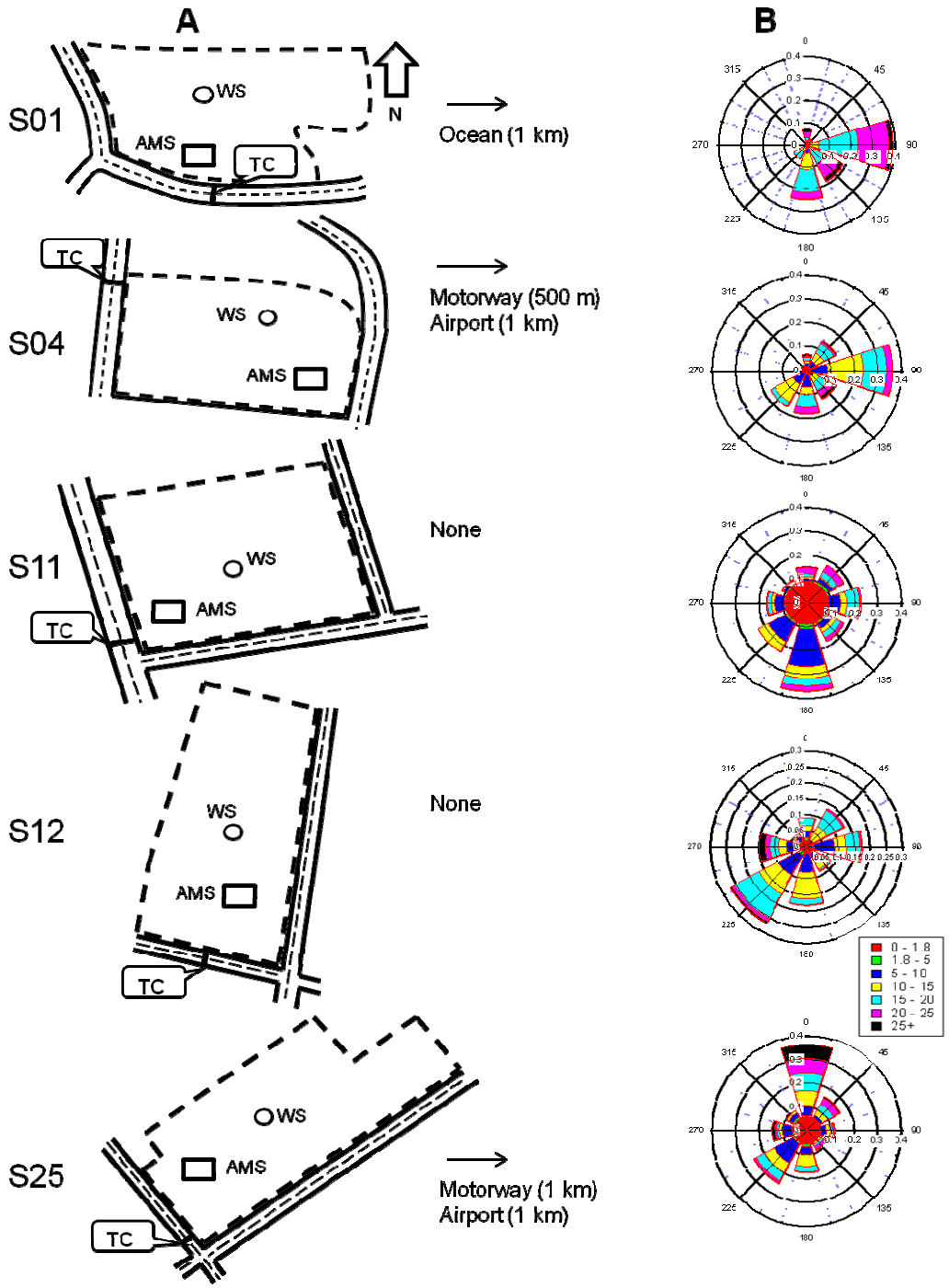

Figure 6-1: Schematic diagrams of schools.

Column A is schematic diagrams of each school (only approximately to scale). AMS represents the location of the classroom with the TOF-AMS, WS the site of weather station and CPC and TC the location of the traffic counter. Direction of additional sources is indicated. Column B is the rose plot for the sampling period. The wind speed (km h^{-1}) legend is the same for all plots

particle number concentration. The weather station and CPC were housed within a trailer, which was located at a site within the school reflecting the best overall exposure of the children. Data from nearby weather stations were also obtained from the Bureau of Meteorology (BOM) as some of the schools may have been affected by local winds due to school buildings. A vacant classroom within each school was used to house the TOF-AMS and ambient outdoor air was sampled through a window using conductive rubber tubing that was approximately 1 m in length. The classroom was approximately 100-150m from the trailer housing the other instrumentation in each school with its relative location given in Figure 6-1. Traffic counts were taken on the busiest road next to the school, indicated in Figure 6-1, referred to as the main road throughout. In the traffic count data, cars, motorbikes and scooters were classified as light vehicles. The medium classification refers to 2, 3 and 4 axel light trucks and the heavy classification to heavy trucks.

6.2.3.1 ***TOF-AMS operation***

A compact TOF-AMS was run at each school. Details of the operation and description of the TOF-AMS has been given elsewhere [15, 16]. In summary, the TOF-AMS is an on-line instrument that quantitatively measures the chemical composition and size distributions of the non-refractory portion of submicron particles (approximately PM_1). The particles are sampled through an aerodynamic lens which focuses the particles into a narrow beam which then enters a particle sizing chamber. After passing through the chamber, volatile and semi-volatile particles are vaporised and ionised before analysis by a time-of-flight mass spectrometer. Typically in the field the TOF-AMS is run in two modes, the PTOF mode which measures particle size and MS mode, which measure the mass spectrum of vaporised particles. For this study the sampling interval was for 5 minutes

alternating equally between PTOF and MS modes. PTOF mode data was not utilised in the current paper due to quality control issues and once this is resolved it may be included in future work.

6.2.4 Quality control

The TOF-AMS was calibrated for ion efficiency (IE) and particle size at the beginning of the sampling with the IE calibrations also done in the middle and at the end of sampling at each school. The calibrations were carried out according to the standard protocols [15, 17, 18] and the detection limits for each chemical species was calculated as 3 times the standard deviation of the signal for ambient air passing through a HEPA filter [19]. This gave an average 5-min detection limits 44, 5, 5, 53 and 8 ng m^{-3} for the organics, nitrates, sulphates, ammonium and chlorides, respectively at all the schools. These values are similar to the corresponding values reported by Drewnick et al. [20], and the average values for each school are given in Table A4-2 (Appendix 4). The use of conductive rubber tubing was not found to introduce artefacts into the measured mass spectra, as the m/z peaks associated with siloxanes [21] were not abnormally elevated.

6.2.5 Data analysis

The TOF-AMS data was processed and analysed using Squirrel v1.51 in IGOR Pro version 6.22. One-way analysis of variance (ANOVA) was used to compare whether the mean concentrations of the different chemical species measured by the TOF-AMS during the weekday and weekend chemical were significantly different. ANOVA was performed using SPSS version 19 (IBM). Quality control checks were preformed on the CPC and weather station data prior to the data being put into a Microsoft Access database.

6.2.5.1 ***Organic Aerosol analysis***

Further analysis of the OA was undertaken by first calculating the f_{43}, f_{44} and f_{60} ratios, which refer to the ratio of the m/z 43, 44 and 60 ions respectively, relative to the total mass of the organic component. Since the OA has been shown to occupy a well-defined triangular region of the f_{43} vs f_{44} plot, known as the triangle plot [12], the f_{43} and f_{44} values were plotted in order to characterise and compare the OA components at each school. LV-OOA has a higher f_{44} and lower f_{43} ratio than SV-OOA therefore LV-OOA occupies the top end of the triangle space in the plot while SV-OOA components are concentrated in the lower part of the triangle. HOA components have an f_{44} that is less than 0.05 and so are found along the base of the triangle. The wide base of the triangle represents the range in the chemical composition of HOA and SV-OOA. This can be used to show the age of the OOA, as the more oxidised and hence more aged OA would be found closer to the top of the triangle [12, 22].

Standard mass spectral profiles of the different OA components, HOA, SV-OOA, LV-OOA and BBOA are given in Ng et al. [10] based upon the analysis of 15 urban datasets. These spectra have been used as reference spectra in this study for identifying the OA components at the schools. The m/z 44 ion is a prominent feature of OOA spectra and is not found in HOA spectra. Thus it can be used to distinguish OOA [10]. Ng et al. [10] showed that the m/z 57 ion is a tracer ion for HOA. Therefore we used this ion to show the influence of HOA to the total OA. The m/z 60 ion is attributed to the fragmentation of levoglucosan, which has been used as a chemical marker for biomass burning [23]. Consequently, the f_{60} was calculated in the current study as a means of determining the influence of BBOA. Cubison et al. [23] established a background level in urban environments for f_{60} to be 0.3% ±0.06%

in ambient OA levels that are mostly secondary in nature, and attributed f_{60} values above the background levels to the influence of BBOA. The O:C ratio was calculated according to Aiken et al. [24] for unit mass resolution data to determine the level of oxidation of the OA.

6.3 RESULTS AND DISCUSSION

6.3.1 General school characteristics

6.3.1.1 ***Meteorological conditions***

The weather conditions at each school are included in Table 6-1. Sampling at S01 and S04 was completed during the summer (November to March) which had an average temperature of 23°C. Sampling for S11, S12 and S25 was during winter (June to August) with an average temperature of 15-16°C. The relatively small difference in temperature between winter and summer is typical for Brisbane due to its subtropical climate. Figure 6-1b displays the wind rose plots for the entire sampling period at each school. As seen in the higher proportion of calm wind, the most stable weather was encountered during sampling at S11.

6.3.1.2 ***Traffic characteristics***

The 24 hour average traffic characteristics at each school are given in Table 6-1. (Note that the percentage traffic composition does not always add to 100% due to unclassified vehicles such as cars with trailers.) S01, S11 and S12 are all situated on suburban streets and this is reflected in the traffic characteristics at the schools. S01 and S12 had the lowest traffic counts consisting of mostly light duty vehicles (LDV). S11 had higher traffic counts than S01 and S12, though with similar traffic composition. S25 was also situated on a suburban road but recorded higher percentage of medium and heavy vehicles passing the school. S04 is situated on a

major road and so had the highest counts and most varied traffic composition, with more heavy duty vehicles (HDV) passing the school.

6.3.2 Average concentration of the chemical species

There was considerable variation in the chemical properties of the sampled particles between the five schools. The average concentration of the chemical species at each school is given in Figure 6-2, with the summary statistics given in Appendix 4 (Table A4-1). In each of the schools the largest fraction is the organic species, followed by ammonium, sulphate, nitrate and chloride. When compared to the other schools, S12 and S25 were found to have higher concentrations of each chemical species, especially the organic fraction. These high mass concentrations may be due to prescribed burning of bushland, which is common in Brisbane during August. For this reason the influence of biomass burning is investigated further in later sections. S01, S04 and S11 have broadly similar profiles with the relative contribution of ammonium and sulphate being the main point of difference between the schools. The percentage of the total mass for ammonium was 26%, 30% and 25%, while for sulphate it was 25%, 19% and 10% for S01, S04, and S11, respectively. The variation in the relative concentrations of sulphate could indicate differences in the age of the NR-PM_1 at the schools, with the age of the OA further investigated in Section 6.3.3.

A comparison of the average mass of the chemical species between weekdays and weekends (see Figure A4-1 in Appendix 4) found that S01, S11 and S25 had higher concentrations on weekdays, particularly organics, which would suggest a traffic related source of these chemical species. At S04 and S12, however, the weekends were found to have the higher concentrations. Nonetheless, the difference between

the weekday and weekend concentrations of all species was not found to be statistically significant ($p>0.05$) at any of the five schools. Therefore this indicates that the emissions were not significantly different between weekday and weekend at the schools, with the influence of traffic discussed further in Section 6.3.4.3. However the limited number of weekends sampled at each school may have influenced the outcomes of the comparison.

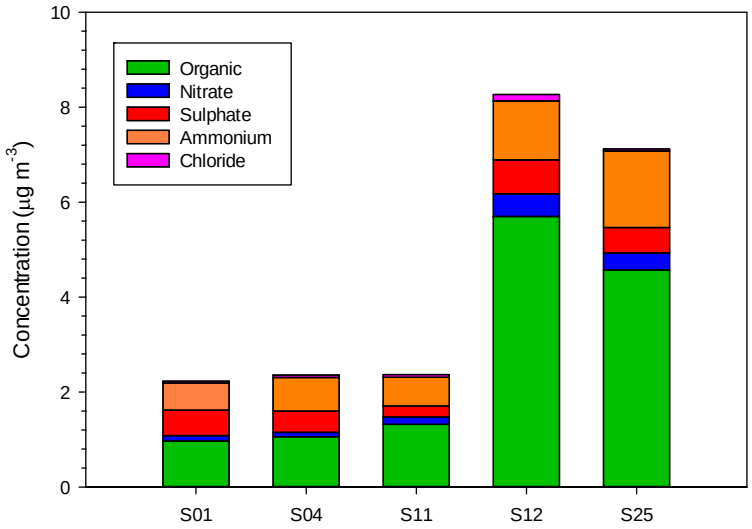

Figure 6-2: Average concentrations of the chemical species at each school.

6.3.3 Characterisation of the Organic Aerosols

The largest particulate matter fraction at each school was the organic component and, as the majority of vehicle emissions are carbonaceous in nature [25], this fraction was analysed in detail to determine whether local primary emissions are a significant source of organic aerosol (OA) at each school. For each school, the average f_{43} and f_{44} for each sampling day were graphed on the triangle plot (Figure 6-3). This enabled the OA component at each school to be classified based upon its level of oxidation.

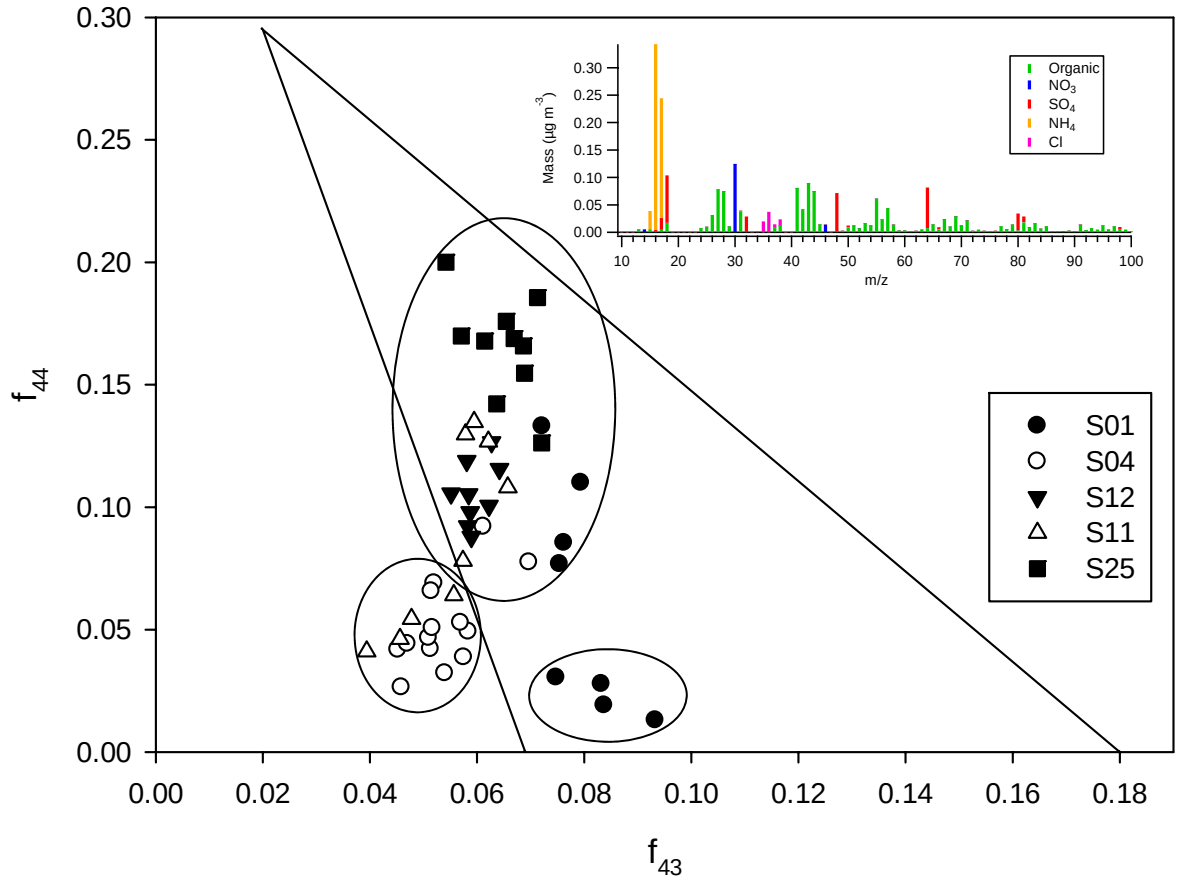

Figure 6-3: Plot of the f_{44} vs f_{43} for each sampling day.
The triangle from Ng et al. [12] is included as a visual aid. The inset mass spectrum is an example of the samples that fall outside the triangle space from S04 and S11.

6.3.3.1 ***Hydrocarbon-like Organic Aerosols***

A group of four days from S01 which has f_{44} <0.05 appeared at the base of the triangle plot, (Figure 6-3), and so readings on these days are likely to be dominated by HOA. This is confirmed by comparison of the average mass spectra for these days with the HOA references spectra [10]. These represent sampling days that has large sharp peaks of OA at around 7am and our hypothesis is that the use of fuel-powered gardening equipment at the school during the measurements skewed the results. However, when these large peaks are removed the spectra still resemble HOA, but at lower concentrations. Therefore the peaks were deemed to be outliers and were

removed for subsequent analysis. The O:C ratio for the S01 HOA samples was 0.17±0.03. This value is slightly higher than that reported for urban combustion Primary OA (POA) [24] but in the range of 0.1 to 0.19 observed for diesel exhaust [26].

6.3.3.2 ***Semi-Volatile Oxygenated Organic Aerosols***

There is a group of samples from S04 and S11 that fall outside of the triangular region in Figure 6-3, and are centred on f_{44} of 0.05. They are characterised by the alkyl fragment series, as per the HOA reference spectra, and also the m/z 43 and 44 ions with approximately equal concentrations (example given in Figure 6-3). These mass spectra most closely resemble the SV-OOA reference spectra in Ng et al. [10]. Therefore this suggests that the OA has undergone some degree of oxidation. At S04 and S11 these samples had an average O:C ratio of 0.27 ± 0.06 and 0.28 ± 0.04, respectively which are in the range of 0.35 ± 0.14 reported by Ng et al. [12] for SV-OOA. The prominence of the alkyl fragment series and the low f_{44} that is around the characteristic level for HOA, suggests a primary precursor which could be considered as slightly aged POA. POA from diesel emissions that have been oxidised for 5 hours was observed to have an O:C ratio that ranged from 0.21to 0.37 [26]. The results for SV-OOA from S04 and S11 fall within this range, further suggesting that aged POA was the source of the SV-OOA at these schools.

Table 6-2: Average values for selected tracer ratios for the sampling days classified by OA type for each school. Note only one value for the LV-OOA data at S04. Uncertainties are 1 standard deviation.

	S01 SV-OOA	**S01 LV-OOA**	**S01 HOA**	**S04 LV-OOA**	**S04 SV-OOA**	**S11 LV-OOA**	**S11 SV-OOA**	**S12 LV-OOA**	**S25 LV-OOA**
O:C	0.39	0.54	0.17	0.43	0.27	0.52	0.28	0.48	0.71
	±0.02	±0.06	±0.03		±0.06	±0.04	±0.04	±0.05	±0.08
f_{43}	0.076	0.076	0.084	0.061	0.053	0.061	0.047	0.06	0.064
	±0.001	±0.005	±0.008		±0.006	±0.003	±0.007	±0.003	±0.006
f_{44}	0.081	0.121	0.023	0.092	0.049	0.12	0.051	0.11	0.17
	±0.006	±0.016	±0.008		±0.014	±0.01	±0.011	±0.012	±0.021
f_{60}	0.0027	0.0028	0.0013	0.0024	0.0023	0.0056	0.0046	0.0094	0.011
	±0.0008	±0.0007	±0.0007		±0.0004	±0.001	±0.002	±0.003	±0.003

Photochemical oxidation of diesel exhaust in an environmental chamber has been shown to resemble that of ambient OOA after a matter of hours [27, 28]. Thus Chirico et al. [26] observed that the total OA from diesel emissions was approximately 80% SOA after 5 hours of ageing. The mass spectra for aged diesel exhaust from Sage et al. [28] are similar to the mass spectra obtained for these samples at S04 and S11. As aging can occur over the course of hours, this would suggest that this POA has been in the atmosphere for a short time period. The dominant wind direction during sampling at S04 was from a major highway (Figure 6-1) and was the likely source of this OA at this school.

6.3.3.3 ***Low-Volatility Oxygenated Organic Aerosols***

The main group is made of sampling days from all schools and is within the SV-OOA and LV-OOA region of the triangle space. Three samples from S01 and S04 at the lower end of the group have mass spectra that resembled SV-OOA reference spectra while the rest resembled the LV-OOA reference spectra [10]. LV-OOA days from S01, S04, S11 and S12 occupy the overlap region between SV-OOA and LV-OOA [12], with mass spectra similar to LV-OOA. S25 samples are clustered at the top of the group and are in the LV-OOA region, indicating that they are the most aged. Although SOA was present at all of the schools, the ages and oxidation levels of OOA differ from school to school. The difference in the SV-OOA and the LV-OOA can be seen in the O:C ratio, where the LV-OOA averaged 0.52 ± 0.05 across S01, S11 and S12. This figure is lower than the range of 0.73±0.14 reported by Ng et al. [12] for LV-OOA which would suggest that it was not fully oxidised OOA. Conversely at S25 the average O:C was 0.71 ± 0.08, which is within the range for LV-OOA from Ng et al. [12] thus more oxidised and aged OA than the OOA observed at S01, S11 and S12, as seen in Figure 6-3. As LV-OOA was found to be

the main type of OOA at the schools, the results would suggest that regional OA was the main source.

6.3.3.4 ***Biomass Burning Organic Aerosols***

The sampling days associated with LV-OOA in S11, S12 and S25 showed the m/z 60 ion, and so biomass burning was a component of the OA at these two schools [23]. Table 6-2 presented the f_{60} values calculated for each school and all sampling days for S01 and S04 are below the urban background level of f_{60} established by Cubison et al. [23]. This indicates that BBOA was not present. As a result, the POA at these schools can be attributed to vehicle emissions. On the other hand, the f_{60} for S11, S12 and S25 is above the urban background levels; hence BBOA was a component of the OA at these schools. Sampling at S11, S12 and S25 was carried out in the winter when prescribed burning in bushland around Brisbane is common, suggesting aged BBOA as a source of LV-OOA at these schools.

6.3.4 Diurnal cycle of Organic Aerosol

The temporal variation of the OA was investigated at each school to determine children's exposure to vehicle emissions during school hours. The diurnal cycle of the organic aerosol is presented as a box plot for each school (Figure 6-4A). In order to give additional insight into the source of the OA over the course of the day, the mean concentrations of the m/z 44, 57 and 60 ions and PNC as a function of time of day are presented as well (Figure 6-4B). The m/z 57 ion is a tracer for HOA and a bimodal cycle in the HOA would indicate that the vehicle emissions are the primary source of HOA. The diurnal cycle of the PNC is indicative of the local sources and where the diurnal variation pattern of PNC is visually similar to that for m/z 57 ion, traffic is the probable source. The m/z 44 ion is a tracer for OOA and peaks in the

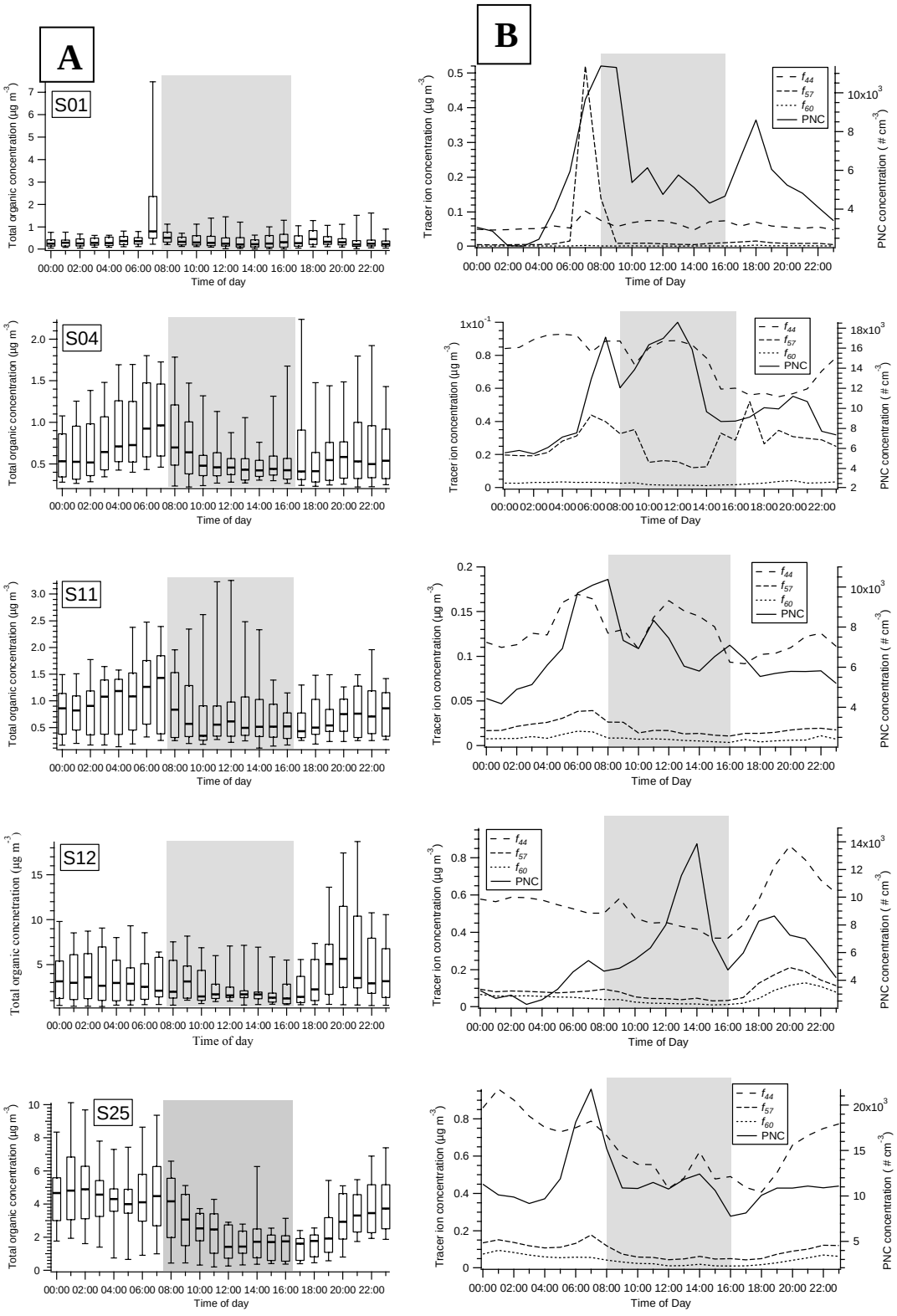

Figure 6-4: The diurnal variation in the organic fraction at each school.Shaded areas highlighting school hours, (9am to 3pm) plus the hour before and after to capture school-related traffic. Column A is a box plot of the diurnal variation of the total organic concentration. Column B is the diurnal variation in the corresponding school in the mean concentration of the m/z 44, 57 and 60 ions and particle number (PNC).

middle of the day indicate that there was photochemical activity resulting in SOA formation [29], with the m/z 60 ion acting as a tracer for biomass burning.

6.3.4.1 ***OA diurnal cycles at individual schools***

6.3.4.1.1 S01 diurnal cycle

The diurnal cycle of the total OA and the tracer ions varied between each school. Therefore, each school will be discussed individually followed by a discussion on trends observed at all the schools. In general, except for the large peak at 7-8am, the lowest average concentration of total OA was seen at S01 (Figure 6-4A). The m/z 57 ion concentration also had a large peak at this time (Figure 6-4B), indicating that this spike in OA was hydrocarbon based. During this time at S01, and at many other schools in the project, school staff was observed to have used fuel-powered gardening equipment. This strongly suggests that the fuel-powered gardening equipment being used in the school grounds was the main contributor to this peak. There was little other variation observed in total OA concentration apart from a slight peak at around 5-6pm, which was also seen in the concentration of the m/z 57 ion, suggesting traffic as the source of HOA at S01. The low concentrations of OA at S01 were likely due to the sea breezes, which would not carry much regional OOA. At S01, the PNC follows the same pattern as the m/z 57 ion (Figure 6-4B); however the afternoon peak was centred on 6pm and so suggests that it is due to peak hour traffic rather than school traffic with the influence of school traffic further discussed in Section 6.3.4.3.

6.3.4.1.2 S04 diurnal cycle

There was a large early morning peak from 5-8am and a smaller peak at around 5pm in the total OA concentration at S04 (Figure 6-4A). A similar diurnal trend was

observed in Figure 6-4B in the m/z 57 ion concentration indicating that traffic emissions were the main contributor to the organic aerosol. The PNC and m/z 57 ion peaked together in the morning pointing to a local traffic source for the large morning peak. From Section 6.3.3.2 the OA at this school was found to resemble aged diesel emissions for most of the sampling period, which indicates that the source was not traffic on the roads directly surrounding the school but on roads further afield. The prevailing wind direction during sampling was easterly from a major highway (Figure 6-1) than the main road surrounding the school. In addition, the traffic pattern at S04 was relatively constant during the day, whereas the traffic pattern on the nearby highway would be expected to be more bimodal, as observed in the f_{57} cycle. Therefore, it was likely that traffic on the nearby highway rather than the surrounding main road was the source.

6.3.4.1.3 S11 diurnal cycle

In Figure 6-4A the total OA concentration at S11 had an early morning peak (6am-8am) followed by small peaks in the middle of the day and the evening, suggesting different sources of OA. The morning peak was also observed in the m/z 57 and 60 ion concentration (Figure 6-4B) indicating a contribution from biomass burning in the morning. However, the m/z 44 ion peaked at midday, suggesting photochemical SOA formation occurred which resulted in the increase in the total OA. Unlike the m/z 57 ion, the m/z 44 and 60 ions were observed to peak in the evening and were also observed at S12 and discussed below. In Figure 6-4B the concentration of the m/z 57 ion peaked in the early morning and decreased to a minimum throughout the day at 2pm, which indicates local sources of HOA [9]. At S11, the PNC and m/z 57 ion concentration peaked together in the morning further implying a local traffic

source of HOA. The absence of a peak in f_{57} during the afternoon may be attributed to increased dilution due to a rise in the boundary layer at this time. Over the measurement period, the mean air temperature during the late afternoon was about 6°C greater than during the morning rush hour period at this school. A similar diurnal variation has previously been observed for HOA and the afternoon decrease in HOA concentration attributed to a rise in the boundary layer by Zhang et al. [9] and Sun et al. [29].

6.3.4.1.4 S12 and S25 diurnal cycle

There were similarities in the OA diurnal cycle at S12 and S25, with the general trend being a minimum concentration in the total OA at midday followed by the peaking of the total OA concentration in the evening, at 8pm and midnight in S12 and S25 respectively (Figure 6-4A). At both schools, the m/z 44 ion concentrations was higher than the concentration of the m/z 57 ion throughout the day (Figure 6-4B) indicating that OOA was the dominant source of OA, particularly during school hours. In Figure 6-4B the trends in diurnal cycle for the m/z 44, 57 and 60 ions followed the diurnal cycle of the total OA concentration (Figure 6-4A) at both schools, suggesting a similar source. There were some differences in the OA component diurnal cycles between the schools, with a peak in m/z 57 ion observed at 9am and 7am, for S12 and S25 respectively. The m/z 57 ion peak at S25 corresponded with a large peak in PNC indicating that local emission, most likely school drop off traffic, was the source of HOA at this school and is investigated further in Section 6.3.4.3.

The m/z 60 ion concentration was higher at S12 and S25, and biomass burning was a component of the OA at these schools. A similar total organic diurnal cycle was

observed by Brown et al. [14], with the evening peak attributed to local biomass burning from residential heating. In Brisbane due to the relatively mild winters, the impact of residential heating is thought to be minimal. Therefore, controlled back burning that is practised during winter in Brisbane [30] is thought to be the main contributor. At S25, the main wind direction was northerly and the large bushfire during sampling did not directly affect the school (Figure 6-1). The build up of BBOA during the night could be due to the inversion layer. At S12, there was not as much controlled burning occurring during the sampling period, and residential wood burning could be contributing to BBOA levels. When the concentration of wood burning particulate matter is higher on the weekend, it can indicate that the wood burning is more discretionary or decorative than for heating [31]. The weekend to weekday ratio of the levels of the m/z 60 ion at S12 was 2.5, which points to discretionary or decorative residential wood burning as source, in addition to that which was present from back burning. The OA was less aged at S12 compared to S25 (Figure 6-3), suggesting a more local source of BBOA.

*6.3.4.2 **Diurnal trends for all schools***

The PNC peaked in the middle of the day at S04, S11, S12 and S25 which shows that the production of secondary aerosols due to nucleation was prominent [32]. At S11 and S25, the middle of the day PNC peak was closely followed by a peak in the OOA tracer ion, m/z 44, as would be expected for SOA formation [33]. The AMS typical lower size cut off is for particles with a diameter of 40-50 nm and so would take some time to detect the particles as they grow. This pattern was seen at S11 during the morning, where the peak in the m/z 44 ion followed the PNC peak closely. However at S04 and S12 the midday PNC peaks were not followed by peaks in the

m/z 44 ion concentration. This may be because the particle size was too small for the AMS to detect. The nucleation events at these schools will be investigated further in future papers.

At all schools, the minimum concentrations of total OA, and in particular HOA tracer ion m/z 57, were found during school hours (9.00 am till 3.00 pm). The OOA was the main OA component that children at school were exposed to as the m/z 44 ion had the highest concentration during school hours. The low m/z 57 ion concentrations show that children's exposure to HOA at the schools was limited because the peaks in concentrations were generally outside of school hours. Only at S04 were school children exposed to vehicle emissions for the whole school day, albeit at the lowest concentration during the day. Contributing factors to the increased exposure to HOA at S04 are higher traffic counts (Table 6-1) and close proximity to a major highway.

*6.3.4.3 **Influence of school traffic on HOA concentrations***

The peaks of the HOA tracer ion concentration at each school overlapped with the school drop off times, around 8 – 9 am. This represents the time of maximum exposure to OA from vehicle emissions for children at school. A similar trend in the variation of particle number concentration was previously observed in urban schools during school drop off and pick up times and was associated with car and bus counts [5]. Therefore, the traffic associated with school drop off is contributing to the concentration of HOA and children's exposure in addition to the morning peak traffic. At S04 and S25 a peak in the HOA tracer ion concentration was observed at pick up time (2 to 4 pm), further suggesting an influence from school traffic to children's exposure of HOA.

Thus the weekday and weekend m/z 57 ion cycles were investigated to determine the influence of school drop off and pick up traffic. As mentioned in Section 6.3.2, only 1 or 2 weekends were sampled at the schools and so these comparisons are done with caution. The comparisons for S04 and S25 are shown in Figure 6-5, with the plots for the other three schools given in the Supporting Information (Figures A4-2 to 4).

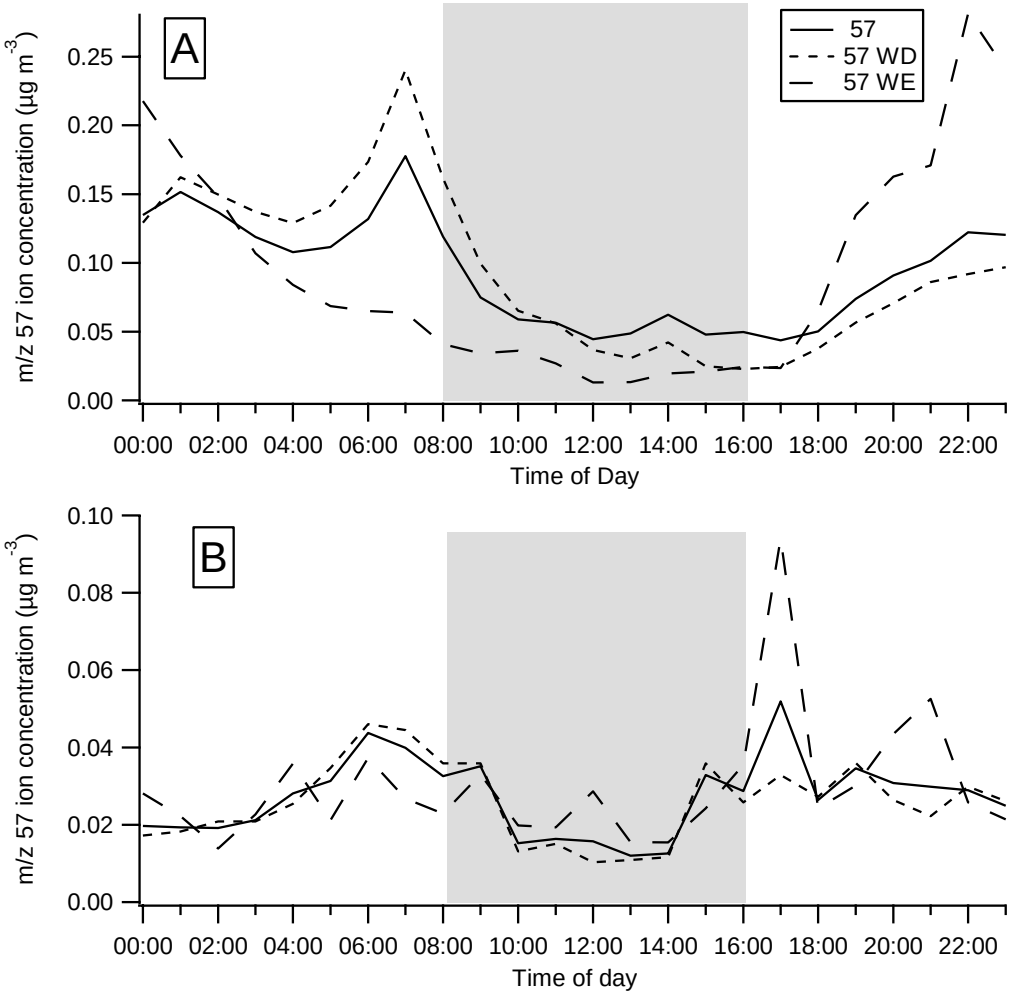

Figure 6-5: Comparison in the diurnal variation in the concentration of the m/z 57 ion for all sampling days (57), weekdays (57 WD) and weekends (57 WE) at S04 (B) and S25 (A).

At S04 the weekend and weekday m/z 57 cycles were similar, an additional confirmation that the morning and afternoon peaks in HOA concentration were not related to school traffic rather from nearby highways as indicated in Section

6.3.4.1.2. The large peak at 7-8am at S01 was not present during the weekends and so must be related to activities within the school, as mentioned in section 3.4.1. At S11, S12 and S25 the presence of HOA during weekdays is likely caused by drop off traffic as there was a peak of m/z 57 ion concentration at the school drop off times that was not seen on the weekends. At S12, there was a large background of OA which may be masking school traffic influence. S11, S12 and S25 had 4, 2 and 3 times, respectively the drop off traffic of both S01 and S04 and this may be the reason why it was more pronounced at these schools.

6.4 CONCLUSIONS

Children's exposure to vehicle emissions was characterised using a TOF-AMS in five urban schools in Brisbane, Australia. At each of the schools the organic fraction was the largest component of the NR-PM_1. The oxidation level of the OA varied from school to school and also within the sampling period at the schools, with secondary OA being the major component. Secondary OA was observed at the schools which ranged in oxidation level from the less aged SV-OOA to the more aged OA that resembled LV-OOA. At two of the schools, S04 and S11, there was OA from nearby highways that was similar to slightly aged vehicle emissions. The more aged OA was observed at three schools, S11, S12 and S25 and at these schools BBOA contributed to the high load of OA. Only one school, S01, had sampling days that were dominated by primary emissions of OA, which may be due to the influence of fuel powered equipment being operated near the TOF-AMS in the school.

The minimum concentration of OA was observed during school hours and based upon the tracer m/z 44 ion, the major organic component that school children were exposed to was OOA. The tracer m/z 57 ion for HOA showed a distinct diurnal

pattern at the schools, with a large peak in the morning that decreased to minimum concentration in the afternoon. School drop off and pick up times represented the times of maximum exposure of school children to HOA at the schools in this study. The variation in the levels of vehicle emissions during the school day highlights the times when future control strategies may be focused in order to limit children's exposure. The results from this study indicates that in general for urban environments, unless schools are located near (<500m) major highways, during school hours the children are exposed predominantly to regional secondary OA as opposed to local emissions. The results from this study will be integrated with other air quality parameters measured at the schools in future publications to gain a holistic picture of factors driving children's exposure at school and the potential health effects. Overall, the results from this study indicate that secondary processes are driving children's exposure at urban school and future work could be focused on better characterisation of SOA which would enable improved understanding of the potential health effects.

ACKNOWLEDGMENTS

This work was supported by the Australian Research Council, Department of Transport and Main Roads (DTMR) and Department of Education and Training (DET) through Linkage Grant LP0990134. Our particular thanks go to Randall Fletcher (DTMR) and Andy Monk (DET) for their vision regarding the importance of this work. We would like to thank Dr Branka Miljevic for training on the use of the TOF-AMS and data analysis. We would also like to thank all members of the UPTECH project, including Dr Guy Marks, Dr Paul Robinson, Prof Kerrie

Mengersen, A/Prof Zoran Ristovski, Dr Mandana Mazaheri, Dr Congrong He, Dr Sama Low Choy, Dr Jaime Mejia, Dr Wafaa Ezz, Prof Gail Williams, Dr Diane Keogh, Mr Rusdin Laiman, Mr Farhad Salimi, Mr Megat Mokhtar, Ms Nitika Mishra, Dr Adriana Cortes, Dr Brett Toelle, Dr Andres Quinones and Dr Pam Kidd for their contribution to this work. We also thank Mr Matthew Falk for his assistance in the classification of the epidemiological studies and his contribution to the discussion of epidemiological study design, as well as Dr Folasade Fatokun (formerly from ILAQH, QUT and currently from the Department of Employment, Economic Development and Innovation) for the initial collection of the literature and Ms Rachael Appleby for her administrative assistance.

6.5 REFERENCES

1. Nel, A., Air Pollution-Related Illness: Effects of Particles. *Science* **2005,** *308*, (5723), 804-806.
2. Ryan, P. H.; Le Masters, G.; Biagini, J.; Bernstein, D.; Grinshpun, S. A.; Shukla, R.; Wilson, K.; Villareal, M.; Burkle, J.; Lockey, J., Is it traffic type, volume, or distance? Wheezing in infants living near truck and bus traffic. *J. Allergy Clin. Immun.* **2005,** *116*, (2), 279-284.
3. Gehring, U.; Wijga, A.; Brauer, M.; Fischer, P.; de Jongste, J.; Kerkhof, M.; Oldenwening, M.; Smit, H.; Brunekreef, B., Traffic-related Air Pollution and the Development of Asthma and Allergies during the First 8 Years of Life. *Am. J. Resp. Crit. Care* **2010,** *181*, (6), 596-603.
4. Mejía, J. F.; Choy, S. L.; Mengersen, K.; Morawska, L., Methodology for assessing exposure and impacts of air pollutants in school children: Data collection, analysis and health effects – A literature review. *Atmos. Environ.* **2011,** *45*, (4), 813-823.
5. Hochstetler, H. A.; Yermakov, M.; Reponen, T.; Ryan, P. H.; Grinshpun, S. A., Aerosol particles generated by diesel-powered school buses at urban schools as a source of children's exposure. *Atmos. Environ.* **2011,** *45*, 1444-1453.
6. Li, C.; Nguyen, Q.; Ryan, P. H.; LeMasters, G. K.; Spitz, H.; Lobaugh, M.; Glover, S.; Grinshpun, S. A., School bus pollution and changes in the air quality at schools: a case study. *J. Environ. Monitor.* **2009,** *11*, (5), 1037-1042.
7. Richmond-Bryant, J.; Bukiewicz, L.; Kalin, R.; Galarraga, C.; Mirer, F., A multi-site analysis of the association between black carbon concentrations and vehicular idling, traffic, background pollution, and meteorology during school dismissals. *Sci. Total Environ.* **2011,** *409*, (11), 2085-2093.
8. Patel, M. M.; Chillrud, S. N.; Correa, J. C.; Feinberg, M.; Hazi, Y.; Deepti, K. C.; Prakash, S.; Ross, J. M.; Levy, D.; Kinney, P. L., Spatial and temporal variations

in traffic-related particulate matter at New York City high schools. *Atmos. Environ.* **2009,** *43*, (32), 4975-4981.
9. Zhang, Q.; Worsnop, D. R.; Canagaratna, M. R.; Jimenez, J. L., Hydrocarbon-like and oxygenated organic aerosols in Pittsburgh: insights into sources and processes of organic aerosols. *Atmos. Chem. Phys.* **2005,** *5*, (12), 3289-3311.
10. Ng, N. L.; Canagaratna, M. R.; Jimenez, J. L.; Zhang, Q.; Ulbrich, I. M.; Worsnop, D. R., Real-Time Methods for Estimating Organic Component Mass Concentrations from Aerosol Mass Spectrometer Data. *Environ. Sci.Technol.* **2011,** *45*, (3), 910-916.
11. Jimenez, J. L.; Canagaratna, M. R.; Donahue, N. M.; Prevot, A. S. H.; Zhang, Q.; Kroll, J. H.; DeCarlo, P. F.; Allan, J. D.; Coe, H.; Ng, N. L.; Aiken, A. C.; Docherty, K. S.; Ulbrich, I. M.; Grieshop, A. P.; Robinson, A. L.; Duplissy, J.; Smith, J. D.; Wilson, K. R.; Lanz, V. A.; Hueglin, C.; Sun, Y. L.; Tian, J.; Laaksonen, A.; Raatikainen, T.; Rautiainen, J.; Vaattovaara, P.; ehn, M.; Kulmala, M.; Tomlinson, J.; Collins, D. R.; Cubison, M. J.; Dunlea, E. J.; Huffman, A.; Onasch, T. B.; Alfarra, M. R.; Williams, P. I.; Bower, K. N.; Kondo, Y.; Schneider, J.; Drewnick, F.; Borrmann, S.; Weimer, S.; Demerjian, K. L.; Salcedo, D.; Cottrell, L.; Griffin, R.; Takami, A.; Miyoshi, T.; Hatakeyama, S.; Jayne, J. T.; Herndon, S. C.; Trimborn, A.; Williams, L. R.; Wood, E. C.; Middlebrook, A.; Kolb, C. E.; Baltensperger, U.; Worsnop, D. R., Evolution of Organic Aerosols in the Atmosphere *Science* **2009,** *326*, 1525-1529.
12. Ng, N. L.; Canagaratna, M. R.; Zhang, Q.; Jimenez, J. L.; Tian, J.; Ulbrich, I. M.; Kroll, J. H.; Docherty, K. S.; Chhabra, P. S.; Bahreini, R.; Murphy, S. M.; Seinfeld, J. H.; Hildebrandt, L.; Donahue, N. M.; DeCarlo, P. F.; Lanz, V. A.; Prévôt, A. S. H.; Dinar, E.; Rudich, Y.; Worsnop, D. R., Organic aerosol components observed in Northern Hemispheric datasets from Aerosol Mass Spectrometry. *Atmos. Chem. Phys.* **2010,** *10*, (10), 4625-4641.
13. Sun, Y. L.; Zhang, Q.; Schwab, J. J.; Chen, W. N.; Bae, M. S.; Hung, H. M.; Lin, Y. C.; Ng, N. L.; Jayne, J.; Massoli, P.; Williams, L. R.; Demerjian, K. L., Characterization of near-highway submicron aerosols in New York City with a high-resolution aerosol mass spectrometer. *Atmos. Chem. Phys.* **2012,** *12*, (4), 2215-2227.
14. Brown, S. G.; Lee, T.; Norris, G. A.; Roberts, P. T.; Collett Jr., J. L.; Paatero, P.; Worsnop, D. R., Receptor modeling of near-roadway aerosol mass spectrometer data in Las Vegas, Nevada, with EPA PMF. *Atmos. Chem. Phys.* **2012,** *12*, (1), 309-325.
15. Drewnick, F.; Hings, S. S.; DeCarlo, P. F.; Jayne, J. T.; Gonin, M.; Fuhrer, K.; Weimer, S.; Jimenez, J. L.; Demerjian, K. L.; Borrmann, S.; Worsnop, D. R., A New Time-of-Flight Aerosol Mass Spectrometer (TOF-AMS)—Instrument Description and First Field Deployment. *Aerosol Sci. Technol.* **2005,** *39*, (7), 637–658.
16. Canagaratna, M. R.; Jayne, J. T.; Jimenez, J. L.; Allan, J. D.; Alfarra, M. R.; Zhang, Q.; Onasch, T. B.; Drewnick, F.; Coe, H.; Middlebrook, A.; Delia, A.; Williams, L. R.; Trimborn, A. M.; Northway, M. J.; DeCarlo, P. F.; Kolb, C. E.; Davidovits, P.; Worsnop, D. R., Chemical and microphysical characterization of ambient aerosols with the Aerodyne aerosol mass spectrometer. *Mass Spectrom. Rev.* **2007,** *26*, 185-222.

17. Jayne, J. T.; Leard, D. C.; Zhang, X.; Davidovits, P.; Smith, K. A.; Kolb, C. E.; Worsnop, D. R., Development of an Aerosol Mass Spectrometer for Size and Composition Analysis of Submicron Particles. *Aerosol Sci. Technol.* **2000,** *33*, (1), 49-70.
18. Jimenez, J. L.; Jayne, J. T.; Shi, Q.; Kolb, C. E.; Worsnop, D. R.; Yourshaw, I.; Seinfeld, J. H.; Flagan, R. C.; Zhang, X.; Smith, K. A.; Morris, J. W.; Davidovits, P., Ambient aerosol sampling using the Aerodyne Aerosol Mass Spectrometer. *J. of Geophys. Res.* **2003,** *108*, (D7), 8425-8438.
19. Zhang, Q.; Canagaratna, M. R.; Jayne, J. T.; Worsnop, D. R.; Jimenez, J. L., Time- and size-resolved chemical composition of submicron particles in Pittsburgh: Implications for aerosol sources and processes. *J. Geophys. Res.* **2005,** *110*, D07S09.
20. Drewnick, F.; Hings, S. S.; Alfarra, M. R.; Prevot, A. S. H.; Borrmann, S., Aerosol quantification with the Aerodyne Aerosol Mass Spectrometer: detection limits and ionizer background effects. *Atmospheric Measurement Techniques* **2009,** *2*, (1), 33-46.
21. Timko, M. T.; Yu, Z.; Kroll, J.; Jayne, J. T.; Worsnop, D. R.; Miake-Lye, R. C.; Onasch, T. B.; Liscinsky, D.; Kirchstetter, T. W.; Destaillats, H.; Holder, A. L.; Smith, J. D.; Wilson, K. R., Sampling Artifacts from Conductive Silicone Tubing. *Aerosol Sci. Technol.* **2009,** *43*, (9), 855-865.
22. Ng, N. L.; Canagaratna, M. R.; Jimenez, J. L.; Chhabra, P. S.; Seinfeld, J. H.; Worsnop, D. R., Changes in organic aerosol composition with aging inferred from aerosol mass spectra. *Atmos. Chem. Phys.* **2011,** *11*, (13), 6465-6474.
23. Cubison, M. J.; Ortega, A. M.; Hayes, P. L.; Farmer, D. K.; Day, D.; Lechner, M. J.; Brune, W. H.; Apel, E.; Diskin, G. S.; Fisher, J. A.; Fuelberg, H. E.; Hecobian, A.; Knapp, D. J.; Mikoviny, T.; Riemer, D.; Sachse, G. W.; Sessions, W.; Weber, R. J.; Weinheimer, A. J.; Wisthaler, A.; Jimenez, J. L., Effects of aging on organic aerosol from open biomass burning smoke in aircraft and laboratory studies. *Atmos. Chem. Phys.* **2011,** *11*, (23), 12049-12064.
24. Aiken, A. C.; DeCarlo, P. F.; Kroll, J. H.; Worsnop, D. R.; Huffman, J. A.; Docherty, K. S.; Ulbrich, I. M.; Mohr, C.; Kimmel, J. R.; Sueper, D.; Sun, Y.; Zhang, Q.; Trimborn, A.; Northway, M.; Ziemann, P. J.; Canagaratna, M. R.; Onasch, T. B.; Alfarra, M. R.; Prevot, A. S. H.; Dommen, J.; Duplissy, J.; Metzger, A.; Baltensperger, U.; Jimenez, J. L., O/C and OM/OC Ratios of Primary, Secondary, and Ambient Organic Aerosols with High-Resolution Time-of-Flight Aerosol Mass Spectrometry. *Environ. Sci. Technol.* **2008,** *42*, (12), 4478-4485.
25. Kleeman, M. J.; Schauer, J. J.; Cass, G. R., Size and Composition Distribution of Fine Particulate Matter Emitted from Motor Vehicles. *Environ. Sci. Technol.* **2000,** *34*, (7), 1132-1142.
26. Chirico, R.; DeCarlo, P. F.; Heringa, M. F.; Tritscher, T.; Richter, R.; Prévôt, A. S. H.; Dommen, J.; Weingartner, E.; Wehrle, G.; Gysel, M.; Laborde, M.; Baltensperger, U., Impact of aftertreatment devices on primary emissions and secondary organic aerosol formation potential from in-use diesel vehicles: results from smog chamber experiments. *Atmos. Chem. Phys.* **2010,** *10*, (23), 11545-11563.
27. Robinson, A. L.; Donahue, N. M.; Shrivastava, M. K.; Weitkamp, E. A.; Sage, A. M.; Grieshop, A. P.; Lane, T. E.; Pierce, J. R.; Pandis, S. N., Rethinking organic aerosols: Semivolatile emissions and photochemical aging. *Science* **2007,** *315*, 1259-1262.
28. Sage, A. M.; Weitkamp, E. A.; Robinson, A. L.; Donahue, N. M., Evolving mass spectra of the oxidized component of organic aerosol: results from aerosol mass

spectrometer analyses of aged diesel emissions. *Atmos. Chem. Phys.* **2008,** *8*, (5), 1139-1152.
29. Sun, Y. L.; Zhang, Q.; Schwab, J. J.; Demerjian, K. L.; Chen, W. N.; Bae, M. S.; Hung, H. M.; Hogrefe, O.; Frank, B.; Rattigan, O. V.; Lin, Y. C., Characterization of the sources and processes of organic and inorganic aerosols in New York city with a high-resolution time-of-flight aerosol mass apectrometer. *Atmos. Chem. Phys.* **2011,** *11*, (4), 1581-1602.
30. Friend, A. J.; Ayoko, G. A.; Stelcer, E.; Cohen, D., Source apportionment of PM2.5 at two receptor sites in Brisbane, Australia. *Environ. Chem.* **2011,** *8*, (6), 569-580.
31. Fuller, G. W.; Green, D. C.; Butterfield, D., A UK-wide assessment of black carbon and PM from wood burning. *Proceedings of European Aerosol Conference, Granada* **2012**.
32. Morawska, L.; Ristovski, Z.; Jayaratne, E. R.; Keogh, D. U.; Ling, X., Ambient nano and ultrafine particles from motor vehicle emissions: Characteristics, ambient processing and implications on human exposure. *Atmos. Environ.* **2008,** *42*, (35), 8113-8138.
33. Zhang, Q.; Stanier, C. O.; Canagaratna, M. R.; Jayne, J. T.; Worsnop, D. R.; Pandis, S. N.; Jimenez, J. L., Insights into the Chemistry of New Particle Formation and Growth Events in Pittsburgh Based on Aerosol Mass Spectrometry. *Environ. Sci. Technol.* **2004,** *38*, (18), 4797-4809.

Chapter 7. First measurements of source apportionment of organic aerosols in the Southern Hemisphere

Leigh R. Crilley, Godwin A. Ayoko and Lidia Morawska

International Laboratory for Air Quality and Health, Institute of Health and Biomedical Innovation, Queensland University of Technology, Brisbane, QLD, 4001, Australia.

(2014), *Environmental Pollution.* 184, 81-88

PREFACE

In this paper was the source apportionment of organic aerosols (OA) at multiple sites as determined by an AMS was described. While these measurements enabled and enhanced the source apportionment of the OA at the schools, this paper scope was broader than children's exposure at school, which was the more the focus of the preceding 3 chapters (4-6). There is limited information on the sources and composition of OA in the Southern Hemisphere as well as the mass spectral variability in source profiles across an urban area, which this paper addressed. The results indicated that the mass spectral profiles of the secondary OA components differed between the schools, whereas the primary emissions profiles were more similar.

Statement of joint authorship of co-authors

The authors listed below have certified* that:

1. they meet the criteria for authorship in that they have participated in the conception, execution, or interpretation, of at least that part of the publication in their field of expertise;
2. they take public responsibility for their part of the publication, except for the responsible author who accepts overall responsibility for the publication;
3. there are no other authors of the publication according to these criteria;
4. potential conflicts of interest have been disclosed to (a) granting bodies, (b) the editor or publisher of journals or other publications, and (c) the head of the responsible academic unit, and
5. they agree to the use of the publication in the student's thesis and its publication on the QUT ePrints database consistent with any limitations set by publisher requirements.

In the case of this chapter:

First measurements of source apportionment of organic aerosols in the Southern Hemisphere, (2014) *Environmental Pollution*, 184; 81-88.

Contributor	Statement of contribution*
Leigh R. Crilley	Performed the field work with the AMS, data analysis and wrote the manuscript
Godwin A. Ayoko*	Provided overall direction for this study and assisted with the data analysis and drafting of the manuscript
Lidia Morawska*	Designed the overall concept of the study and assisted with the data interpretation and manuscript preparation

Principal Supervisor Confirmation

I have sighted email or other correspondence from all Co-authors confirming their certifying authorship.

PROF GODWIN AYOKO — Name

Signature

22/11/2013 — Date

ABSTRACT

An Aerodyne aerosol mass spectrometer was deployed at five urban schools to examine spatial and temporal variability of organic aerosols (OA) and positive matrix factorization (PMF) used for the first time in the Southern Hemisphere to apportion the sources of the OA across an urban area. The sources identified included hydrocarbon-like OA (HOA), biomass burning OA (BBOA) and oxygenated OA (OOA). At all sites, the main source was OOA, which accounted for 62-73% of the total OA mass and was generally more oxidized compared to those reported in the Northern Hemisphere. This suggests that there are differences in aging processes or regional sources in the two hemispheres. Unlike HOA and BBOA, OOA demonstrated instructive temporal variations but not spatial variation across the urban area. Application of cluster analysis to the PMF-derived sources offered a simple and effective method for qualitative comparison of PMF sources that can used in other studies.

KEYWORDS: Aerosol Mass Spectrometry, organic aerosols, urban environments, positive matrix factorization

7.1 INTRODUCTION

In an urban environment, OA have been frequently shown to be the largest component of ambient particles in the non-refractory PM_1 (mass concentration of particles with a diameter less than 1 μm) ([1] and references therein). One analytical instrument for quantitative measurements of the chemical composition of OA with a high temporal resolution is the Aerodyne Aerosol Mass Spectrometer (AMS) [2]. One technique, which has been successfully applied to the OA mass spectra from AMS datasets, is positive matrix factorization (PMF) [3, 4]. PMF is a quantitative technique that requires no prior knowledge of the sources before analysis. The

application of PMF has allowed for the variability in the OA to be extracted resulting in the apportionment of distinct OA factors to better model the source contributions [3].

In many urban datasets, the two main components that are extracted by PMF are hydrocarbon-like OA (HOA), and oxygenated OA (OOA) [4-6]. HOA has been shown to be correlated with primary tracers such as CO and NO_x and is considered representative of primary emissions [4, 5]. The OOA component is representative of secondary OA and can be further broken down into two subsets based upon the degree of volatility and oxidation [3]. These sub components are known as semi-volatile OOA (SV-OOA) and low-volatility OOA (LV-OOA) [3, 4]. SV-OOA is less oxidised and hence freshly formed OOA while the LV-OOA is more aged and oxidised OOA, and are usually derived from regional sources. However, there is a continuum of oxidation levels between fresh OOA and the more aged OOA and when this is considered with the dynamic nature of OA there can be substantial variability in the mass spectra of the factors.

Thus the OA in an urban environment is highly complex and originates from a number of local and regional sources. Many of the studies investigating the source apportionment of OA were conducted based at one site within a city (see e.g. [6-8]).Therefore, conducting measurements at a number of locations around one urban area for extended periods would give more accurate representation of the OA and the spatial and temporal variation in the source profiles for that urban area. There has been limited research on the spectral variability of PMF- derived source factors of OA from multiple sites within one urban environment. Studies that have used an

AMS at multiple sites have been mobile measurements conducted on road and focused on vehicle emissions [10] or with limited time at a particular site [11]. Mohr et al. [11] found that though the chemical composition of PM_1 around Zurich in winter had a uniform distribution, by sampling at multiple sites the contribution of local sources could be distinguished. To date research has been predominantly carried out in North America and Europe (See [9]), with measurements required in the Southern Hemisphere to improve understanding of the global budget of secondary OA [12].

Considering the aforementioned gaps in knowledge, the aim of the current study was the source apportionment of OA at five locations around the subtropical city of Brisbane, Australia. Thus the source apportionment of the OA in an urban environment using PMF was performed, for the first time to the author's knowledge in the Southern Hemisphere. The similarities of the mass spectra for the PMF derived factors were compared using cluster analysis to quantitatively analyze the variability in the source profiles between the sites. Conditional probability function is as far as we know, applied for the first time to PMF- derived factors from AMS OA data to analyze the direction of the main contributions of sources, and their relationship with the local sources in this study.

7.2 METHOD

7.2.1 Sampling sites and methodology

Brisbane is a subtropical city with a rapidly growing population and as such the contribution of vehicle emissions and other anthropogenic sources to air pollution is

increasing. An Aerodyne compact Time-Of-Flight Aerosol Mass Spectrometer (TOF-AMS) [2, 13] was deployed at five schools in different suburbs in the metropolitan Brisbane area, which are referred to as S01, S04, S11, S12 and S25. This study was a part of a larger project at these schools designed to study the effect of ultrafine particles from traffic emissions on children's health (www.ilaqh.qut.edu.au/Misc/UPTECH%20Home.htm). Twenty-five schools participated in this project, however measurements with the TOF-AMS was conducted at only five schools due to various logistical reasons, and their locations are shown in Figure 1. The schools selected were not near any other large source of air pollution including large infrastructure projects except traffic emissions. Measurements at S01 and S04 were conducted during summer whereas for S11, S12 and S25 it was performed in winter. As Brisbane is a subtropical city, the variation between the seasons is limited with winter typically drier than the summer months.

Detailed description of the sampling method, meteorology, TOF-AMS operation and the schools are given in Crilley et al. [14]. Briefly, the TOF-AMS was housed in a vacant classroom within the school and sampled for 2-3 weeks at each site with a 5 min interval. The TOF-AMS was calibrated for ion efficiency according to the standard protocols [13, 15, 16]. In addition to the TOF-AMS, a NO_x, and CO gas analyser (Ecotech, Knoxfield, Australia) and an automatic weather station (Monitor Sensor, Caboolture, Australia) were also deployed at the schools. These instruments were housed within a trailer at a site within the school grounds reflecting the best overall exposure to the pollutants present. The trailer site was located between 50-150 m from the classroom with the TOF-AMS. The sampling heights for the TOF-AMS varied between 1.5-2 m at the sites and the gas analyzers were 3 m at all sites.

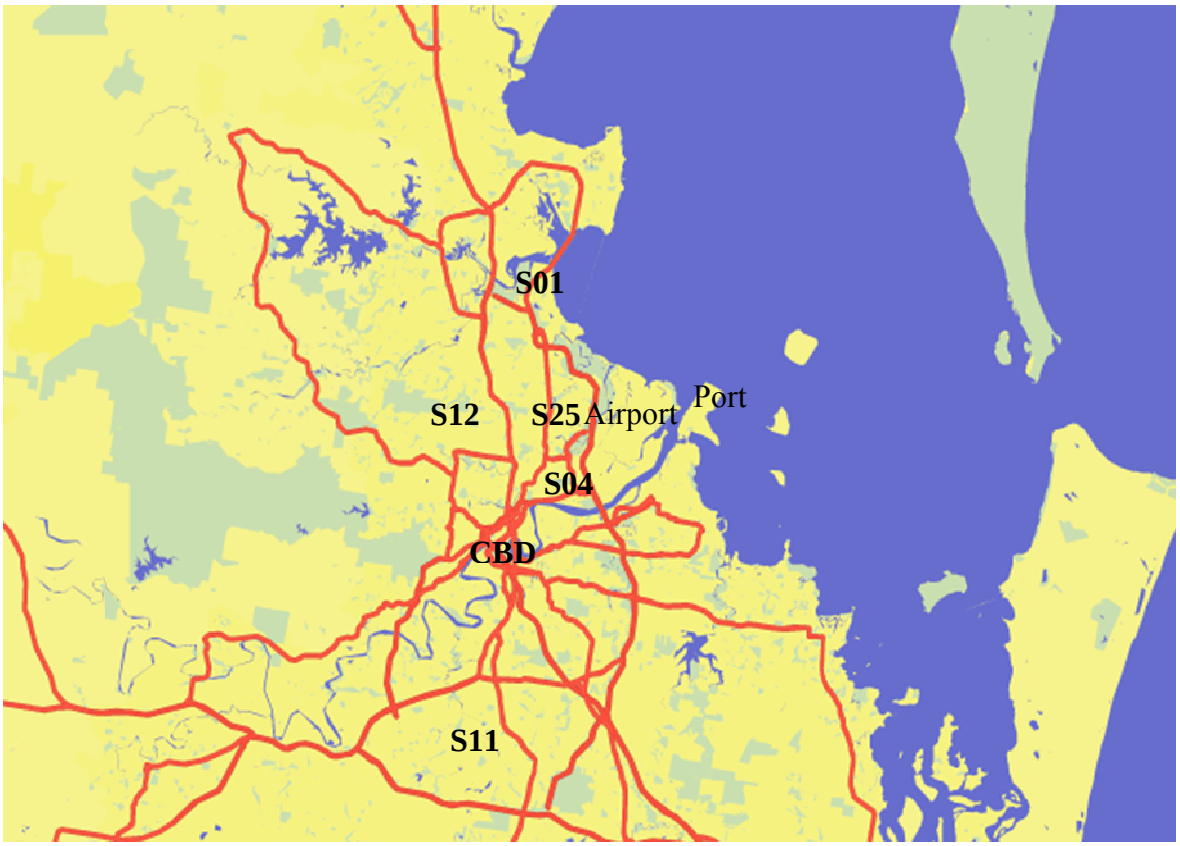

Figure 7-1: Map of Brisbane city indicating the locations of sites and potential sources. Green areas represent bushland and major roads are shown in orange. CBD indicates the central business district.

7.2.2 Data Analysis

7.2.2.1 ***PMF analysis***

The TOF-AMS data was processed and analyzed using Squirrel v1.51 in IGOR Pro v6.22. Squirrel was used to generate the organic and error matrices in the m/z range 13-300 for subsequent PMF analysis. PMF analysis was applied to the organic fraction data at each location using PMF2 developed by Paatero and Tapper [17] and the PMF evaluation tool (PET) for IGOR Pro as described in Ulbrich et al. [4]. Pre-treatment of the data prior to PMF analysis as set out in Zhang et al. [18] was applied to the organic data from each location. Details of the pre-treatment are presented in Appendix 5, section A5.1 and Table A5-1. The seed and F-peak values were varied

to find the best solution. For each site, the F-peak was found to be at a minimum at zero while the optimum seed varied. The number of factors chosen at each site was based upon the guidelines described in Ulbrich et al. [4] and Zhang et al. [18].

The solution chosen did not necessarily have the lowest Q/Q_{exp} value, as it would frequently continue to decrease with the number of factors, rather it showed a sharp decrease in the Q/Q_{exp} value, which indicated that the minimum number of factors has been obtained [4]. Also, the scaled residuals for each solution was checked to ensure that they were normally distributed, centred on zero and with a reasonable standard deviation [18]. For each factor in a solution the mass spectra, O:C ratio, diurnal cycle, percentage mass contributions and correlations with other species were examined to further determine the best solution. Variability in the source contributions were assessed using 20 bootstrap runs.

The mass spectra for the factors in a solution were analysed as a further aid in determining the optimum solution for each site. Firstly, the mass spectra from a solution were compared with the reference mass spectra from Ng et al. [19] or primary source spectra (e.g. [20]) by visual inspection. Thus the mass spectra obtained for a solution had to be matched to a known source profile, and if a solution contained a mass spectrum that did not resemble a known source profile, then this solution was rejected. In a solution, if splitting of factors became apparent, by giving similar or unreal source mass spectra, the solution with a lesser number of factors was used. In addition, if the a solution contained a factor that accounted for less than 5% of the mass, then this factor was unlikely to be from a real source, so this solution was not used [4].

Further validation of the source identification was determined using the O:C ratio, diurnal cycle and correlations with other species. An estimation of the O:C ratio was calculated according to Aiken et al. [21] for unit mass resolution data and compared to previous work in the literature [9]. The diurnal cycle was determined as certain sources would be expected to have a distinct diurnal cycle, for example a bimodal diurnal cycle for the HOA factor. Pearson's correlations analysis was performed using SPSS (v19) and each factor was correlated with concentrations of CO and NO_x as well as the AMS determined concentrations of nitrate, sulphate and ammonium. Thus the combination of these three analyses was used to further support the source identification of a given factor.

Where only one OOA type factor was identified, no attempt was made to classify it as either SV-OOA or LV-OOA as there is no distinct marker to differentiate them. Where multiple OOA type factors were identified, they were differentiated as either SV-OOA or LV-OOA depending on the level of oxidation, with the most oxidized factor classified as LV-OOA and vice versa. Thus it may be more appropriate to label these factors as less-oxygenated OOA and more oxygenated OOA [18]. However the more widely applied nomenclatures of SV-OOA and LV-OOA were used for consistency across the sites.

7.2.2.2 ***Comparison of PMF factors***

Once the number of factors was chosen for the PMF solution at each site, cluster analysis and conditional probability function analysis were applied. Hierarchical cluster analysis was applied to the mass spectra from of each of the PMF factors identified at each site, to find the similarities between the factors. Hierarchical cluster

analysis was performed in SPSS v19 using the between groups linkage cluster method, and a squared Euclidean distance. Conditional probability function (CPF) is an analysis tool to find the direction of the source contributions. This was accomplished by combining the wind direction and speed data at each site with the source contributions from the PMF analysis, as described in Lee and Hopke [22], and also Friend et al. [23]. The differences in the time intervals for the wind and TOF-AMS data meant that the hourly wind data was applied to each of the TOF-AMS data point for that hour ([23] and references therein). CPF analysis calculates the number of events where the source contribution is greater than the 75th percentile in a particular direction. Thus the contribution of local sources could be determined for each location.

7.3 RESULTS AND DISCUSSION

7.3.1 PMF solutions for each school

At each site the number of factors selected varied from two to four and the selected solutions met the criteria for Q/Q_{exp}, factor mass spectra and the scaled residuals described previously. A two factor solution was chosen for S01 and S04 as the OOA factor in the three factor solutions split into two factors with mass spectra that did not resemble any known sources at both sites. A three factor solution was chosen for S11 as the four factor solution gave a factor that only accounted for 4.8% of the mass. At S12, a three factor solution was also selected as splitting of the OOA factor appeared to occur in the four factor solution. A four factor solution was chosen for S25 as the additional factor in the five factor solution accounted for less than 5% of the mass [4].

Table 7-1: Summary of the PMF solutions at each school. Variability given for the percentage contribution is 1 standard deviation calculated in bootstrapping analysis.

	Q/Q_{exp}	Factor	Assignment	Percentage contributions	O:C	Correlations ($r^2 > 0.7$)
S01	0.48	1	OOA	71 ± 1.1	0.69	NO_3^-
		2	HOA	29 ± 0.62	0.08	
S04	2.52	1	OOA	64 ± 0.78	0.57	NO_3^-
		2	HOA	36 ± 0.73	0.13	
S11	2.71	1	OOA	62 ± 2.1	0.93	NO_3^-, NH_4^+
		2	HOA	23 ± 0.66	0.08	NO_3^-, NH_4^+
		3	BBOA	14 ± 1.9	0.44	NO_3^-
S12	3.2	1	SV-OOA	28 ± 1.0	0.26	CO, NO_x
		2	LV-OOA	45 ± 1.2	0.97	NO_3^-
		3	BBOA	26 ± 0.35	0.31	NO_3^-
S25	3.14	1	SV-OOA	32 ± 3.3	0.83	
		2	LV-OOA	38 ± 3.1	1.25	NO_3^-
		3	HOA	20 ± 1.1	0.08	NO_3^-, CO, NO_x
		4	BBOA	10 ± 0.54	0.1	NO_3^-

In Table 7-1, a summary of the results for each site is given, and includes the O:C ratio, percentage mass contribution and correlations to other species for the factors identified. The solution for each site, which included the mass spectra, time series and diurnal cycles of each factor are given in the Appendix 5 (Figures A5-1 to 15). OOA was identified at all of the sites, but was separated into SV-OOA and LV-OOA at only two sites. HOA was identified at four of the sites, whereas a BBOA factor was identified at three of the sites. Representative mass spectra for each of these identified sources are given in Figure 7-2. In the next section, the reasons for the source identification of the PMF-derived factors are outlined.

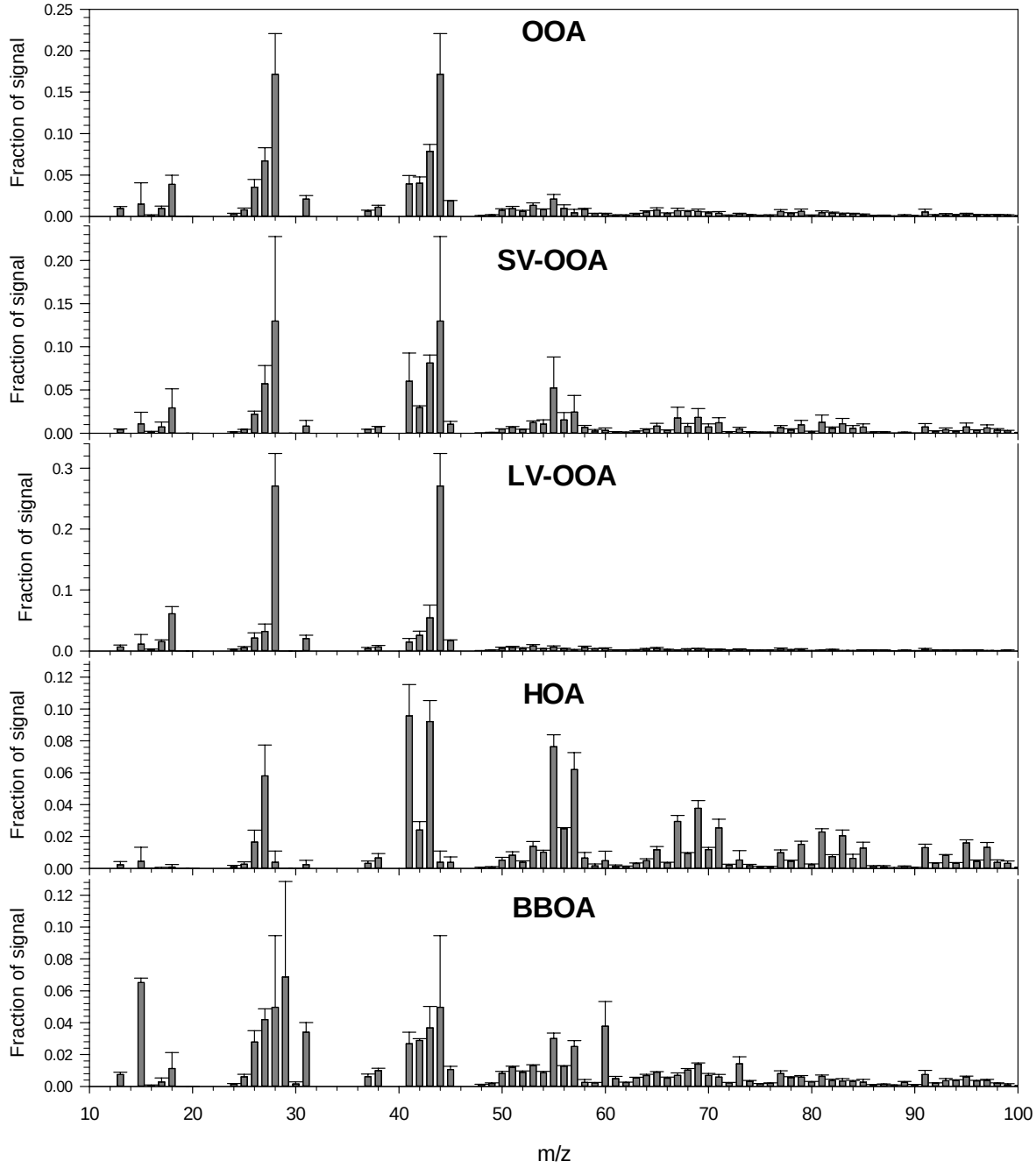

Figure 7-2: Average mass spectra for the different OA sources identified across the sites. Error bars represent 1 standard deviation.

7.3.2 Source identification of the PMF factors

7.3.2.1 ***OOA factors***

All of the OOA mass spectral profiles identified at all of the sites were characterised by the prominence of the m/z 44 ion. From Table 7-1, the OOA factor/s accounted for between 62-73% of the total OA mass and so was the main OA component at all

of the sites in Brisbane. The percentage of the OA accounted for by the OOA factor/s is in agreement with other studies in urban environments ([18] and references therein). At S01, S04 and S11 the OOA factor and the SV-OOA and LV-OOA factor mass spectra from S12 and S25 closely resembled the corresponding standard mass spectrum from Ng et al. [19]. The LV-OOA factor at S12 and S25 was characterized by having a higher concentration of the m/z 44 ion relative to the other ions and was thus more oxidized.

Across the sites the oxidation of the OOA factor varied as indicated by the differing O:C ratios (Table 7-1). In general, the OOA factor(s) at S11, S12 and S25 had a higher O:C ratio compared to S01 and S04, indicating that the OOA was more aged at S11, S12 and S25. The exception was the SV-OOA factor at S12 which had a notably lower O:C ratio (0.26) than the other OOA factors (Table 7-1). In Table 7-2, the O:C ratios from PMF derived OOA factors is given for selected urban sites for comparison with the results from this study. These selected urban areas include sub-tropical locations (Mexico City and PRD region, China) and sites affected by regional sources (Beijing and PRD region, China). The SV-OOA factor for S12 was the only one that was within the range (Table 7-2) reported by Ng et al. [9] from 43 datasets in the Northern Hemisphere for SV-OOA. All of the other OOA factors were in or above the range for LV-OOA from Ng et al. [9]. Therefore the SV-OOA factor for S12 was likely to be from a different source from the other OOA, and is investigated further in Sections 7.3.3.

Table 7-2: O:C ratios for PMF derived factors SV-OOA and LV-OOA for selected urban sites around the world.
*Huang et al (2010) identified two distinct OOA factors but did not call them SV-OOA and LV-OOA rather OOA-1 and OOA-2 as they were unlike the LV-OOA and SV-OOA standard spectra.

Location	SV-OOA	LV-OOA	Reference
Mexico City	0.52	0.83	[21]
Northern Hemisphere	0.35±0.14	0.73±0.14	[9]
New York	0.38	0.63	[26]
Beijing	0.47*	0.48*	[6]
PRD Region, China	0.45	0.59	[29]

That the O:C ratio for majority of the OOA factors at the sites studied was within the LV-OOA range from Ng et al. [9] points to the OOA being highly oxidized in Brisbane. At S11, S12 and S25 the factor classified as either OOA/LV-OOA had an O:C ratio that exceeded the LV-OOA range, with S25 recording the highest O:C ratio for a LV-OOA factor at 1.25. In addition, the 'SV-OOA' factor for S25 was in the top end of the range for LV-OOA [9] and was the same as reported for the LV-OOA factor at another subtropical city, Mexico City [21]. In general, the O:C ratios for the OOA factor/s from this study are higher than the corresponding factors listed in Table 7-2. Therefore this indicates that the regional OA in Brisbane is more oxidized and aged compared to other cities around the world.

From Table 7-1, none of the OOA factors were found to be correlated with sulphate, rather they were generally correlated with nitrate. Sulphate has generally been associated with more oxidized and regional OOA and nitrate with fresher, less oxidized OOA ([18] and references therein). However, Hersey et al. [7] proposed that on a fundamental chemical basis there is no reason why nitrate should correlate better with SV-OOA as opposed to LV-OOA. The OOA factors that were correlated

with nitrate had a range of O:C ratios. The O:C ratio difference indicates that there was a distinct difference in the source of the OOA factors that was probably seasonal as S01, S04 were sampled in summer whereas S11, S12, S25 were sampled in winter. Thus the less oxidized OOA at S01 and S04 may be due to increased local photochemical SOA formation while at S11, S12 and S25 the OOA source was more regional [7, 18]. In addition, the increased rainfall during summer may be removing secondary aerosol before they become highly aged resulting in lower levels of oxidation. A seasonal difference in the source of secondary aerosols is further supported by fact that the ammonium at S11, S12 and S25 was highly correlated ($r^2 >$ 0.7) with both sulphate and nitrate whereas at S01 and S04 this was not the case.

From Table 7-1 it is apparent that unlike the SV-OOA factor, the LV-OOA factor at S25 was correlated with nitrate. This indicates that there is a difference in the origins of the two OOAs. In Figure A5-16 (Appendix 5) the CPF analysis for OOA are shown, and revealed that the main source contributions for the two OOA factors at S25 were from different origins. Therefore the two OOA factors at S25 represent different regional sources of OA. Apart from at S25, the CPF analysis, as expected did not provide information about the location of the sources OOA at the other sites. This is because the OOA was predominately secondary OA and therefore from a regional source rather than a local point source.

7.3.2.2 ***HOA factors***

At four of the sites a HOA factor was identified and its mass spectra was characterized by the presence of the hydrocarbon ion series peaks (m/z 41, 43 , 55, 57 etc) and closely resembled the standard HOA mass spectra given in Ng et al. [19]. The HOA factors accounted for 20-36% of the OA mass (Table 7-1) and as such

were a large source of the OA. For all four of the HOA factors the O:C ratios were less than 0.13 (Table 7-1), which is in the range expected for HOA in urban locations ([9] and references therein). At the four sites, the O:C ratios for the HOA factors also points to vehicle emissions as the source [24]. Similar diurnal cycles for the HOA factors were found (Figures A5-6 to 8, A5-10) in that it did not follow the bimodal cycle normally associated with vehicle emissions rather that it peaked only in the morning. A similar diurnal pattern has been observed before for HOA and the absence of a HOA peak attributed to a general rise in the boundary layer [25, 26]. Thus the diurnal cycle of HOA in the current work can be attributed to local HOA emissions [25].

The HOA factors were not correlated with the primary emission tracers CO and NO_x except for at S25 (Table 7-1). With the vertical sampling height similar for all instruments, the lack of correlation maybe due to the instruments not being co-located at the sites. The concentrations of primary source emissions are expected to be more dynamic than regional sources. Therefore due to the distance between instruments the concentrations of HOA may have varied, resulting in the lack of correlation. The inconclusive evidence for the HOA factors by the correlation analysis with tracer species led the use of conditional probability function analysis to justify the source identification.

The most informative results from the CPF analysis were found for the HOA factors, as they were from a local primary source and is shown in Figure 7-3. A HOA factor was identified at four sites with the exception of S12 (Table 7-1). HOA has been used in previous work as a surrogate for vehicle emissions in urban environments

[27, 28]. As can be seen in Figure 7-3, the CPF analysis results from each site shows that the main contributions for HOA factor were coming from the road closest to the AMS. The diurnal cycle of the HOA factors suggested local emissions of HOA, and the CPF analysis further confirms vehicle emissions was the case as the main source contributions were from the nearest roads. At S12 the CPF results for SV-OOA factor also indicated that main source contributions were from a surrounding road. The SV-OOA factor at S12 was shown by cluster analysis to be spectrally similar to the HOA factors (See Section 7.3.3), and combined with the main direction of the source being from the surrounding roads, indicates a contribution from fresh vehicle emissions in this source factor at S12. However, the relatively high intensity of the m/z 44 ion in the SV-OOA factor at S12 indicates that it has been aged and the source may be slightly aged vehicle emissions from a nearby arterial road (1km to the east of the S12). Thus at S12 the SV-OOA factor is likely a mixture of vehicle emissions from both sources.

7.3.2.3 ***BBOA factors***

The BBOA factor identified at the S11, S12 and S25 was characterized by the presence of the m/z 60 and 73 ions, which have been used as marker for biomass burning as these peaks are associated with levoglucosan [19]. At the three sites the O:C ratio of the BBOA factor was found to vary. S11 and S12 had an O:C ratio of 0.44 and 0.31, respectively which was comparable to the expected ratio for BBOA of 0.3-0.4 [21] whereas at S25 the O:C ratio was found to be lower at 0.1, which is more indicative of cooking OA (COA) [6, 20]. However the mass spectrum of COA does not generally include the m/z 60 and 73 ions [6, 20] therefore the BBOA factor

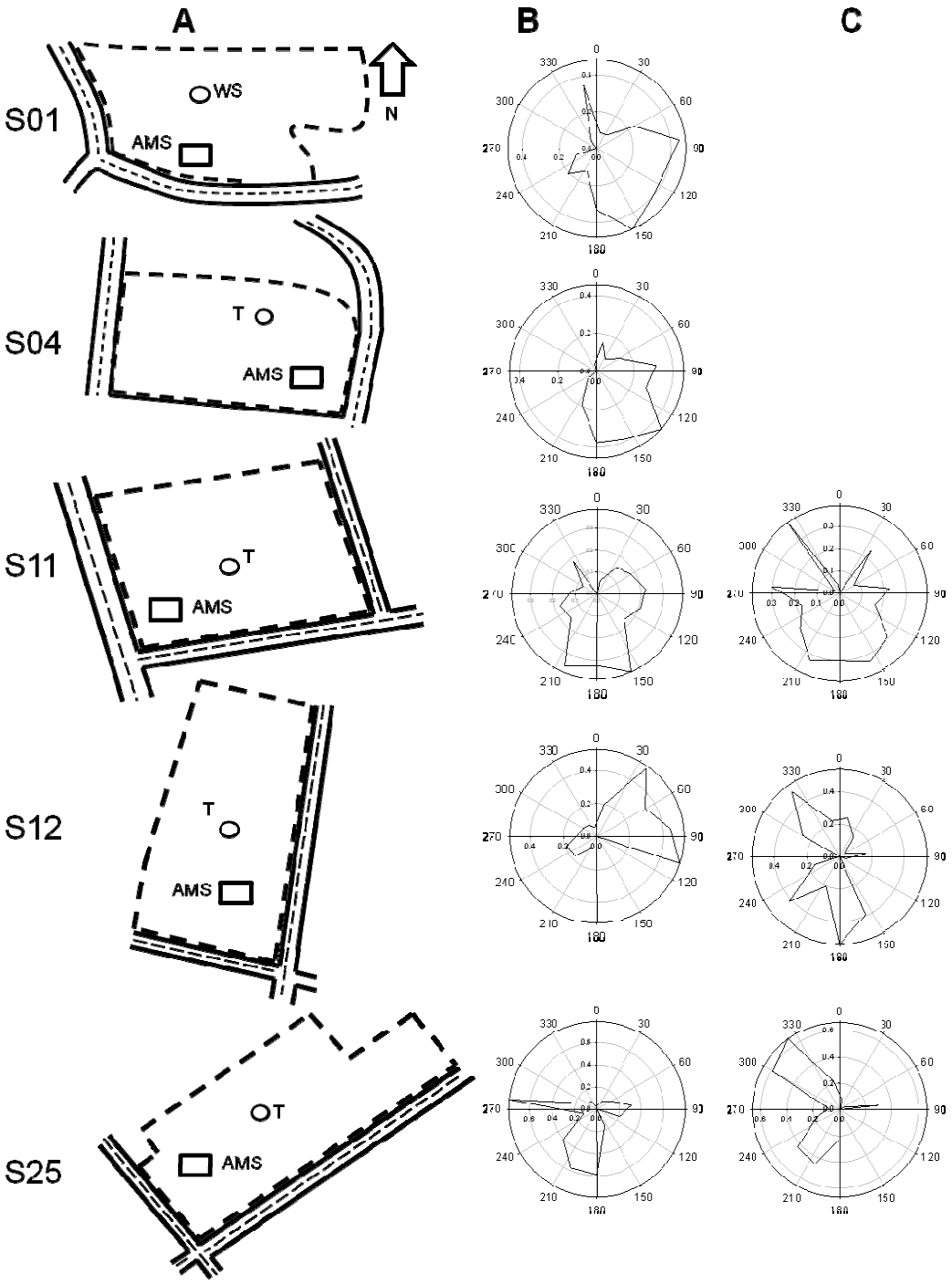

Figure 7-3: Schematic diagrams at each school and CPF results.
Column A are schematic diagrams of each school (only approximately to scale). AMS represents the location of the classroom with the TOF-AMS and T the site of the trailer housing the gas analysers, weather station and CPC. Column B and C are the CPF results for HOA/SV-OOA and BBOA factors, respectively at each school.

at S25 may be a mixture of both COA and BBOA. The higher O:C ratio at S11 compared to the other sites indicated that the BBOA was more aged. That the BBOA was only identified at the sites sampled in the winter points to a seasonal influence that was not due to meteorology but source operation. In Brisbane back burning of bush land near the city is a common practice during winter, and a seasonal influence has been noted for Brisbane in biomass burning previously [23]. Thus there may be a seasonal trend in the BBOA factor for Brisbane but the limited seasonal data for this study limits the conclusions that can be drawn in this regard.

For the BBOA factors when there was a known source of biomass burning, the CPF analysis detected this contribution (Figure 7-3). During the sampling at S25 there was a large bushfire to the west, which was the direction of the BBOA source at this site. CPF analysis of the SV-OOA factor (Figure A5-16) and the BBOA factor (Figure 7-3) at S25 indicated that largest contributions to these two factors were from the west. This information along with correlation (r^2 of 0.6) of SV-OOA and BBOA factor time series points to aged OA from bushfires to west of the site as the source of the SV-OOA at S25.

At S11 and S12 there were no known point sources of biomass burning such as a bushfire and this indicates that there were multiple source contributions, which probably includes a discretionary domestic wood burning source such as braziers. The diurnal cycle of the BBOA factor at S11 and S12 showed evening peaks (Figures A5-8 and A5-9, Appendix 5), which have previously been attributed to domestic heating [8]. Overall, the use of CPF analysis on PMF-derived TOF-AMS

factors is best suited for sources that have a distinct geographical origin, such as vehicle emissions from nearby roads or local bushfires.

7.3.3 Cluster Analysis

As many of the same sources were identified across the sites, hierarchical cluster analysis was used to analyze the similarities in the mass spectrum of the factors identified at the sites. The results are presented in Figure 7-4 as a dendrogram. The most notable aspect from Figure 7-4 is that the primary OA (POA) and secondary OA (SOA) have separated into two distinct clusters and are discussed in the following two sections.

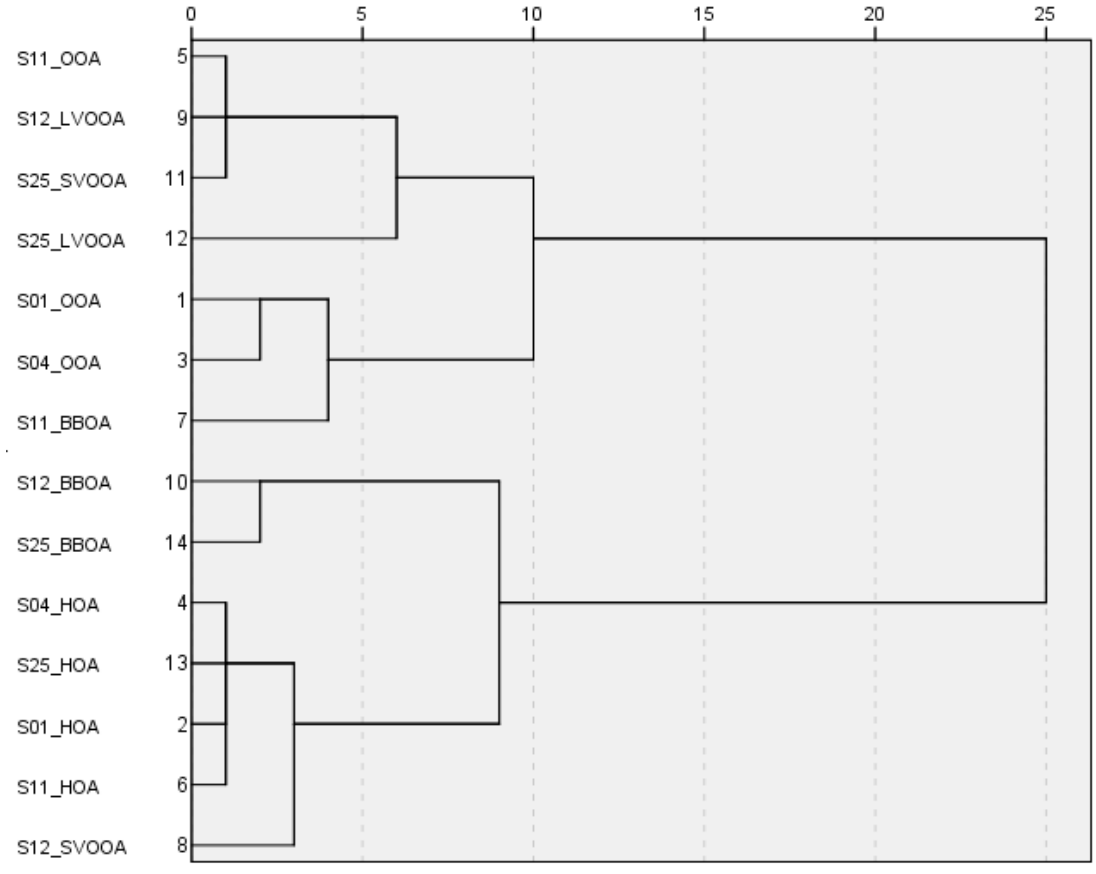

Figure 7-4: Dendrogram of hierarchical cluster analysis of the identified factors from every school.

7.3.3.1 ***POA cluster***

The POA cluster contains one SV-OOA, all of the HOA and most of the BBOA factors. As indicated by the low linkage distance, the HOA factors were all very similar, which points to the same HOA source at the four sites. Clustered with the HOA factors was the SV-OOA factor at S12 signifying that it was from the same source but slightly aged; and this acts as further confirmation to the CPF results discussed previously. The BBOA factors from S11 and S25 were also found to be similar as they were clustered together. As these two BBOA factors were also more similar to the other POA (HOA factors) than the OOA factors, it suggests that fresh BBOA was the source.

7.3.3.2 ***SOA cluster***

From Figure 7-4, the SOA cluster contained the rest of the OOA factors and the BBOA from S11. Thus the BBOA factor at S11 was more aged compared to the BBOA factor from S12 and S25, as indicated by the higher O:C ratio for S11 BBOA factor. The OOA factors from S01 and S04 were similar but distinct from the other OOA factors at S11, S12 and S25, therefore pointing to differences in the OOA composition. From Table 7-1, the O:C ratio was found to be different for the two clusters, with the OOA factors from S01 and S04 having a lower ratio compared to S11, S12 and S25 indicating that the last three sites the OOA were more aged. This may be a seasonal trend as the measurements at S11, S12 and S25 were conducted in winter while S01 and S04 were performed in summer. The OOA in summer may be more influenced by photochemical SOA formation and may therefore be less aged [7]. Also of note from Figure 7-4 was that the assignment of SV-OOA and LV-OOA was only relevant for differentiating between the oxidation levels of the OOA factors identified at a specific site. This can be seen in Figure 7-4, where the LV-OOA and

SV-OOA factors at S11 and S25, respectively were clustered and thus had similar mass spectra.

7.4 CONCLUSIONS

The source apportionment of the OA at five sites in a subtropical city was performed using PMF, for the first time to our knowledge in the Southern Hemisphere. The sources identified at each site varied; however the main source at all of the sites was OOA, accounting for 62-73% of the total OA mass. CPF analysis applied to determine the direction of the source contributions and aided the source identification of the primary factors. Cluster analysis was able to group the PMF- derived factors into POA (containing the HOA and BBOA) and SOA (with the OOA) clusters and is therefore a simple yet effective method for qualitative comparison of PMF factors from different sites that could be utilized in future studies. Overall, the SOA factors were more oxidized than previous results from the Northern Hemisphere and points to differences in the aging processes or regional sources in the Southern Hemisphere. Further work at more locations around the Southern Hemisphere is required to confirm this hypothesis.

Appendix 5

Appendix 5 contains information on the data pre-treatment prior to PMF analysis, as well as the mass spectra, time series and diurnal cycles for the selected PMF solutions at each school.

ACKNOWLEDGMENTS

This work was supported by the Australian Research Council (ARC), QLD Department of Transport and Main Roads (DTMR) and QLD Department of Education, Training and Employment (DETE) through Linkage Grant LP0990134.

Our particular thanks go to R. Fletcher (DTMR) and B. Robertson (DETE) for their vision regarding the importance of this work. We would also like to thank Prof G. Marks, Dr P. Robinson, Prof K. Mengersen, Prof Z. Ristovski, Dr M. Mazaheri, Dr C. He, Dr G. Johnson, Dr R. Jayaratne, Dr S. Low Choy, Prof G. Williams, W. Ezz, F. Salimi, S. Clifford, M. Mokhtar, N. Mishra, R. Laiman, L. Guo, Prof C. Duchaine, Dr H. Salonen, Dr X. Ling, Dr J. Davies, Dr L. Leontjew Toms, F. Fuoco, Dr A. Cortes, Dr B. Toelle, A. Quinones, P. Kidd, E. Belousova, Dr M. Falk, Dr F. Fatokun, Dr J. Mejia, Dr D. Keogh, Prof T. Salthammer, R. Appleby and C. Labbe for their contribution to the UPTECH project. We also thank Dr Adrian Friend for providing the map used in Figure 1.

7.5 REFERENCES

1. Jimenez, J. L.; Canagaratna, M. R.; Donahue, N. M.; Prevot, A. S. H.; Zhang, Q.; Kroll, J. H.; DeCarlo, P. F.; Allan, J. D.; Coe, H.; Ng, N. L.; Aiken, A. C.; Docherty, K. S.; Ulbrich, I. M.; Grieshop, A. P.; Robinson, A. L.; Duplissy, J.; Smith, J. D.; Wilson, K. R.; Lanz, V. A.; Hueglin, C.; Sun, Y. L.; Tian, J.; Laaksonen, A.; Raatikainen, T.; Rautiainen, J.; Vaattovaara, P.; ehn, M.; Kulmala, M.; Tomlinson, J.; Collins, D. R.; Cubison, M. J.; Dunlea, E. J.; Huffman, A.; Onasch, T. B.; Alfarra, M. R.; Williams, P. I.; Bower, K. N.; Kondo, Y.; Schneider, J.; Drewnick, F.; Borrmann, S.; Weimer, S.; Demerjian, K. L.; Salcedo, D.; Cottrell, L.; Griffin, R.; Takami, A.; Miyoshi, T.; Hatakeyama, S.; Jayne, J. T.; Herndon, S. C.; Trimborn, A.; Williams, L. R.; Wood, E. C.; Middlebrook, A.; Kolb, C. E.; Baltensperger, U.; Worsnop, D. R., Evolution of Organic Aerosols in the Atmosphere *Science* **2009,** *326*, 1525-1529.

2. Canagaratna, M. R.; Jayne, J. T.; Jimenez, J. L.; Allan, J. D.; Alfarra, M. R.; Zhang, Q.; Onasch, T. B.; Drewnick, F.; Coe, H.; Middlebrook, A.; Delia, A.; Williams, L. R.; Trimborn, A. M.; Northway, M. J.; DeCarlo, P. F.; Kolb, C. E.; Davidovits, P.; Worsnop, D. R., Chemical and microphysical characterization of ambient aerosols with the Aerodyne aerosol mass spectrometer. *Mass Spectrom. Rev.* **2007,** *26*, 185-222.

3. Lanz, V. A.; Alfarra, M. R.; Baltensperger, U.; Buchmann, B.; Hueglin, C.; Prévôt, A. S. H., Source apportionment of submicron organic aerosols at an urban site by factor analytical modelling of aerosol mass spectra. *Atmos. Chem. Phys.* **2007,** *7*, (6), 1503-1522.

4. Ulbrich, I. M.; Canagaratna, M. R.; Zhang, Q.; Worsnop, D. R.; Jimenez, J. L., Interpretation of organic components from Positive Matrix Factorization of aerosol mass spectrometric data. *Atmos. Chem. Phys.* **2009,** *9*, (9), 2891-2918.
5. Zhang, Q.; Alfarra, M. R.; Worsnop, D. R.; Allan, J. D.; Coe, H.; Canagaratna, M. R.; Jimenez, J. L., Deconvolution and Quantification of Hydrocarbon-like and Oxygenated Organic Aerosols Based on Aerosol Mass Spectrometry. *Environ. Sci. Technol.* **2005,** *39*, (13), 4938-4952.
6. Huang, X. F.; He, L. Y.; Hu, M.; Canagaratna, M. R.; Sun, Y.; Zhang, Q.; Zhu, T.; Xue, L.; Zeng, L. W.; Liu, X. G.; Zhang, Y. H.; Jayne, J. T.; Ng, N. L.; Worsnop, D. R., Highly time-resolved chemical characterization of atmospheric submicron particles during 2008 Beijing Olympic Games using an Aerodyne High-Resolution Aerosol Mass Spectrometer. *Atmos. Chem. Phys.* **2010,** *10*, (18), 8933-8945.
7. Hersey, S. P.; Craven, J. S.; Schilling, K. A.; Metcalf, A. R.; Sorooshian, A.; Chan, M. N.; Flagan, R. C.; Seinfeld, J. H., The Pasadena Aerosol Characterization Observatory (PACO): chemical and physical analysis of the Western Los Angeles basin aerosol. *Atmos. Chem. Phys.* **2011,** *11*, (15), 7417-7443.
8. Brown, S. G.; Lee, T.; Norris, G. A.; Roberts, P. T.; Collett Jr., J. L.; Paatero, P.; Worsnop, D. R., Receptor modeling of near-roadway aerosol mass spectrometer data in Las Vegas, Nevada, with EPA PMF. *Atmos. Chem. Phys.* **2012,** *12*, (1), 309-325.
9. Ng, N. L.; Canagaratna, M. R.; Zhang, Q.; Jimenez, J. L.; Tian, J.; Ulbrich, I. M.; Kroll, J. H.; Docherty, K. S.; Chhabra, P. S.; Bahreini, R.; Murphy, S. M.; Seinfeld, J. H.; Hildebrandt, L.; Donahue, N. M.; DeCarlo, P. F.; Lanz, V. A.; Prévôt, A. S. H.; Dinar, E.; Rudich, Y.; Worsnop, D. R., Organic aerosol components observed in Northern Hemispheric datasets from Aerosol Mass Spectrometry. *Atmos. Chem. Phys.* **2010,** *10*, (10), 4625-4641.
10. Canagaratna, M. R.; Jayne, J. T.; Ghertner, D. A.; Herndon, S. C.; Shi, Q.; Jimenez, J. L.; Silva, P. J.; Williams, P.; Lanni, T.; Drewnick, F.; Demerjian, K. L.; Kolb, C. E.; Worsnop, D. R., Chase Studies of Particulate Emissions from in-use New York City Vehicles. *Aerosol Sci. Technol.* **2004,** *38*, 555-573.
11. Mohr, C.; Richter, R.; DeCarlo, P. F.; Prévôt, A. S. H.; Baltensperger, U., Spatial variation of chemical composition and sources of submicron aerosol in Zurich during wintertime using mobile aerosol mass spectrometer data. *Atmos. Chem. Phys.* **2011,** *11*, (15), 7465-7482.
12. Spracklen, D. V.; Jimenez, J. L.; Carslaw, K. S.; Worsnop, D. R.; Evans, M. J.; Mann, G. W.; Zhang, Q.; Canagaratna, M. R.; Allan, J.; Coe, H.; McFiggans, G.; Rap, A.; Forster, P., Aerosol mass spectrometer constraint on the global secondary organic aerosol budget. *Atmos. Chem. Phys.* **2011,** *11*, (23), 12109-12136.
13. Drewnick, F.; Hings, S. S.; DeCarlo, P. F.; Jayne, J. T.; Gonin, M.; Fuhrer, K.; Weimer, S.; Jimenez, J. L.; Demerjian, K. L.; Borrmann, S.; Worsnop, D. R., A New Time-of-Flight Aerosol Mass Spectrometer (TOF-AMS)—Instrument Description and First Field Deployment. *Aerosol Sci. Technol.* **2005,** *39*, (7), 637–658.
14. Crilley, L. R.; Ayoko, G. A.; Jayaratne, E. R.; Salimi, F.; Morawska, L., Aerosol Mass Spectrometric analysis of the chemical composition of non- refractory PM1 samples from school environments in Brisbane, Australia. *Sci. Tot. Environ.* **2013,** *458-460,* 81-89.
15. Jayne, J. T.; Leard, D. C.; Zhang, X.; Davidovits, P.; Smith, K. A.; Kolb, C. E.; Worsnop, D. R., Development of an Aerosol Mass Spectrometer for Size and

Composition Analysis of Submicron Particles. *Aerosol Sci. Technol.* **2000,** *33*, (1), 49-70.
16. Jimenez, J. L.; Jayne, J. T.; Shi, Q.; Kolb, C. E.; Worsnop, D. R.; Yourshaw, I.; Seinfeld, J. H.; Flagan, R. C.; Zhang, X.; Smith, K. A.; Morris, J. W.; Davidovits, P., Ambient aerosol sampling using the Aerodyne Aerosol Mass Spectrometer. *J. Geophys. Res.* **2003,** *108*, (D7), 8425-8438.
17. Paatero, P.; Tapper, U., Positive matrix factorization: A non-negative factor model with optimal utilization of error estimates of data values. *Environmetrics* **1994,** *5*, (2), 111-126.
18. Zhang, Q.; Jimenez, J.; Canagaratna, M.; Ulbrich, I.; Ng, N.; Worsnop, D.; Sun, Y., Understanding atmospheric organic aerosols via factor analysis of aerosol mass spectrometry: a review. *Anal. Bioanal. Chem.* **2011,** *401*, (10), 3045-3067.
19. Ng, N. L.; Canagaratna, M. R.; Jimenez, J. L.; Zhang, Q.; Ulbrich, I. M.; Worsnop, D. R., Real-Time Methods for Estimating Organic Component Mass Concentrations from Aerosol Mass Spectrometer Data. *Environ. Sci. Technol.* **2011,** *45*, (3), 910-916.
20. Mohr, C.; Huffman, J. A.; Cubison, M. J.; Aiken, A. C.; Docherty, K. S.; Kimmel, J. R.; Ulbrich, I. M.; Hannigan, M.; Jimenez, J. L., Characterization of Primary Organic Aerosol Emissions from Meat Cooking, Trash Burning, and Motor Vehicles with High-Resolution Aerosol Mass Spectrometry and Comparison with Ambient and Chamber Observations. *Environ. Sci. Technol.* **2009,** *43*, (7), 2443-2449.
21. Aiken, A. C.; DeCarlo, P. F.; Kroll, J. H.; Worsnop, D. R.; Huffman, J. A.; Docherty, K. S.; Ulbrich, I. M.; Mohr, C.; Kimmel, J. R.; Sueper, D.; Sun, Y.; Zhang, Q.; Trimborn, A.; Northway, M.; Ziemann, P. J.; Canagaratna, M. R.; Onasch, T. B.; Alfarra, M. R.; Prevot, A. S. H.; Dommen, J.; Duplissy, J.; Metzger, A.; Baltensperger, U.; Jimenez, J. L., O/C and OM/OC Ratios of Primary, Secondary, and Ambient Organic Aerosols with High-Resolution Time-of-Flight Aerosol Mass Spectrometry. *Environ. Sci. Technol.* **2008,** *42*, (12), 4478-4485.
22. Lee, J. H.; Hopke, P. K., Apportioning sources of PM2.5 in St. Louis, MO using speciation trends network data. *Atmos. Environ.* **2006,** *40, Supplement 2*, (0), 360-377.
23. Friend, A. J.; Ayoko, G. A.; Stelcer, E.; Cohen, D., Source apportionment of PM2.5 at two receptor sites in Brisbane, Australia. *Environ. Chem.* **2011,** *8*, (6), 569-580.
24. Chirico, R.; DeCarlo, P. F.; Heringa, M. F.; Tritscher, T.; Richter, R.; Prévôt, A. S. H.; Dommen, J.; Weingartner, E.; Wehrle, G.; Gysel, M.; Laborde, M.; Baltensperger, U., Impact of aftertreatment devices on primary emissions and secondary organic aerosol formation potential from in-use diesel vehicles: results from smog chamber experiments. *Atmos. Chem. Phys.* **2010,** *10*, (23), 11545-11563.
25. Zhang, Q.; Worsnop, D. R.; Canagaratna, M. R.; Jimenez, J. L., Hydrocarbon-like and oxygenated organic aerosols in Pittsburgh: insights into sources and processes of organic aerosols. *Atmos. Chem. Phys.* **2005,** *5*, (12), 3289-3311.
26. Sun, Y. L.; Zhang, Q.; Schwab, J. J.; Demerjian, K. L.; Chen, W. N.; Bae, M. S.; Hung, H. M.; Hogrefe, O.; Frank, B.; Rattigan, O. V.; Lin, Y. C., Characterization of the sources and processes of organic and inorganic aerosols in New York city with a high-resolution time-of-flight aerosol mass spectrometer. *Atmos. Chem. Phys.* **2011,** *11*, (4), 1581-1602.

27. Sun, Y. L.; Zhang, Q.; Schwab, J. J.; Chen, W. N.; Bae, M. S.; Hung, H. M.; Lin, Y. C.; Ng, N. L.; Jayne, J.; Massoli, P.; Williams, L. R.; Demerjian, K. L., Characterization of near-highway submicron aerosols in New York City with a high-resolution aerosol mass spectrometer. *Atmos. Chem. Phys.* **2012,** *12*, (4), 2215-2227.
28. Allan, J. D.; Williams, P. I.; Morgan, W. T.; Martin, C. L.; Flynn, J. L.; Nemitz, E.; Phillips, G. J.; Gallagher, M. W.; Coe, H., Contributions from transport, solid fuel burning and cooking to primary organic aerosols in two UK cities. *Atmos. Chem. Phys.* **2010,** *10*, (2), 647-668.
29. He, L.-Y.; Huang, X.-F.; Xue, L.; Hu, M.; Lin, Y.; Zheng, J.; Zhang, R.; Zhang, Y.-H., Submicron aerosol analysis and organic source apportionment in an urban atmosphere in Pearl River Delta of China using high-resolution aerosol mass spectrometry. *J. Geophys. Res.* **2011,** *116*, (D12), D12304.

Chapter 8. Analysis of organic aerosols collected on filters by Aerosol Mass Spectrometry for source identification

Leigh R. Crilley[1,2], Godwin A. Ayoko[1,2] and Lidia Morawska[1,2].

[1]International Laboratory for Air Quality and Health, Queensland University of Technology, Brisbane, QLD, 4001, Australia.

[2]Institute of Health and Biomedical Innovation, Queensland University of Technology, Brisbane, QLD, 4059, Australia.

(2013) *Analytica Chimica Acta.* 803, 91-96.

PREFACE

Field deployment of the AMS was not possible at all of the participating schools. Therefore this paper aimed to test and validate a novel methodology for the analysis of organic aerosols collected on filters by an AMS. The methodology was validated using the AMS data from the five schools where it sampled and gave good qualitative results. This enabled the main source of the organic aerosols to be determined at all of the schools in the project giving complementary information to Chapters 4 and 5.

Statement of joint authorship of co-authors

The authors listed below have certified* that:

1. they meet the criteria for authorship in that they have participated in the conception, execution, or interpretation, of at least that part of the publication in their field of expertise;
2. they take public responsibility for their part of the publication, except for the responsible author who accepts overall responsibility for the publication;
3. there are no other authors of the publication according to these criteria;
4. potential conflicts of interest have been disclosed to (a) granting bodies, (b) the editor or publisher of journals or other publications, and (c) the head of the responsible academic unit, and

5. they agree to the use of the publication in the student's thesis and its publication on the QUT ePrints database consistent with any limitations set by publisher requirements.

In the case of this chapter:

Analysis of organic aerosols collected on filters by Aerosol Mass Spectrometry for source identification, (2013) *Analytica Chimica Acta*, 803, 91-96.

Contributor	Statement of contribution*
Leigh R. Crilley	Conceived the study design, performed the field work, laboratory experiments, data analysis and wrote the manuscript.
Godwin A. Ayoko*	Provided overall direction for this study and assisted with the data analysis and drafting of the manuscript
Lidia Morawska*	Designed the overall concept of the study and assisted with the data interpretation and manuscript

Principal Supervisor Confirmation

I have sighted email or other correspondence from all Co-authors confirming their certifying authorship.

PROF GODWIN AYOKO — Name

Signature

22/11/2013 — Date

ABSTRACT

Aerosol mass spectrometers (AMS) are powerful tools in the analysis of the chemical composition of airborne particles, particularly organic aerosols which are gaining increasing attention. However, the advantages of AMS in providing on-line data can be outweighed by the difficulties involved in its use in field measurements at multiple sites. In contrast to the on-line measurement by AMS, a method which involves sample collection on filters followed by subsequent analysis by AMS could significantly broaden the scope of AMS application. We report the application of such an approach to field studies at multiple sites. An AMS was deployed at 5 urban schools to determine the sources of the organic aerosols at the schools directly. PM_1 aerosols were also collected on filters at these and 20 other urban schools. The filters were extracted with water and the extract run through a nebulizer to generate the aerosols, which were analysed by an AMS. The mass spectra from the samples collected on filters at the 5 schools were found to have excellent correlations with those obtained directly by AMS, with r^2 ranging from 0.89 to 0.98. Filter recoveries varied between the schools from 40 -115%, possibly indicating that this method provides qualitative rather than quantitative information. The stability of the organic aerosols on Teflon filters was demonstrated by analysing samples stored for up to two years. Application of the procedure to the remaining 20 schools showed that secondary organic aerosols were the main source of aerosols at the majority of the schools. Overall, this procedure provides accurate representation of the mass spectra of ambient organic aerosols and could facilitate rapid data acquisition at multiple sites where AMS could not be deployed for logistical reasons.

KEYWORDS: Organic Aerosols, Aerosol Mass Spectrometry, Source, Filter samples

8.1 INTRODUCTION

One of the more significant advancements in aerosol science in the past 20 years has been the development of aerosol mass spectrometers [1]. These instruments allow the chemical composition of airborne particles to be determined at higher temporal resolutions than traditional filter-based chemical analytical methods [2]. The Aerodyne Aerosol Mass Spectrometer (AMS), one of the more widely used types of these instruments measures quantitatively the chemical composition of the near-refractory particles with an aerodynamic diameter less than 1 μm (PM_1). Recent attention has focused on the organic fraction as measured by the AMS, as it is frequently the largest component in urban air [3]. Further simplification of the organic fraction into two main components based upon key mass to charge ratio (m/z) ions in the mass spectrum is possible: hydrocarbon-like organic aerosols (HOA) and oxygenated organic aerosols (OOA). The HOA component is characteristic of primary organic aerosols while the OOA can be considered as a surrogate for secondary organic aerosols [4, 5], thus the AMS offers insights into the origin of ambient organic aerosols.

The chemical composition information and high time resolution offered by the AMS can however be outweighed by the numerous difficulties in field measurements with an AMS, including the transportation, set-up, maintenance and the need for adequate housing of the instrument. By comparison, filter based sampling is relatively easy and an inexpensive method to perform in the field, and the filters can be easily stored. Therefore a procedure that can allow for the analysis of filter samples obtained from the field by an AMS back in the laboratory, would improve the scope

and application of the AMS markedly, particularly for sampling across many sites during one project.

Preliminary results from an AMS studies of filter samples extracted by water was described previously [6]. Based on these promising results we thus undertook a comprehensive study to test and validate this approach using samples at multiple sites where an AMS directly measured the ambient OA. In the current study, PM_1 filter samples were collected at 25 urban schools whereas an AMS sampled at five of the 25 schools. For the remaining 20 schools, the filter extraction method was applied retrospectively to the PM_1 filter samples in order to determine the water soluble organic aerosols mass spectra at these schools. Based on the determined mass spectrum, the source of the organic aerosols was investigated at each school to determine the contributions of primary and secondary sources.

8.2 METHOD

8.2.1 Sampling Sites

This paper utilises TOF-AMS measurements and PM_1 filter samples that were collected as a part of a larger study investigating the effect of ultrafine particles from traffic emissions on children's health, known as UPTECH (www.ilaqh.qut.edu.au/Misc/UPTECH%20Home.htm). The twenty-five schools selected are referred to as S01 to S25 and were in different suburbs of the Brisbane Metropolitan area. The schools that participated were not near any major pollution sources apart from traffic emissions. Measurements at the schools were conducted from October 2010 to August 2012. More details of the school sites and sampling conditions at the AMS schools can be found in Crilley et al. [7].

8.2.2 AMS field operation

An Aerodyne compact Time-Of-Flight Aerosol Mass Spectrometer (TOF-AMS) was used for this work and a description of the instrument and its operation has been given previously [8, 9]. In brief, the TOF-AMS is an on-line instrument that measures quantitatively both the size distribution and chemical composition of the non-refractory portion of approximately PM_1 particles. An aerodynamic lens is used to sample the particles, which are focused into a narrow beam prior to entering the sizing chamber. After passing through the chamber, volatile and semi-volatile particles are thermally vaporised and then ionised before analysis by a time-of-flight mass spectrometer. The TOF-AMS was available to run at only 5 schools, S01, S04, S11, S12 and S25, which will be referred to as the "AMS schools" throughout the paper, with the remaining schools referred to as "non-AMS schools". A full description of the TOF-AMS field operation is available in Crilley et al. [7]. In brief, the TOF-AMS was housed in a vacant classroom within the school and sampled continuously with a five-minute interval for two to three weeks at each school. Ambient outdoor air was sampled at a sampling height of about 1.5 m.

8.2.3 Filter sampling method

PM_1 filters were collected at all of the 25 schools and the filter set-up was housed within a trailer at a site that was assumed to give the best overall exposure. This site was never more than 150 m from the classroom housing the TOF-AMS at the corresponding school. Filters were collected using a PM_1 cyclone, with the required flow rate for the cyclone maintained by critical orifices. Four filters were collected at each school, over a sampling interval of 24 hours (8 am till 8 am the following morning), Monday till Friday with a typical sample volume of 8.2 m^3. Samples were

collected on 47 mm, 0.2 μm pore size commercially available Teflon filters (Whatman) and the sampling inlets were approximately 3 m off the ground. At the schools where the TOF-AMS sampled, the distance between the TOF-AMS classroom and filter sampling site varied from 50 to 150 m. The filter sampling and TOF-AMS measurements were conducted concurrently at the schools. After sampling, the filters were placed in a Petri dish, sealed in a plastic ziplock bag and stored for analysis.

8.2.4 Filter extraction and analysis method

Extraction of the water soluble organic aerosols (WSOA) from the PM_1 filter samples and subsequent analysis by TOF-AMS was conducted at the International Laboratory for Air Quality and Health, Queensland University of Technology. In the extraction method employed in this study, the filters were submerged in 25 ml of Milli-Q water (18.2 MΩ cm) and ultrasonicated for 45 minutes. To ensure enough particle mass was extracted for subsequent analysis on the TOF-AMS, the four filters collected at each school were extracted individually, one after the other into one solution. The filter extract solution was run through a nebulizer to generate the aerosols and then dried over silica, prior to being introduced into the TOF-AMS. For the analysis of the filter extract solution, the TOF-AMS was operated using the same settings employed during the school measurements, except that the sampling interval was reduced from 5 minutes to 1 minute.

8.2.5 Quality Control

Routine calibration of the ionization efficiency for the TOF-AMS was conducted according to the standard protocols [9-11] in both the schools and in the laboratory for the filter testing. Using the method set out in Zhang et al. [12], the detection limit

for the organic fraction was calculated for the filter MS analysis to be on average 78 ± 23 ng m^{-3}. This was comparable with the average detection limit for organics observed by Zhang et al. [12] and previous sampling of ambient air at the AMS schools [7].

8.2.6 Data Analysis

TOF-AMS data was processed and analysed using Squirrel v1.51 in IGOR Pro v6.22. In this study only the organic fraction mass spectrum was compared. For the validation of the filter extraction method, only TOF-AMS data that corresponded to the filter sampling times were used. The average organic mass spectrum (MS) calculated from these times will be referred to as the ambient MS throughout the paper. At each of the 5 schools where a TOF-AMS was deployed the ambient MS was correlated to the average mass spectrum from the filter extract solution, which will be referred to as the filter MS. For every filter MS the m/z 15, 29 and 31 ions were found to be outliers as they were at least an order of magnitude higher than in the ambient MS and were subsequently removed.

Pearson's correlation coefficients and associated errors were calculated using SPSS v19. Errors for the correlation coefficients were calculated by bootstrapping analysis at a 95% confidence interval using 1000 bootstrap samples. All correlations reported for the comparison of ambient and filter MS were found to be significant below a 0.01 level. Filter recoveries were calculated by comparing the total mass of the organic m/z ions as determined the TOF-AMS for the ambient sampling and filter samples.

Standard mass spectral profiles of the different OA components, HOA, SV-OOA, LV-OOA and BBOA are given in Ng et al. [13] based upon the analysis of 15 urban datasets. These spectra have been used as reference spectra in this study for comparison with the filter MS for identifying the main source of the OA. There have been several m/z ions which have been shown to be key ions in the analysis of ambient organic aerosol (OA) and these include the m/z 44 and 57 ions [13]. The m/z 44 and 57 ions have been shown to be tracer ions for oxygenated OA (OOA) and hydrocarbon-like OA (HOA), respectively. OOA is considered as a surrogate for secondary OA, while the HOA is similar to vehicle emissions [4, 5] . Thus the m/z 44 and 57 ions are used as tracer ions for secondary OA and vehicle emissions in this study for determining the sources at the schools.

One way of comparing the OA from different sites is to plot the f_{43} and f_{44} ratios. The f_{43} and f_{44} ratio refer to the ratio of the m/z 43 and 44 ions, respectively, to the total organic mass. OA has been shown to occupy a defined triangle space within this plot, and can give information on the degree of oxidation of the OA [14]. HOA components have an f_{44} that is less than 0.05 and so are found along the base of the triangle. OOA has a higher f_{44} ratio and thus can be used to show the degree of oxidation of the OOA, so that the more oxidised and hence more aged OA are found closer to the top of the triangle [14, 15].

8.3 RESULTS AND DISCUSSION

8.3.1 Validation of the filter extraction method

In Figure 8-1, the ambient and filter mass spectra for each school are given, along with the Pearson's correlation coefficient between the filter and ambient MS. Excellent agreements between the ambient and filter MS was found with the

Pearson's correlation coefficient ranging from 0.89 to 0.98, a similar result to El Haddad et al. [6], thus indicating that the OA was successfully extracted from the filters. One negative aspect of the filter MS was the low concentration of fragments above m/z 60, suggesting that the large organic compounds may not have been extracted completely. S01 and S04 were found to have slightly lower correlations than the other three schools. The precise reasons for this observation are currently unknown. However it is probably due to the fact that the OA at these schools were less oxidized and therefore less water-soluble. S01 and S04 were sampled in November 2010 and March 2011, respectively and were analysed on the AMS in November 2012, which demonstrates the stability of WSOA sampled on Teflon filters. Therefore, this technique can be applied to samples collected over two years ago. Provided the filter are stored below 25°C and away from sources of contamination a true representation of the MS of the WSOA can still be obtained.

Filter recoveries varied between the schools from 40-115%. Teflon filters that were used for the sampling may have contributed to the variable recoveries, as Teflon repels water, thus inhibiting the extraction. However, the filter MS from these schools still showed the overall character of the ambient MS and are therefore representative of the ambient OA at the schools indicating that it is a good qualitative method. To further compare the filter MS and ambient MS, the correlations were determined between key m/z ions, 43, 44 and 57. The filter and ambient f_{43}, f_{44} and

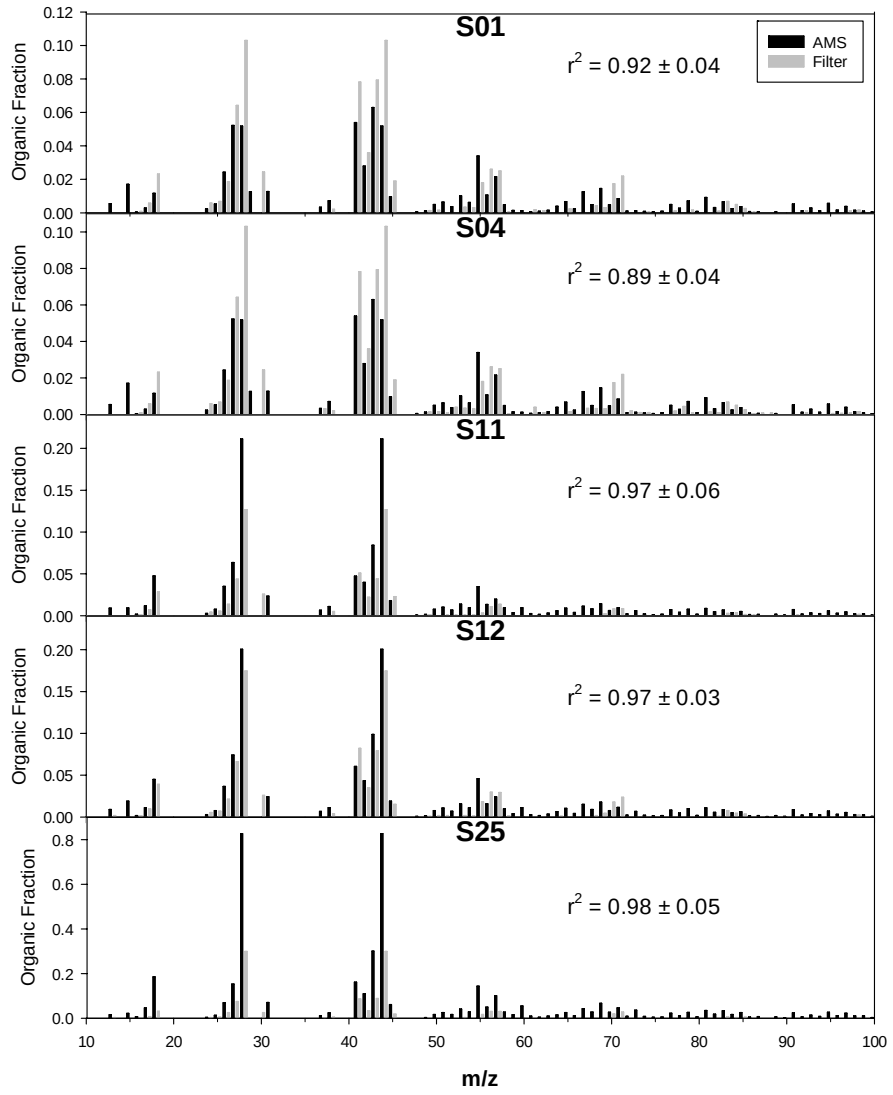

Figure 8-1: Comparison of the ambient and filter mass spectra at the five AMS schools, with the Pearson's correlations shown.

f_{57} ratios, gave Pearson's correlation coefficient scores of 0.84 ± 0.49, 0.94 ± 0.04 and 0.89 ± 0.25, respectively at a significant level of 0.05. Though there was a large error associated with the f_{43} ratio, the values from the ambient and filter MS were within 10% of each other at all 5 schools. As the m/z 43 and 57 ions are associated more with fragments from HOA than the more oxidized OOA [13], the likely cause of the large errors was that the HOA is less water soluble. Overall, the high

correlations coefficients found for these key tracer ions indicate that this extraction method can be used for a qualitative assessment of the source of the OA.

8.3.2 Comparison of sources at the schools

As the filter extraction and analysis method produced good qualitative results it was applied to the filters from the remaining 20 schools. The filter MS results from all the schools are summarized in Table 8-1; with example filter MS from selected schools representative of the three observed OA types shown in Figure 8-3. In Appendix 6, Figures A61-3, the filter MS for the additional schools are given. To aid in the comparison of the OA at each school, the f_{43} and f_{44} ratios were plotted as shown in Figure 8-2.

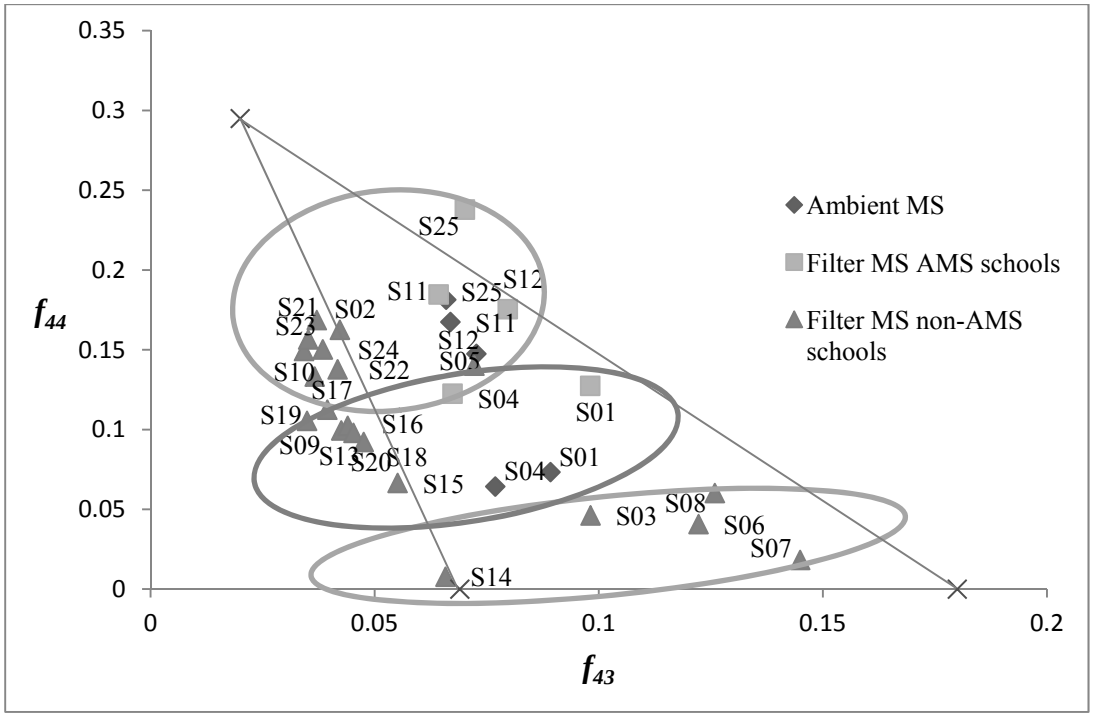

Figure 8-2: Plot of the f_{44} v f_{43} ratios for the ambient and filter MS for the schools where the AMS was deployed and the filer MS from the remaining 20 schools.

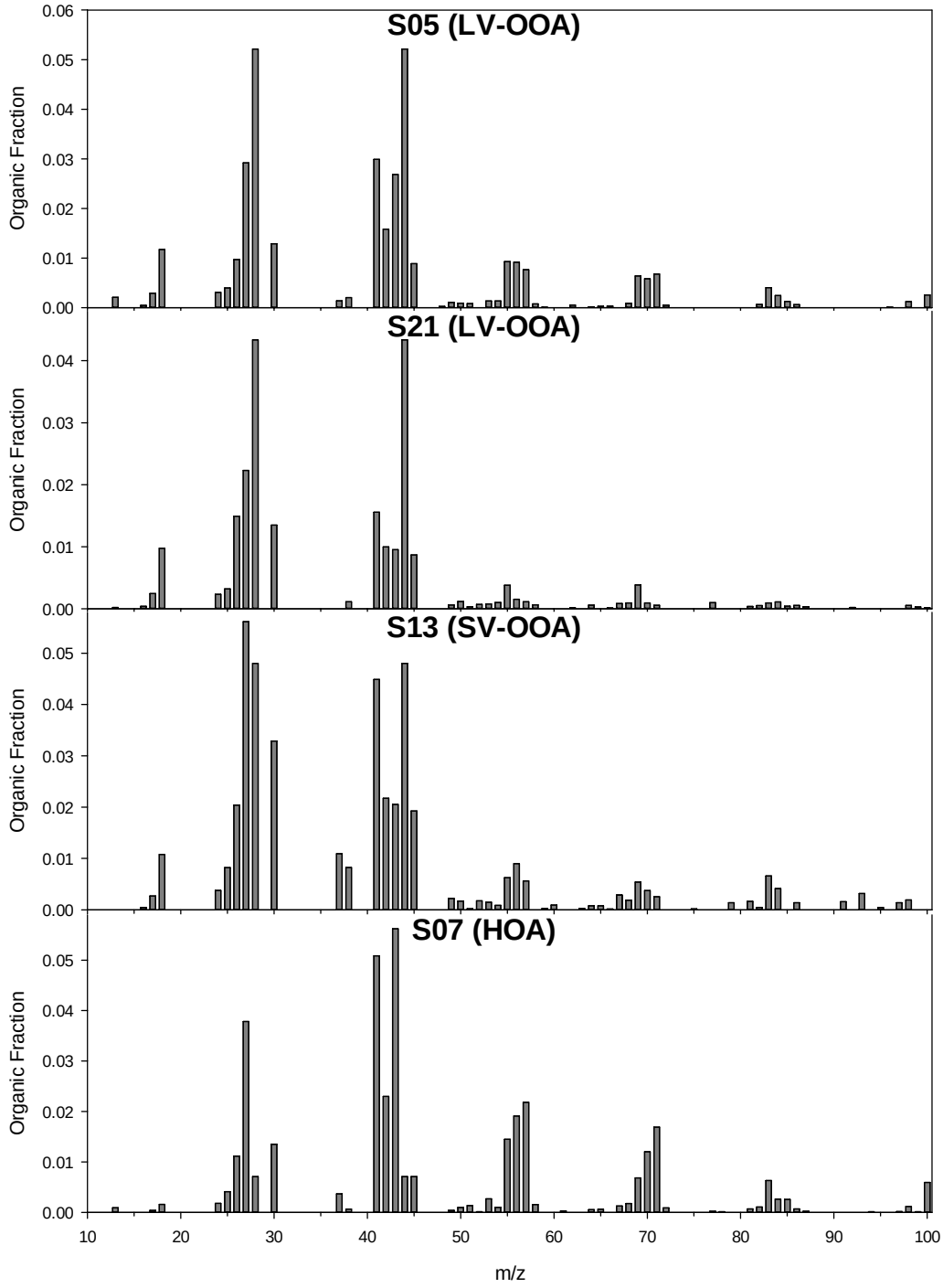

Figure 8-3: Filter MS from selected schools as examples of the different types of organic aerosols.

In Figure 8-2 there are three clusters of schools, separated based upon the f_{44} ratio and therefore source of the OA. From Figure 8-2, the OA at the AMS schools was found to be either SV-OOA or LV-OOA at S01, S04 and S11, S12, S25, respectively in agreement with the results from Crilley et al. [7]. When the AMS and non-AMS

schools were found to have a similar type of organic MS, the MS agreed well by visual inspection, having similar prominent ions.

Table 8-1: The filter MS values for f_{44} and f_{57} for the non-AMS schools and the type of OA based upon comparison to reference spectra.

School	f_{44}	f_{57}	Type of OA
S02	0.163	0.013	LV-OOA
S03	0.046	0.048	HOA
S05	0.140	0.021	LV-OOA
S06	0.041	0.050	HOA
S07	0.018	0.056	HOA
S08	0.060	0.047	HOA
S09	0.105	0.012	LV-OOA
S10	0.149	0.010	LV-OOA
S13	0.099	0.012	SV-OOA
S14	0.008	0.007	HOA
S15	0.067	0.006	SV-OOA
S16	0.102	0.013	LV-OOA
S17	0.133	0.005	LV-OOA
S18	0.098	0.009	SV-OOA
S19	0.113	0.002	LV-OOA
S20	0.092	0.005	SV-OOA
S21	0.169	0.004	LV-OOA
S22	0.138	0.006	LV-OOA
S23	0.157	0.003	LV-OOA
S24	0.150	0.000	LV-OOA

8.3.2.1 ***Hydrocarbon-like organic aerosols***

The schools with a f_{44} ratio less than 0.05 which included S03, S06-8 and S14 (Table 8-1) were in the HOA region of Figure 8-2 [14]. These schools had a filter MS that were similar to the HOA standard spectra from Ng et al. [13] because the strongest peaks are the m/z 41 and 43 ions; confirming the HOA nature of the OA. From Table 8-1, the schools in the HOA region also had the highest f_{57} ratios, with the exception of S14. This is as expected, as the m/z 57 ion has been shown to be a tracer ion for HOA [13] and further confirms the source identification. At S14 the m/z 43 and 57

ion peaks did not have the same intensity as the m/z 41 and 55 ion peaks (Figure A6-2), as would be expected for HOA [13]. Therefore at S14 another primary source of OA was dominant, and was likely to be cooking OA (COA), as previous studies have shown that the intensity of the m/z 55 is much stronger than that of the m/z 57 ion in the MS for COA [16, 17].

*8.3.2.2 **Oxygenated organic aerosols***

Most of the schools had an f_{44} ratio above 0.05 and are therefore in the OOA region of the triangle plot (Figure 8-2) [14]. Of the schools in the OOA regions, the distinction between SV-OOA and LV-OOA at the schools was not always clear due to the oxidation levels of ambient OOA being a continuum. However, a separation between SV-OOA and LV-OOA is present in Figure 8-2, with the two groups of schools having distinct differences in the MS and are separated based upon the level of oxidation. In the middle of the triangle plot S01, S04, S13, S15, S18 and S20 have clustered with f_{44} ratios between 0.067 – 0.099 (Table 8-1), and are within the region associated with SV-OOA [14]. Also these schools had MS with prominent peaks at m/z 41, 43 and 44 (See Figures 8-1 and 8-3) and in this respect were more similar to the standard SV-OOA MS from Ng et al. [13], confirming the source identification. At S01 and S04 the WSOA MS was found to resemble the SV-OOA standard spectra, for both the ambient and filter MS. These were similar to the filter MS from the non-AMS schools, S13, S15, S18 and S20 and were characterized by approximately equal intensities of the m/z 41, 43 and 44 ions. In our previous work [7], we attributed the SV-OOA at S04 to slightly aged vehicle emissions from nearby highways due to the similarities of the MS for aged diesel exhaust obtained by Sage et al. [18]. Therefore, slightly aged vehicle emissions were likely to be a dominant source at S13, S15, S18 and S20.

The remaining schools which formed the third and largest cluster had f_{44} ratios that were higher than the other two groups, ranging from 0.102 – 0.169 (Table 8-1). This group were in the LV-OOA region and the MS from these schools (See Figures 8-1 and 8-3) had a strong m/z 44 ion peak intensity relative to the other peaks, and were thus similar to the LV-OOA standard MS [13] indicating a regional source of the OA at these schools [5,14]. At S11, S12 and S25 the LV-OOA MS were also consistent for the ambient and filter MS as they were all within the LV-OOA region of the triangle plot (Figure 8-2). In addition, the LV-OOA filters MS at the non-AMS schools (Table 8-1) were similar to ambient MS from S11, S12 and S25, characterized by a strong m/z 44 ion concentration relative to other m/z ions. In Figure 8-2, the filter MS from the non-AMS schools also fell within the LV-OOA region of Figure 8-2, however these were generally separate from S11, S12 and S25, with the exception of S05. These variations were likely as a result of differences in the regional OA present during sampling at the AMS and non-AMS schools which is conceivable as the sampling at the schools was undertaken at different times of the year.

8.4 CONCLUSIONS

Overall, the simple procedure described in this paper, which involved water extraction of filter samples followed by analysis on a TOF-AMS has been shown to provide an accurate representation of the MS of ambient OA. Application of this procedure enabled the source of the OA to be distinguished between primary and secondary sources at the schools where a TOF-AMS was not deployed. Therefore this offers a simplified approach to field measurements at multiple sites and also

extended the possible applications of TOF-AMS to locations where deployment is difficult. In addition, the current paper demonstrated the stability of the WSOA on Teflon filters, enabling the analysis of samples that were stored for up to two years. Possible future work should aim to improve the extraction method to enable more quantitative measurements and thus extending it to the other chemical species measured by an AMS.

ACKNOWLEDGMENTS
We would like to thank Prof Urs Baltensperger, Paul Scherrer Institut for useful discussions on the procedure adapted in this study. This work was supported by the Australian Research Council (ARC), Department of Transport and Main Roads (DTMR) and Department of Education, Training and Employment (DETE) through Linkage Grant LP0990134. Our particular thanks go to R. Fletcher (DTMR) and B. Robertson (DETE) for their vision regarding the importance of this work. We would also like to thank all members of the UPTECH project, including Prof G. Marks, Dr P. Robinson, Prof K. Mengersen, Prof Z. Ristovski, Dr M. Mazaheri, Dr C. He, Dr G. Johnson, Dr R. Jayaratne, Dr S. Low Choy, Prof G. Williams, W. Ezz, F. Salimi, L. Crilley, S. Clifford, M. Mokhtar, N. Mishra, R. Laiman, L. Guo, Prof C. Duchaine, Dr H. Salonen, Dr X. Ling, Dr J. Davies, Dr L. Leontjew Toms, F. Fuoco, Dr A. Cortes, Dr B. Toelle, A. Quinones and P. Kidd for their contribution to this work. We thank former ILAQH, QUT members Dr M. Falk, Dr F. Fatokun, Dr J. Mejia and Dr D. Keogh for their contributions at the early stage of the project. Thanks also to Prof T. Salthammer from Fraunhofer WKI in Germany for VOC analysis, R. Appleby and C. Labbe for their administrative assistance.

8.5 REFERENCES

1. McMurry, P. H., A review of atmospheric aerosol measurements. *Atmos. Environ.* **2000,** *34*, (12-14), 1959-1999.

2. Laskin, A.; Laskin, J.; Nizkorodov, S. A., Mass spectrometric approaches for chemical characterisation of atmospheric aerosols: critical review of the most recent advances. *Environ. Chem.* **2012,** *9*, (3), 163-189.
3. Jimenez, J. L.; Canagaratna, M. R.; Donahue, N. M.; Prevot, A. S. H.; Zhang, Q.; Kroll, J. H.; DeCarlo, P. F.; Allan, J. D.; Coe, H.; Ng, N. L.; Aiken, A. C.; Docherty, K. S.; Ulbrich, I. M.; Grieshop, A. P.; Robinson, A. L.; Duplissy, J.; Smith, J. D.; Wilson, K. R.; Lanz, V. A.; Hueglin, C.; Sun, Y. L.; Tian, J.; Laaksonen, A.; Raatikainen, T.; Rautiainen, J.; Vaattovaara, P.; ehn, M.; Kulmala, M.; Tomlinson, J.; Collins, D. R.; Cubison, M. J.; Dunlea, E. J.; Huffman, A.; Onasch, T. B.; Alfarra, M. R.; Williams, P. I.; Bower, K. N.; Kondo, Y.; Schneider, J.; Drewnick, F.; Borrmann, S.; Weimer, S.; Demerjian, K. L.; Salcedo, D.; Cottrell, L.; Griffin, R.; Takami, A.; Miyoshi, T.; Hatakeyama, S.; Jayne, J. T.; Herndon, S. C.; Trimborn, A.; Williams, L. R.; Wood, E. C.; Middlebrook, A.; Kolb, C. E.; Baltensperger, U.; Worsnop, D. R., Evolution of Organic Aerosols in the Atmosphere *Science* **2009,** *326*, 1525-1529.
4. Zhang, Q.; Alfarra, M. R.; Worsnop, D. R.; Allan, J. D.; Coe, H.; Canagaratna, M. R.; Jimenez, J. L., Deconvolution and Quantification of Hydrocarbon-like and Oxygenated Organic Aerosols Based on Aerosol Mass Spectrometry. *Environ. Sci. Technol.* **2005,** *39*, (13), 4938-4952.
5. Lanz, V. A.; Alfarra, M. R.; Baltensperger, U.; Buchmann, B.; Hueglin, C.; Prévôt, A. S. H., Source apportionment of submicron organic aerosols at an urban site by factor analytical modelling of aerosol mass spectra. *Atmos. Chem. Phys.* **2007,** *7*, (6), 1503-1522.
6. El Haddad, I.; Slowik, J. G.; Baltensperger, U.; Prévôt, A. S. H. *In Proceeeding of the European Aerosol Conference*, *Granada*. 2012.
7. Crilley, L. R.; Ayoko, G. A.; Jayaratne, E. R.; Salimi, F.; Morawska, L., Aerosol Mass Spectrometric analysis of the chemical composition of non- refractory PM1 samples from school environments in Brisbane, Australia. *Sci. Total Environ.* **2013,** *458-460,* 81-89.
8. Canagaratna, M. R.; Jayne, J. T.; Jimenez, J. L.; Allan, J. D.; Alfarra, M. R.; Zhang, Q.; Onasch, T. B.; Drewnick, F.; Coe, H.; Middlebrook, A.; Delia, A.; Williams, L. R.; Trimborn, A. M.; Northway, M. J.; DeCarlo, P. F.; Kolb, C. E.; Davidovits, P.; Worsnop, D. R., Chemical and microphysical characterization of ambient aerosols with the Aerodyne aerosol mass spectrometer. *Mass Spectrom. Rev.* **2007,** *26*, 185-222.
9. Drewnick, F.; Hings, S. S.; DeCarlo, P. F.; Jayne, J. T.; Gonin, M.; Fuhrer, K.; Weimer, S.; Jimenez, J. L.; Demerjian, K. L.; Borrmann, S.; Worsnop, D. R., A New Time-of-Flight Aerosol Mass Spectrometer (TOF-AMS)—Instrument Description and First Field Deployment. *Aerosol Sci. Technol.* **2005,** *39*, (7), 637–658.
10. Jayne, J. T.; Leard, D. C.; Zhang, X.; Davidovits, P.; Smith, K. A.; Kolb, C. E.; Worsnop, D. R., Development of an Aerosol Mass Spectrometer for Size and Composition Analysis of Submicron Particles. *Aerosol Sci. Technol.* **2000,** *33*, (1), 49-70.
11. Jimenez, J. L.; Jayne, J. T.; Shi, Q.; Kolb, C. E.; Worsnop, D. R.; Yourshaw, I.; Seinfeld, J. H.; Flagan, R. C.; Zhang, X.; Smith, K. A.; Morris, J. W.; Davidovits, P., Ambient aerosol sampling using the Aerodyne Aerosol Mass Spectrometer. *J. Geophys. Res.* **2003,** *108*, (D7), 8425-8438.

12. Zhang, Q.; Canagaratna, M. R.; Jayne, J. T.; Worsnop, D. R.; Jimenez, J. L., Time- and size-resolved chemical composition of submicron particles in Pittsburgh: Implications for aerosol sources and processes. *J. Geophys. Res.* **2005,** *110*, D07S09.
13. Ng, N. L.; Canagaratna, M. R.; Jimenez, J. L.; Zhang, Q.; Ulbrich, I. M.; Worsnop, D. R., Real-Time Methods for Estimating Organic Component Mass Concentrations from Aerosol Mass Spectrometer Data. *Environ. Sci. Technol.* **2011,** *45*, (3), 910-916.
14. Ng, N. L.; Canagaratna, M. R.; Zhang, Q.; Jimenez, J. L.; Tian, J.; Ulbrich, I. M.; Kroll, J. H.; Docherty, K. S.; Chhabra, P. S.; Bahreini, R.; Murphy, S. M.; Seinfeld, J. H.; Hildebrandt, L.; Donahue, N. M.; DeCarlo, P. F.; Lanz, V. A.; Prévôt, A. S. H.; Dinar, E.; Rudich, Y.; Worsnop, D. R., Organic aerosol components observed in Northern Hemispheric datasets from Aerosol Mass Spectrometry. *Atmos. Chem. Phys.* **2010,** *10*, (10), 4625-4641.
15. Ng, N. L.; Canagaratna, M. R.; Jimenez, J. L.; Chhabra, P. S.; Seinfeld, J. H.; Worsnop, D. R., Changes in organic aerosol composition with aging inferred from aerosol mass spectra. *Atmos. Chem. Phys.* **2011,** *11*, (13), 6465-6474.
16. Huang, X. F.; He, L. Y.; Hu, M.; Canagaratna, M. R.; Sun, Y.; Zhang, Q.; Zhu, T.; Xue, L.; Zeng, L. W.; Liu, X. G.; Zhang, Y. H.; Jayne, J. T.; Ng, N. L.; Worsnop, D. R., Highly time-resolved chemical characterization of atmospheric submicron particles during 2008 Beijing Olympic Games using an Aerodyne High-Resolution Aerosol Mass Spectrometer. *Atmos. Chem. Phys.* **2010,** *10*, (18), 8933-8945.
17. Mohr, C.; DeCarlo, P. F.; Heringa, M. F.; Chirico, R.; Slowik, J. G.; Richter, R.; Reche, C.; Alastuey, A.; Querol, X.; Seco, R.; Peñuelas, J.; Jiménez, J. L.; Crippa, M.; Zimmermann, R.; Baltensperger, U.; Prévôt, A. S. H., Identification and quantification of organic aerosol from cooking and other sources in Barcelona using aerosol mass spectrometer data. *Atmos. Chem. Phys.* **2012,** *12*, (4), 1649-1665.
18. Sage, A. M.; Weitkamp, E. A.; Robinson, A. L.; Donahue, N. M., Evolving mass spectra of the oxidized component of organic aerosol: results from aerosol mass spectrometer analyses of aged diesel emissions. *Atmos. Chem. Phys.* **2008,** *8*, (5), 1139-1152.

Chapter 9. Conclusions

9.1 RESEARCH SUMMARY AND OUTCOMES

A comprehensive review of the relevant literature revealed a number of gaps in the understanding in the sources of children's exposure to airborne particles at school and their potential toxicity. In the literature review vehicle emissions were identified as the main primary sources of airborne fine particles in urban areas including Brisbane. Children were identified in the literature review as being highly susceptible to the detrimental health effects of vehicle emissions. Schools were chosen as the location of main body of research as children spend a large portion of the day at school and schools are controllable environments in which to measure exposure for large cohorts. Furthermore schools are unique urban environments as they are affected not only by local primary sources but also emissions from school related activities such as drop-off/pick up traffic. However, the concentration of vehicle emissions and the contribution of local and school traffic at school are not known. In addition, it is not known whether it is vehicle emissions or other primary and secondary sources that are the main sources of children's exposure at school. As vehicle emissions are mostly carbonaceous in nature, a focus of the research was on the source identification and apportionment of OA as there is limited information on the source profiles in Southern Hemisphere cities. Overall, the variation in concentration of vehicle emissions and secondary aerosols during school hours and the factors contributing to increased exposure at schools are not known.

In general, there is limited literature on children's exposure to vehicle emissions and other sources at school [1]. *Thus the main objective of this study was to determine the sources of ambient particles that children are exposed to at school and the driving factors.* Without adequate information on the chemical and physical properties of airborne particles at school, an assessment of the potential toxicity is not possible. Therefore along with the primary objective, *a secondary objective was to determine the potential toxicity of the vehicle emissions based upon the chemical composition*. To address these two objectives, this thesis comprised of a pilot tunnel study on

vehicle emissions and a comprehensive program of research on the chemical composition of airborne particles at urban schools. Selected established and novel analytical techniques were drawn from the literature and applied at the participating schools to determine the source contributions and driving factors, as well as the potential toxicity. This body of research resulted in the production of six peer-reviewed papers in fields of analytical, atmospheric, environmental chemistry and air pollution (Chapter 3-8) that aimed to address these objectives as outlined in the next paragraphs.

The initial pilot study, presented in the first paper (Chapter 3) was conducted in a tunnel in Brisbane to probe the effect of traffic counts and composition on the levels traffic emissions and its toxicity. This represented the first on-road measurements of particle associated oxidative potential of vehicle emissions under 'real world' dilutions. Thus it addressed the second objective by enabling the key parameters affecting the toxicity of vehicle emissions to be determined, which were subsequently applied in the analysis of children's exposure at urban schools.

The physical and chemical properties of fine airborne particles were investigated at 25 urban schools in Brisbane to determine the sources and driving factors of children's exposure at school. The analytical techniques selected from the literature for this research were well suited to the source identification and apportionment of ambient particles to address the primary objective. In one paper (Chapter 4), the $PM_{2.5}$ EC and OC concentrations were analysed with the aim of distinguishing the contributions from primary and secondary sources to the carbonaceous aerosols. This enabled the factors contributing to the observed levels of vehicle emissions and SOA, along with the characteristics of high exposure schools to be established. In addition to the EC and OC sampling, the trace elemental composition of the PM_1 fraction was analysed at each school to give complementary information on the sources at the schools, such as from non-exhaust vehicle emissions and industry.

The paper comprising Chapter 5 presents the analysis of the trace elemental PM_1 composition at the schools and addresses both the primary and secondary objectives.

Investigating the elemental composition of the airborne particles allowed for the contributing sources to be determined. The PM_1 elemental composition was compared to the $PM_{2.5}$ composition in Brisbane in the literature to ascertain the size distribution of the heavy metals and therefore the potential toxicity. Alongside the filter analysis conducted at the schools, an AMS was deployed at selected schools as it high time resolution afforded more detailed analysis detailed analysis on the contributing sources and factors.

A particular focus of the AMS analysis was on OA as it is the typically the largest component in urban areas [2] and vehicle emissions are mostly carbonaceous [3]. The high time resolution offered by an AMS compared to the filter analysis allowed for the temporal variation in the OA and its components (both primary and secondary) to be determined. The concentration of vehicle emissions that children are actually exposed to during school hours at school and the influence of local and school traffic were explored in the paper forming chapter 6. The sources of OA, the largest component of the NR-PM_1, at the schools was analysed in accordance with the primary objective. In Chapter 7 the source apportionment of the OA was performed using an advanced data analysis technique, Positive Matrix Factorisation (PMF). The contributing sources at the schools were determined and the primary and secondary sources compared using multivariate techniques to determine the variation of the source profiles. As field deployment of the AMS was not possible for every school, a novel filter based method for the analysis of the OA by AMS was developed and validated. Thus the main source of the OA at all 25 schools was identified (Chapter 8). Therefore this methodology offers a simplified approach to field measurements with an AMS and also extends its application to locations where deployment is difficult.

Therefore the six research papers presented addressed the primary and secondary objectives of this thesis, and resulted in the following research outcomes. The pilot tunnel study found that the total traffic counts were better correlated with pollutant levels and oxidative potential than the traffic composition (gasoline and diesel

vehicles). This knowledge was applied to determine the driving factors to children's exposure at school in the five papers in this thesis that investigated the physical and chemical properties of ambient fine particles at urban schools (Chapters 4 - 8). These five papers revealed different aspects to children's exposure at school as well as several common characteristics, as detailed in the next section.

9.1.1 Children's Exposure at School

Each of the five papers used different analytical and data techniques to investigate different aspects of children's exposure at school. It should be noted that the results from this thesis do not necessarily indicate which school were most polluted; rather the focus was on determining the contributing sources and the driving factors. From the different analytical techniques applied in this study, several common characteristics were observed in the ambient particles at the schools. Overall, there were five types of sources, which included secondary sources (both organic and sulphate), biomass burning, shipping, vehicle and industrial emissions were identified at the schools through Chapters 4-8. A common finding from all of the papers was that children were predominantly exposed secondary rather than primary particles emissions at school. From the PMF analysis in Chapter 7, the OOA factors demonstrated a temporal rather than a spatial variation and were more unique than the primary source factor profiles. The apparent lack of spatial variation indicates that PMF-derived factors from a receptor site are applicable across an urban area. At the majority of the schools, the SOA was generally highly oxidised, so it was attributed to regional sources. However, some influence from both freshly formed SOA related to increased solar radiation as well as a source attributed to slightly aged vehicle emissions was observed.

Vehicle emissions were generally the largest anthropogenic source at the schools. The vehicle emissions sources was characterised by Pb, Br, Mn and Ti (Chapter 5) and EC and POC (Chapter 4). The highest concentrations of vehicle emissions were generally observed at schools near busy roads and total traffic counts rather than traffic composition were the better indicator of the levels of vehicle emissions at the schools. The wind direction relative to surrounding roads was also an important parameter in the observed concentrations of vehicle emissions, and the effect was

explicitly demonstrated in the Chapter 7 with the CPF analysis of HOA factors. In addition to the local traffic emissions, school-related traffic was found to possibly contribute to elevated concentrations of Pb, Br and Ni as the concentrations were elevated at the schools compared to other Brisbane locations [4]. Drop-off and pick up times observed to be the periods of maximum exposure for children at school to vehicle emissions. This highlights times where future control strategies may be focused in order to limit children's exposure. Overall, the findings from the research conducted for this thesis lead to the conclusions outlined in the next section.

9.2 CONCLUSIONS

The research conducted in this thesis led to the following conclusions:

1. Total traffic volume as opposed to traffic composition was a better indicator of vehicle particle emissions and their potential toxicity.
2. The toxic heavy metals (Cr, Pb, Ni, V, Cu and Zn) were predominantly found in the PM_1 fraction which suggests it is potentially a better fraction to use when studying the health effects of airborne particles.
3. Unless a school is located near (<500m) a major road, during school hours children are exposed predominantly to regional SOA rather than vehicle emissions.
4. Levels of vehicle emissions at the schools were primarily dependent on total traffic counts on surrounding roads and secondly on the wind direction relative to the surrounding roads.
5. School drop off and pick up times represented the periods of maximum exposure to vehicle emissions for school children at the schools studied.
6. While local meteorology affected the measured concentrations, overall the range of concentrations measured can be considered as representative of children's exposure to vehicle emissions and SOA at schools with similar traffic conditions.

9.3 FUTURE WORK

This thesis aimed to identify the sources of ambient particles at urban schools with a particular focus on vehicle emissions and the driving factors. From the literature, the

size and chemical composition of airborne particle are both thought to play a role in the associated health effects; however the relative contributions of both are still unclear [5]. In this thesis, PM_1 rather than $PM_{2.5}$ was identified as a potentially better fraction to use in studies examining the health effects of airborne particles. Further validation of this hypothesis is required in terms of the chemical composition and potential toxicity of PM_1 fraction. In addition, comparative epidemiological studies to confirm that PM_1 is a better indicator of the detrimental health effects associated with airborne particles would be of benefit. Moreover, the trends observed in the pilot study should be validated by future work and if found to be correct would signal the need to consider the total traffic volume as a key parameter in evaluating the toxicity of ultrafine and fine particles emissions.

Throughout this thesis, secondary sources rather than vehicle emissions were found to be the largest contributing source at the majority of urban schools as they were not near a busy road. However, it was outside the scope of the current work to fully determine the contributing factors to SOA concentrations at the schools. Understand the contributing factors to SOA concentrations is of importance as it is likely to have different health effects to vehicle emissions and other primary source emissions owing to the different chemical composition [6]. However, a more complete understanding of the chemical composition of SOA is needed to gain further insight into the health effects of SOA. Thus future work could focus on developing techniques to better distinguish between the influence of background regional SOA and SOA that are formed locally. The comparison of the different PMF-derived OOA factors at the schools revealed that the discrimination between SV-OOA and LV-OOA was only relevant to a particular site and not across Brisbane and improving this distinction could be focus of future work.

The novel methodology described for the analysis of OA on filter samples by AMS should be improved to make it a quantitative rather than a qualitative technique. Areas that could be optimized include the filter paper used and apparatus used for extraction. This would allow the filter method to be applied to the other non-refractory chemical species and would significantly improve the scope and possible applications of the AMS and reduce opportunities lost due to instrument downtime.

This thesis forms part of a larger study that aimed to determine the effect of traffic emissions on children's health. The results from the current study will be incorporated with the findings from investigations into the other measured air quality parameters such as particle number concentration, particle size distribution, gaseous species (CO, CO_2, NO_x, SO_2) and specific organic species (such as polycyclic aromatic hydrocarbons). Thus the whole project aimed to achieve a holistic picture of children's exposure to vehicle emissions and other contributing sources at school. In addition to the air quality measurements, cardiovascular and respiratory health testing was performed on the children at the participating school. The health data should be analysed in conjunction with the air quality measurements with intention of addressing the overall aim of the UPTECH project, namely to determine the effects of long term exposure to traffic emissions on children.

9.4 REFERENCES

1. Mejía, J. F.; Choy, S. L.; Mengersen, K.; Morawska, L., Methodology for assessing exposure and impacts of air pollutants in school children: Data collection, analysis and health effects – A literature review. *Atmos. Environ.* **2011,** *45*, (4), 813-823.
2. Jimenez, J. L.; Canagaratna, M. R.; Donahue, N. M.; Prevot, A. S. H.; Zhang, Q.; Kroll, J. H.; DeCarlo, P. F.; Allan, J. D.; Coe, H.; Ng, N. L.; Aiken, A. C.; Docherty, K. S.; Ulbrich, I. M.; Grieshop, A. P.; Robinson, A. L.; Duplissy, J.; Smith, J. D.; Wilson, K. R.; Lanz, V. A.; Hueglin, C.; Sun, Y. L.; Tian, J.; Laaksonen, A.; Raatikainen, T.; Rautiainen, J.; Vaattovaara, P.; ehn, M.; Kulmala, M.; Tomlinson, J.; Collins, D. R.; Cubison, M. J.; Dunlea, E. J.; Huffman, A.; Onasch, T. B.; Alfarra, M. R.; Williams, P. I.; Bower, K. N.; Kondo, Y.; Schneider, J.; Drewnick, F.; Borrmann, S.; Weimer, S.; Demerjian, K. L.; Salcedo, D.; Cottrell, L.; Griffin, R.; Takami, A.; Miyoshi, T.; Hatakeyama, S.; Jayne, J. T.; Herndon, S. C.; Trimborn, A.; Williams, L. R.; Wood, E. C.; Middlebrook, A.; Kolb, C. E.; Baltensperger, U.; Worsnop, D. R., Evolution of Organic Aerosols in the Atmosphere *Science* **2009,** *326*, 1525-1529.
3. Kleeman, M. J.; Schauer, J. J.; Cass, G. R., Size and Composition Distribution of Fine Particulate Matter Emitted from Motor Vehicles. *Environ. Sci. Technol.* **2000,** *34*, (7), 1132-1142.
4. Friend, A. J.; Ayoko, G. A.; Stelcer, E.; Cohen, D., Source apportionment of PM2.5 at two receptor sites in Brisbane, Australia. *Environ. Chem.* **2011,** *8*, (6), 569-580.
5. Harrison, R. M.; Smith, D. J. T.; Kibble, A. J., What is responsible for the carcinogenicity of PM2.5? *Occup. Environ. Med.* **2004,** *61*, (10), 799-805.
6. Robinson, A. L.; Donahue, N. M.; Shrivastava, M. K.; Weitkamp, E. A.; Sage, A. M.; Grieshop, A. P.; Lane, T. E.; Pierce, J. R.; Pandis, S. N., Rethinking

organic aerosols: Semivolatile emissions and photochemical aging. *Science* **2007,** *315*, 1259-1262.

Appendices

Appendix 1 (Chapter 3)

A1-1.0 Profile of particle number and mass concentrations by distance through the tunnel

The profile of the particle number and mass concentrations for the sampling trips that were classified as with HDV and without HDV are given as Figures A1-1 to A1-4. The classification was done visually, with sampling trips where a HDV was observed were classified as with HDV and so these sampling trips were grouped together and their profiles calculated.

A1-2.0 Dilution ratio calculations

Dilution ratios for campaign III was calculated according to the method described in Ntziachristos et al. [1]. The percentage diesel fraction was assumed to be sum of the medium and long vehicles. As approximately 95% of passenger vehicles in Australia are gasoline powered [2], the short vehicles were not considered for the calculation of the diesel fraction. The input parameters that were used for the calculation of exhaust CO_2 were the same as listed in Ntziachristos et al. [1], and as this tunnel contains both uphill and flat road sections the parameters were averaged where appropriate.

A1-3.0 Correction factor for 3007 CPC

The comparison between a 3022 and 3007 was performed and can be seen in Figure A1-5. This was done to determine a correction factor for the 3007 measurements for concentrations above 10^5 particles cm^{-3}. The correction factor was determined to be $y = 3.66x10^4e^{0.0000112x}$ for when $x > 10^5$ p cm^{-3} ($r^2 = 0.98$)

A1-4.0 Open road mean concentrations

For each campaign the mean open road concentrations of particle number and mass that were measured along the route taken from the Queensland University of Technology campus to the tunnel are tabled in Table A1-11. The concentrations of particle number, particle mass and ROS from the open road measurement campaign that was conducted on a road with similar traffic volume and road characteristics are also given in Table A1-1.

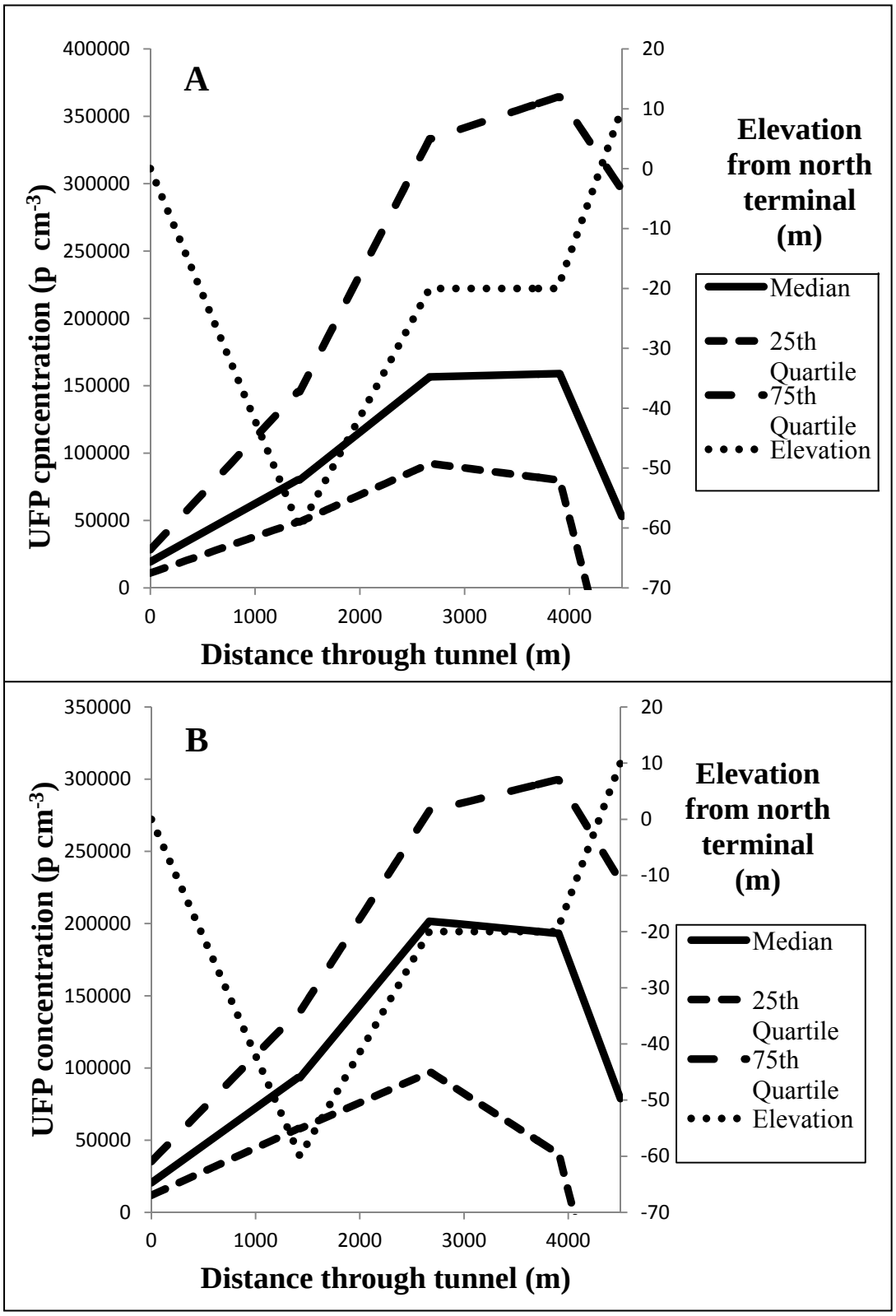

Figure A1-1: Particle number concentration evolution by distance through the tunnel for southbound tunnel runs without HDV (A) and with HDV (B)

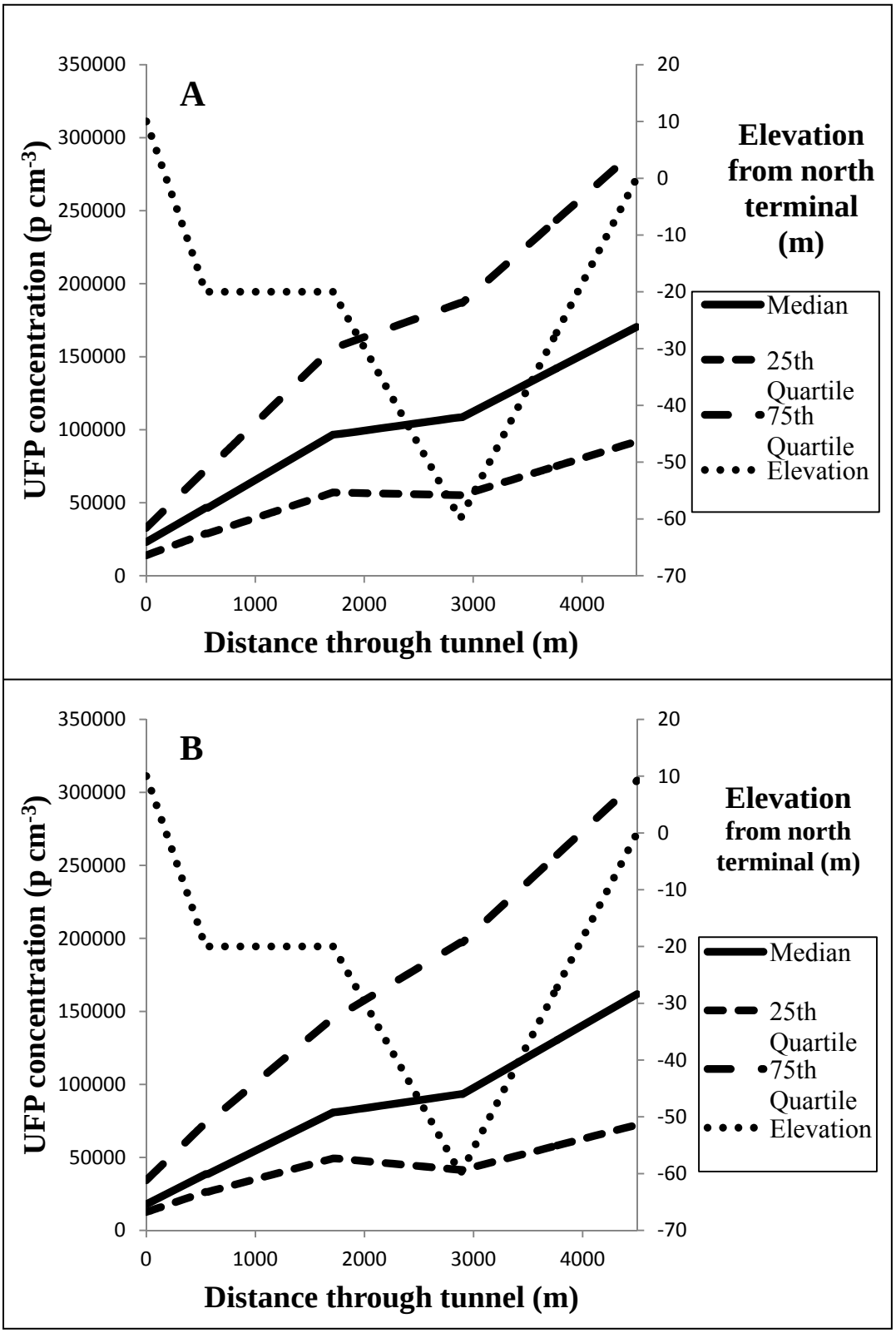

Figure A1-2: Particle number concentration evolution by distance through the tunnel for northbound tunnel runs without HDV (A) and with HDV (B)

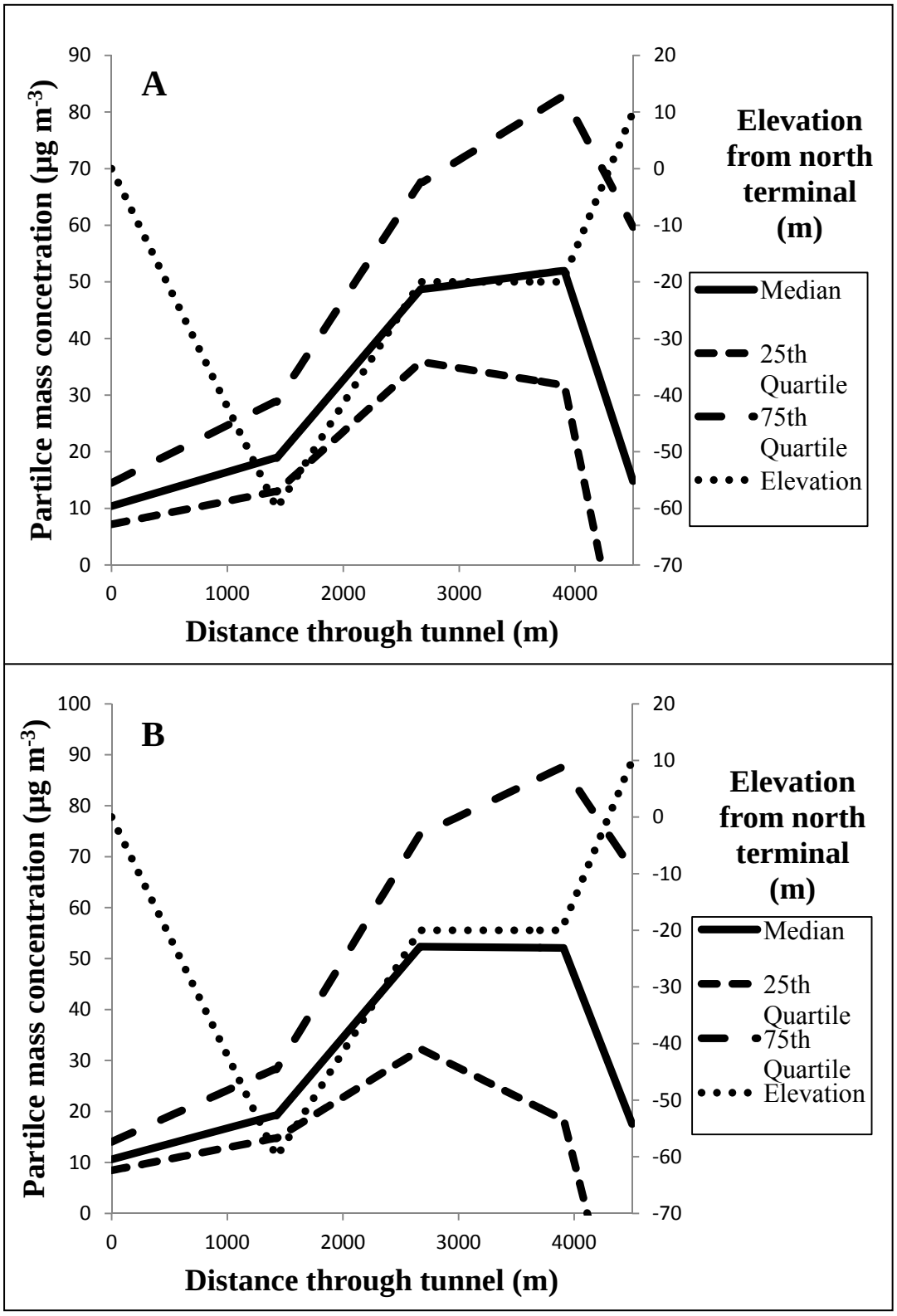

Figure A1-3: Particle mass concentration evolution by distance through the tunnel for southbound tunnel runs without HDV (A) and with HDV (B)

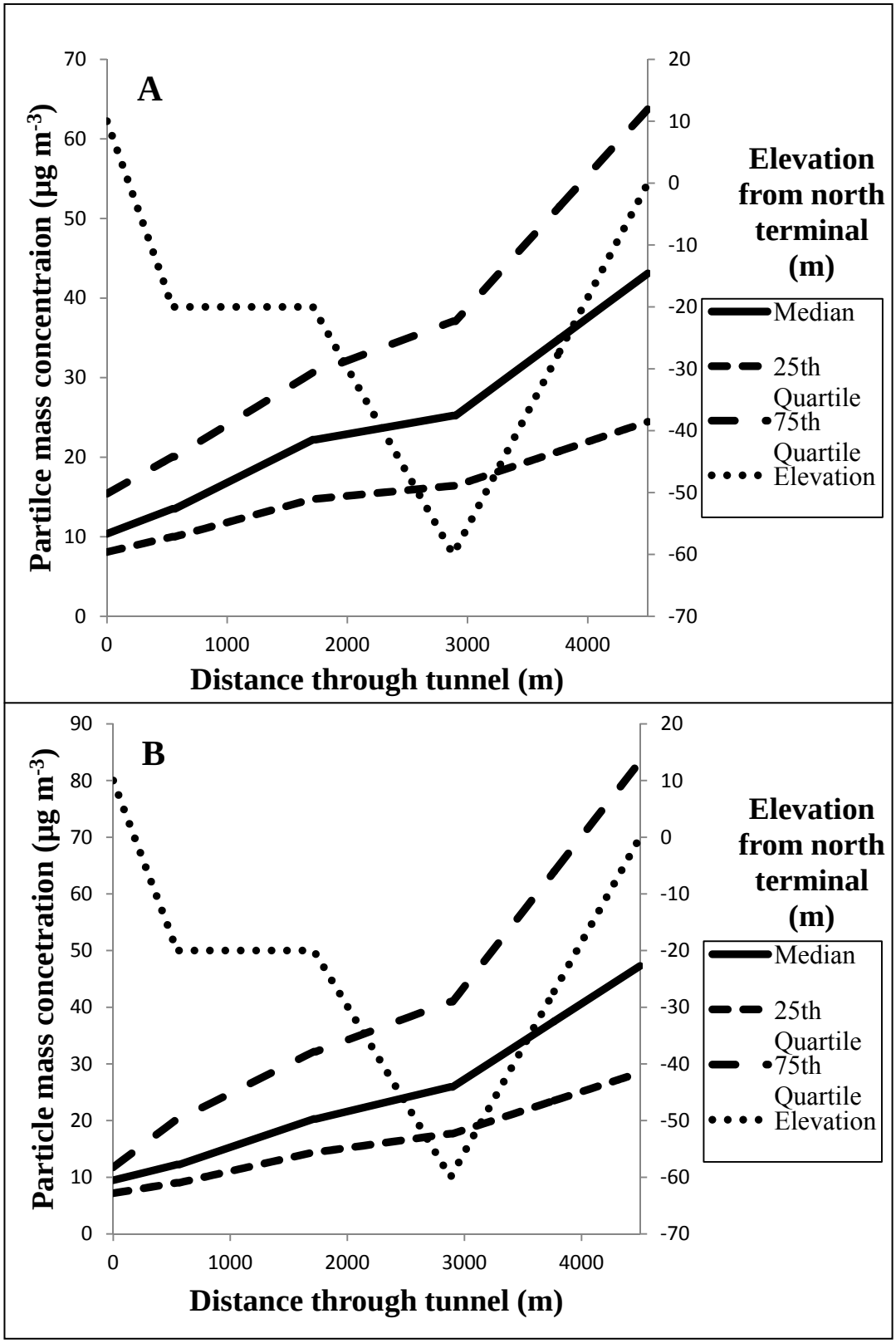

Figure A1-4: Particle mass concentration evolution through the tunnel for northbound tunnel runs without HDV (A) and with HDV (B)

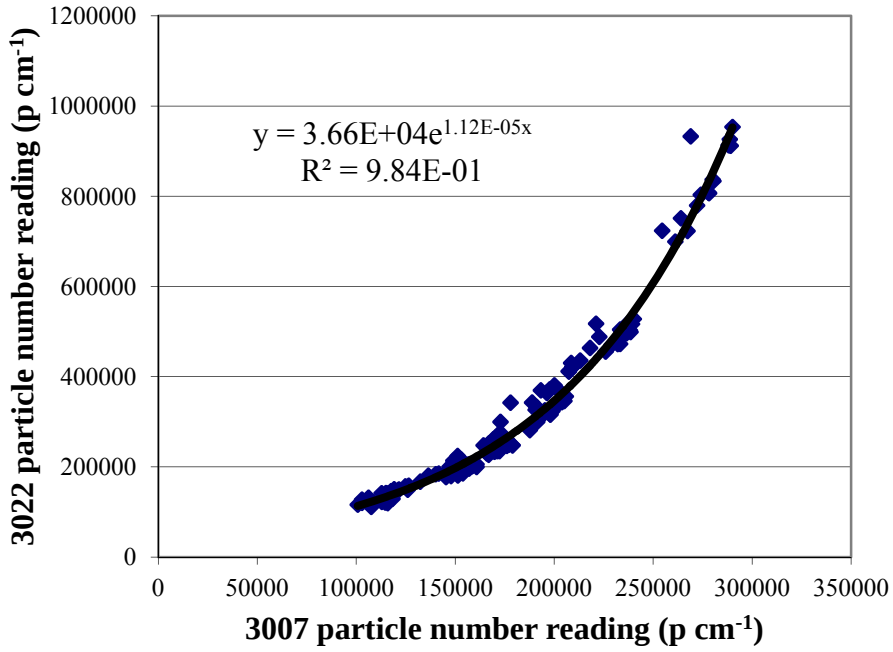

Figure A1-5: Comparison between a 3007 and 3022 CPC

Table A1-1: Mean concentrations for open road measurements

Campaign	I	II	III	Open road
UFP number (p cm^{-3})	3x10^4	4.59x10^4	2.92x10^4	2.35x10^4
Particle mass (µg m^{-3})	11	12	13	9
ROS (nmol mg^{-1})	Not measured			< Detection limit

A5.0 References

1. Ntziachristos, L.; Ning, Z.; Geller, M. D.; Sioutas, C., Particle Concentration and Characteristics near a Major Freeway with Heavy-Duty Diesel Traffic. *Environ. Sci. Technol.* **2007,** *41*, (7), 2223-2230.

2. Knibbs, L. D.; de Dear, R. J.; Morawska, L.; Mengersen, K. L., On-road ultrafine particle concentration in the M5 East road tunnel, Sydney, Australia. *Atmos. Environ.* **2009,** *43*, (22-23), 3510-3519.

Appendix 2 (Chapter 4)

A2.1 Impact of traffic counts at individual schools

At two schools, S12 and S20 there was a public holiday during sampling and these were found to have a corresponding decrease in traffic counts, as shown in Table A2-2. The influence on the traffic on the EC concentrations and the OC/EC at these schools was investigated with the results in Table A2-2. At S12 there was little difference between the EC and OC/EC values for the public holiday and the rest of the week, while at S20 there was a noticeable difference. The total traffic counts were higher and showed a greater decrease at S20 compared to S12 and this was the likely reason for the marked differences. This also points to one of the main sources of the carbonaceous aerosol at S20 being vehicle emissions due to the observed decrease in EC concentration and increased OC/EC during the public holiday.

A2.2 OC and EC fractions

Analysis of the OC and EC fractions can give a further insight into the source of the carbonaceous aerosols, with the average concentration for each fraction for all the schools given in Figure A2-2. The average concentrations of the OC and EC fractions at each school are given in Table A2-3. The most abundant OC fractions at the schools were generally OC2 and OC3, which comprised the majority of the OC. No OC1 fraction was found in any of the samples, with varying amounts of OC4 and PC. The EC1 and EC2 fractions were the most abundant of the EC fraction, with little EC3 found at the schools. The more abundant fractions observed at the schools, OC2, OC3, EC1 and EC2, have been associated with vehicle emissions in previous work [1-3]. This would point to vehicle emissions, in general, being one of the main sources of OC and EC at the schools.

The concentrations of char-EC and soot-EC and char-EC/soot-EC at each school was calculated according to the method described by Han et al. [4] to give insight into the source of the EC and are given in Table A2-4. In general, the EC was in the soot form at each school. The source for soot-EC is primarily vehicle emission, specifically diesel emissions [4] indicating that the source of the EC at the schools was vehicular. In addition, the char-EC/soot-EC ratio at all schools with the exception of S05 was below 1. Since the char-EC/soot-EC ratio from vehicles emissions is less than 1 [3], the observed ratio at all the schools further indicated that the EC was primarily emitted from vehicles.

A2.3 References

1. Sahu, M.; Hu, S.; Ryan, P. H.; Le Masters, G.; Grinshpun, S. A.; Chow, J. C.; Biswas, P., Chemical compositions and source identification of PM2.5 aerosols for estimation of a diesel source surrogate. *Sci. Total Environ.* **2011,** *409*, (13), 2642-2651.
2. Kim, E.; Hopke, P. K.; Edgerton, E. S., Improving source identification of Atlanta aerosol using temperature resolved carbon fractions in positive matrix factorization. *Atmos. Environ.* **2004,** *38*, (20), 3349-3362.
3. Cao, J. J.; Lee, S. C.; Ho, K. F.; Fung, K.; Chow, J. C.; Watson, J. G., Characterization of Roadside Fine Particulate Carbon and its Eight Fraction in Hong Kong. *Aerosol Air Qual. Res.* **2006,** *6*, (2), 106-122.
4. Han, Y.; Cao, J.; Chow, J. C.; Watson, J. G.; An, Z.; Jin, Z.; Fung, K.; Liu, S., Evaluation of the thermal/optical reflectance method for discrimination between char- and soot-EC. *Chemosphere* **2007,** *69*, (4), 569-574.

Table A2-1: Average weather and traffic conditions at each school during the sampling period. Solar radiation values in bold were affected by shade. N/A = Not Available

School	Date	Temp. (°C)	Solar radiation (W m^{-2})	RH (%)	Wind speed (m s^{-1})	Prominent wind direction	Frequency of wind from main road (%)	Direction of main road	Traffic count (veh hr^{-1})	% Light	% Med	% Heavy
S01	Nov-10	24.5	548.1	61	5.47	East	0	South	291	95.4	3.8	0.7
S02	Oct-10	24.4	606.3	63	4.32	East	49	East	1418	95.0	4.7	0.3
S03	Nov-10	25.2	**365.6**	59	1.74	Northeast	3	Southwest	542	98.1	1.8	0.1
S04	Mar-11	26.4	N/A	55	2.71	East	0	West	1331	86.4	8.6	2.2
S05	Mar-11	23.9	318.7	73	1.86	Southeast	30	South	1096	96.3	3.1	0.4
S06	May-11	18.7	373.9	61	4.41	West	0	East	475	86.8	8.6	3.3
S07	Jun-11	19.6	318.2	58	0.85	South	0	Northeast	1564	94.9	4.0	0.6
S08	Jun-11	17.5	354.5	59	1.89	West	45	West	1039	86.1	13.3	0.6
S09	Jul-11	16.9	427.6	58	2.47	West	0	North	1994	89.5	4.2	1.9
S10	Aug-11	19.4	445.4	56	3.2	East	14	West	1471	94.4	3.8	0.8
S11	Aug-11	20.3	472.7	64	3.28	S/SW	23	South	765	94.7	2.5	0.9
S12	Aug-11	18.6	**412.5**	54	1.16	West	8	S/SW	294	96.7	2.9	0.3
S13	Oct-11	24.6	**315.2**	57	1.73	East	3	West	1021	94.9	4.3	0.5
S14	Oct-11	24.3	469.4	62	1.37	Southeast	15	East	262	95.5	3.8	0.5
S15	Nov-11	29.0	853.8	46	5.01	Northeast	0	West	1357	91.5	6.6	0.8
S16	Nov-11	27.0	608.8	67	1.24	North	38	North	89	98.1	1.2	0.6
S17	Dec-11	26.5	555.3	60	1.2	Southeast	17	East	1128	95.1	3.2	0.7
S18	Mar-12	24.7	349.6	59	1.54	Southeast	0	West	62	97.4	2.6	0.0
S19	Mar-12	25.2	480.8	69	4.86	Southeast	10	South	1715	88.6	3.7	2.4
S20	Apr-12	21.8	314.4	61	0.79	S/SW	2	East	1949	95.8	2.9	0.9
S21	Jun-12	16.9	**67.3**	51	1.24	West	0	North	249	97.2	2.1	0.5
S22	Jun-12	19.5	408.5	50	1	Northwest	44	W/NW	783	96.3	3.1	0.5
S23	Jul-12	18.8	311.0	52	0.79	South	3	Southeast	1038	70.1	29.2	0.5
S24	Aug-12	19.2	510.4	27	4.58	West	2	North	271	97.1	2.4	0.4
S25	Aug-12	20.3	451.8	58	4.76	North	18	S/SW	584	91.5	7.0	1.2

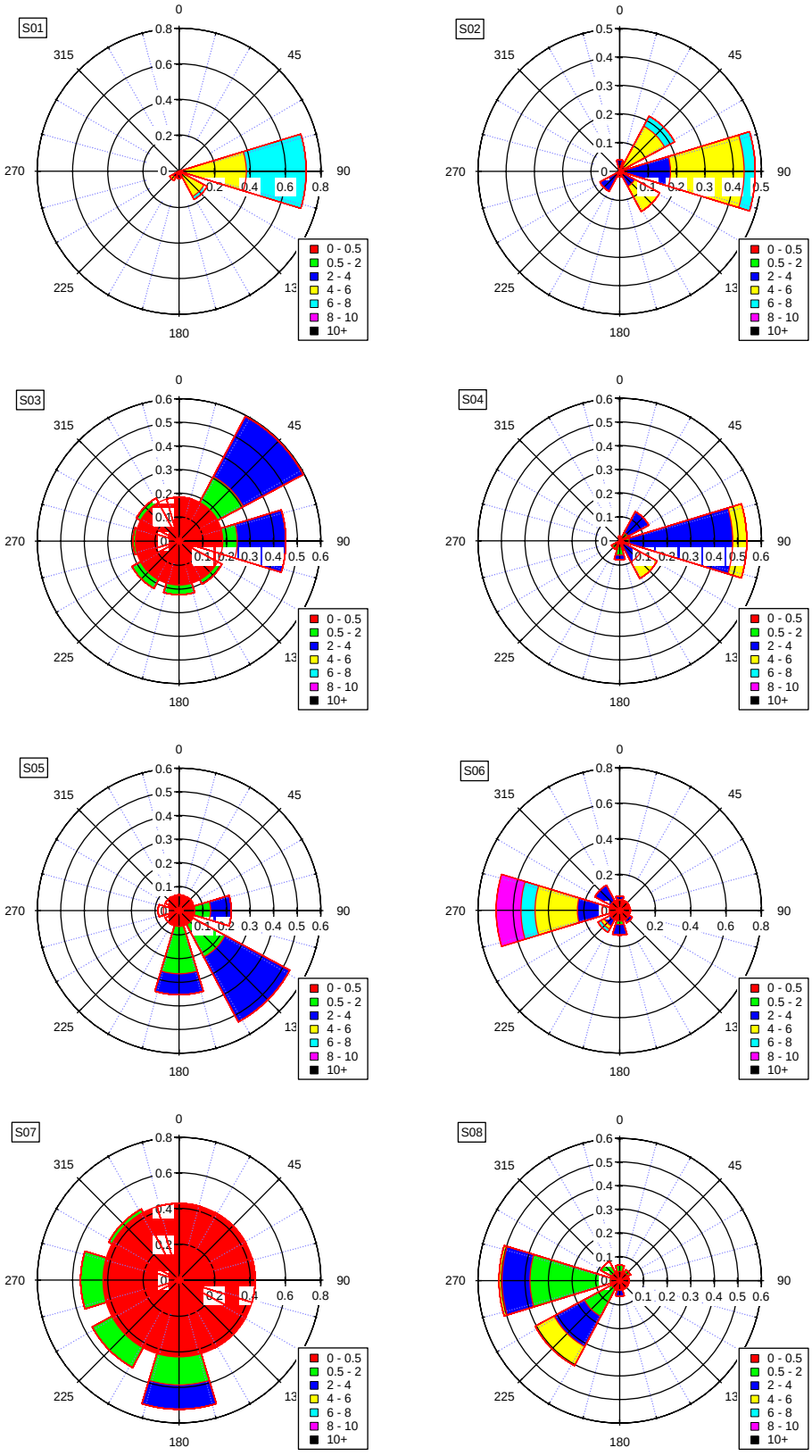
S01
S02
S03
S04
S05
S06
S07
S08
0
45
90
135
180
225
270
315
0 - 0.5
0.5 - 2
2 - 4
4 - 6
6 - 8
8 - 10
10+

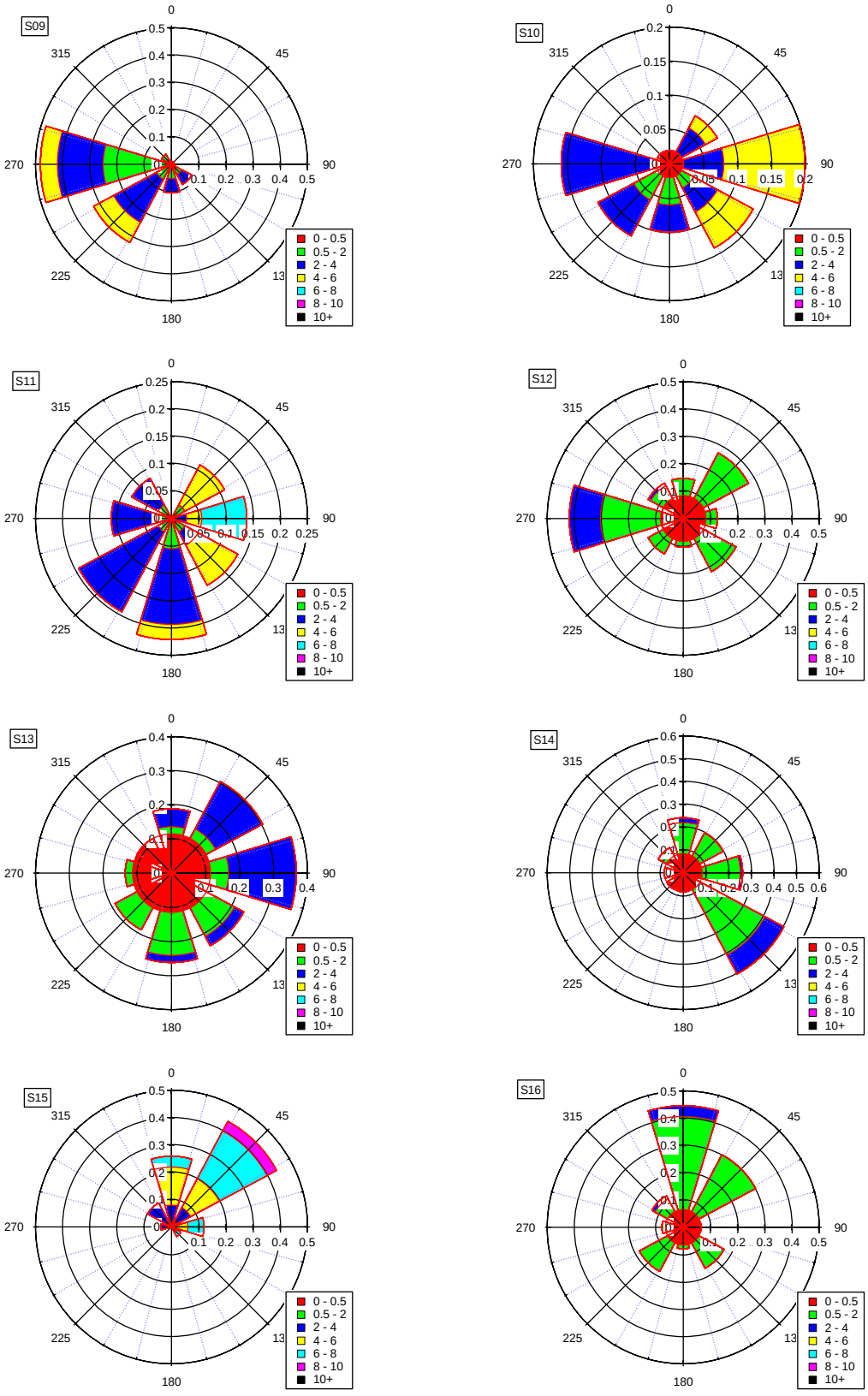
S09
S10
S11
S12
S13
S14
S15
S16
0
45
90
135
180
225
270
315
0 - 0.5
0.5 - 2
2 - 4
4 - 6
6 - 8
8 - 10
10+

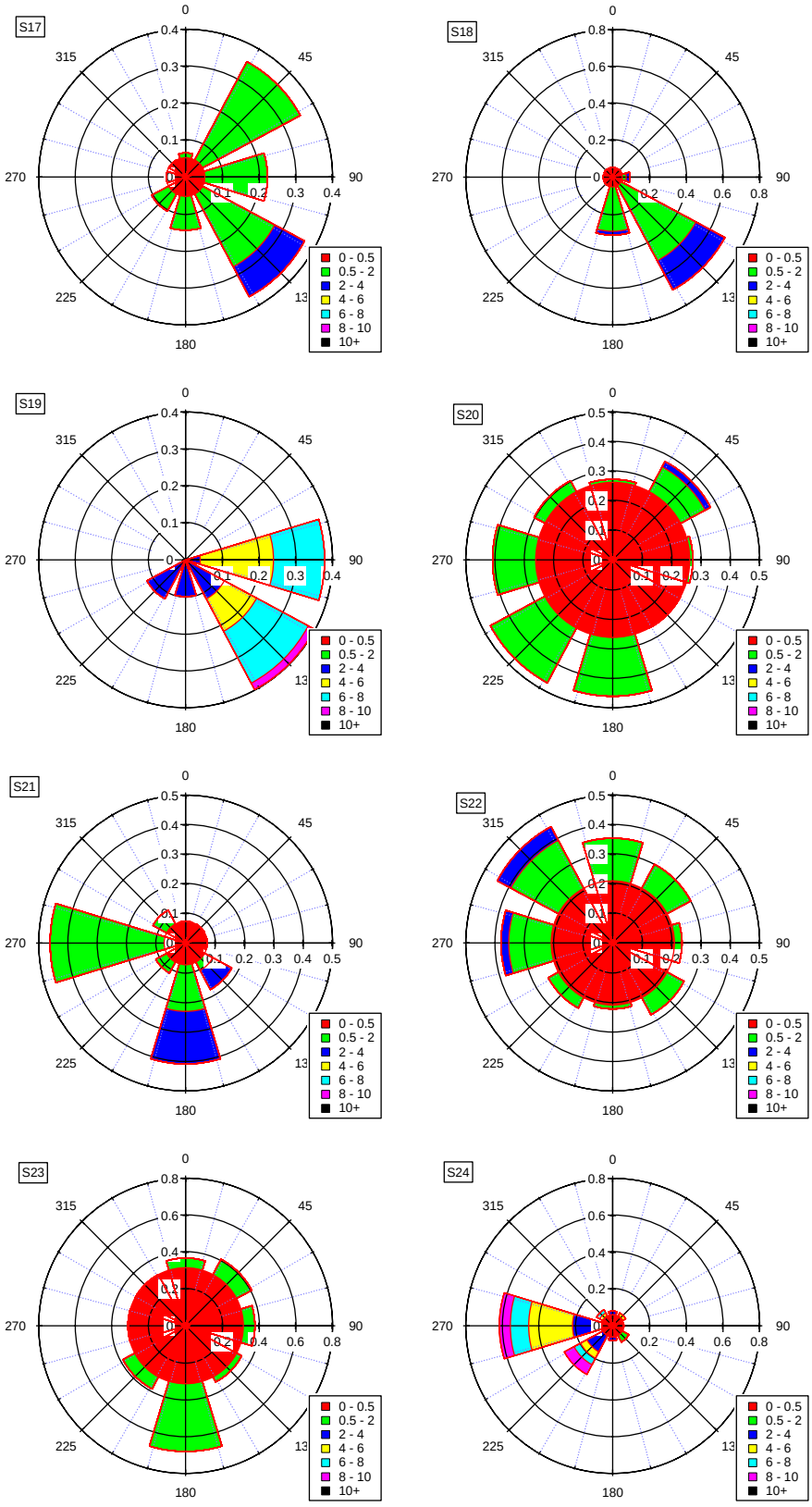
S17
S18
S19
S20
S21
S22
S23
S24
0 - 0.5
0.5 - 2
2 - 4
4 - 6
6 - 8
8 - 10
10+

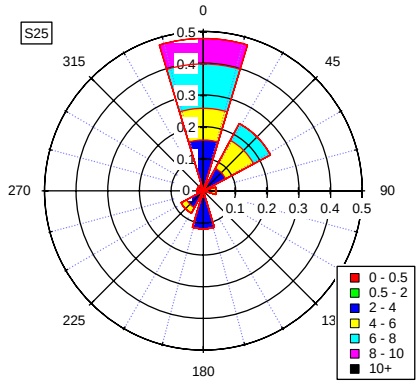

Figure A2-1: Rose plots of the entire sampling period at each school. Wind speed is in m s^{-1}.

Table A2-2: Difference in the traffic counts, EC concentrations and OC/EC for schools where the sampling period included public holidays (PH). The PH values refer to the values on the public holiday while the average values refer to the average over the other four normal school days. The uncertainty given is one standard deviation.

School	Traffic average (veh hr^{-1})	Traffic PH (veh hr^{-1})	EC average (µg m^{-3})	EC PH (µg m^{-3})	OC/EC average	OC/EC PH
S12	316	203	0.43 ± 0.18	0.39	4.5 ± 1.68	5.0
S20	2158	1110	1.09 ± 0.28	0.34	2.1 ± 0.65	3.8

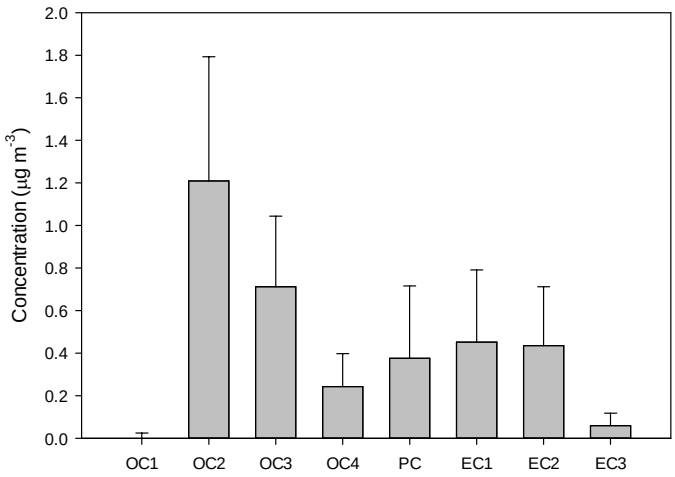

Figure A2-2: Average concentrations of the OC and EC fraction across all the schools. Error bars are on standard deviation

Table A2-3: Average concentrations of the OC and EC fractions at each school.

	Average concentration (µg m^{-3})								*Standard Deviation (µg m^{-3})*							
School	**OC1**	**OC2**	**OC3**	**OC4**	**PC**	**EC1**	**EC2**	**EC3**	**OC1**	**OC2**	**OC3**	**OC4**	**PC**	**EC1**	**EC2**	**EC**
S01	0.00	1.56	0.79	0.20	0.27	0.21	0.20	0.04	0.02	0.14	0.14	0.04	0.12	0.15	0.18	0
S02	0.00	2.17	1.06	0.32	0.55	0.53	0.68	0.15	0.02	0.42	0.32	0.12	0.22	0.16	0.14	0
S03	0.00	2.49	0.53	0.14	0.17	0.23	0.19	0.02	0.02	0.30	0.06	0.04	0.07	0.05	0.04	0
S04	0.00	1.79	0.71	0.16	0.07	0.31	0.39	0.01	0.02	0.42	0.10	0.07	0.03	0.10	0.08	0
S05	0.00	1.14	0.56	0.14	0.00	0.23	0.27	0.00	0.01	0.23	0.16	0.12	0.14	0.12	0.09	0
S06	0.00	1.09	0.39	0.08	0.24	0.26	0.54	0.12	0.01	0.17	0.16	0.04	0.07	0.19	0.43	0
S07	0.00	1.40	0.91	0.37	0.28	0.62	0.83	0.11	0.01	0.28	0.30	0.11	0.35	0.38	0.63	0
S08	0.02	2.01	0.79	0.60	0.25	0.51	0.50	0.19	0.01	0.82	0.50	0.29	0.24	0.23	0.15	0
S09	0.01	1.20	0.53	0.14	0.34	0.25	0.25	0.11	0.02	0.30	0.14	0.05	0.08	0.03	0.03	0
S10	0.00	1.38	0.82	0.34	0.60	0.72	0.66	0.09	0.01	0.19	0.20	0.11	0.27	0.24	0.16	0
S11	0.00	0.83	0.61	0.33	1.09	1.04	0.62	0.07	0.01	0.05	0.48	0.24	0.70	0.92	0.34	0
S12	0.00	0.71	0.64	0.22	0.37	0.42	0.32	0.05	0.01	0.40	0.29	0.08	0.22	0.18	0.17	0
S13	0.00	1.29	0.93	0.27	0.90	0.82	0.61	0.03	0.01	0.27	0.26	0.13	0.29	0.23	0.11	0
S14	0.00	1.18	0.83	0.36	0.50	0.62	0.37	0.06	0.01	0.24	0.19	0.07	0.18	0.21	0.11	0
S15	0.00	1.87	0.57	0.24	0.34	0.41	0.28	0.04	0.01	0.21	0.20	0.08	0.17	0.14	0.09	0
S16	0.00	1.12	0.59	0.17	0.22	0.31	0.36	0.04	0.01	0.27	0.18	0.08	0.17	0.10	0.15	0
S17	0.00	1.07	0.59	0.22	0.35	0.36	0.30	0.03	0.00	0.35	0.16	0.09	0.18	0.16	0.21	0
S18	0.02	0.90	0.88	0.31	0.20	0.33	0.29	0.01	0.01	0.15	0.35	0.16	0.07	0.05	0.01	0
S19	0.00	0.86	0.51	0.15	0.21	0.16	0.27	0.05	0.01	0.25	0.23	0.08	0.17	0.05	0.13	0
S20	0.00	0.94	0.60	0.21	0.31	0.45	0.70	0.10	0.01	0.26	0.27	0.09	0.24	0.21	0.34	0
S21	0.00	0.30	0.16	0.13	0.09	0.07	0.19	0.06	0.01	0.16	0.24	0.16	0.10	0.03	0.04	0
S22	0.00	0.87	0.76	0.16	0.29	0.51	0.79	0.07	0.01	0.13	0.43	0.15	0.32	0.39	0.25	0
S23	0.00	0.71	0.70	0.16	0.26	0.33	0.57	0.05	0.01	0.13	0.24	0.05	0.17	0.11	0.15	0
S24	0.00	0.62	1.02	0.30	0.73	0.73	0.31	0.00	0.00	0.19	0.36	0.14	0.36	0.44	0.13	0
S25	0.00	0.70	1.25	0.41	0.85	0.94	0.52	0.02	0.00	0.11	0.28	0.11	0.27	0.34	0.17	0

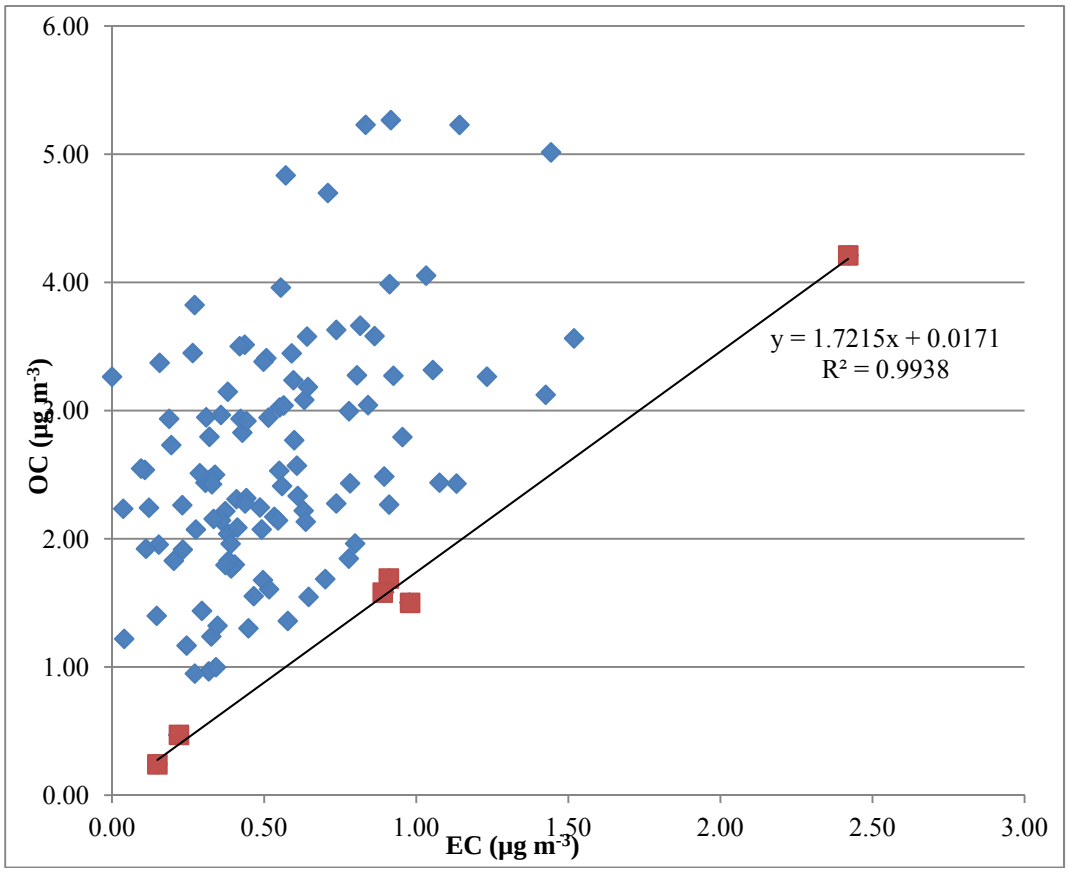

Figure A2-3: Plot of OC and EC concentrations to determine the OC/EC_{min}

Table A2-4: Average calculated char-EC and soot-EC concentration in μg m^{-3} and char-EC/soot-EC ratio for each school

School ID	Char-EC	Soot-EC	Char-EC/soot-EC
S01	0.01	0.23	0.06
S02	0.01	0.82	0.01
S03	0.06	0.21	0.28
S04	0.25	0.40	0.62
S05	0.24	0.25	0.99
S06	0.06	0.66	0.09
S07	0.34	0.94	0.36
S08	0.26	0.68	0.38
S09	0.01	0.36	0.03
S10	0.13	0.75	0.17
S11	0.07	0.69	0.10
S12	0.05	0.36	0.15
S13	0.01	0.64	0.02
S14	0.12	0.43	0.27
S15	0.08	0.32	0.25
S16	0.10	0.39	0.25
S17	0.04	0.33	0.12
S18	0.13	0.30	0.44
S19	0.04	0.32	0.13
S20	0.15	0.80	0.19
S21	0.02	0.25	0.08
S22	0.22	0.87	0.25
S23	0.09	0.62	0.15
S24	0.03	0.31	0.10
S25	0.1	0.54	0.19

Table A2-5: PROMETHEE ranking results for the schools from the most preferred school to least. Φ represents the net preference flow used for the ranking.

Ranking	School	Net outranking flow (Φ)
1	S21	0.31
2	S19	0.19
3	S05	0.15
4	S01	0.12
5	S17	0.12
6	S09	0.12
7	S12	0.11
8	S03	0.10
9	S16	0.10
10	S18	0.08
11	S06	0.05
12	S23	0.05
13	S15	0.04
14	S24	0.02
15	S04	0.02
16	S14	-0.05
17	S20	-0.07
18	S22	-0.11
19	S13	-0.11
20	S25	-0.14
21	S11	-0.15
22	S10	-0.18
23	S02	-0.25
24	S08	-0.27
25	S07	-0.28

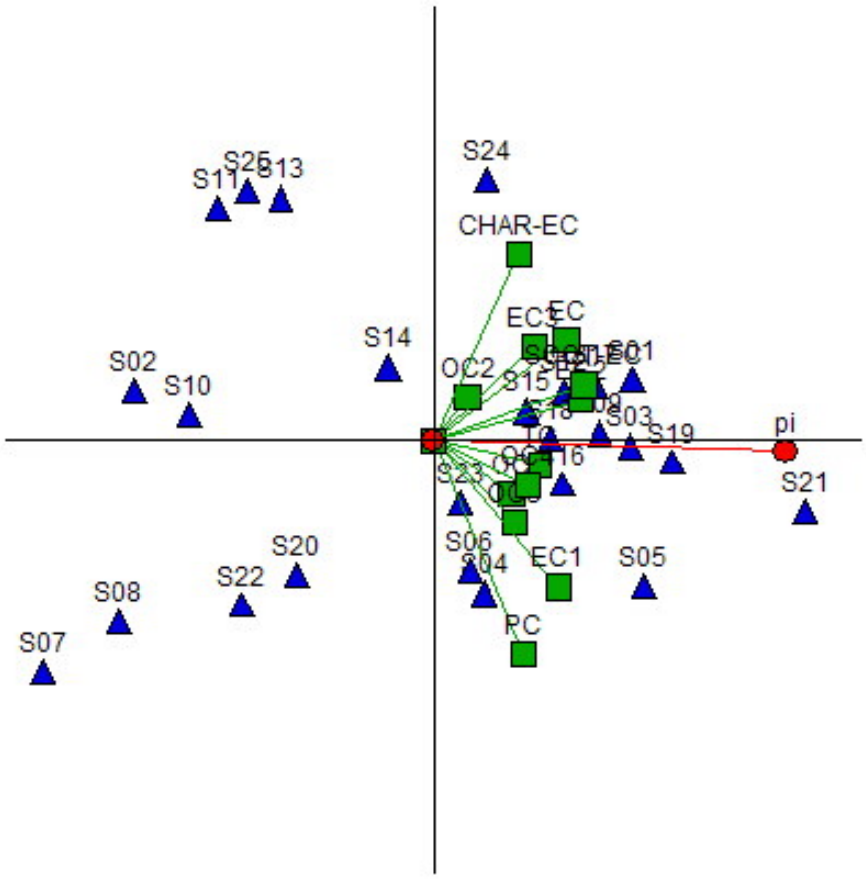

Figure A2-4: GAIA plot of the OC and EC components.

Appendix 3 (Chapter 5)

Table A3-1: Summary of the minimum detection limits (MDL) for each element in ng m^{-3}. Note for Na the PIGE analysis program only calculates a MDL when Na is detected.

	Average	Min	Max
Na	0.0	0.0	0.0
Al	18.7	8.1	36.9
Si	11.5	5.1	23.0
P	10.3	4.7	20.6
S	9.6	4.4	19.1
Cl	10.0	4.7	19.7
K	9.1	4.2	17.5
Ca	8.5	3.9	16.3
Ti	6.9	3.0	13.0
V	5.8	2.5	10.7
Cr	4.6	1.9	8.2
Mn	3.8	1.6	6.8
Fe	3.5	1.4	6.5
Co	4.0	1.6	7.8
Ni	3.3	1.4	6.2
Cu	3.5	1.6	6.7
Zn	4.0	1.7	7.7
Br	12.7	5.8	25.5
Sr	32.4	15.2	70.0
Cd	40.8	0.0	648.7
Pb	20.3	9.4	40.7

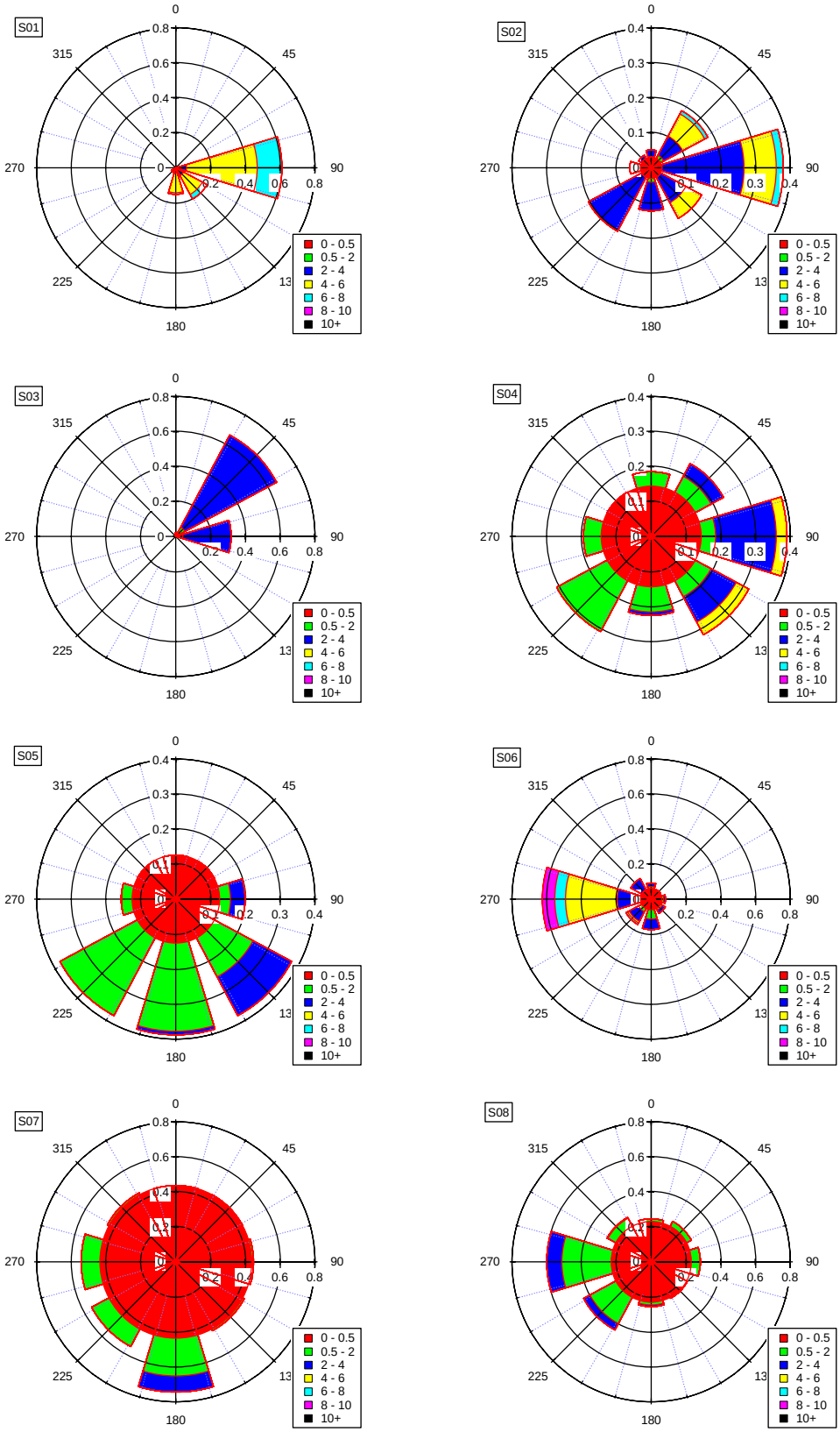
S01
S02
S03
S04
S05
S06
S07
S08
0
45
90
135
180
225
270
315
0 - 0.5
0.5 - 2
2 - 4
4 - 6
6 - 8
8 - 10
10+

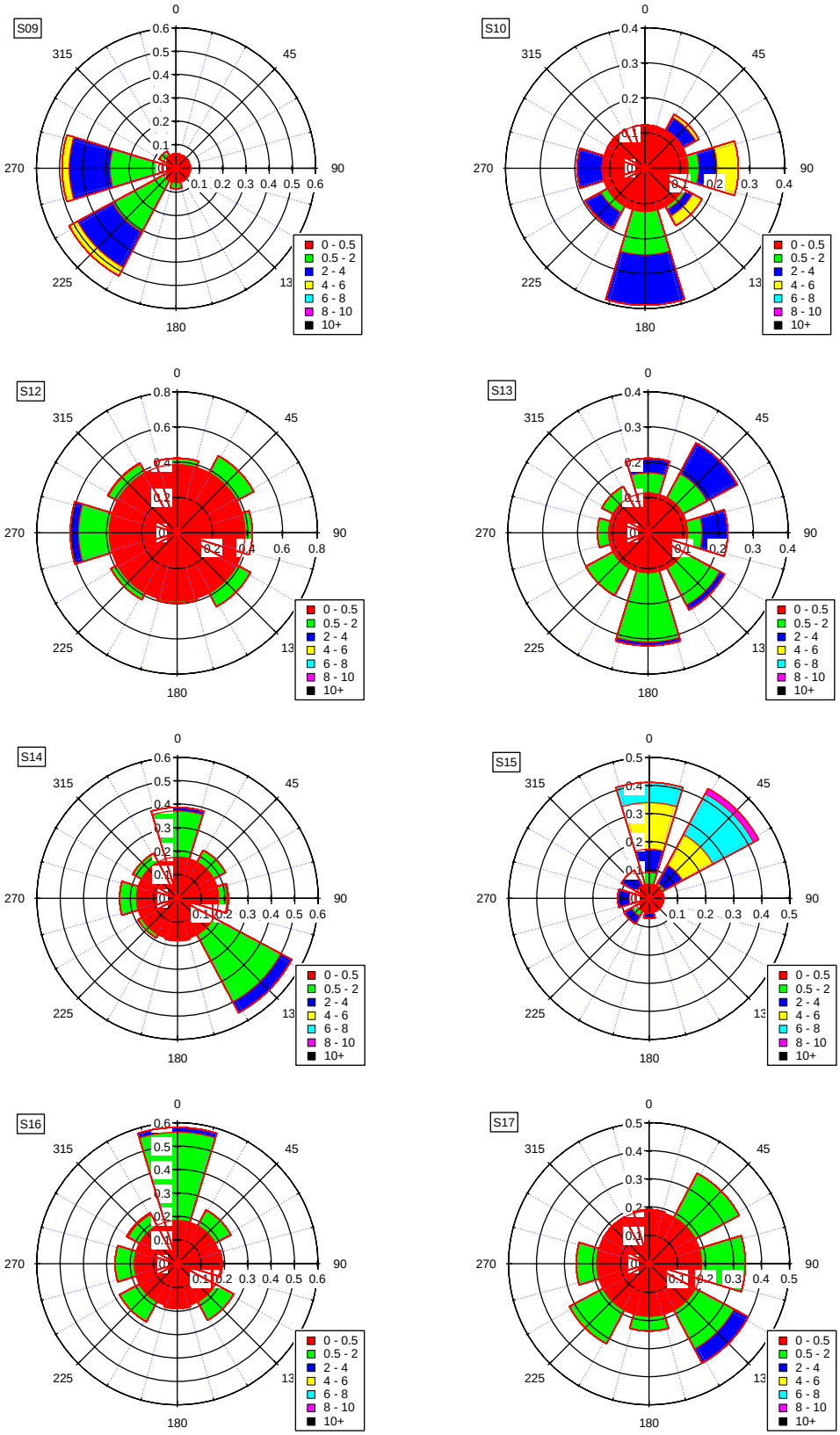
S09
S10
S12
S13
S14
S15
S16
S17
0
45
90
135
180
225
270
315
0 - 0.5
0.5 - 2
2 - 4
4 - 6
6 - 8
8 - 10
10+

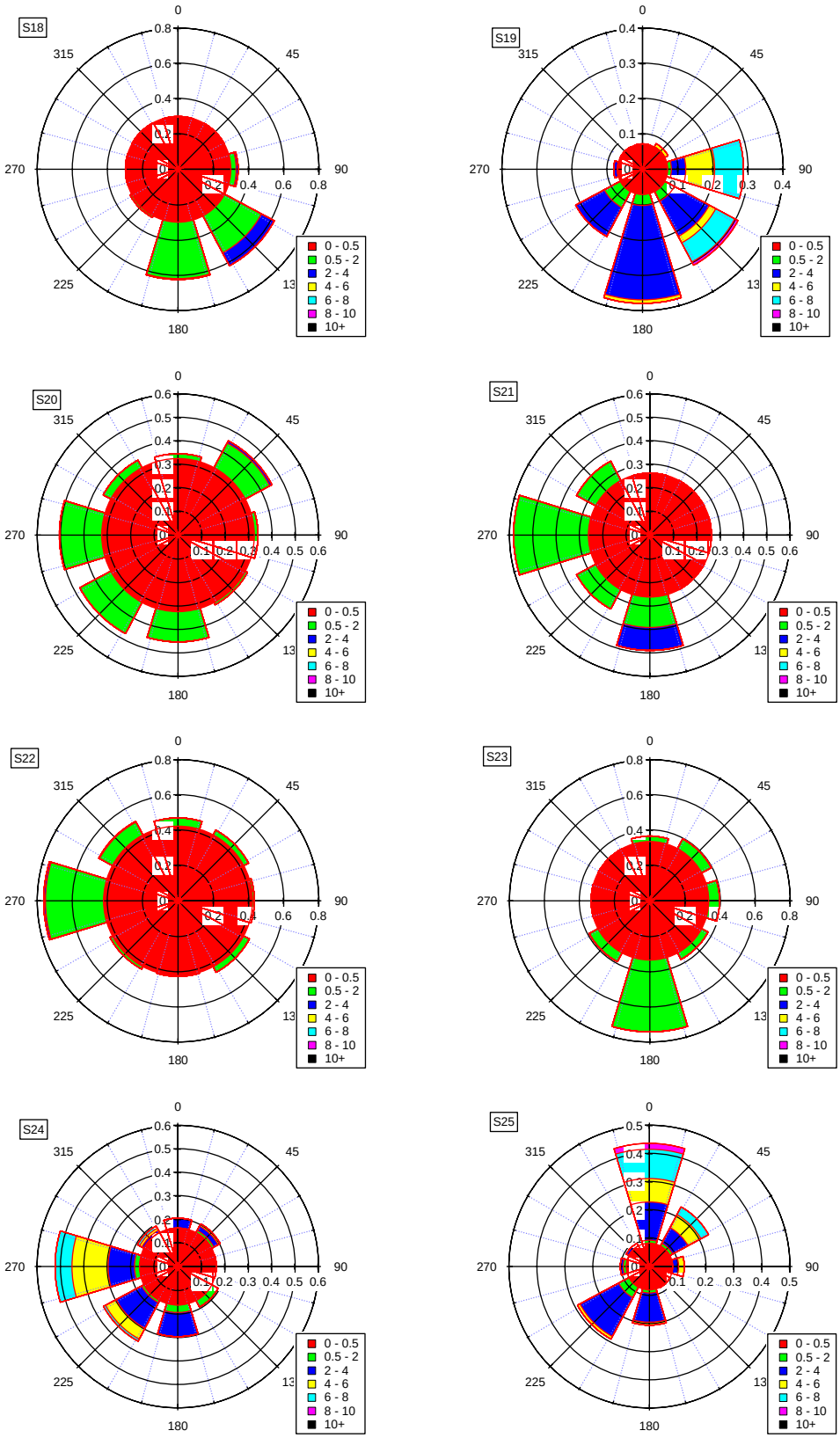

Figure A3-1: Wind rose plots of the sampling period at each school

Table A3-3: Principal Component Analysis for all of the schools.

	Component		
	1	2	3
Al	-0.12	-0.15	***0.80***
SI	***0.95***	0.19	0.14
P	***0.92***	-0.01	0.17
S	***0.91***	0.05	0.34
Cl	***0.90***	0.01	-0.04
K	0.43	0.46	0.49
Ca	***0.91***	0.19	0.22
Ti	***0.72***	0.19	-0.07
V	***0.82***	0.37	-0.08
Cr	***0.96***	0.19	0.02
Mn	***0.94***	0.23	-0.06
Fe	-0.14	***0.91***	-0.20
Ni	***0.67***	0.40	-0.20
Cu	***0.92***	0.10	0.04
Zn	0.28	***0.77***	0.06
Br	***0.97***	0.11	-0.03
Sr	***0.96***	0.19	-0.06
Pb	***0.96***	0.13	-0.02
Co	***0.85***	0.00	-0.01
Cd	***0.95***	0.10	-0.07
Variance (%)	66.1	77.3	83.3
Eiginvalue	13.22	2.24	1.19

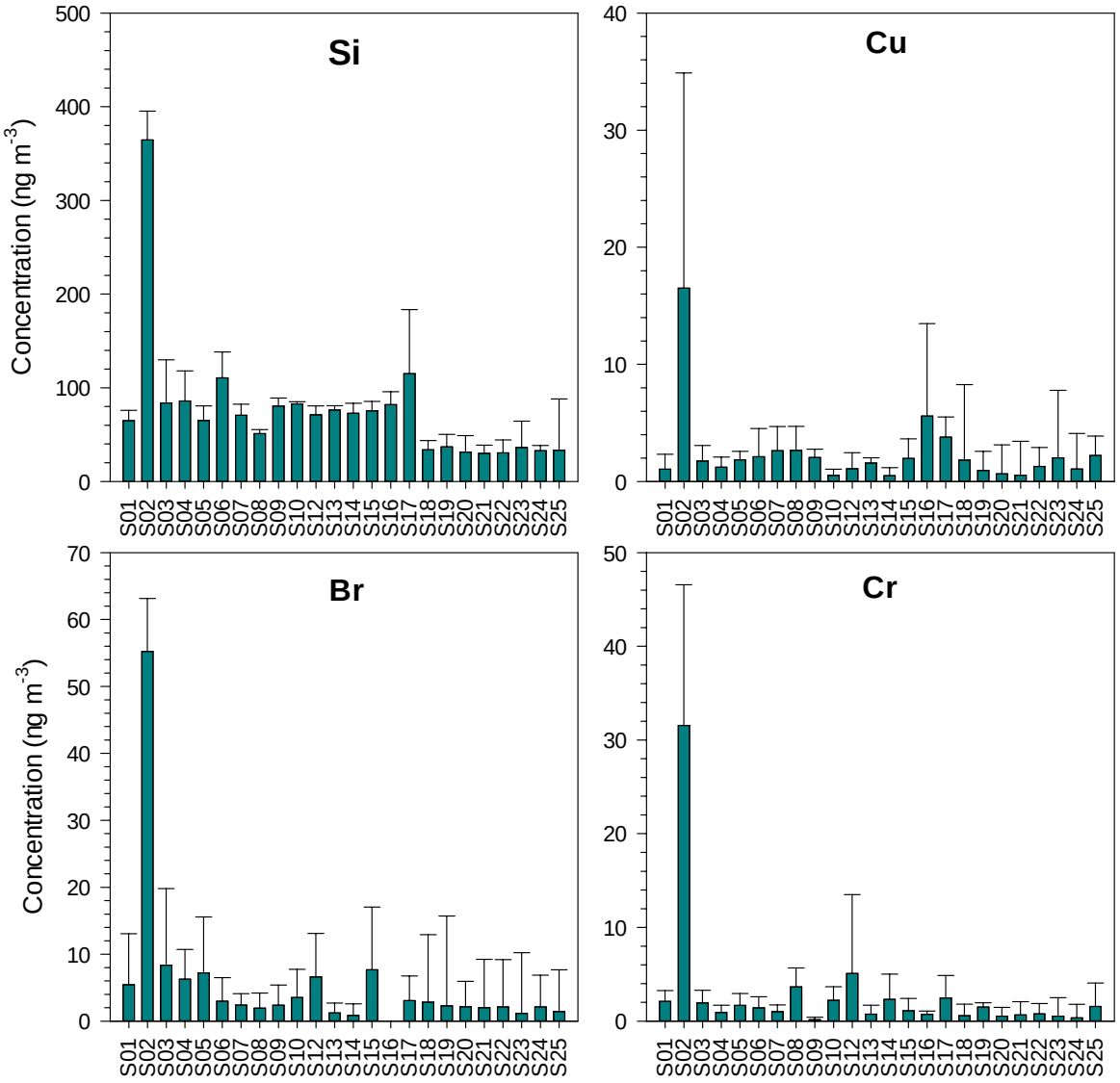

Figure A3-2: Average PM_1 concentrations of selected elements at all of the schools. Error bars represent 1 standard deviation

Appendix 4 (Chapter 6)

Table A4-1: Summary statistics of the concentration of the chemical species measured by the AMS at each school.

		Organics	Nitrates	Sulphates	Ammonium	Chlorides
S01	Mean	0.68	0.10	0.47	0.15	0.03
	Median	0.31	0.09	0.46	0.14	0.03
	Max.	205.60	0.34	1.33	0.71	0.79
	Min.	0.00	0.02	0.00	0.00	0.00
	Std Dev.	4.66	0.05	0.17	0.13	0.04
S04	Mean	0.77	0.08	0.38	0.18	0.04
	Median	0.54	0.07	0.25	0.14	0.03
	Max.	57.85	0.71	5.90	1.61	0.89
	Min.	0.08	0.02	0.00	0.00	0.00
	Std Dev.	1.20	0.06	0.38	0.13	0.03
S11	Mean	0.87	0.15	0.18	0.15	0.05
	Median	0.73	0.09	0.13	0.13	0.03
	Max.	5.00	0.78	1.18	0.78	1.15
	Min.	0.02	0.03	0.00	0.00	0.02
	Std Dev.	0.67	0.12	0.14	0.10	0.06
S12	Mean	3.57	0.42	0.59	0.31	0.10
	Median	2.13	0.26	0.46	0.24	0.06
	Max.	37.89	2.11	2.66	1.39	1.34
	Min.	0.09	0.04	0.00	0.00	0.02
	Std Dev.	3.60	0.38	0.46	0.25	0.12
S25	Mean	2.86	0.29	0.38	0.35	0.03
	Median	2.33	0.19	0.36	0.30	0.01
	Max.	17.54	2.41	1.35	1.61	1.47
	Min.	0.00	0.04	0.03	0.05	0.00
	Std Dev.	2.42	0.28	0.25	0.23	0.06

Table A4-2: Detection limits for the chemical species at each school in ng m^{-3}

School	Organics	Nitrates	Sulphates	Ammonium	Chloride
S04	31	6	7	96	6
S11	59	6	5	36	11
S12	36	3	4	53	6
S25	48	4	4	26	9

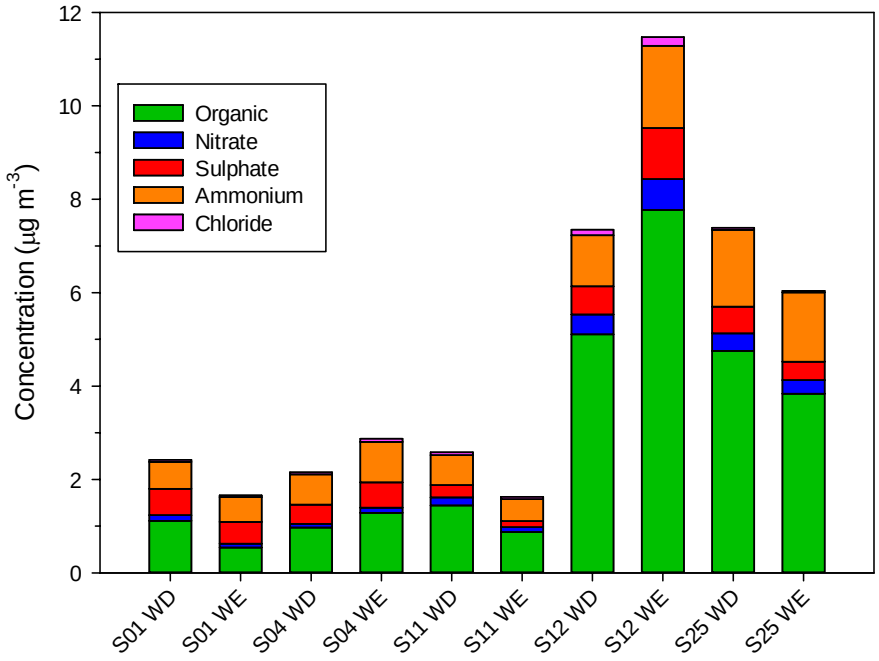

Figure A4-1: Average concentrations of the chemical species at each school for the weekday (WD) and weekend (WE).

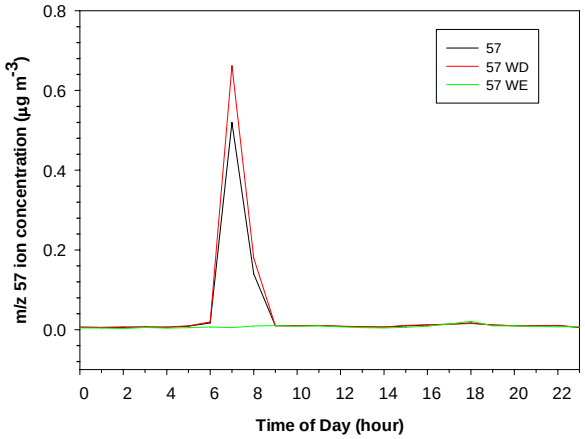

Figure A4-2: Comparison in the diurnal variation in the concentration of the HOA tracer ion, m/z 57 for all sampling days (57), weekdays (57 WD) and weekends (57 WE) at S01.

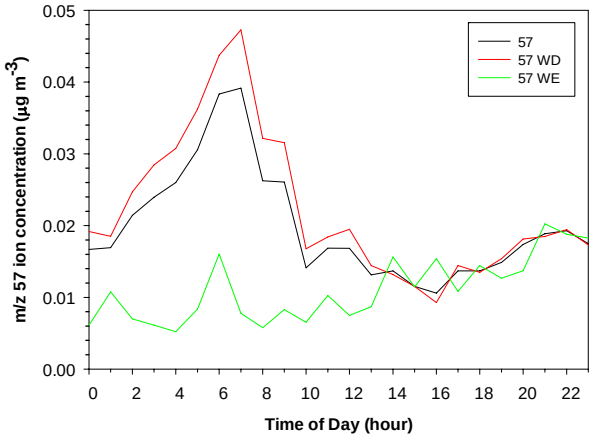

Figure A4-3: Comparison in the diurnal variation in the concentration of the HOA tracer ion, m/z 57 for all sampling days (57), weekdays (57 WD) and weekends (57 WE) at S11.

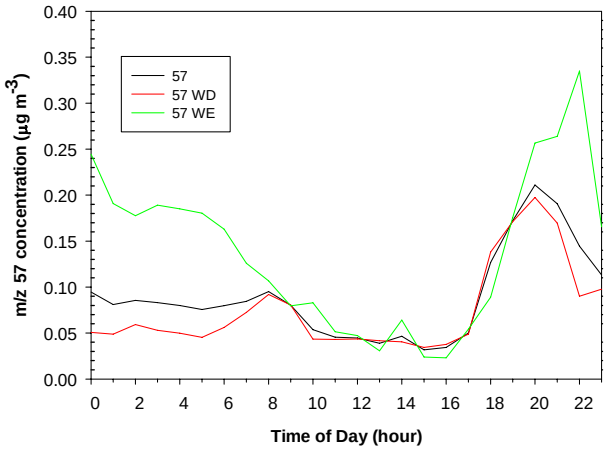

Figure A4-4: Comparison in the diurnal variation in the concentration of the HOA tracer ion, m/z 57 for all sampling days (57), weekdays (57 WD) and weekends (57 WE) at S12.

Appendix 5 (Chapter 7)

A5-1.1 Data pre-treatment

Pre-treatment of the data prior to PMF analysis as set out in Zhang et al. [1] was applied to the organic data from each location. The pre-treatment applied included the removal of any outlier peaks identified in the time series of organic fraction concentration as having unusually high concentrations. These peaks were removed as PMF analysis looks for patterns within the data set and any outliers overly affect the structure of the data. Data from calibration periods and High Efficiency Particle Air (HEPA) filter blanks such as the first weekend of S25 were also removed prior to PMF analysis, as they were perceived to be compromised in the field. Additional pre-treatment including checking the signal to noise ratio (SNR) for each m/z ion and any m/z ion found to have a weak SNR (SNR<2) were downgraded by a factor of 2 [2]. As recommended by Ulbrich et al. [2], the m/z 44 was downgraded along with the m/z ions associated with the m/z 44 in the fragmentation table (m/z 16, 17, 18, 19, 20 and 28) by the square root of 7 for each school. Table S1 lists the number of outlier peaks removed for each school dataset and also the number of weak m/z that were downgraded. From Table S1, S01 only had 55 m/z ions had a strong signal, and these m/z ions were all associated with the alkyl fragment ion series ($C_nH_{2n+1}^+$ (m/z 29, 43, 57, 71 etc) and $C_nH_{2n-1}^+$ (m/z 27, 41, 55, 69 etc)). There were very strong peaks in the concentration of the total organic fraction around 7am each weekday morning at this school, which were attributed to fuel powered gardening equipment at the school [3] and this may be the cause of the large number of weak m/z ions.

A5.2 References

1. Zhang, Q.; Jimenez, J.; Canagaratna, M.; Ulbrich, I.; Ng, N.; Worsnop, D.; Sun, Y., Understanding atmospheric organic aerosols via factor analysis of aerosol mass spectrometry: a review. *Anal. Bioanal. Chem.* **2011,** *401*, (10), 3045-3067.
2. Ulbrich, I. M.; Canagaratna, M. R.; Zhang, Q.; Worsnop, D. R.; Jimenez, J. L., Interpretation of organic components from Positive Matrix Factorization of aerosol mass spectrometric data. *Atmos. Chem. Phys.* **2009,** *9*, (9), 2891-2918.
3. Crilley, L. R.; Ayoko, G. A.; Jayaratne, E. R.; Salimi, F.; Morawska, L., Aerosol Mass Spectrometric analysis of the chemical composition of non- refractory PM1 samples from school environments in Brisbane, Australia. *Sci. Total Environ.* **2013,** *458-460*, 81-89.

Table A5-1: Summary of the data pre-treatment for each school.

School	No. of weak m/z	No. of Data points	No. of outliers
S01	215	4079	32
S04	0	4084	14
S11	62	2673	2
S12	3	2416	12
S25	1	3002	7

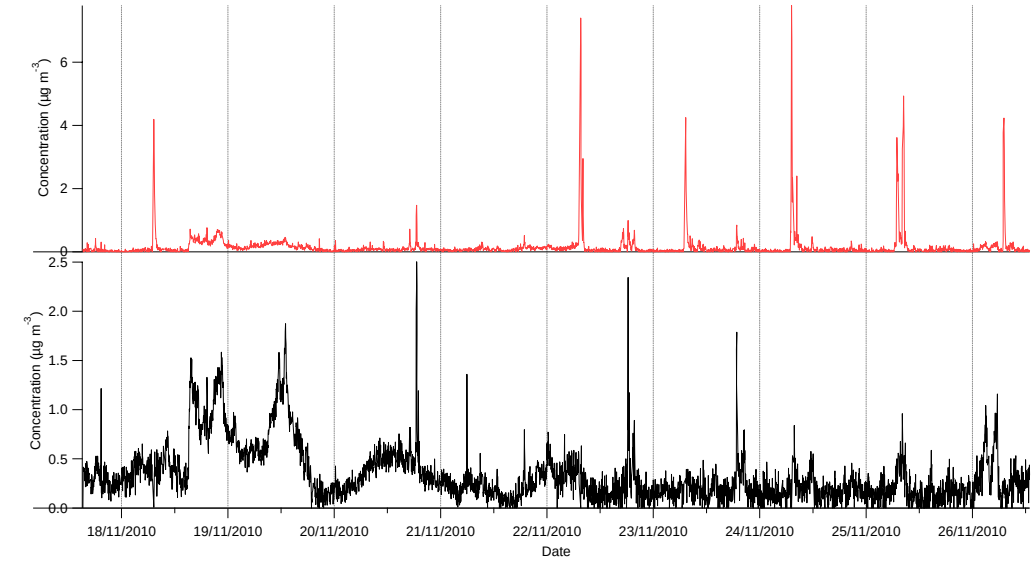

Figure A5-1: Time series of the two factor solution at S01. The HOA and OOA factors are red and black, respectively.

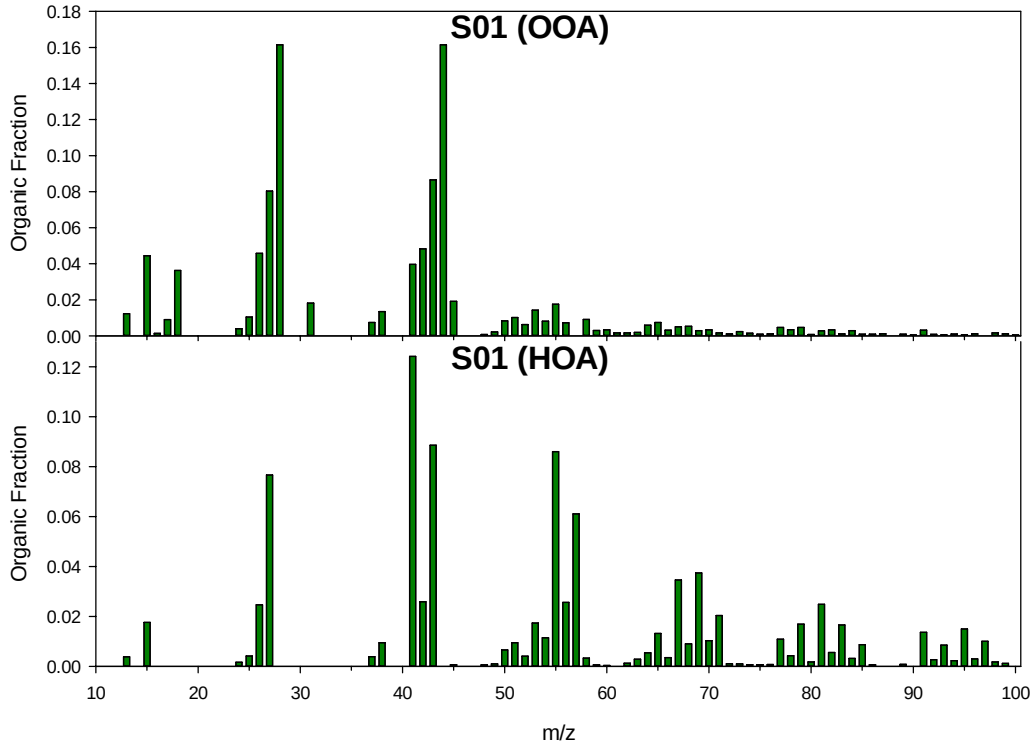

Figure A5-2: Mass spectra of the two factors from S01, labelled with the source.

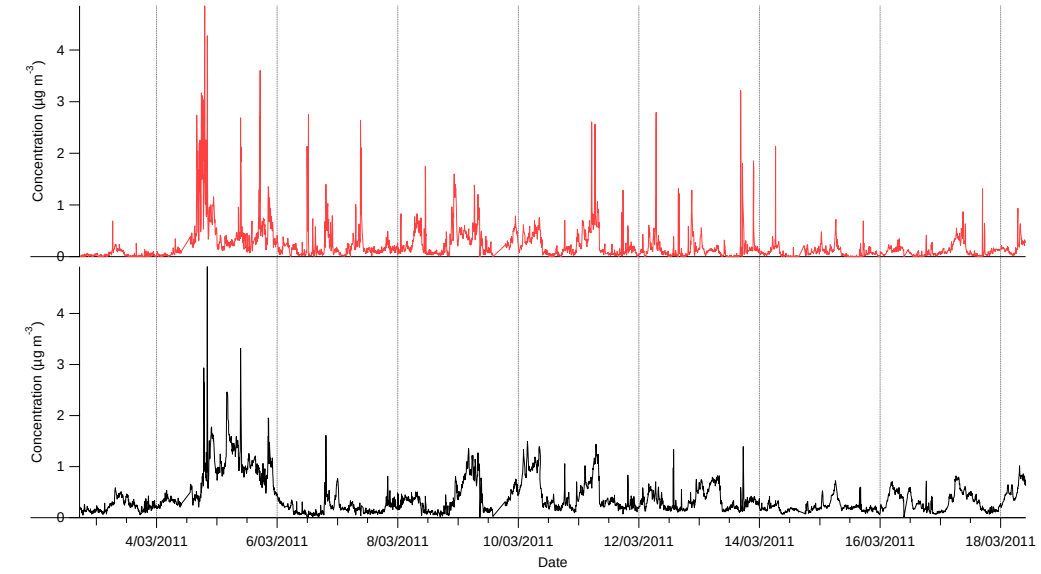

Figure A5-3: Time series of the two factor solution at S04. The HOA and OOA factors are red and black, respectively.

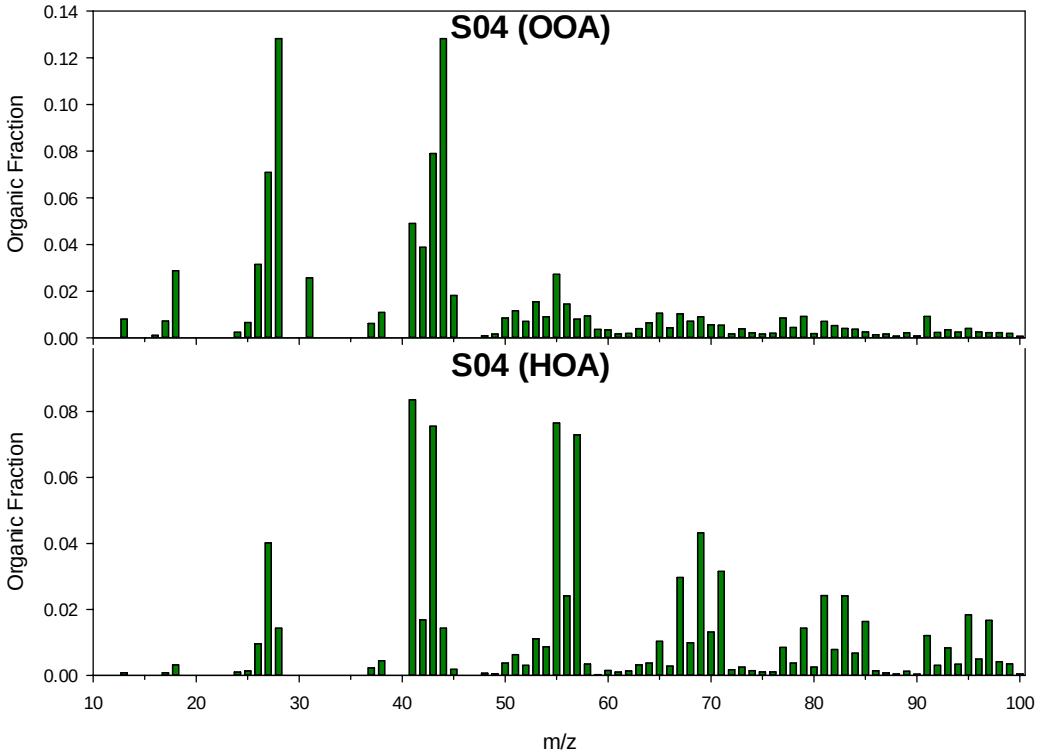

Figure A5-4: Mass spectra of the two factors from S04, labelled with the source.

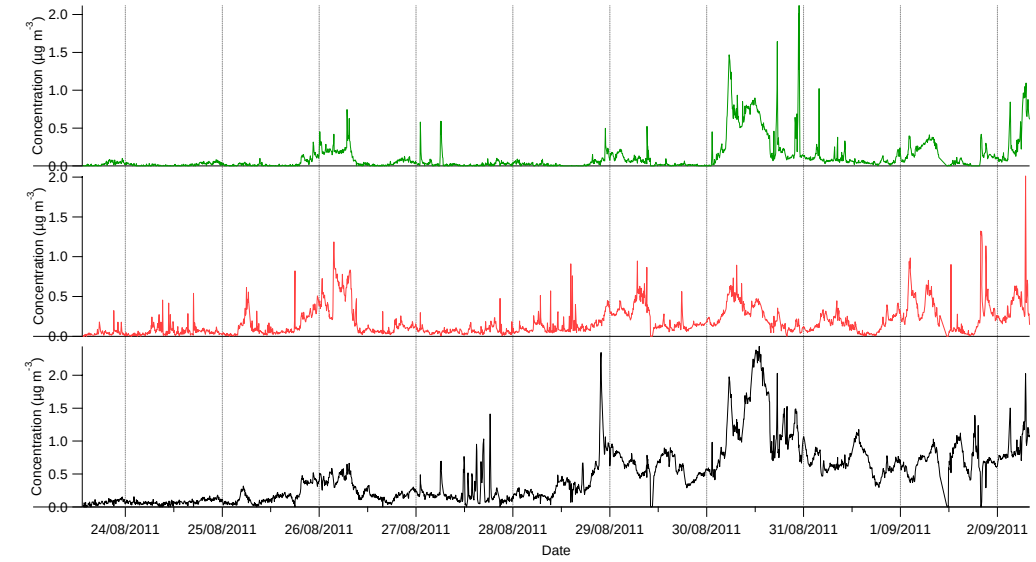

Figure A5-5: Time series of the three factor solution at S11. The OOA, HOA and BBOA factors are black, red and green, respectively.

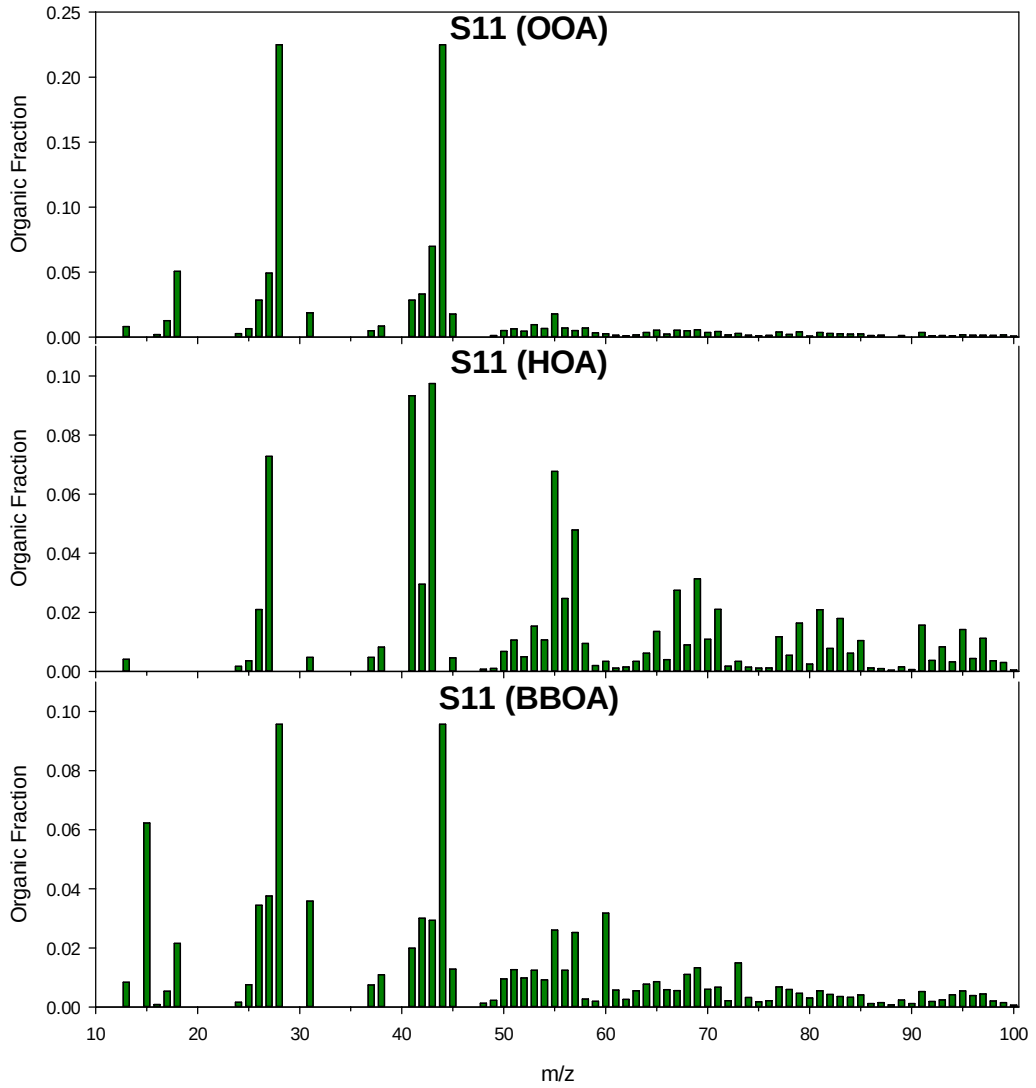

Figure A5-6: Mass spectra of the three factors from S11, labelled with the source.

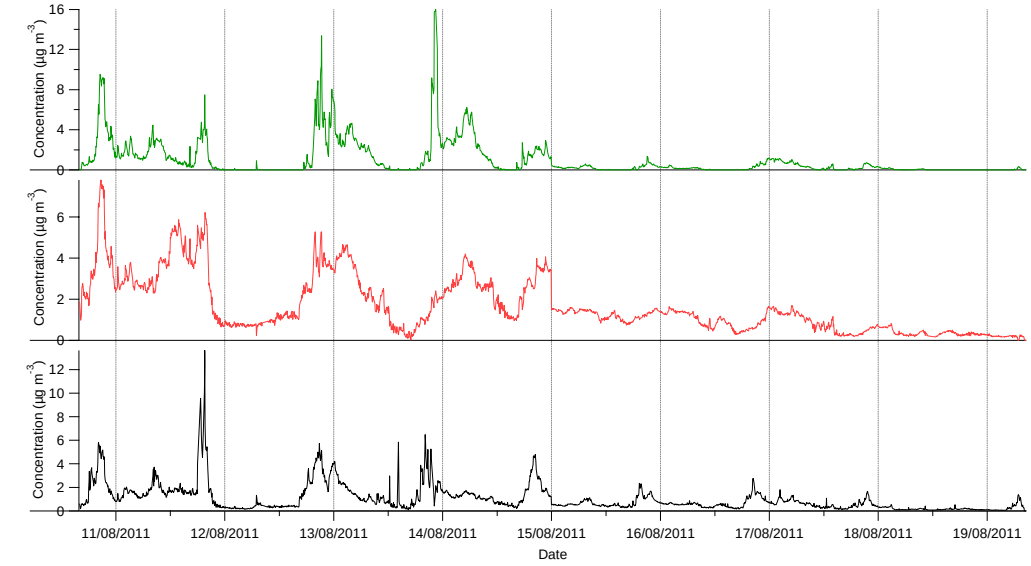

Figure A5-7: Time series and diurnal cycles of the three factor solution at S12. The SV-OOA, LV-OOA and BBOA factors are black, red and green, respectively.

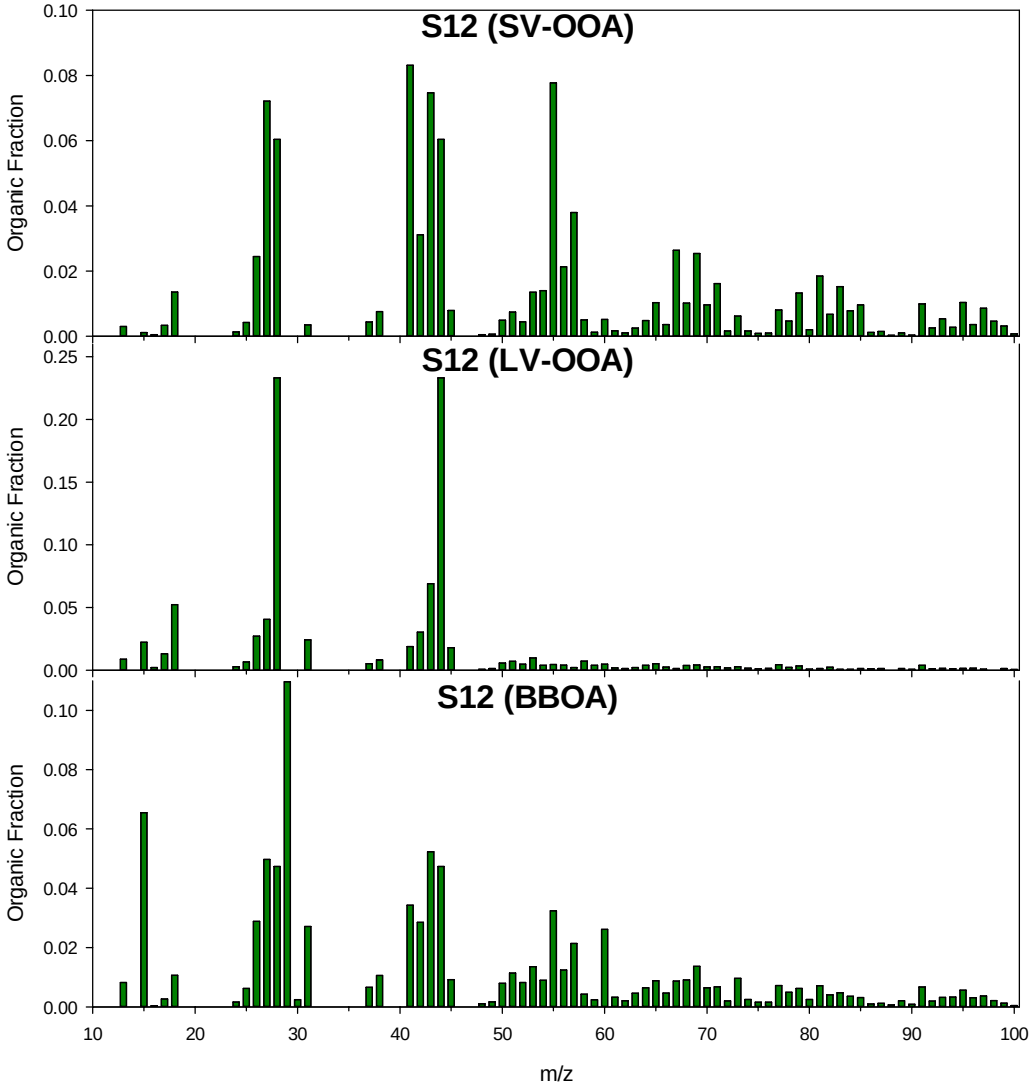

Figure A5-8: Mass spectra of the three factors from S12, labelled with the source.

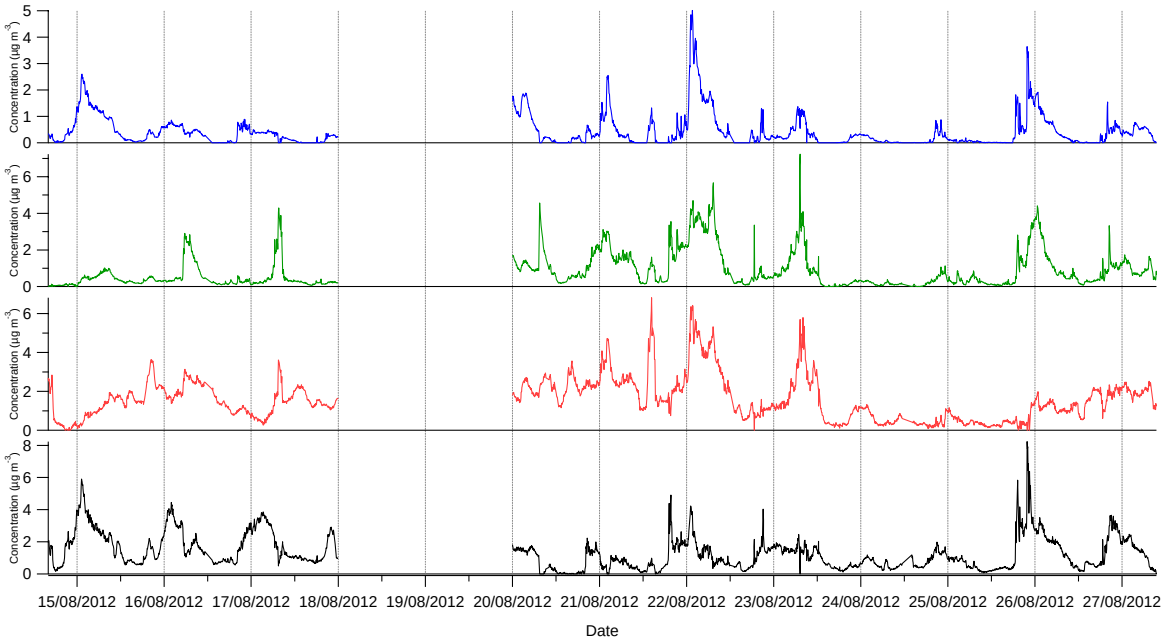

Figure A5-9: Time series of the four factor solution at S25. The SV-OOA, LV-OOA, HOA and BBOA factors are black, red, green and blue, respectively.

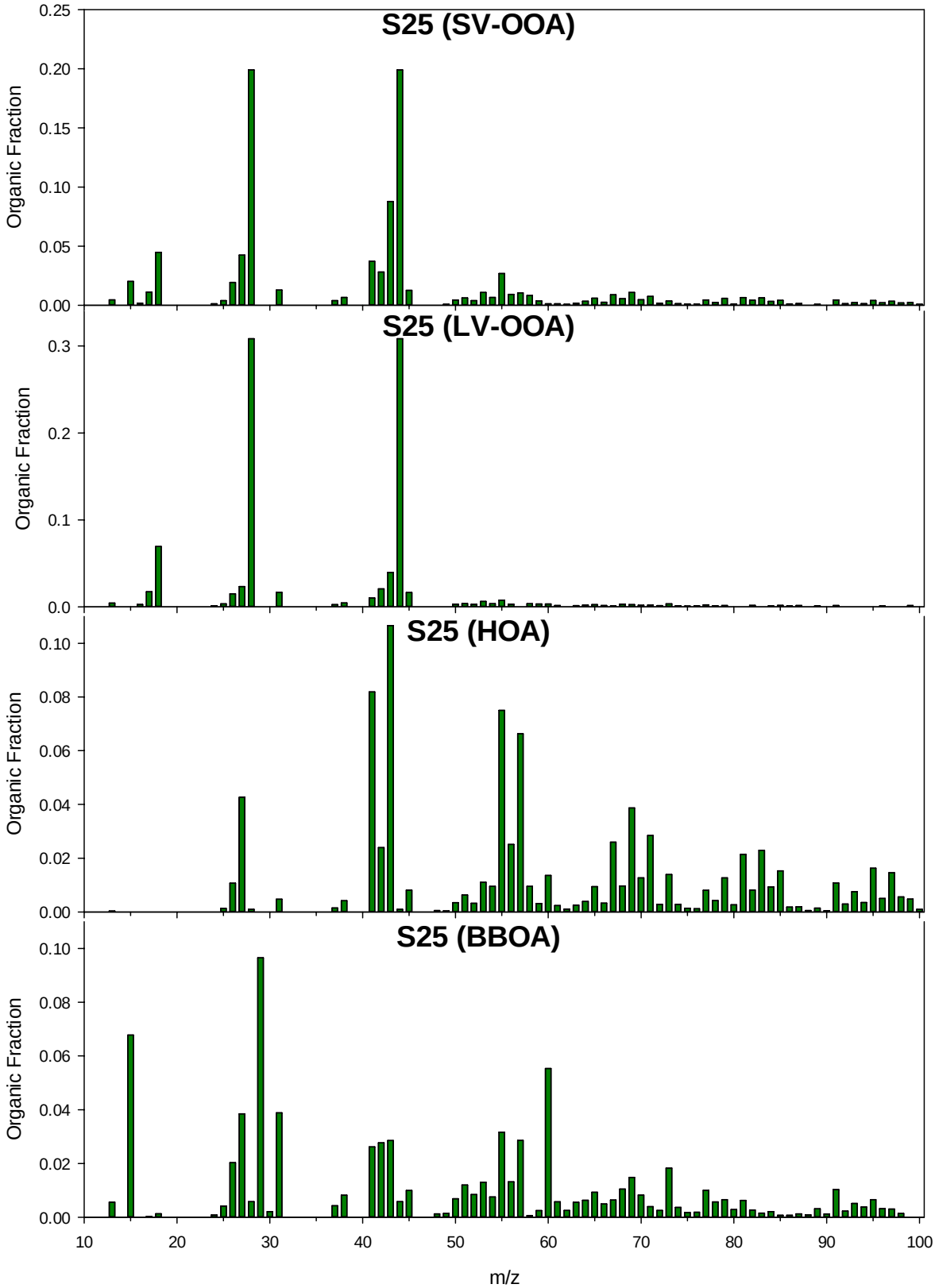

Figure A5-10: Mass spectra of the four factors from S25, labelled with the source.

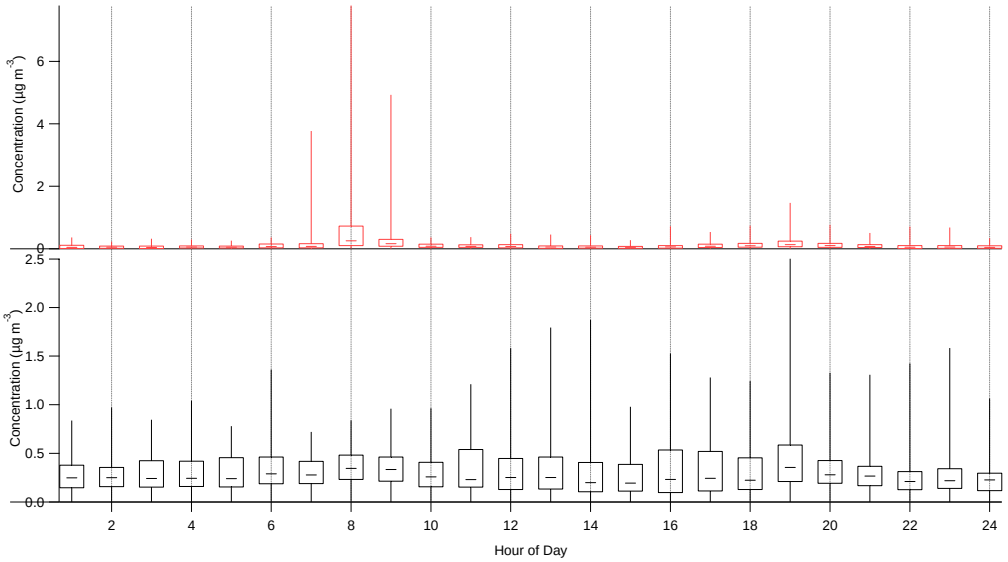

Figure A5-11: Box plots of the diurnal variation at S01. The HOA and OOA factors are red and black, respectively.

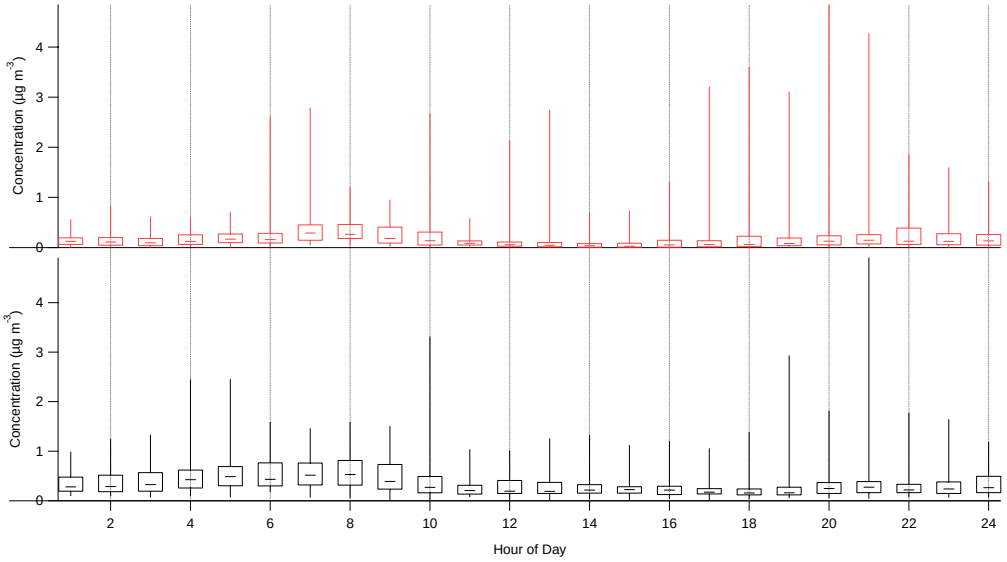

Figure A5-12: Box plots of the diurnal variation at S04. The HOA and OOA factors are red and black, respectively.

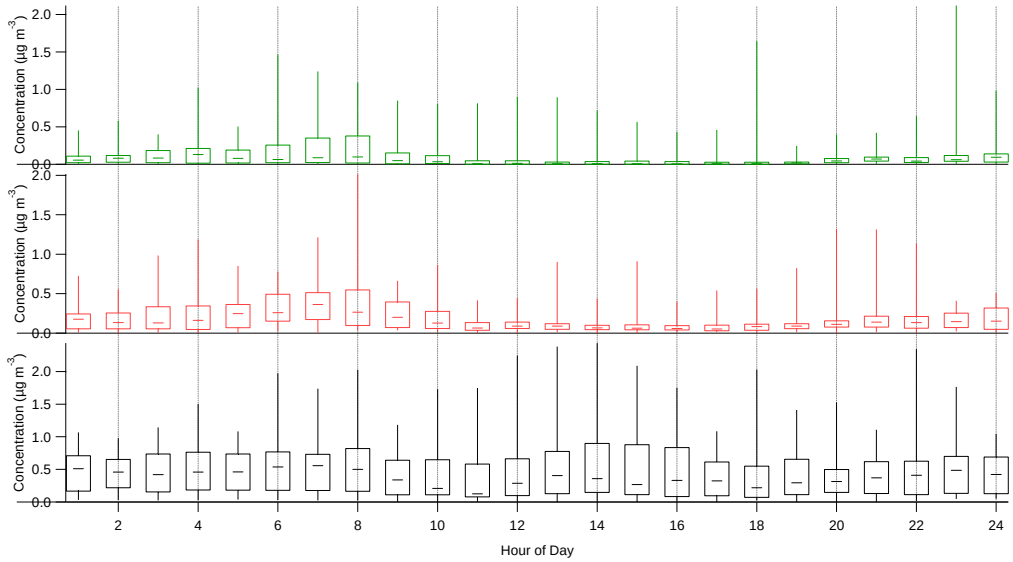

Figure A5-13: Box plots of the diurnal variation of the three factor solution at S11. The OOA, HOA and BBOA factors are black, red and green, respectively.

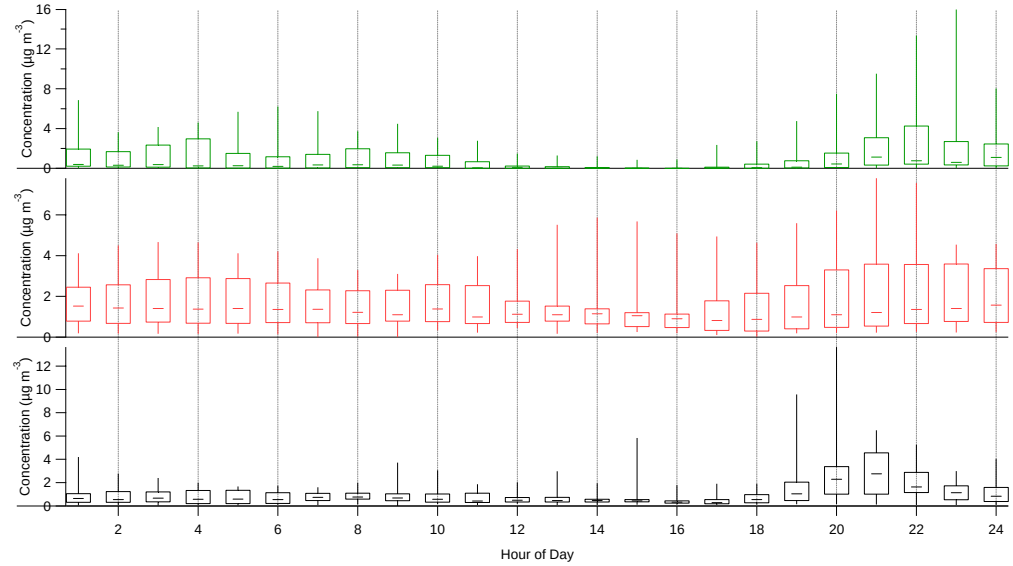

Figure A5-14: Box plots of the diurnal variation of the three factor solution at S12. The SV-OOA, LV-OOA and BBOA factors are black, red and green, respectively.

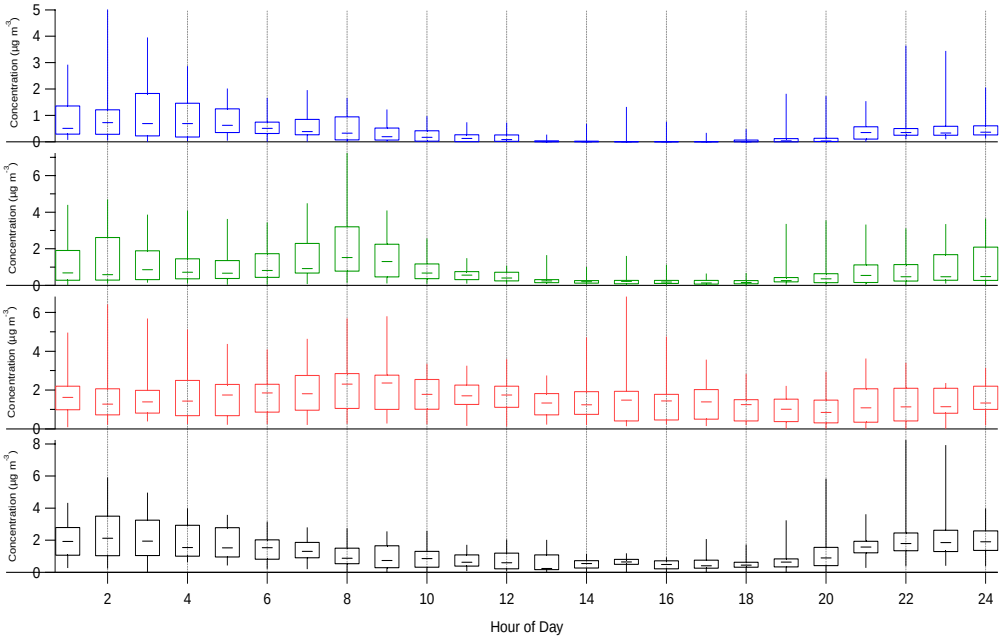

Figure A5-15: Box plots of the diurnal variation of the three factor solution at S25. The SV-OOA, LV-OOA, HOA and BBOA factors are black, red, green and blue, respectively.

S01

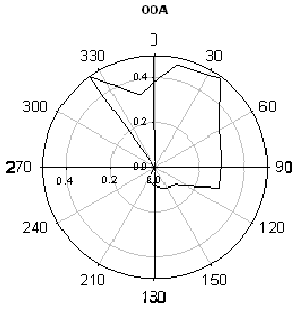

S04

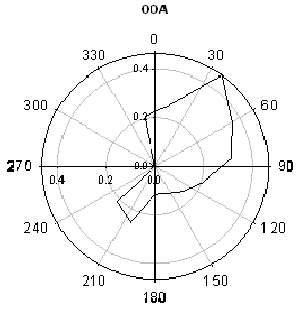

S11

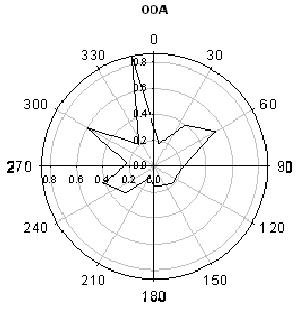

S12

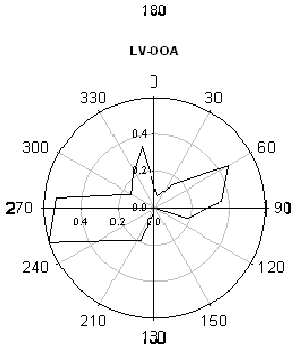

S25

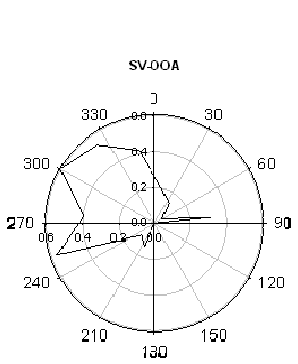

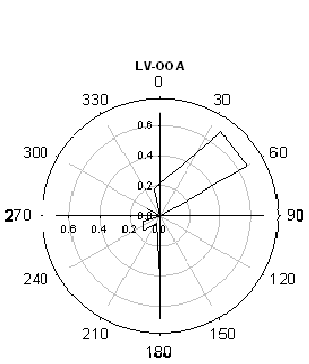

Figure A5-16: CPF graphs for the OOA factor/s at each school.

Appendix 6 (Chapter 8)

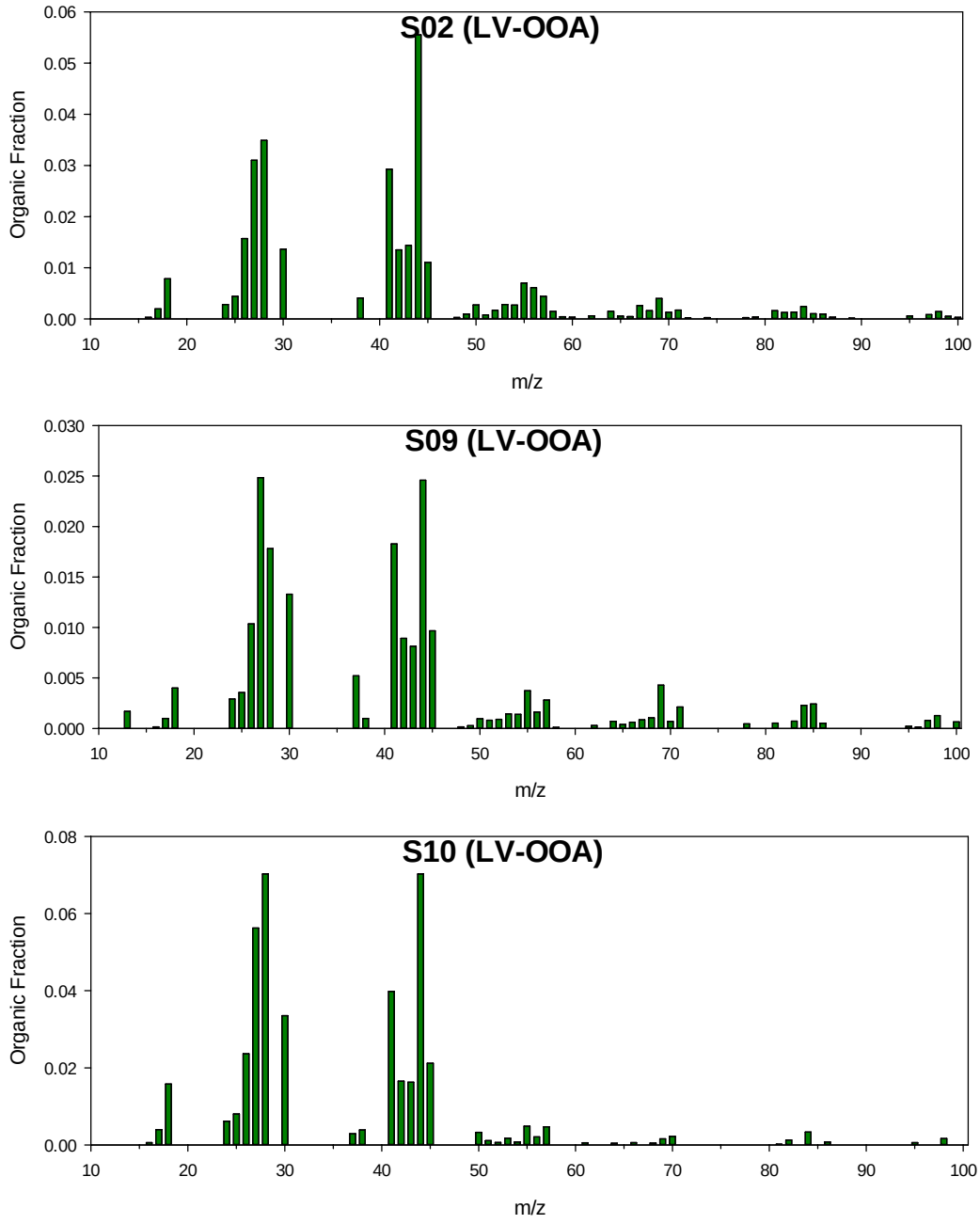

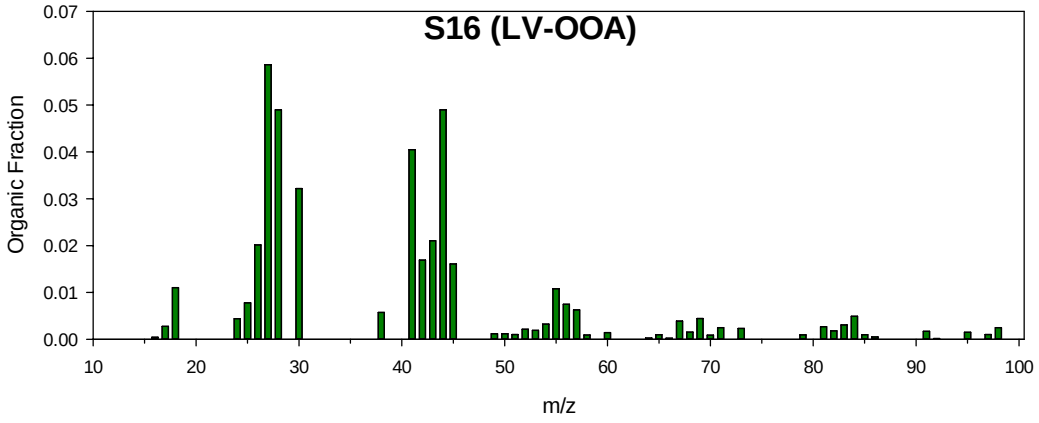
S16 (LV-OOA)
Organic Fraction
0.07
0.06
0.05
0.04
0.03
0.02
0.01
0.00
10
20
30
40
50
60
70
80
90
100
m/z

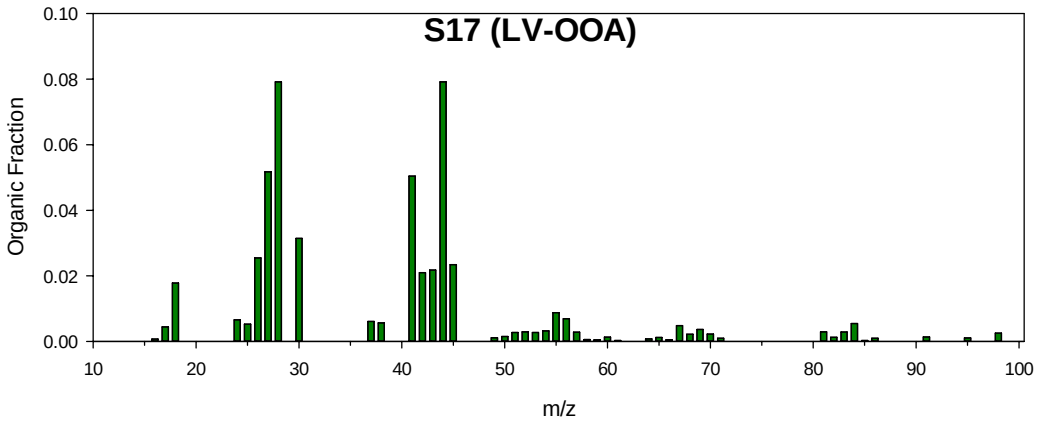
S17 (LV-OOA)
Organic Fraction
0.10
0.08
0.06
0.04
0.02
0.00
10
20
30
40
50
60
70
80
90
100
m/z

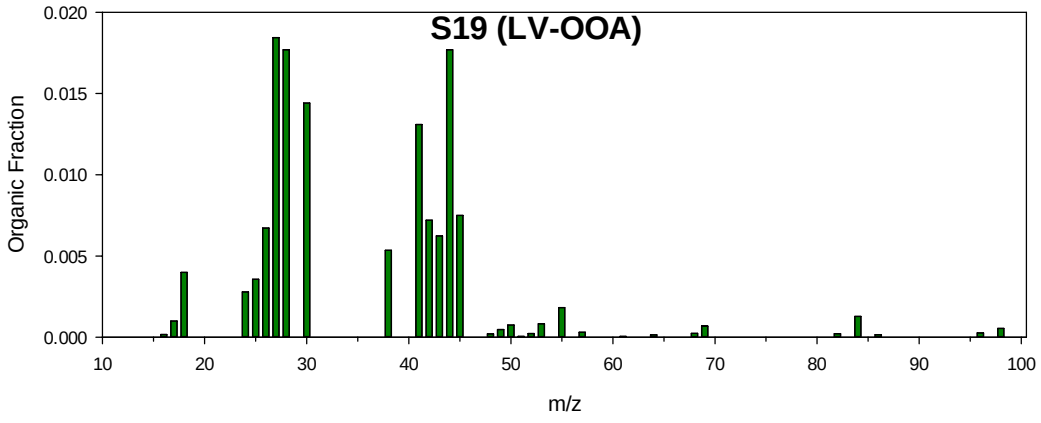
S19 (LV-OOA)
Organic Fraction
0.020
0.015
0.010
0.005
0.000
10
20
30
40
50
60
70
80
90
100
m/z

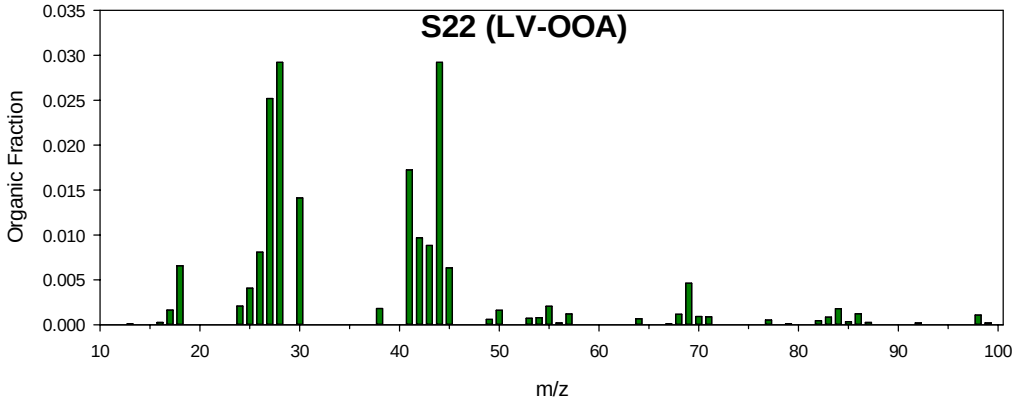
S22 (LV-OOA)
Organic Fraction
0.035
0.030
0.025
0.020
0.015
0.010
0.005
0.000
10
20
30
40
50
60
70
80
90
100
m/z

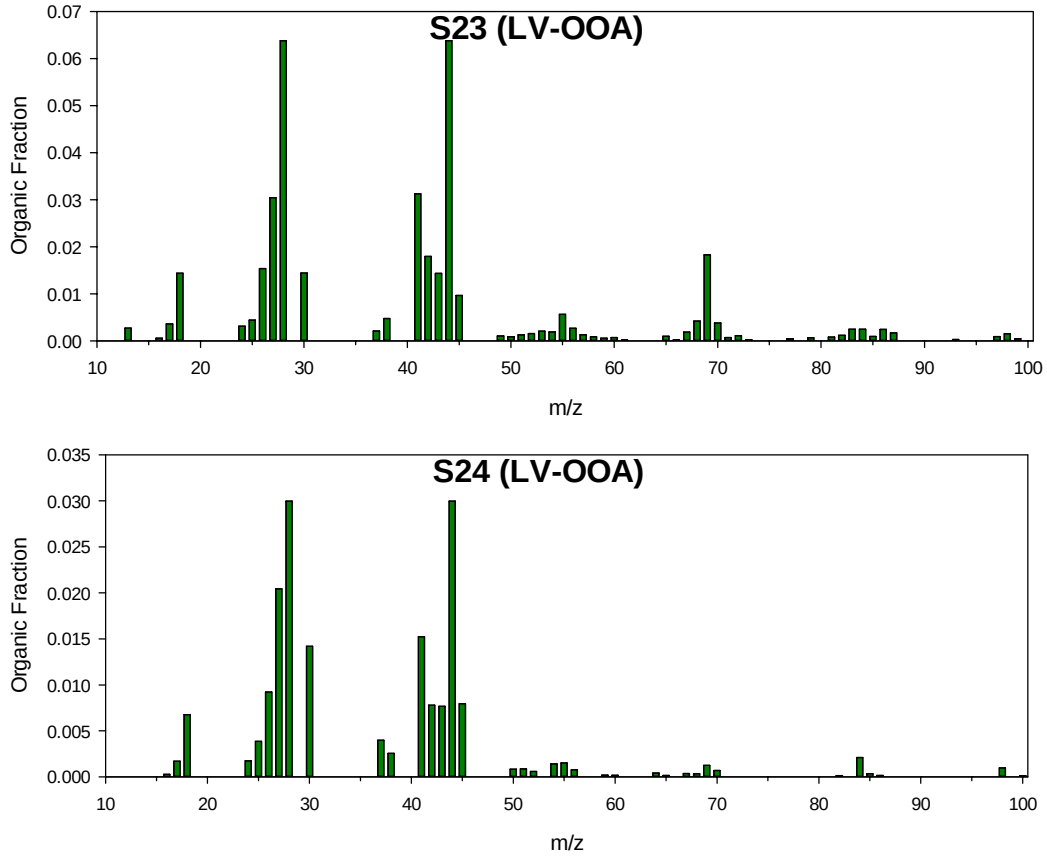

Figure A6-1: Filter extract mass spectra at the schools where the water soluble organic aerosols were classified as LV-OOA

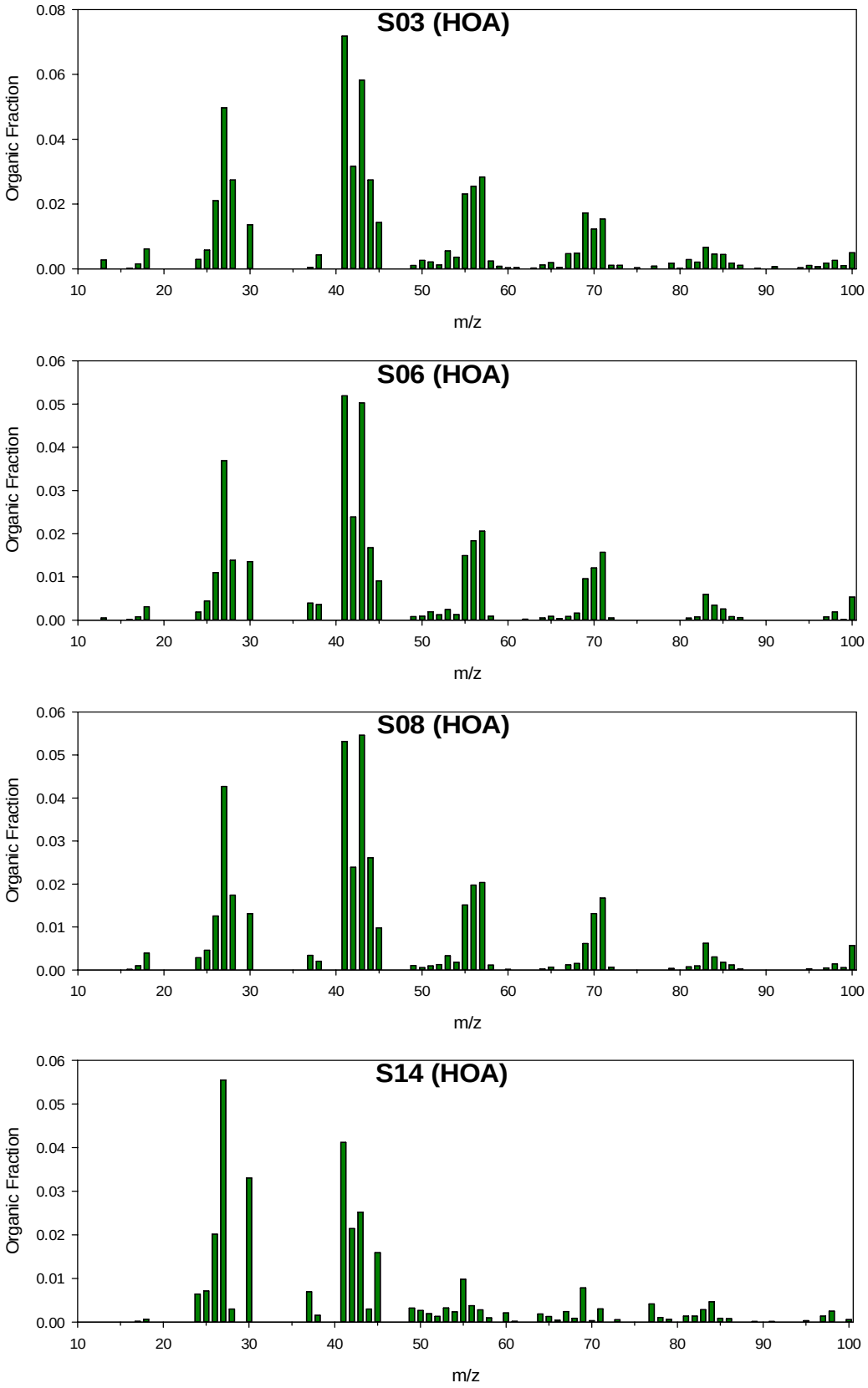

Figure A6-2: Filter extract mass spectra at the schools where the water soluble organic aerosols were classified as HOA

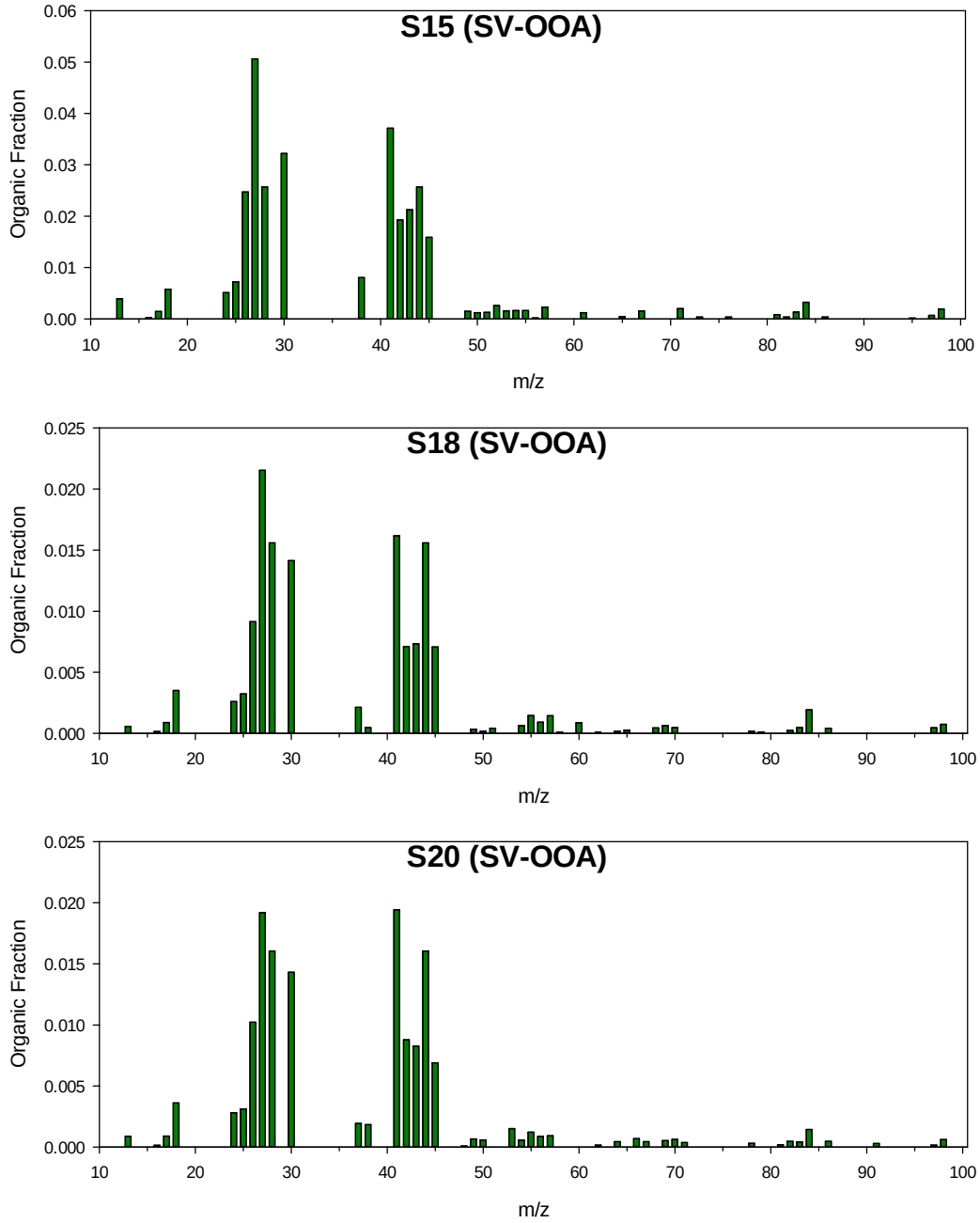

Figure A6-3: Filter extract mass spectra at the schools where the water soluble organic aerosols were classified as SV-OOA